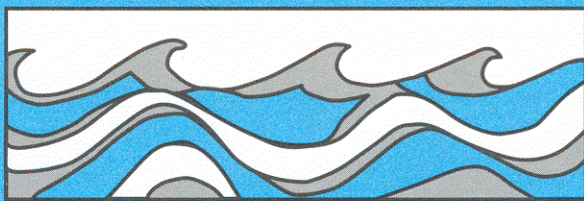


University of Washington
Department of Civil and Environmental Engineering



STATE ESTIMATION AND HYPOTHESIS
TESTING: A FRAMEWORK FOR THE
ASSESSMENT OF MODEL COMPLEXITY AND
DATA WORTH IN ENVIRONMENTAL
SYSTEMS

John R. Yearsley



Water Resources Series
Technical Report No. 116
June 1989

Seattle, Washington
98195

Department of Civil Engineering
University of Washington
Seattle, Washington 98195

**STATE ESTIMATION AND HYPOTHESIS TESTING: A
FRAMEWORK FOR THE ASSESSMENT OF MODEL COMPLEXITY
AND DATA WORTH IN ENVIRONMENTAL SYSTEMS**

John R. Yearsley

Water Resources Series
Technical Report No. 116

June 1989

ABSTRACT

The primary objective of this dissertation was to demonstrate methods that can be used to assess model complexity and data worth in environmental systems. The methodology was developed within the framework of hypothesis testing and state estimation and demonstrated by application to two well-known environmental systems, the global carbon cycle and a lake ecosystem. These two environmental systems were chosen because of the interest they hold for environmental scientists and planners, and because there is a large body of data and research that provides the required empirical foundations for applying and testing the methodology.

For purposes of this dissertation, it was assumed that the large pool of available data and knowledge was sufficient to develop a reference system model that could produce outputs characteristic of the two prototype systems. This provided a rationale for the generation of observations with Monte Carlo simulation techniques. The results of previous research were used to construct reference models of both the global carbon cycle and a lake ecosystem. Populations generated by these reference models provided the observations used in assessing both the methodology and important features of the two environmental systems.

The populations generated by the reference models were used to explore issues of model complexity and data worth for both linear and nonlinear process and measurement models. This was done, for both environmental systems, by postulating several levels of model complexity for the process models and several levels of error for the measurement models. The tests of model validity and the analysis of data worth and model complexity were performed under the controlled, idealized conditions. These conditions were established by the reference system models used to represent each of the two systems. Under these conditions, the methodology was successfully demonstrated, given certain assumptions regarding the process and measurement models. For the global carbon cycle, the postulated process models were assumed to be perfect; i.e., no model error, and the measurement error was assumed to be normally distributed. In the case of the lake ecosystem, errors in the postulated process models were assumed to be normally distributed and the measurement error log-normally distributed.

ACKNOWLEDGMENTS

The research described in this report is based upon the doctoral dissertation of the author. While conducting the research described herein, the author received guidance and support from the following:

Dr. Dennis Lettenmaier, the dissertation advisor, was the source of solutions for many of the technical problems which arose. His editing of the report was thorough and constructive. Most important, he provided just the right amount of guidance to keep things moving.

Professors Steve Burges, Brian Mar, Richard Palmer, and Jeff Richey were always helpful and, most of all, great sources of encouragement.

The author was a full time employee of the U.S. Environmental Protection Agency during the four-year period in which the research was conducted. The agency contributed to the completion of the research in a number of ways. Computer resources at the U.S. Environmental Protection Agency Region 10 were used for the Monte Carlo simulations. Robert Courson, Director of the Environmental Services Division, William Schmidt, Chief of the Technical Support Branch and Pat Cirone, Chief of the Health and Environmental Assessment Section were all very helpful and understanding throughout, allowing flexible work schedules as well as encouragement and support.

TABLE OF CONTENTS

	Page
List of Figures	v
List of Tables.....	viii
CHAPTER	
1 INTRODUCTION	1
1.1. Elements of Environmental Assessment.....	1
1.2. Important Concepts	5
1.3. Research Objectives.....	13
2 LITERATURE REVIEW	15
2.1. Needs Assessment.....	15
2.2. Application of Models to Environmental Analysis	20
2.3. Survey of Appropriate Methods.....	23
2.3.1 State Estimation	23
2.3.2 Hypothesis Testing	26
2.3.3 Analysis of Complex Systems	26
2.3.4 Monte Carlo Method.....	30
2.4. Summary.....	31
3 DESCRIPTION OF METHODOLOGY.....	32
3.1. State-Space Structure	32
3.2. Hypothesis Testing	36
3.3. State Estimates Applied to Sequential Testing	44
3.4. Application to Environmental Assessment	47
3.5. Application of Hypothesis Testing to Model Validity... ..	54
4 LINEAR MODELS: AN ASSESSMENT OF MODEL COMPLEXITY AND DATA WORTH IN THE GLOBAL CARBON CYCLE.....	56
4.1. Background.....	56
4.2. Scope of Analysis.....	57
4.3. Model of the Global Carbon Cycle.....	59
4.4. Monte Carlo Methods.....	65
4.5. Model Complexity	67
4.6. Results.....	73
4.7. Summary.....	91

TABLE OF CONTENTS

CHAPTER	Page
5	NONLINEAR MODELS: AN ASSESSMENT OF MODEL COMPLEXITY AND DATA WORTH IN AN HYPOTHETICAL LAKE ECOSYSTEM..... 92
	5.1. Introduction..... 92 5.2. Scope of Analysis..... 95 5.3. Monte Carlo Methods..... 100 5.4. Measurement Error..... 106 5.5. Model of the Lake Ecosystem 112
	5.5.1 Environmental Characteristics 112 5.5.2 Ecosystem Model Parameters..... 115
	5.6. Model Complexity 116
	5.6.1 Model I..... 117 5.6.2 Model II..... 118 5.6.3 Model III..... 120
	5.7. Results-Constant Environmental Conditions 122
	5.7.1 Parameter Estimates..... 124 5.7.2 Model Validation 139 5.7.3 Time to Identify Hypotheses..... 146
	5.8. Results-Simlated Natural Conditions 151
	5.8.1 Parameter Estimates..... 162 5.8.2 Model Validation 169 5.8.3 Time to Determine Correct Hypotheses 172
	5.9. Conclusions..... 175
6	SUMMARY AND CONCLUSIONS..... 177
	6.1. Summary..... 177 6.2. Conclusions..... 179
	6.2.1 Primary Objectives..... 179 6.2.2 Secondary Objectives..... 180
	6.3. Recommendations..... 185

TABLE OF CONTENTS

	Page
BIBLIOGRAPHY	189
APPENDIX I: STATE-SPACE STRUCTURE FOR THE GLOBAL CARBON CYCLE	201
APPENDIX II: A DESCRIPTION OF THE REFERENCE MODEL FOR THERMAL ENERGY	206
APPENDIX III: A DESCRIPTION OF THE REFERENCE MODEL FOR ECOSYSTEM DYNAMICS.....	212
APPENDIX IV: FILTER DERIVATION FOR THE NONLINEAR ECOSYSTEM MODELS.....	228

LIST OF FIGURES

Figure Number	Page
1.1	Schematic of systems approach2
1.2	Flow diagram of environmental assessment.....4
1.3	Temperature in an hypothetical lake as an example of environmental state variable6
1.4	The three different types of states estimates8
3.1	Relationships between the state variable, inputs and outputs in a system described by state-space structure 33
3.2	Distribution of the random variable, ξ , under the null and alternative hypotheses 37
3.3	Schematic of hypothesis testing for a sequential test 39
3.4	Decision regions for sequential tests 42
3.5	Environmental system with inputs before and after development 48
3.6	Trajectory of state variables, \mathbf{x} , in an environmental system before and after development..... 51
3.7	Hypothetical trajectory of decision variables ξ_0 and ξ_1 before and after development..... 53
4.1	Model of global carbon cycle..... 60
4.2	Comparison of simulated and modeled atmospheric CO_2 64
4.3	Simulated deviations of carbon from equilibrium conditions for the atmosphere, terrestrial biota, intermediate/deep ocean and ocean surface 74
4.4	Time history of the power to reject the null hypothesis for three models of the global carbon cycle 79
4.5	Time required to detect input from the terrestrial biota when measurement error of atmospheric carbon is varied 86
4.6	Time required to detect input from the terrestrial biota when measurement error of terrestrial bioa carbon is varied..... 87
4.7	Time required to detect input from the terrestrial biota when measurement error of soil carbon is varied 88
4.8	Time required to detect input from the terrestrial biota when measurement error of deep/intermediate ocean carbon is varied 89
4.5	Time required to detect input from the terrestrial biota when measurement error of ocean surface carbon is varied..... 90
5.1	Schematic diagram of system of reference models used to generate ecosystem state variables 96
5.2	Postulated models of three different levels of model complexity 98
5.3	The reference ecosystem idealized as a continuously stirred tank reactor (CSTR)102
5.4	Fluxes contributing to the heat budget of the prototype lake.....103
5.5	Nutrient and energy flow in prototype ecosystem105

LIST OF FIGURES

Figure Number	Page
5.6	Simulated phytoplankton in reference ecosystem for three nutrient loading scenarios.....125
5.7	Simulated inorganic phosphorus in reference ecosystem for three nutrient loading scenarios126
5.8	Simulated zooplankton biomass in reference ecosystem for three nutrient loading scenarios127
5.9	Means and standard deviation of apparent settling velocity for Model I as a function of measurement error131
5.10	Means and standard deviations for parameter estimates for Model II as a function of measurement error132
5.11	Means and standard deviations for parameter estimates for Model III as a function of measurement error134
5.12	Cost function for true parameters of Model III versus cost function for estimated parameters when $P_{in}=0.05$ mg/l and $CV=0.5$140
5.13	Simulated and observed trajectory of phytoplankton for parameter set with pathologic behavior.....141
5.14	Power to reject null hypothesis for Models I,II and III when $P_{in}=0.01$ mg/l.....143
5.15	Power to reject null hypothesis for Models I,II and III when $P_{in}=0.02$ mg/l.....144
5.16	Power to reject null hypothesis for Models I,II and III when $P_{in}=0.05$ mg/l.....145
5.14	Power to reject null hypothesis for Model III with true parameters147
5.18	Typical ten-year trajectory of river inflow, Q, based upon data from the Cedar River at Renton, Washington.....154
5.19	Typical ten-year trajectory of daily average solar radiation based upon data from the Seattle-Tacoma International airport155
5.20	Typical ten-year trajectory of simulated total phosphorus in the river inflow based upon characteristics of the Cedar River at Renton, Washington.....156
5.21	Typical ten-year trajectories for three classes of phyto- under simulated natural conditions.....158
5.22	Typical ten-year trajectory of dissolved inorganic phosphorus (PO_4 -P) under simulated natural conditions.....159
5.23	Typical ten-year trajectories for two classes of zooplankton under simulated natural conditions.....160
5.24	Typical ten-year trajectory of simulated water temperature in the hypothetical lake ecosystem161

LIST OF FIGURES

Figure Number		Page
5.25	Mean and standard deviations of apparent settling velocity, w_s , for Model I using complex reference model under simulated natural conditions	163
5.26	Mean and standard deviations of parameter estimates for Model II using complex reference model under simulated natural conditions	164
5.27	Mean and standard deviations of parameter estimates for Model II using complex reference model under simulated natural conditions	167
5.28	Power to reject null hypothesis for Models I, II, III under simulated natural conditions for $\Delta P/P_{in}=0.1$	170
5.29	Power to reject null hypothesis for Models I, II, III under simulated natural conditions for $\Delta P/P_{in}=0.2$	171

LIST OF TABLES

Table Number		Page
2.1	Federal laws associated with the application of mathematical models of environmental systems.....	16
4.1	Parameter values used in the nonlinear model of the global carbon cycle	62
4.2	Scenarios used to test hypotheses regarding the consumption of fossil fuels and terrestrial biota.....	66
4.3	Coefficient matrix for 15-compartment model.....	68
4.4	Coefficient matrix for 6-compartment model	71
4.5	Coefficient matrix for 4-compartment model	72
4.6	Contributions of various compartment to the likelihood function compared to the theoretical contribution.....	82
5.1	Range of coefficient of variation for eight ecosystem variables in Saginaw Bay, Lake Huron	107
5.2	Coefficient of variation of observations of three ecosystems variables in Moses Lake, Washington using three different sampling strategies.....	108
5.3	The coefficient of variation in the estimates of the numbers of several species of zooplankton using various sampling devices.....	109
5.4	Slope, intercept and R^2 for least squares analysis of eq. (5.7).....	115
5.5	Parameter values used in the simplified ecosystem	
5.6	Scenarios for nutrient loading rate and coefficient of variation of measurement evaluated in the first stage of the ecosystem models tests.....	123
5.7	Parameter set, θ , for Models I, II and III that were included in the estimation process	129
5.8	Characteristics of Model I for identifying correct hypothesis for nine scenarios of measurement error and nutrient loading.....	149
5.9	Characteristics of Model II for identifying correct hypothesis for nine scenarios of measurement error and nutrient loading.....	149
5.10	Characteristics of Model III for identifying correct hypothesis for nine scenarios of measurement error and nutrient loading.....	150
5.11	Values of parameters used in the complex ecosystem reference model	152
5.12	Characteristics of Model I for identifying correct hypothesis for six scenarios of measurement error and nutrient loading	173
5.13	Characteristics of Model II for identifying correct hypothesis for six scenarios of measurement error and nutrient loading	173
5.14	Characteristics of Model III for identifying correct hypothesis for six scenarios of measurement error and nutrient loading	174

CHAPTER 1

INTRODUCTION

1.1. Elements of Environmental Assessment

As the demands placed by modern civilizations on the natural environment increase, the need to understand and assess environmental impacts also grows. Fulfilling this need is possible only when the processes affecting the environment can be described by scientific laws or relationships, and the effects associated with these processes can be observed. Furthermore, it is useful to structure this knowledge within the framework of a scientific discipline. Given the existence of scientific laws or relationships and observable effects, systems analysis provides such a structure for performing assessments of environmental impacts. Defining an environmental system and the state of the system are fundamental components of this structure.

An environmental system is a specific segment of the environment which can be treated, in some sense, as a self-contained entity. It is assumed that this segment interacts with the rest of environment only through external driving forces (see Figure 1.1). The state of the system is defined by one or more qualities of the system that are measurable. The measurable qualities are called state variables. The boundaries of an environmental system in space, time, and number of state variables are determined by the scale of the processes for which the environmental assessment is being performed. Environmental systems can have global spatial scales, time scales of decades, and highly aggregated measures of the system state such as population, capital investment, pollution and natural resources (Forrester, 1969; Meadows and Meadows, 1972). They can be as small as a freshwater pond with times scales of hours or days and state variables that include chemical and biological constituents such as dissolved oxygen, nutrients and biomass.

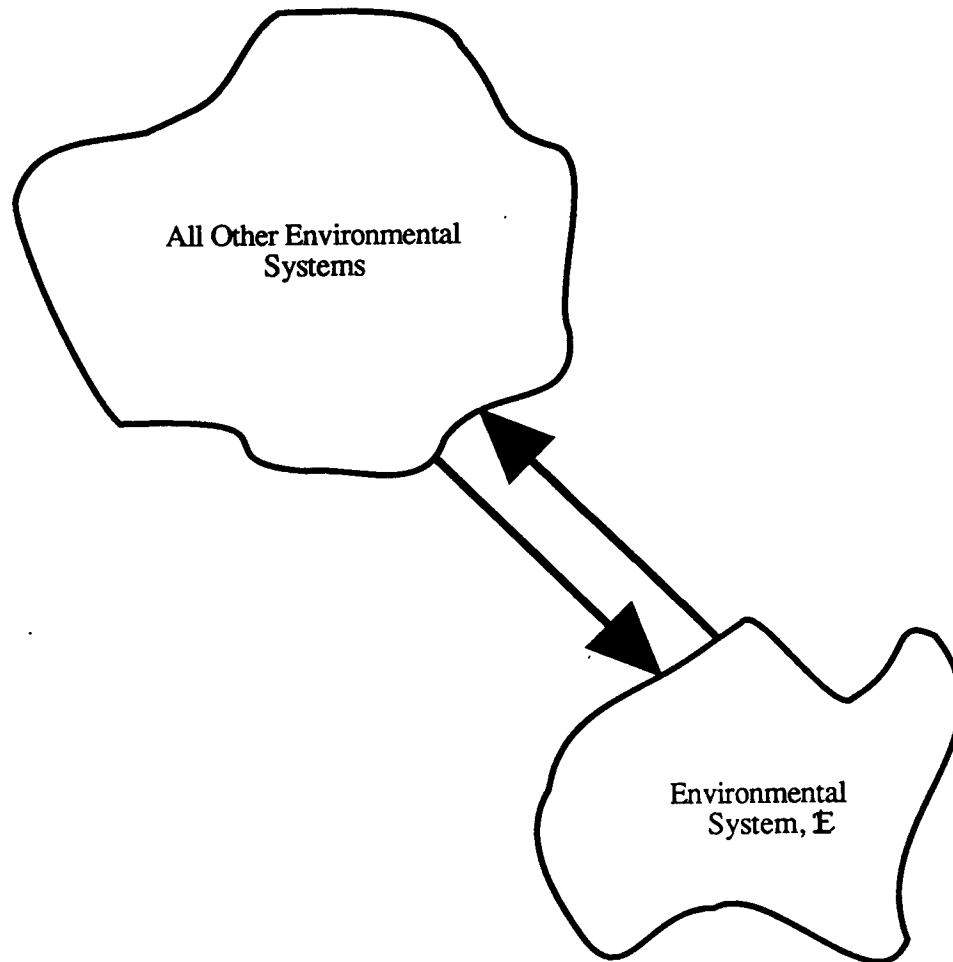


Figure 1.1. Schematic diagram showing idealized interaction between environmental system, \mathbf{E} , and all other environmental systems.

One way of characterizing or estimating both the state of environmental systems and the impact of human development on these systems is by making direct measurements of the system's state variables. Another way of obtaining such estimates is by constructing abstractions or models of the system based on physical, chemical, or biological laws. The existence of such laws implies that information about the process of interest has been obtained from prior observations of the system of interest or from other systems that behave similarly. These other systems may include both natural and controlled (laboratory) systems. Estimates of the system state variables can then be obtained from either the observations, the model, or some combination of the two.

For purposes of environmental assessment state estimates are used both to detect changes in the environment and to determine the forces or effects that have caused the changes. The state estimates are used to construct decision variables. Environmental assessment is accomplished by defining rules which can be applied to the decision variables for determining whether or not there has been an impact. The process can be characterized schematically as shown in Figure 1.2.

However, capital and human resources are needed for both the collection of data and the development of models. Those who develop programs to assess environmental impact must decide how the resources should be allocated to obtain the most information. Factors that must be included in the development of these programs include:

- The precision and accuracy of available measurement methods
- The amount of variability in the ecosystem, E , that can be explained by models derived from observations and known scientific laws or relationships
- The state of the knowledge of ecosystems structure
- The purpose of the assessment to which the model and data are being applied
- The costs or benefits associated with outcomes of the assessment

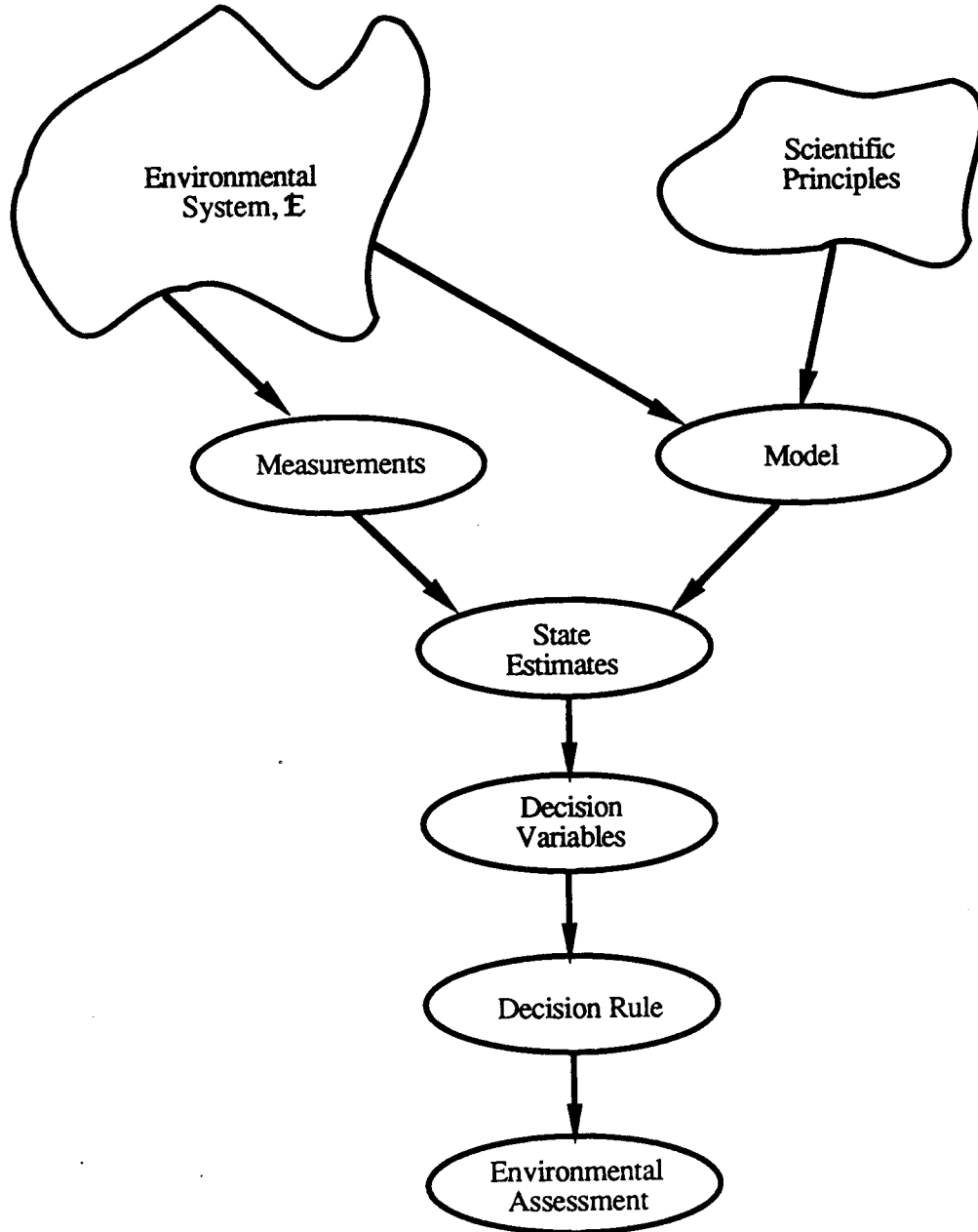


Figure 1.2. Flow diagram showing the way in which measurements of the environmental system, E , and scientific principles are used to make environmental assessments.

Recognizing that these are the important elements of environmental assessment, methods that can be used to characterize the worth of data and value of developing models of the ecosystem are needed.

1.2. Important Concepts

State estimation and hypothesis testing provide a framework for comparing the relative value of devoting resources collecting data versus developing more complex models. Estimates of the state of an environmental system are obtained by first identifying the measurable properties, the state variables. Their values, or levels, are determined by the initial conditions, the effects of driving forces, and the processes that result in change. Water temperature, for example, could be used as a state variable to characterize the thermal state of a water body such as a lake or reservoir (Fig. 1.3). At any specific point in time, t_s , the temperature, would summarize the effects of past inputs such as solar radiation, river inflow, and thermal discharges. A measurement of the temperature with some instrument, such as a thermistor, would be one way of obtaining an estimate of the system's thermal state. The mechanism by which the measurements are transformed to estimates of the temperature of the water body is called the measurement model.

If enough is known about the dynamics of the system in terms of physical, chemical and biological processes, it may be possible to construct a model that describes the evolution of the state variables in time. Such a model provides another means of obtaining an estimate of the system state and is called a process model. In the example of the thermal state of the lake, the laws of thermodynamics and knowledge of the lake's heat budget could be used to construct a model of the process describing the water

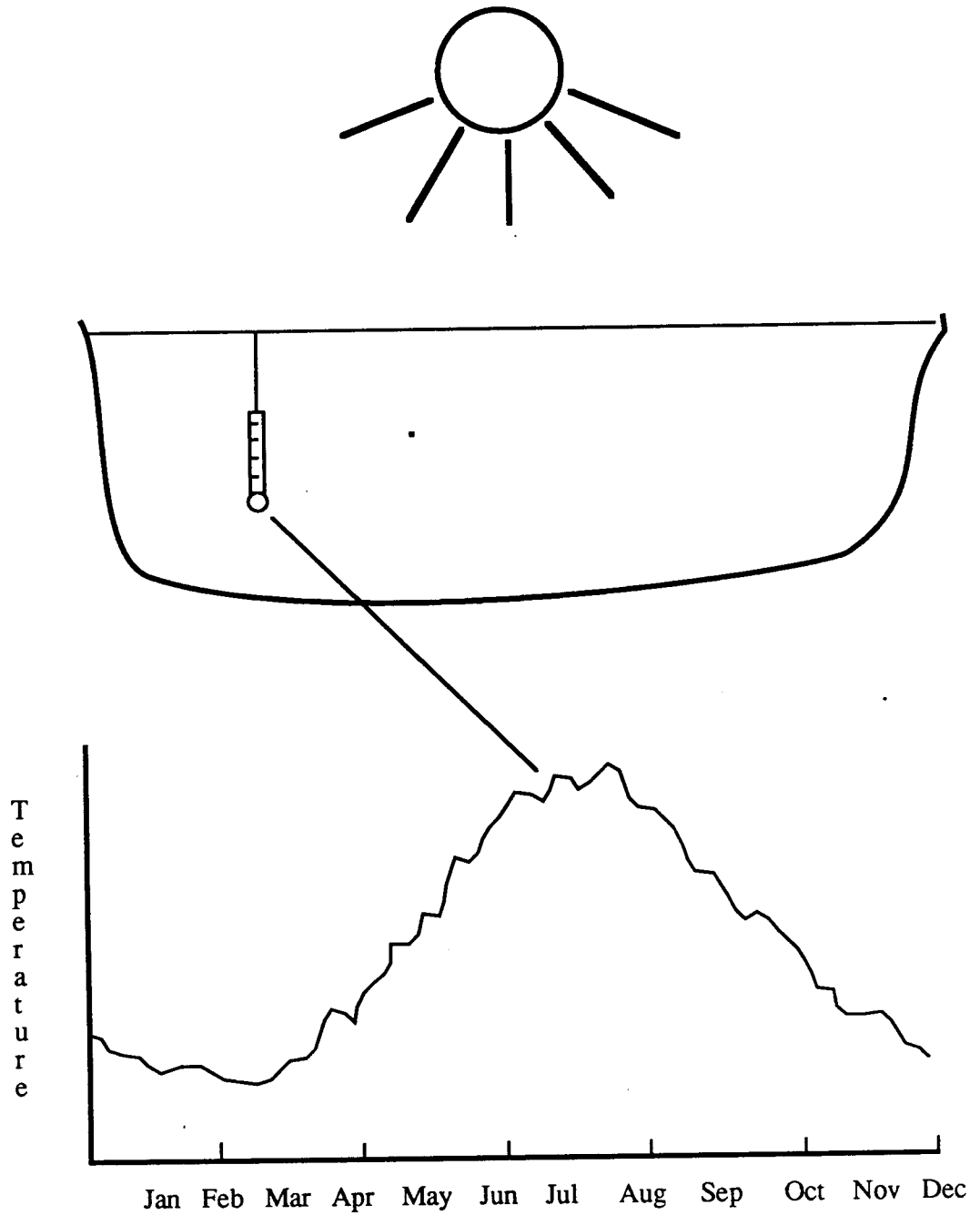


Figure 1.3. Temperature at an arbitrary location in a hypothetical lake as an example of an observable environmental state variable.

temperature as a function of time. The process model can be used to obtain estimates of the state variable, water temperature. Similarly, thermistors or thermometers could be used to measure of water temperature as a function of time. The measurement model would also provide an estimate of the state variable, water temperature. By combining the estimates obtained from both measurement model and process model it is possible to obtain state estimates for the present, past, or future. The definition of state estimates for each of these three cases have been defined as follows (Gelb,1974; Schweppe, 1973):

- Filtering: The time of the state estimate coincides with the time of the last observation (Fig. 1.4a).
- Smoothing: The time of the state estimate falls within the time span of the observations (Fig. 1.4b).
- Prediction: The time of the state estimate occurs after the last observation (Fig. 1.4c).

Filtering and smoothing are appropriate for diagnosing environmental impacts. That is, they can be used for analyzing observed changes in the state of the system before and after project implementation. Such estimates are important for determining compliance with environmental standards and assuring enforcement of environmental regulations.

Prediction, or estimating the state of an ecosystem at some time in the future, also plays an important role in environmental assessment. Determining the potential environmental impacts of proposed development scenarios, establishing permit limitations for waste discharges, and developing long-range environmental plans, are examples of the ways in which prediction is applied to environmental assessment. However, there is generally a high degree of variability in natural systems in addition to the uncertainties associated with environmental models. The variance in state estimates may increase rapidly as the interval between the time of the last observation and the time

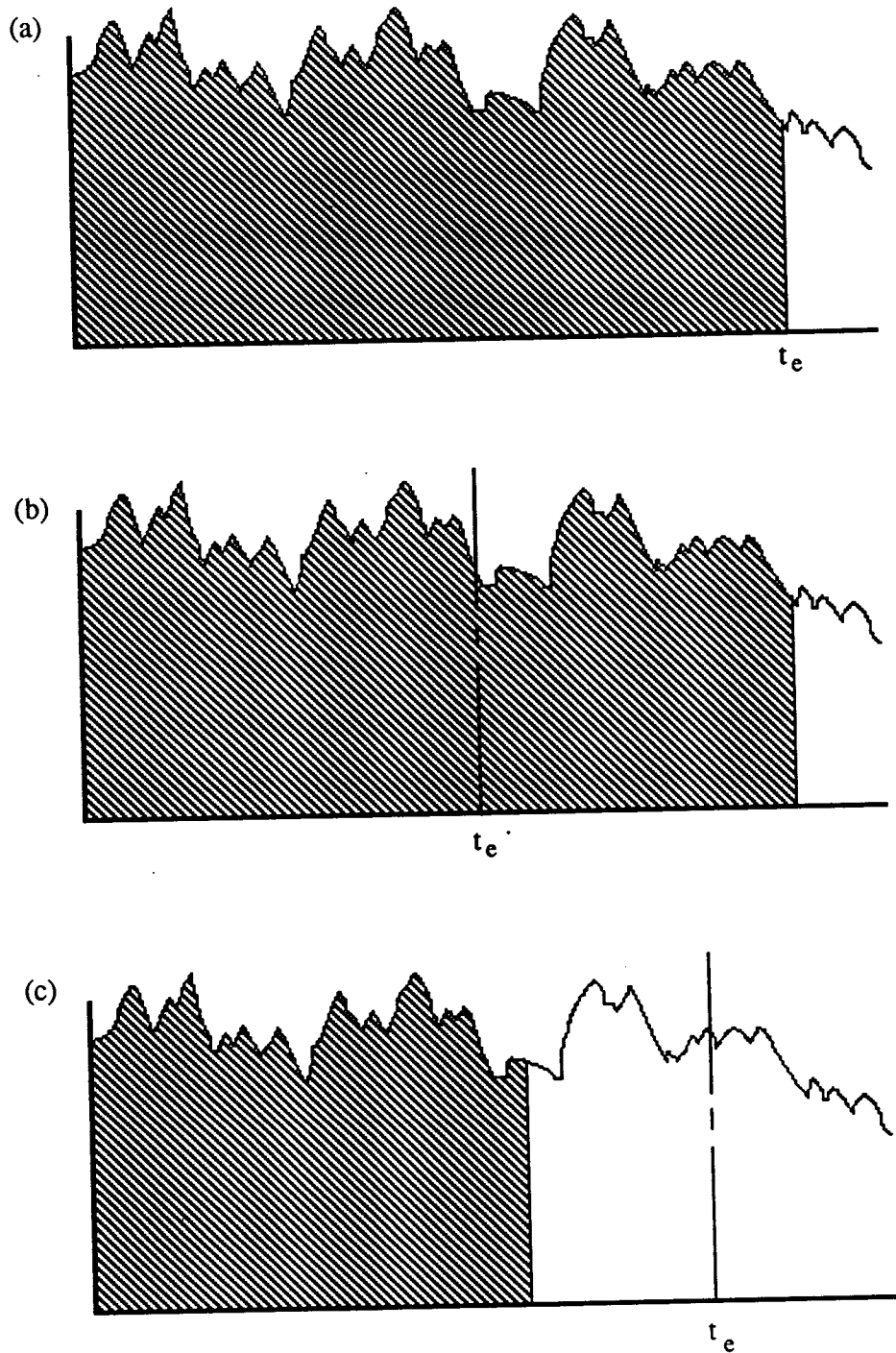



Figure 1.4. The three different types of states estimates at time, t_e : (a) filtering; (b) smoothing; and (c) predicting; for observations that span the time period shown by the shading: .

of the prediction increases. As a result, the accuracy of predicted state estimates may be limited. This has been a source of concern for both resource managers and environmental scientists. This concern has motivated analyses such as the one performed by McLaughlin and Wood (1988), who developed techniques for evaluating the accuracy of model predictions using a distributed parameter approach.

This work, however, will focus on diagnosis of environmental systems. More specifically, it will focus on state estimates obtained by filtering. Filtering gives an estimate of the present state by combine the present estimate of the state from the measurement model with the present estimate from the process model. Smoothing could also be used for diagnosis. However, filtering provides real-time estimates of the state and is much simpler to implement than smoothing. For the cases in which real-time estimates are not needed, it is not clear that the improved accuracy resulting from smoothing is great enough to warrant its implementation (Meditch, 1973).

The Kalman filter (Kalman, 1960; Kalman and Bucy, 1961) is a state estimation method for linear systems that integrates the measurement system model with a model of the process dynamics. The Kalman filter assumes the measurement and systems equations can be modeled by a structure of the form:

$$\dot{\mathbf{x}}(t) = \mathbf{F}(t)\mathbf{x}(t) + \mathbf{G}(t)\mathbf{w}(t) + \mathbf{B}(t)\mathbf{u}(t) \quad (1.1)$$

$$\mathbf{z}(t) = \mathbf{H}(t)\mathbf{x}(t) + \mathbf{y}(t) \quad (1.2)$$

where

$\mathbf{x}(t)$ = the vector of systems state variables¹

$\mathbf{u}(t)$ = the vector of known and deterministic inputs

$\mathbf{w}(t)$ = uncertain white input disturbance

$\mathbf{v}(t)$ = uncertain white observation disturbance

$\mathbf{z}(t)$ = the vector of observations

$\mathbf{F}(t)$, $\mathbf{G}(t)$, $\mathbf{B}(t)$ = the system coefficient matrix

$\mathbf{H}(t)$ = the measurement system coefficient matrix

The Kalman filter gives an estimate of the state of the system described by equations (1.1) and (1.2) for which the error of the estimate is unbiased and the sum of the squared error is a minimum. For these constraints, the filter determines, at each point in time, the weight that should be given to the estimate obtained from the system model

¹ The development follows the conventions of style and notation found in the works of Schweppe (1973) and Gelb (1974). Vectors are written as bold-faced, underlined, lower-case Greek or English letters. Matrices are written as bold-faced, upper-case Greek or English letters, while elements of matrices are the same Greek or English letters in plain text (not bold-faced or underlined) with subscripts. For example, an $(n \times 1)$ vector might be denoted by \mathbf{a} , while an $(n \times m)$ matrix would be denoted by \mathbf{A} . The elements of \mathbf{a} and \mathbf{A} would be written as a_i and A_{ij} , respectively. Script \mathcal{H} , \mathcal{L} , \mathcal{R} , \mathcal{T} (\mathcal{H} , \mathcal{L} , \mathcal{R} , and \mathcal{T}) are used to denote important variables in hypothesis testing. Script \mathcal{V} , with superscript, n , (\mathcal{V}^n) is an n -dimensional vector space. Subscripts associated with the state variables, probability distribution functions and hypotheses refer to a specific hypothesis. For example, the state variables, \mathbf{x}_j , are associated with the j^{th} hypothesis, \mathcal{H}_j .

(eq. (1.1)) compared to the weight given the estimate from the measurement model (eq. (1.2)). These weights are a function of the variance of the process model error, $\underline{w}(t)$, and the variance of the measurement model error, $\underline{v}(t)$. Because of the filter's elegant simplicity, it has been applied to a wide variety of problems. Under certain conditions, the Kalman filter can be applied to nonlinear problems by using linearization. The Kalman filter combines the models of the system process with observations to obtain an estimate of the system state as well as an estimate of the uncertainty of the state estimate. It is well suited for analyzing the relative importance of developing the process model compared to that of obtaining measurements of the system.

In the case of an environmental system for which there has been an intervention due to some form of development, determining whether or not the estimate of the system state represents adverse environmental impacts is often appropriate. Typically this is done by comparing the model (or models) that estimate the present system state with a model of the system under conditions of no intervention. The objective is to determine whether changes in the state of the system are due to random fluctuations or are a result of the interventions. Hypothesis testing provides a means to achieve this goal.

The first step in hypothesis testing is to establish two or more hypotheses about the process and measurement models that describe the state of the system. A decision variable and decision rule must then be developed (see Figure 1.2). A decision variable is one or more numbers derived from the estimates of the state for each hypothesis. The decision variables for each of the hypotheses are then compared by applying the decision rule to determine which hypothesis is true. The likelihood function is commonly used as a decision variable and, for state estimates defined in terms of filtering, it can be obtained from the output of the Kalman filter (Sage and Melsa, 1971; and Schweppe, 1973). The likelihood function is the joint probability of the vector of observations, $\underline{z}(t)$, for a given

hypothesis about the probability density function. For Gaussian processes, the natural logarithm of the likelihood function obtained from Kalman filter is the weighted sum of the squares of the difference between the observations at some time t and the expected value of the state at the time, t , conditioned on a previous observation at time $t' < t$. The log likelihood function is a statistic that can be used to test hypotheses regarding the state of the system.

The roles of model complexity and data worth are determined by the formulation of the Kalman filter. In equations (1.1) and (1.2) the number of state variables included in the vector, $\mathbf{x}(t)$ and the structure of the coefficient matrices, $\mathbf{F}(t)$, $\mathbf{G}(t)$, and $\mathbf{B}(t)$ determine the level of complexity. A common, though not necessarily correct, assumption is that increasing the level of complexity of the systems model leads to a reduction in the system error, $\mathbf{w}(t)$, and, as a result, yields better state estimates. The worth of data can be examined in terms of the magnitude of the the measurement error, $\mathbf{v}(t)$, and the structure of the observation matrix, $\mathbf{H}(t)$, in equation (1.2).

The concept of the reference system model is also used in this report. Though not directly related to the concepts of state estimation and hypothesis testing, it forms the basis for the experimental design. It is apparent from Figure 1.2 that observations obtained from the environmental system make up the essential elements of environmental assessment. Observations are necessary both for purposes of obtaining state estimates from the measurement model and for identifying process models. However, observations of environmental systems are generally expensive to obtain and the experiments are difficult to control. A reference system model (McLaughlin and Wood, 1988) is a mathematical construct of a system for which it is assumed the output represents the true population of system state variables. Samples from the output of the reference system model are treated as measurements of the system. In this report,

samples from the reference system model will generally be described as "synthetically generated observations."

The success of experiments that use reference systems models depends on how well the dynamics of the prototype system are known. Even when the dynamics are well known the assumption that the reference system model perfectly represents the true system is dangerous. Such a belief can lead to circular reasoning and incorrect conclusions regarding model validity. The reference system model should be viewed as a form of laboratory experiment that is not identical to the actual environmental system, but that attempts to capture important features of the prototype system. It is this latter view that provides the basis for using reference system models in this report.

1.3. Research Objectives.

The primary objective of the report is to respond to the need for methods that can be used to characterize the worth of data and value of developing models of the ecosystem. More specifically, the objective is to use state estimation and hypothesis testing to establish paradigms for:

- Testing the validity of environmental models
- Assess the contribution of measurement error and model complexity to detecting environmental change.

Case studies of two important environmental systems, the global carbon cycle and lake ecosystems, will be used to construct the paradigms. These systems were chosen for two reasons. Both are significant environmental issues and a great deal of effort has been devoted to understanding both systems. The global carbon cycle is an important environmental system because changes in atmospheric CO₂ due to the consumption of fossil fuels and terrestrial biota may have far reaching effects on the earth's climate

(Seidel and Keyes, 1983). The primary interest in lake ecosystems has been due to concern that accelerated rates of eutrophication can seriously impair lake water quality. The principal cause of accelerated eutrophication is the input of nutrients from anthropogenic sources associated with municipal, industrial, and agricultural activities (Vollenweider, 1968). For purposes of environmental assessment, resources are currently being committed to the design of monitoring programs and the development of process models for both of these environmental systems.

- Synthetically generated observations from the reference systems models will be a fundamental part of the analysis. The reservoir of knowledge about these systems provides a sound basis for the development of the reference system models. Based on the assumption that the reference systems models adequately describe the prototypes, the following are secondary objectives of the report:

- Assess the effects of measurement error and model complexity on the validity of models of the global carbon cycle and lake ecosystems
- Assess the effects of measurement error and model complexity on the ability to detect environmental changes in the two ecosystems

CHAPTER 2

LITERATURE REVIEW

This literature review will serve three purposes. First, it will assess the need for evaluating model complexity and data worth in environmental assessments. Second, it will characterize the range of environmental problems for which mathematical models have proven useful. Finally, it will survey methods which are appropriate for the analysis of model complexity and data worth.

2.1 Needs Assessment

The value placed on maintaining environmental quality in the United States is reflected in the major legislation passed by Congress during the past twenty years. The Clean Water Act, the Clean Air Act, the National Environmental Protection Act, and the Toxic Substance Control Act (TSCA) are examples of environmental laws which characterize the nation's environmental ethic. These laws have established requirements for evaluating the impacts of development before a specific project is undertaken, and the required assessments often involve mathematical modelling. A comprehensive list of Federal laws, the responses to which have utilized mathematical modelling, is given in Table 2.1.

The environmental assessments required by environmental laws fall into the following areas:

- Protection of human health
- Maintenance of the integrity of ecosystems
- Balancing environmental, economic, and political needs

Table 2.1. Federal laws associated with the application of mathematical models of environmental systems.

Clean Water Act (Public Law 95-217)	Sections 107, 201, 208, 209, 301, 302,303, 307,311,314,316, 404, and 405.
Toxic Substances Control Act (Public Law 94-469)	Sections 4, 5, and 6.
National Environmental Policy Act (Public Law 91-190)	Sections 102 and 103
Surface Mining Control and Reclamation Act (Public Law 95-87))	Sections 506, 510, and 515
Coastal Zone Management Act (Public Law 94-370)	Section 305
Safe Drinking Water Act (Public Law 93.523))	Sections 1412, 1421, 1422, 1424, 1443, and 1444
Resource Conservation and Recover Act (Public Law 94-580)	Sections 1008 and 8006
Endangered Species (Public Law 93-205)	Section 7
Soil and Water Conservation (Public Law 95-192)	Sections 5 and 6
Water Resources Planning (Public Law 89-80)	Section 102
Executive Order No. 11988 (Floodplain Management)	
Flood Control Act of 1936 and and Amendments	Sections 1, 2, and 3
National Flood Insurance Act of 1968	Section 73

Table 2.1 (continued). Federal laws associated with the application of mathematical models of environmental systems

Water Research and Development Act (Public Law 95-467)	Section 1360
Federal Reclamation Act of 1902 and Amendments	43 U.S.C. 421 and 422
Atomic Energy Act of 1954	10 CFR 20, 50, 61.
Clean Air Act (1977 as amended)	Sections 123, 165 and 320 Section 165 Section 320

Ott (1976) provides numerous examples of the ways in which environmental models have been used in support of environmental legislation.

Mathematical models have been also widely used in the development and implementation of environmental policies. The Office of Technology Assessment (Friedman et al., 1984), in a study of water quality modeling, concluded that mathematical models are sophisticated tools for analyzing water resource issues that significantly improve the basis for decision-making and can substantially reduce the cost of managing water resources.

Barnwell and Krenkel (1982) described the need for water quality models, within the context of environmental decision-making, in three management contexts: screening, planning, and design. They reviewed the application of screening models in several rivers, impoundments and estuaries and made some qualitative conclusions regarding their effectiveness. They concluded that for rivers and impoundments the results were fair to excellent, while in estuaries they were poor to excellent. They describe a

successful application of a sophisticated planning model by the Northern Virginia Planning District Commission (NVPDC). The NVPDC used the model, in conjunction with an extensive data collection program, to examine the long-term water quality impacts of land development patterns and best management practice strategies in the Occoquan River Basin. Barnwell and Krenkel (1982) state that the use of models in design is probably the most common application of water quality modeling in the United States. As an example, they describe the application of QUAL-II (Roesner et al., 1981) on the Holston River in Tennessee. The model was used to develop a permit under the National Pollution Discharge Elimination System (NPDES) which led to improved dissolved oxygen in the river.

Despite the optimism expressed by some, the use of mathematical models has often been criticized and challenged. Although some of this criticism has focused on the scientific basis for mathematical models (e.g., Harris, 1980), there is also much that is related to the fact that the development and application of models for environmental issues must be done at the interface between science and policy-making and management. With respect to issues not directly related to the scientific aspects of model development, Mitsch (1983) identified several reasons for failure of models to achieve the potential characterized in the OTA assessment:

- The propensity of models to continually get bigger and more complex; require more and more data; have poorly defined objectives, and be understood by only a few individuals
- Unrealistic expectations, on the part of water resources managers, regarding the kinds of problems models can solve with a given level of resources
- Overselling of the capabilities and potential for mathematical modeling.

The source for much of this criticism, according to Cale et al, (1983), is that there is no agreement on the best way to build, analyze, and evaluate mathematical

models. Cale et al (1983) state that the most important question is validation of ecological models, and the inability to construct valid models is a serious impediment to their acceptance.

Thomann (1982) describes two reasons for developing mathematical models of natural water systems. The first is to increase the level of understanding of cause-effect relationships, and the second is to use the knowledge to perform environmental analysis and provide support for decision-making. Thomann (1982) notes the increase in complexity of water quality models from the linear systems model describing the biological oxygen demand (BOD)-dissolved oxygen (DO) model developed by Streeter and Phelps (1925) to the multistate, nonlinear models used to simulate the interaction of physical, chemical, and biological systems in marine and freshwater systems such as the Water Quality Analysis Simulation Program (DiToro et al., 1981). Thomann (1982) concludes that this increase in complexity requires that careful attention be given to evaluating model credibility. He suggests four stages necessary for establishing the credibility of a model at a specific site:

- **Model development:** The specification of the model structure or model identification, based on knowledge of the physical, biological and chemical processes affecting the system. Model development also includes the estimation of the parameters comprising the model, as well as a description of the external inputs which drive the system. Model identification and parameter estimation should be based on prior information obtained from field studies and laboratory experimentation, independent of the site under consideration.
- **Model calibration:** The comparison of model results with data collected at the site under consideration to determine if the model provides reasonable simulations as initially formulated in Step 1. If model results do not compare well with observations, parameters and input are calibrated within limits suggested by similar studies reported in the scientific literature.
- **Model Verification:** The testing of the calibrated model is tested using a data set that is independent from that used to develop and calibrate the model. According to Thomann (1982), it is essential that the range of physical, chemical, or biological conditions for which the verification is valid be clearly stated. Thomann (1982) suggests a number of measures that might be appropriate for quantifying the degree of verification. These include regression

analyses, relative error, comparison of means using the t-test and the root mean square error.

- **Model post-audit:** Examination and verification of the model's predictive performance after it has been used to develop an environmental control program.

Thomann's (1982) work represents an attempt to formalize the process for establishing model credibility. However, he does not describe specific procedures for incorporating hypothesis testing nor does he deal specifically with the issue of the amount and quality of data necessary to develop accurate models.

2.2. Application of Models to Environmental Analysis

Models with varying levels of complexity have been developed for aquatic, atmospheric, and terrestrial ecosystems. Concern about atmospheric pollution on scales varying from hundreds of meters to global dimensions has led to the development of a number of models. The United States Environmental Protection Agency (EPA) uses a wide variety of diffusion/advection models to control the environmental effects of air pollutants such as sulfur dioxide, carbon monoxide, nitrogen oxides, and particulate matter (EPA, 1980a). The models are used to determine the emission rates of air pollutants such that the appropriate criteria for air quality are satisfied. These emission rates form the basis for permits issued under the Clean Air Act.

On a global scale, air quality models have been used for planning to avoid large-scale environmental effects resulting from increased atmospheric CO₂ (Seidel and Keyes, 1983). Concerns about global impacts on air quality have led to the development of models of atmospheric pollutants. Particular emphasis has been placed on characterizing the distribution of CO₂ in the atmosphere because of its effect on the earth's heat balance (Seidel and Keyes, 1983). Early efforts by Eriksson and Welander (1956), Craig (1957) and Revelle and Suess (1957) were rather simple models of the exchange of carbon

between the atmosphere, oceans, and the biosphere. Both Eriksson and Welander (1955) and Revelle and Suess (1957) concluded that anthropogenic sources of CO₂ were not contributing significantly to the levels of CO₂ in the atmosphere. More recently, the results of long-term observations by Keeling et al. (1976) have provided data for more complex models of the CO₂ interactions between atmosphere, oceans, and land biota (Bacastow and Keeling, 1973; Bjorkstrom, 1979; Bolin, 1977; Machta, 1978; Oeschger et al., 1975; Siegenthaler and Oeschger, 1978; Stuiver, 1978; and Woodwell et al., 1978). As a result of model development and the collection of data, the importance of anthropogenic sources, including consumption of fossil fuels and clearing of the tropical rain forests, has become better understood. The EPA (Seidel and Keyes, 1983), for example, has integrated an eight-compartment model of the global carbon cycle with an atmospheric temperature model (Hansen et al., 1981) to obtain preliminary estimates of the impacts of fossil fuel consumption on the global heat budget .

Much of the interest in mathematical models of water quality has been motivated by a concern for the impact of waste discharges on dissolved oxygen and temperature of both freshwater and marine environments. Mathematical models of dissolved oxygen have changed little in concept since the work done by Streeter and Phelps (1925). These concepts have been extended to the dissolved oxygen budgets of more complex systems, and expanded to include source/sink terms such as sediment oxygen demand, nitrogenous oxygen demand, algal respiration, and photosynthetic production of oxygen (O'Connor and DiToro, 1970). A great deal of effort has been devoted to obtaining consistent estimates of important rate constants (Zison et al., 1978) The major advances have been in the development of solution techniques which make possible the application of dissolved oxygen models to steady-state and time-dependent problems in rivers, lakes and estuaries (Crim and Lovelace, 1973; Johanson et al., 1976; Roesner et al., 1981).

Requirements for the analysis of thermal pollution emerged during the late 1950's as attention focused on the effects of cooling water discharges (Edinger and Geyer, 1965) and impoundments (Raphael, 1962) on the temperature regimes of rivers, lakes, and reservoirs. These first temperature models were based on heat-budget techniques (Wunderlich and Gras, 1967) formulated in terms of linear first- or second-order differential equations and did not require complex solution techniques. The temperature models have since been extended to include more complex environments. The increase in complexity has, however, been primarily associated with expanding the methods to include time-dependence and variability in three spatial dimensions rather than significant changes in heat transfer (Isaji and Spaulding, 1981)

Application of the principles of conservation of mass expressed in differential form have also been used by ecologists (Riley et al., 1949; Riley, 1965; Steele, 1965; Lotka, 1956) to describe structure and productivity of ecosystems. Temperature and dissolved oxygen have important roles in biological systems. It is not surprising that these models of biological systems would be combined with models of temperature, dissolved oxygen, and nutrients as complex ecosystems models. Chen's (1970) conceptual model is one of the first examples. Others, similar in concept, are those of DiToro et al., 1975; DiToro and Matystik, 1980; Baca et al., 1973; Scavia and Park, 1976; Behrens et al., 1975; and Water Resources Engineers, Inc., 1975). These models are all linear in terms of the state variables. However, they all incorporate non-linear growth-limiting functions, generally in the form of Michaelis-Menten kinetics, into the model structure.

Complex models of terrestrial ecosystems have evolved at a rate similar to those associated with aquatic ecosystems. As a result of the International Biological Program, for example, compartmental models were developed for several complex ecosystems

including the Grassland Biome (Innis, 1975), the Eastern Deciduous Biome (Goodall, 1975), the Tundra Biome (Miller et al., 1975) and the Coniferous Forest Biome (Overton, 1975).

A difficulty common to all mathematical models is that the amount of on-site or laboratory data required to verify model structure and estimate model parameters can be prohibitive. Friedman et al., (1984), for example, report that the federal government alone spends approximately \$50 million per year on water-related mathematical models. Furthermore, there is no systematic approach for determining the improvement in accuracy that would result from increasing (or decreasing) the complexity of models.

2.3. Survey of Appropriate Methods

2.3.1. State Estimation

Assessing environmental change can be considered a problem in state estimation. According to Gelb (1974), the purpose of state estimation is to obtain an estimate of the state of a system from knowledge of system dynamics, measurement error statistics, and *a priori* information about the initial state of the system. As noted in Chapter 1, there are three types of estimation problems: (1) filtering, or estimating the state at the time of the last observation; (2) smoothing, or estimating the state of a system at a time prior to the last observation; and (3) prediction, or estimating the state of a system after the last observation.

The work of Kalman (1960) and Kalman and Bucy (1961) provides the theoretical basis for the most widely used state estimation method, the Kalman filter. The Kalman filter provides unbiased estimates of the state variables under conditions of minimum variance. It also provides estimates of the variance of the difference between the estimated state and the true state. The filter is based on the assumption that the system

model is linear. Optimal estimation for linear systems has been extended to the more general nonlinear case by applying first- or second-order Taylor expansions to the nonlinear equations. The extended Kalman filter (EKF) and the linearized Kalman filter (Gelb, 1974) are examples of Taylor series approximations used for minimum variance estimators. While these approximations expand the scope of applications for state estimation methods, they also introduce some difficulties associated with stability and reliability of model error estimates (Lettenmaier and Burges, 1975; Bowles and Grenney, 1978)

A number of applications of filtering to the design of aquatic monitoring programs have been reported. Moore (1971) used the EKF to find the optimal space/time distribution of sampling for a river in which the water quality constituents of interest included temperature, zooplankton, phytoplankton, nitrate, nitrite, ammonia, phosphate, and total dissolved solids. Moore et al. (1976) developed monitoring strategies for the National Eutrophication Survey with an EKF design developed from a simplified nonlinear eutrophication model. Moore et al.'s (1976) work described hypothetical trade offs between sample uncertainty and sampling frequency. Dandy and Moore (1979) applied state estimation methods to the examination of both short-term (standards violations) and long-term (water quality assessment) problems. Kitanidis et al. (1978) have also described application of the Kalman filter to detection of standards violations. Canale et al. (1980) described a Kalman filter method for obtaining an optimal monitoring strategy for lake eutrophication problems. Although Canale et al. (1980) were able to use the method in a limited way, they concluded that computational burdens associated with its implementation were too great for practical applications of the method.

Lettenmaier (1975) formulated the EKF for a steady-state water quality model that included such constituents as dissolved oxygen (DO), biological oxygen demand (DO),

inorganic nitrogen, inorganic phosphorus, temperature, and coliform bacteria. The purpose of his study was to find the space/time tradeoff for sampling that would maximize the power of detecting long-term linear trends or step increases. The filter provided the spatial distribution of the estimation error. After the natural error was added to the estimation error, the resulting variance was used to estimate the power of detecting a trend as a function of effective independent sample size. For a fixed number of samples per year, the optimal sample station locations were obtained using a weighted spatial average of this power. The weighting factors were included so that the relative importance of various water quality constituents could be considered.

A number of researchers have used state estimation techniques for estimating model parameters. Beck and Young (1976) used the EKF to quantify the dynamics of algal oxygen production in a DO/BOD model of the Cam River. Bowles and Grenney (1978) and Constable and MacBean (1979) also used the EKF to analyze DO in rivers. They estimated the rate constants for BOD, DO, and nitrification, as well as the state variables and variance of the state estimates. Koivo and Phillips (1971; 1972; 1976) used the EKF to obtain optimal estimates of several parameters in a DO/BOD model of rivers. Loaiciga and Marino (1985) used an approach based on the Kalman filter to obtain parameter estimates and develop stochastic controls for reservoir operation.

These studies have provided a great deal of insight into the design of monitoring programs. Some of them, as discussed above, have had parameter estimation as an objective. However, they have all assumed a known and fixed level of system structure and complexity. Since the Kalman filter formulation includes both the process and measurement dynamics, it is, as suggested by Lettenmaier (1975), a logical tool for examining model complexity, as well as for monitoring design.

2.3.2. Hypothesis Testing

The value of increasing model complexity can be judged quantitatively by making hypotheses about models and then testing the validity of the hypotheses. For the analysis of environmental impact, the Analysis of Variance (ANOVA) has been the classical way of testing hypotheses (see, e.g., McKenzie et al., 1977) using Neyman-Pearson theory. The models used for ANOVA are limited to testing for changes in means and the interactions of means. The Kalman filter makes it possible to apply hypothesis testing to estimates of states that change with time. Sage and Melsa (1971) have developed a methodology for using the Kalman filter to assess model validity based on hypothesis testing. In their method, the Kalman filter is used to describe the time trajectory of the likelihood function. When the state variables are generated by a Gaussian process the ratio of the likelihood function for the alternate hypothesis, \mathcal{H}_1 , and that of the null hypothesis, \mathcal{H}_0 , provides a sufficient statistic for testing. Sage and Melsa (1971) and Schweppe (1973) show how the methodology can be used to determine when the difference between two models of a system can first be detected. Willsky and Jones (1976) have applied the method with success to certain aerospace problems. Although problems of dimensionality (Lettenmaier, 1979) impose a limit on the size of the system to which the Kalman filter can be applied, the method does have promise for applications to the detection of environmental changes.

2.3.3. Analysis of Complex Systems

One of the primary goals in ecological modeling is to obtain an understanding of environmental systems. Implicit in this goal is the assumption that increased complexity necessarily leads to a better model of the system. Increasing complexity makes it possible to examine the way in which scientific assumptions affect systems dynamics,

but it is not necessarily of practical benefit for assessing environmental impact. This is particularly true if all portions of the system are not strongly coupled or if aggregating the dynamics of certain compartments will provide an appropriate description. Furthermore, estimation of model parameters becomes more costly and less certain as model complexity increases. Godfrey (1983), for example, states that parameters can be estimated for no more than three simply connected compartments, even with noise-free measurements. Increasing complexity may or may not improve model accuracy, but it does increase costs. These costs are associated with obtaining correct estimates of model parameters and determining model structure. Optimal model complexity is a function of the marginal increase in accuracy and the marginal cost of system identification and parameter estimation.

For complex electrical, mechanical, economic, and social systems, a number of methods for reducing complexity have been developed. Jamshidi (1983) characterizes time-domain methods as being either aggregation or perturbation methods. For linear systems, many of the aggregation methods are based on knowledge of the systems characteristics. These characteristics can be described in terms of the eigenvalues of the system. For a system with n independent eigenvalues, described by the equation:

$$A\mathbf{x} = \dot{\mathbf{x}}$$

where,

$A = n \times n$ coefficient matrix

$\mathbf{x} = n \times 1$ vector of states

$\dot{\mathbf{x}} = n \times 1$ vector of the time derivatives of the states

the system response will be a linear combination of the eigenvectors associated with each of the eigenvalues. For some driving forces, some number $m < n$ of the eigenvectors may be the dominant contributors to the system response. Davison's (1966) has developed a method for obtaining solutions in which dominant modes are retained. The ratio of the responses of the retained modes is the same in the reduced system as in the complete system. Aoki (1968) has also shown that methods such as Davison's (1966) are a forms of aggregation. Litz (1982) has expanded Davison's method by developing a method which minimizes the error resulting from neglecting the nondominant modes. These methods require initial knowledge of the eigenvalues of the system, which can be difficult to determine for a large, complex system. The aggregation methods have been applied to a number of economic problems and the dominant modes methods have been used in the application to mechanical and electrical systems. Although there has been some interest in the effect of aggregation on ecosystem analysis (e.g., O'Neill and Rust, 1979), the techniques described in this section have apparently not been previously applied to environmental systems.

Perturbation methods can be applied to both linear and nonlinear systems models when the system can be separated into parts that respond at different time scales. In the simplest case, such a system has two modes, called a fast mode and slow mode, respectively. The fast mode responds at a time scale of t_f , while the slow mode responds at a time scale t_s that is much greater than t_f ($t_s \gg t_f$). If the slow part of the system is only weakly connected to the fast part then the two systems can be uncoupled and solved, approximately, as separate systems (Milne, 1965). If the fast and slow modes are not weakly coupled then the singular perturbation method can be applied (Kokotovic et al., 1976). For small times, $t \cong t_f$, the slow modes can be considered to be at their initial values and only the fast modes are included in the solution. For large times, $t \gg t_f$, the

fast modes can be considered to have reached steady-state values and only the slow modes are considered. Mahmoud (1982) has extended the perturbation method to allow separation of a complex system into n modes and discusses the specific case when $n=3$ (slow, medium, and fast modes).

DeCaprariis (1984) has used perturbation analysis to separate the fast and slow variables in a lake ecosystem model. He then used stochastic analysis to describe the autocorrelation function of the fast variables, transformed the problem into the frequency domain, and concluded from an examination of the functional form of the variance spectrum that the need for a complex model increased as the eutrophic level of the system increased. De Caprariis' method is not quantitative but suggests that examining the frequency domain is another way in which to approach the question of model complexity.

The concepts described in the papers above are appropriate for the analysis of complex systems and have been applied to electrical, mechanical, economic, and ecological systems. Another approach that ecologists have taken is to characterize ecosystems structure in terms of qualities such as resilience and stability (Hannon, 1973; Finn, 1976; Webster et al., 1975; Carney et al., 1981; Turner and DeAngelis, 1982). These techniques are generally appropriate for linear systems only. System eigenvalues are the basis for the way in which indices are determined and, therefore, can be related to the order reduction methods discussed above.

The techniques for aggregation will be applied to the analysis of the complexity of linear systems in the study of the global carbon cycle (Chapter 4). The methods for nonlinear systems are not as well developed as the ones for linear systems. Therefore, the analysis of complexity for the nonlinear lake ecosystems models will rely on ad hoc techniques.

2.3.4. Monte Carlo Method

The primary emphasis in this study is on state estimation and hypothesis testing. However, observations are needed to test and demonstrate the methods. Long-term, comprehensive data sets for ecosystems are rare. The data that are available are often archived in a form not easily adapted to use by those not involved in the data collection. The choice in this study has been, therefore, to rely on observations generated by Monte Carlo simulations. By doing so, the quality of data and the frequency of sampling can be controlled.

The method has proven useful in hydrology (Salas et al., 1980), and there are numerous examples of the application of Monte Carlo methods to ecosystems analysis. Ward and Vanderholm (1973) used Monte Carlo simulation in conjunction with a dispersion model for conservative constituents. They used the simulated observations to develop cost effective monitoring designs for detecting spills and for detecting long-term water quality trends. Heidtke and Armstrong (1979) used data from Monte Carlo simulations to design a monitoring program for detecting violations of water quality standards for chlorides.

In another kind of application, Fedra (1980; 1982) and Fedra et al. (1981) evaluated model accuracy and uncertainty in a model of lake eutrophication. The results were used to determine the range of parameter values that satisfied a set of constraints developed from actual observations. Hornberger and Spear (1980), Hornberger (1980) and Scavia et al. (1981) used simulation methods to describe uncertainty in the estimates of DO, BOD, DO productivity, nutrient balance, and algal population dynamics. Gardner et al. (1980) examined six different formulations of a simple predator-prey ecosystem with Monte Carlo methods. Tiwari and Hobbie (1976) and Tiwari et al. (1978) examined

the effect that randomness in initial conditions, model parameters and forcing functions had on ecosystems models.

2.4. Summary

As the need for quantitative description of ecosystems increases, there is a corresponding increase in the need for methods of testing model validity of these models and for assessing the amount of information obtained from such models. A variety of techniques have been developed that are appropriate for these purposes, most of which have been applied to electrical or mechanical systems. The literature review, however, has revealed no comprehensive methods which have been applied to ecosystem models.

CHAPTER 3

DESCRIPTION OF METHODOLOGY

State estimation and hypothesis testing are the methods which will be used to characterize the worth of data and value of developing models of the ecosystem. This chapter outlines the way in which these methods can be applied to testing model validity and making environmental assessments.

3.1. State-Space Structure

The methods described in this work are developed within the framework of state-space models of environmental systems. The use of state-space models gives the method a considerable generality because state-space models have been applied to a wide variety of environmental analysis. Systems with state-space structure are those for which there is a relationship between the input and output of a system (Fig. 3.1; Lewis, 1977). For linear systems this can be described (after Schweppe, 1973) as:

Discrete time

Process model:

$$\mathbf{x}((n+1)\Delta) = \Phi(n\Delta) \mathbf{x}(n\Delta) + \Delta\Gamma(n\Delta) \mathbf{u}(n\Delta) + \Delta\mathbf{B}(n\Delta) \mathbf{u}(n\Delta) \quad (3.1)$$

Measurement model:

$$\mathbf{z}(n\Delta) = \mathbf{H}(n\Delta) \mathbf{x}(n\Delta) + \mathbf{v}(n\Delta) \quad (3.2)$$

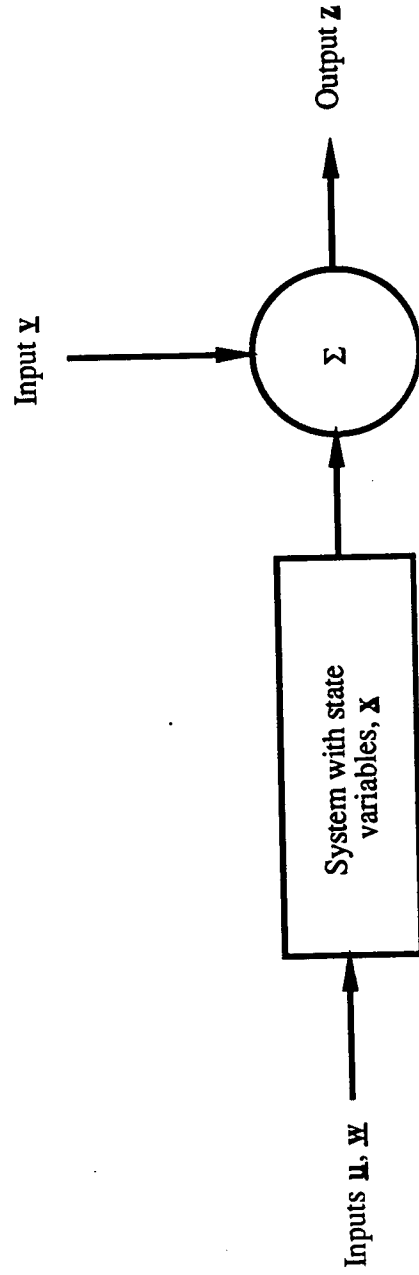


Figure 3.1. Relationships between the state variable, inputs and outputs in a system described by state-space structure.

Continuous time

Process model:

$$\frac{d}{dt} \mathbf{x}(t) = \mathbf{F}(t) \mathbf{x}(t) + \mathbf{G}(t) \mathbf{w}(t) + \mathbf{B}(t) \mathbf{u}(t) \quad (3.3)$$

Measurement model:

$$\mathbf{z}(t) = \mathbf{H}(t) \mathbf{x}(t) + \mathbf{v}(t) \quad (3.4)$$

where

\mathbf{x} = the vector of the true state of the system

\mathbf{u} = a known input vector

\mathbf{w} = the random input vector for the system, with a zero mean and covariance, $\mathbf{Q}(n)$

\mathbf{v} = the random input vector error for the measurement model, with a zero mean and covariance, $\mathbf{R}(n)$

\mathbf{z} = the vector of outputs

t = time

Δ = time increment (in the work that follows, $\Delta = 1$, without loss of generality)

n = number of time increments

Φ, Γ, Λ = the system coefficient matrices in discrete time

$\mathbf{F}, \mathbf{G}, \mathbf{B}$ = the system coefficient matrices in continuous time

\mathbf{H} = the measurement system coefficient matrix

For nonlinear systems, the corresponding models are given by

$$\underline{\mathbf{x}}(n+1) = \Phi[\underline{\mathbf{x}}(n), \underline{\mathbf{w}}(n), \underline{\mathbf{u}}(n), n] \quad (3.5)$$

$$\underline{\mathbf{z}}(n) = \mathbf{H}[\underline{\mathbf{x}}(n), n] + \underline{\mathbf{y}}(n) \quad (3.6)$$

for discrete time, and

$$\frac{d\underline{\mathbf{x}}(t)}{dt} = \mathbf{F}[\underline{\mathbf{x}}(t), \underline{\mathbf{w}}(t), \underline{\mathbf{u}}(t), t] \quad (3.7)$$

$$\underline{\mathbf{z}}(t) = \mathbf{H}[\underline{\mathbf{x}}(t), \underline{\mathbf{y}}(t), t] \quad (3.8)$$

for continuous time. \mathbf{F} and \mathbf{H} are known nonlinear functions.

Given these mathematical descriptors, consider a specific interval of time, T_t , for a system with p state variables, $\underline{\mathbf{x}}$, q output variables, $\underline{\mathbf{z}}$, and r forcing functions, $\underline{\mathbf{u}}$. The state variables span the state space, \mathcal{V}^p , the output variables span the output space, \mathcal{V}^q , and the forcing functions span the control or input space, \mathcal{V}^r . The matrices, \mathbf{F} , \mathbf{G} , \mathbf{F} , and \mathbf{G} are of dimension $q \times q$, the dimension of \mathbf{B} is $q \times r$, and the dimension of \mathbf{H} is $q \times p$. The vector $\underline{\mathbf{w}}$ is of dimension $q \times 1$ and the dimension of the vector $\underline{\mathbf{y}}$ is $p \times 1$. The concept of a state implies that when the value of the state variables in the space, \mathcal{V}^p , is known at time, t_0 ($t_0 \in T_t$), the response of the system for $t \in T_t > t_0$ can be found for any given input in the space, \mathcal{V}^r . The matrix \mathbf{H} transforms $\underline{\mathbf{x}}$ into $\underline{\mathbf{z}}$ in the absence of a random forcing vector, $\underline{\mathbf{y}}$.

The state-space structure formulated above is quite general and has been applied to a wide variety of electrical, mechanical, economic and social systems, as well as ecosystems analysis. The analysis will be made specific to the problem of interest, namely state estimation, by choosing $\underline{\mathbf{x}}$ as the vector of environmental state variables, $\underline{\mathbf{z}}$

as the vector of measurements of the state variables, \underline{w} as the vector of random errors in the process model, and \underline{y} as the vector of errors associated with the measurements. In general, observations are made at discrete intervals in time. Therefore, for most purposes, it is convenient to formulate the system equations in terms of discrete time. In the discussion that follows only equations (3.1) through (3.2) and (3.4) through (3.6) are necessary for the analysis.

3.2. Hypothesis Testing

The purpose of environmental assessment is to determine if there is a change in the environmental system of interest. Given that there is a change, it is generally important to determine the cause of the change. This can be accomplished by stating the problem in terms of various hypotheses about system behavior, then establishing test procedures for deciding which hypothesis is correct. The test procedure is based on a decision variable developed from the system. Within the context of hypothesis testing, this decision variable is generally a test statistic. For the j^{th} hypothesis, the test statistic has a particular probability distribution p_j when the hypothesis \mathcal{H}_j is true (see Figure 3.2). Observations of the test statistic are used to determine the likelihood that one of the hypotheses is true, that is, it is producing the observations.

In general there can be M hypotheses. However, in this study, as in most applications of hypothesis testing, the testing will be of a binary nature, with a null hypothesis, \mathcal{H}_0 , and an alternative hypothesis, \mathcal{H}_1 . The performance of the test can then be characterized by the probability of making one of two kinds of error, commonly characterized as Type I and Type II error. Type I error is the probability of rejecting the null hypothesis, \mathcal{H}_0 , when it is, in fact, true. Type II error is the probability of accepting the null hypothesis, \mathcal{H}_0 , when it is false. The Type I error probability, α , has

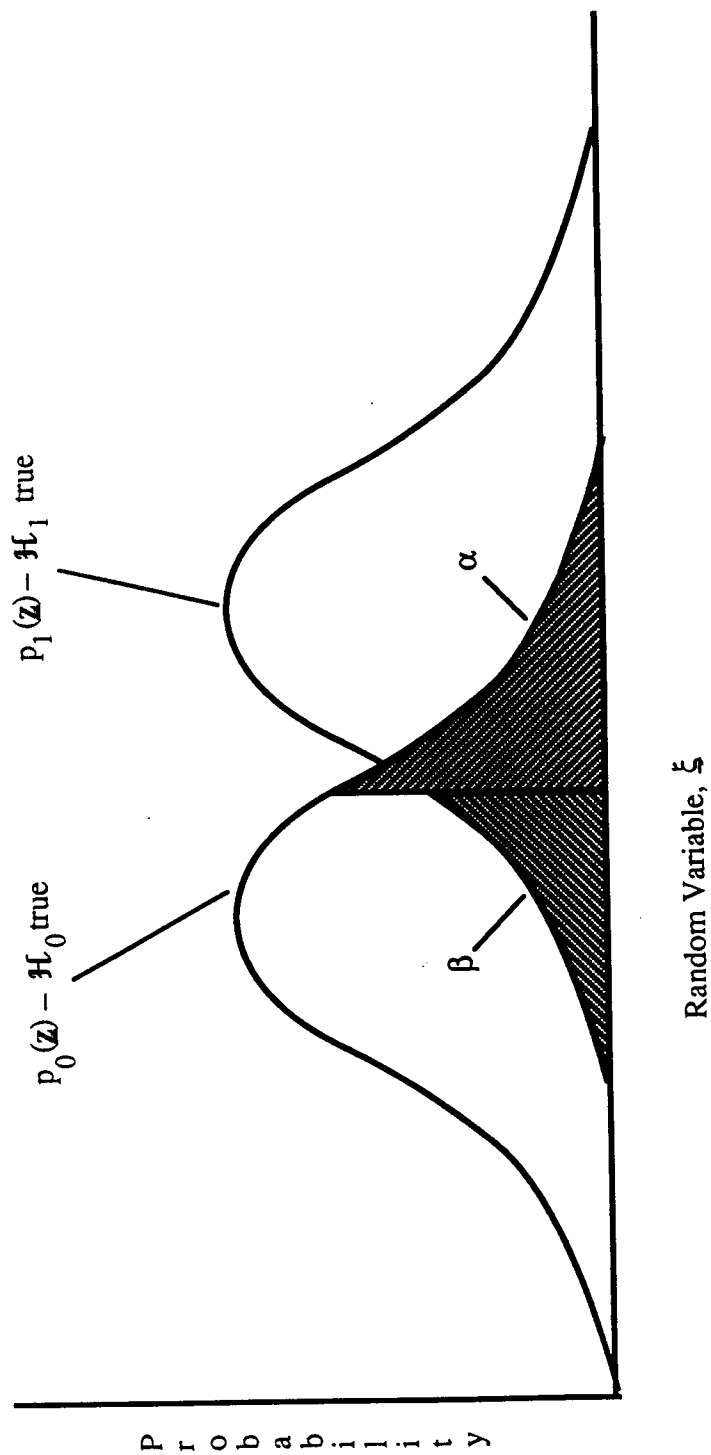


Figure 3.2. Distribution of the random variable, ξ , under the null hypothesis, \mathcal{H}_0 , and alternative hypothesis, \mathcal{H}_1 , showing Type I error, α , and Type II error, β .

also been called the probability of a false alarm (Sage and Melsa, 1971) or producer's risk (Larsen and Marx, 1981). Type II error probability, β , has been called the probability of a miss, or consumer's risk. The power of a test, $1 - \beta$, is the probability of rejecting the null hypothesis, \mathcal{H}_0 , when the alternative hypothesis, \mathcal{H}_1 , is true.

The hypothesis testing is done by constructing a set of rules (Ghash, 1970) which use the data to accept or reject the validity of the j^{th} hypothesis, \mathcal{H}_j . The rules can be formulated in terms of two different types of sample designs. One is a fixed sample design in which the hypothesis test is performed on a fixed number of observations. The other, which is of interest here, is that of sequential design.

Given a fixed sample design with a sample size N , the standard way of formulating the problem is to develop a test for \mathcal{H}_0 against \mathcal{H}_1 which minimizes the probability of Type II error, β , when the probability of Type I error, α , is less than or equal to some preassigned value. Traditional applications of hypothesis testing (e.g., McKenzie et al., 1977; Thomas et al., 1978), such as ANOVA, are formulated in this way. Testing of this kind has formed the basis of most monitoring program designs for purposes of assessing environmental impact. In these cases the hypotheses are stated in terms of conditions before and after an expected change. This approach is data intensive and usually site-specific. In addition, the application of classical parametric methods using fixed sample designs, such as ANOVA, can lead to incorrect conclusions if all the statistical assumptions are not met (Millard et al, 1985).

In many cases, however, more efficient sample designs can be obtained by using sequential analysis as proposed by Wald (1947) and further developed by Van Trees (1959) and Sage and Melsa, (1971). The sequential test is formulated by dividing the sample space into three mutually exclusive regions (see Figure 3.3), \mathcal{R}^0 , \mathcal{R}^1 and \mathcal{R} , where each \mathcal{R} spans an m -dimensional space of observations. The boundaries between

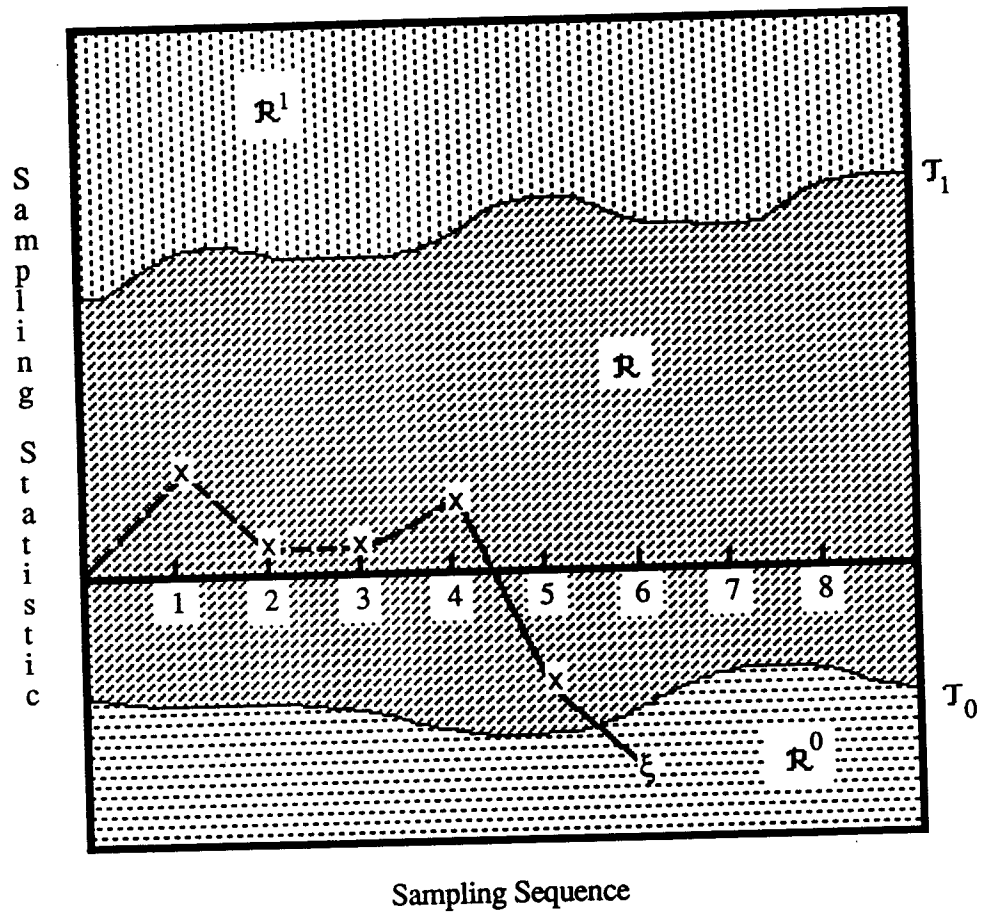


Figure 3.3. Schematic diagram of hypothesis testing for a sequential test. The test is performed at each point in the sequence (x). Testing continues as long as the point remains in the sample space, \mathcal{R} , and ceases when it enters either \mathcal{R}^0 or \mathcal{R}^1 . The upper and lower thresholds are T_0 and T_1 , respectively.

the regions are determined by the thresholds \mathcal{T}_0 and \mathcal{T}_1 . An observation of the system is made at time, $K = 1$ and the decision variable is computed. If the decision variable for the first observation is in \mathcal{R}^0 , the hypothesis test \mathcal{H}_0 is accepted. If it lies in \mathcal{R}^1 , the hypothesis \mathcal{H}_0 is rejected (\mathcal{H}_1 accepted). If the decision for the first observation is in \mathcal{R} , a second sample is taken ($K = 2$) and the process is repeated. The process continues ($K = 3, \dots, N$) until either \mathcal{H}_0 or \mathcal{H}_1 is accepted.

The two basic quantities required in hypothesis testing are a decision function and decision rule (Schweppe, 1973). The decision function converts the observations into one or more numbers (statistics) and the decision rule provides a structure for making a decision based the output from the decision function. Wald (1947) defined the decision function for sequential testing in terms of the likelihood function. Given a set of N observations, \mathbf{z} , the likelihood function, \mathcal{L}_j , is the joint probability of z_1, z_2, \dots, z_N , given that the j^{th} hypothesis is true. It can be expressed as

$$\mathcal{L}_j = p_j(z_1) p_j(z_2) p_j(z_3) \dots p_j(z_N) = \prod_{t=1}^N p_j(z_t) \quad (3.9)$$

where $p_j(\mathbf{z}_N) = p_j(\mathbf{z}_N | \mathcal{H}_j)$ is the probability density function of the random vector \mathbf{z}_N , given the j^{th} hypothesis

$$\mathcal{H}_j : \mathbf{z}_N = \mathbf{z}_{Nj} \quad (3.10)$$

The likelihood function can be developed for multiple hypotheses for which sequential tests can be performed. In this work, however, only binary tests will be considered ($j=0,1$). The decision function proposed by Wald (1947) is the ratio of the the likelihood functions, $\mathcal{L} = \mathcal{L}_1/\mathcal{L}_0$. The decision rule requires two thresholds, an upper threshold, \mathcal{T}_1 ,

for deciding when to choose the alternate hypothesis, \mathcal{H}_1 , and a lower threshold, \mathcal{T}_0 , for deciding when to choose the null hypothesis, \mathcal{H}_0 . Based on this formulation of the decision function and decision rule, the process can be stated as:

- Take a sample at $k=K$ and compute the likelihood ratio, \mathcal{L} .
- Accept \mathcal{H}_0 if $\mathcal{L} < \mathcal{T}_0$ and terminate sampling.
- Accept \mathcal{H}_1 if $\mathcal{L} > \mathcal{T}_1$ and terminate sampling.
- Increment K and return to Step 1 if $\mathcal{T}_0 < \mathcal{L} < \mathcal{T}_1$.

The thresholds, \mathcal{T}_0 and \mathcal{T}_1 , can be related to the Type I error, α , and the Type II error, β , by the following argument. Consider first the case when a sample is taken at time $k=K$ and results in the condition that the likelihood ratio, \mathcal{L} , is equal to the threshold, \mathcal{T}_1 . That is

$$\mathcal{L} = \frac{p(\mathbf{z}_N | \mathcal{H}_1)}{p(\mathbf{z}_N | \mathcal{H}_0)} = \mathcal{T}_1 \quad (3.11)$$

The result of integrating over the decision region, \mathcal{D}_1 for the alternate hypothesis, \mathcal{H}_1 , as shown in Figure 3.4, is

$$\int_{\mathcal{D}_1} p(\mathbf{z}_N | \mathcal{H}_1) d\mathbf{z} = \mathcal{T}_1 \int_{\mathcal{D}_1} p(\mathbf{z}_N | \mathcal{H}_0) d\mathbf{z} \quad (3.12)$$

The term on the left side of the equation is the power of the test for the conventional approach to hypothesis testing, $1-\beta$, while the term under the integral on the righthand side is the Type I error, α . The threshold, \mathcal{T}_1 , is then

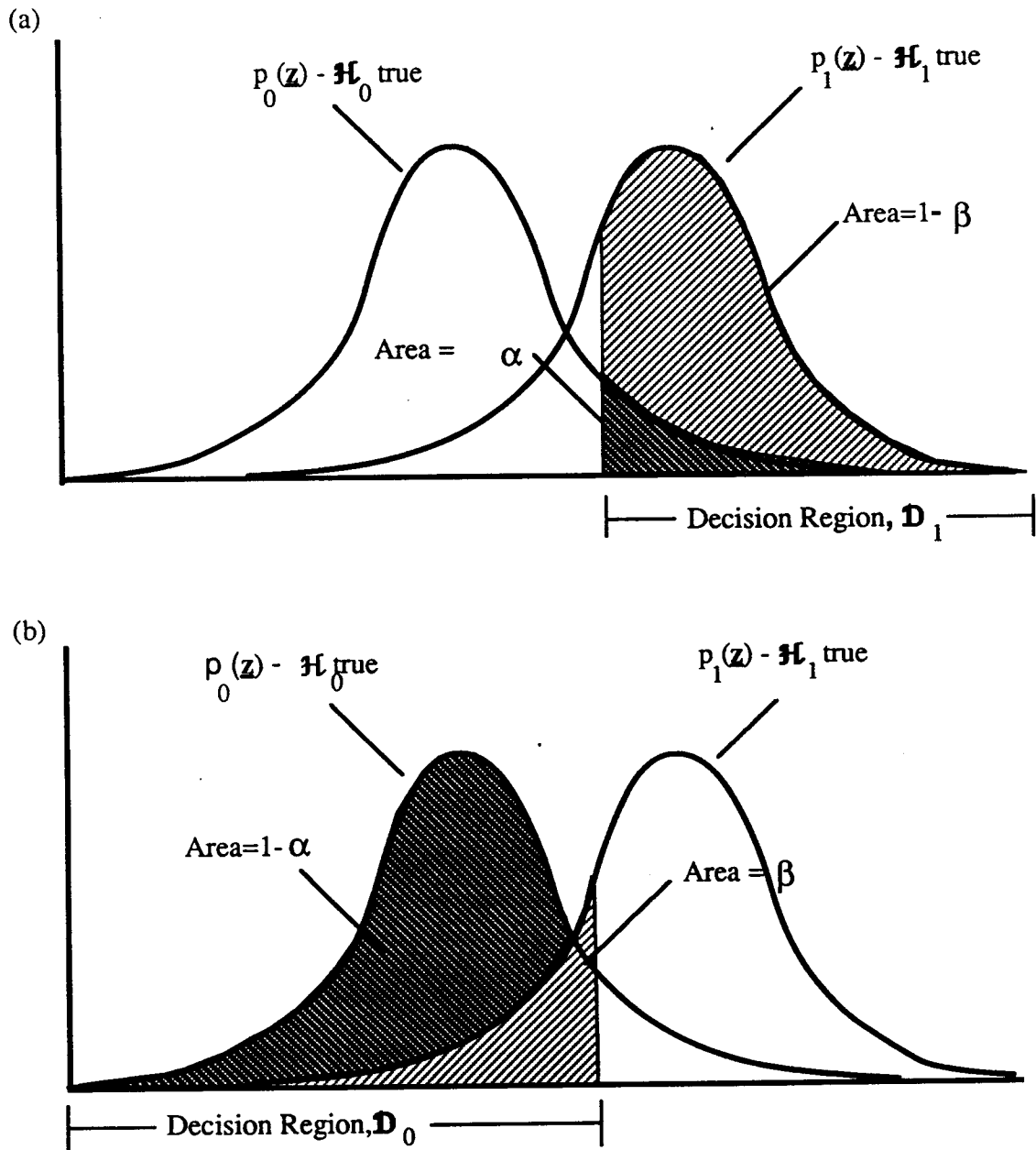


Figure 3.4. Decision regions, \mathcal{D} , for (a) sequential test results in acceptance of \mathcal{H}_0 and (b) sequential test results in acceptance of \mathcal{H}_1 .

$$\mathcal{T}_1 = \frac{1 - \beta}{\alpha} \quad (3.13)$$

Similarly, if a sample is taken at $k=N$, and the likelihood ratio is equal to the lower threshold, \mathcal{T}_0 , then

$$\mathcal{L} = \frac{p(\mathbf{z}_N | \mathcal{H}_1)}{p(\mathbf{z}_N | \mathcal{H}_0)} = \mathcal{T}_0 \quad (3.14)$$

By integrating over the decision region, \mathcal{D}_0 , we obtain

$$\int_{\mathcal{D}_0} p(\mathbf{z}_N | \mathcal{H}_1) d\mathbf{z} = \mathcal{T}_0 \int_{\mathcal{D}_0} p(\mathbf{z}_N | \mathcal{H}_0) d\mathbf{z} \quad (3.15)$$

It can be seen that

$$\mathcal{T}_0 = \frac{\beta}{1 - \alpha} \quad (3.16)$$

In actual practice, the log likelihood function, $\xi_j(\mathbf{z})$, defined as the natural logarithm of the likelihood function, \mathcal{L}_j , is more commonly used. Transforming the likelihood function by taking the logarithm does not affect the usefulness of the statistic and makes the form of the function simpler by replacing products with sums. This is particularly useful when the distribution of \mathbf{z}_N is Gaussian, as will be the case for the analyses conducted in this study. Assuming a sample is taken at time $k=N$, the decision rules using the log likelihood functions are as shown in Table 3.1.

Table 3.1 Decision rules for sequential hypothesis tests

Status of Decision Variable	Decision Rule
$\xi_1(N) - \xi_0(N) < \ln \mathcal{T}_0$,	Choose \mathcal{H}_0
$\xi_1(N) - \xi_0(N) > \ln \mathcal{T}_1$	Choose \mathcal{H}_1
$\ln \mathcal{T}_0 < \xi_1(N) - \xi_0(N) < \ln \mathcal{T}_1$	Continue sampling

3.3. State Estimation Applied to Sequential Testing

For dynamic systems, estimation theory, using the state space formulation of equations (3.1) through (3.8), provides a formalism for combining the process and measurement systems to obtain an optimal estimate of the true state for linear systems. As defined earlier, the estimate obtained at the same time as the last measurement is made is called filtering. A widely used filtering technique for estimating the state of linear systems is the Kalman filter (Kalman, 1960; Kalman and Bucy, 1961), as previously discussed. The Kalman filter gives optimal estimates that are unbiased and minimize the mean squared estimation error, where the estimation error is the difference between the true state and the estimated state.

For the purposes of sequential testing, a very useful application of the Kalman filter is in calculating the log likelihood function, ξ_j , when the systems are formulated in terms of state-space models. For linear state-space models (eqs. (3.1) and (3.2)), the log likelihood function, ξ_j , is given (according to Schweppe, 1973) by

$$\xi_j(N) = -\frac{1}{2} \sum_{n=1}^N \delta_j^T(n) [\mathbf{H}_j(n) \Sigma_j(n|n-1) \mathbf{H}_j^T(n) + \mathbf{R}_j(n)]^{-1} \delta_j(n) \quad (3.17)$$

where

$$\delta_j(n+1) = \mathbf{z}(n+1) - \mathbf{H}_j(n+1) \Phi_j(n) \mathbf{x}_j(n|n) - \mathbf{m}_j(n+1) \quad (3.18)$$

$$\mathbf{x}(n|n) = \Phi(n-1) \mathbf{x}(n-1|n-1) + \mathbf{K}(n) (\mathbf{z}(n) - \mathbf{H}(n) \Phi(n-1) \mathbf{x}(n-1|n-1)) \quad (3.19)$$

$$\Sigma_j(n+1|n) = \Phi(n) \Sigma(n|n) \Phi(n)^T + \Gamma(n) \mathbf{Q}(n) \Gamma(n)^T \quad (3.20)$$

$\mathbf{x}(n|n)$ = the updated estimate of the state of the system at the n^{th} time step

$\mathbf{x}(0|0)$ = the initial estimate of the state of the system

$\mathbf{K}(n)$ = the Kalman gain matrix at the n^{th} time step

$\Sigma_j(n|n) = [\mathbf{I} - \mathbf{K}(n) \mathbf{H}(n)] \Sigma_j(n|n-1)$, the updated error covariance matrix at the n^{th} time step

$\Sigma_j(0|0)$ = the initial error covariance

$\mathbf{m}_j(n)$ = the vector of the deterministic (mean) values of the n system states at the n^{th} time step.

For the nonlinear case (eqs. (3.5) and (3.6)), the most commonly used approach is to linearize the nonlinear problem about some nominal trajectory, and then solve it in the same way as the linear problem described above (Schweppe, 1973; Sage and Melsa, 1971; and Gelb, 1974). The nominal trajectory, $\mathbf{x}_{\text{nom}}(n+1)$, $n=1, \dots, N$, is a function of the previous state, $\mathbf{x}_{\text{nom}}(n)$, and the time, n . The evolution of the trajectory is described by

$$\mathbf{x}_{\text{nom}}(n+1) = \Phi[\mathbf{x}_{\text{nom}}(n), n] \quad (3.21)$$

eq. (3.18) through (3.20) become, respectively,

$$\delta_j(n+1) = \mathbf{z}(n+1) - \mathbf{H}_j(n+1)\Phi^{[1]}[\mathbf{x}_{\text{nom}}(n), n]\mathbf{x}_j(n|n) - \mathbf{x}_{j, \text{nom}}(n+1) \quad (3.22)$$

$$\begin{aligned} \mathbf{x}(n|n) &= \mathbf{x}(n|n+1) + \mathbf{K}(n)[\mathbf{z}(n) - \mathbf{H}[\mathbf{x}_{\text{nom}}(n), n] \\ &\quad - \mathbf{H}[\mathbf{x}_{\text{nom}}(n), n]^{(1)}[\mathbf{x}(n|n-1) - \mathbf{x}_{\text{nom}}(n)] \end{aligned} \quad (3.23)$$

$$\begin{aligned} \mathbf{x}(n|n) &= \mathbf{x}(n|n-1) + \mathbf{K}(n)[\mathbf{z}(n) - \mathbf{H}[\mathbf{x}_{\text{nom}}(n), n] \\ &\quad - \mathbf{H}[\mathbf{x}_{\text{nom}}(n), n]^{(1)}[\mathbf{x}(n|n-1) - \mathbf{x}_{\text{nom}}(n)] \end{aligned} \quad (3.24)$$

where the elements of the matrices, $\mathbf{H}^{[1]}[\mathbf{x}_{\text{nom}}(n), (n)]$ and $\Phi^{[1]}[\mathbf{x}_{\text{nom}}(n), (n)]$, are the first-order terms in the Taylor series expansion of $\mathbf{H}[\mathbf{x}(n), n]$ and $\mathbf{F}[\mathbf{x}(n), (n)]$, respectively, as follows:

$$\mathbf{H}^{(1)}[\mathbf{x}_{\text{nom}}(n), n] = \left. \frac{\partial \mathbf{H}(\mathbf{x}, n)}{\partial \mathbf{x}} \right|_{\mathbf{x}(n) = \mathbf{x}_{\text{nom}}(n)} = \mathbf{J}_{\mathbf{x}}(\mathbf{H}) \quad (3.25)$$

$$\Phi^{(1)}[\mathbf{x}_{\text{nom}}(n), n] = \left. \frac{\partial \Phi(\mathbf{x}, n)}{\partial \mathbf{x}} \right|_{\mathbf{x}(n) = \mathbf{x}_{\text{nom}}(n)} = \mathbf{J}_{\mathbf{x}}(\Phi) \quad (3.26)$$

$\mathbf{J}_{\mathbf{x}}(\mathbf{H})$ is the Jacobian matrix of \mathbf{H} with respect to the vector, \mathbf{x} , and $\mathbf{J}_{\mathbf{x}}(\Phi)$ is the Jacobian matrix of Φ with respect to the vector, \mathbf{x} .

Once the nominal trajectory, $\mathbf{x}_{\text{nom}}(n)$, has been chosen, the analysis can proceed exactly as in the case for the linear state-space models. There are a number of

possibilities for the choice of the nominal trajectory. The case of the extended Kalman filter (EKF) results when the nominal trajectory for the n^{th} time step is obtained from the state estimate for that time step prior to updating, $\hat{\mathbf{x}}(n|n)$. From a theoretical viewpoint this is most sound approach since, as Gelb (1974) states, the EKF reduces to the conventional Kalman filter when the system dynamics and measurements are linear. It does, however, have some drawbacks, particularly with respect to the computational burden imposed by making the filter gain, $\mathbf{K}(n)$, a function of the state estimate, $\hat{\mathbf{x}}(n|n)$. This means that the gain must be computed every time the filter is used to obtain an estimate of the state. When the gain is independent of the state estimate, the gain can be computed beforehand and does not change so long as the nominal trajectory does not change. This alternate approach, in which the nominal trajectory is specified prior to processing the measurement data, is called the linearized Kalman filter.

3.4. Application to Environmental Assessment

For illustrative purposes consider the environmental system, E , which experiences some development. Furthermore, assume that the state of the system can be described by a vector of state variables, \mathbf{x} . As shown in Figure 3.5, this system is driven by the forcing function, $\mathbf{B}\mathbf{u}$, comprised of a natural component acting up until the time $t=t_d$ after which the inputs from the development are added to the natural forcing functions. The true time history of the state variables before (E_0) and after (E_1) is shown in Figure 3.6. The objective of environmental assessment is to determine whether or not E_0 is different from E_1 . Within the framework of hypothesis testing, this could be stated in terms of the following two hypotheses:

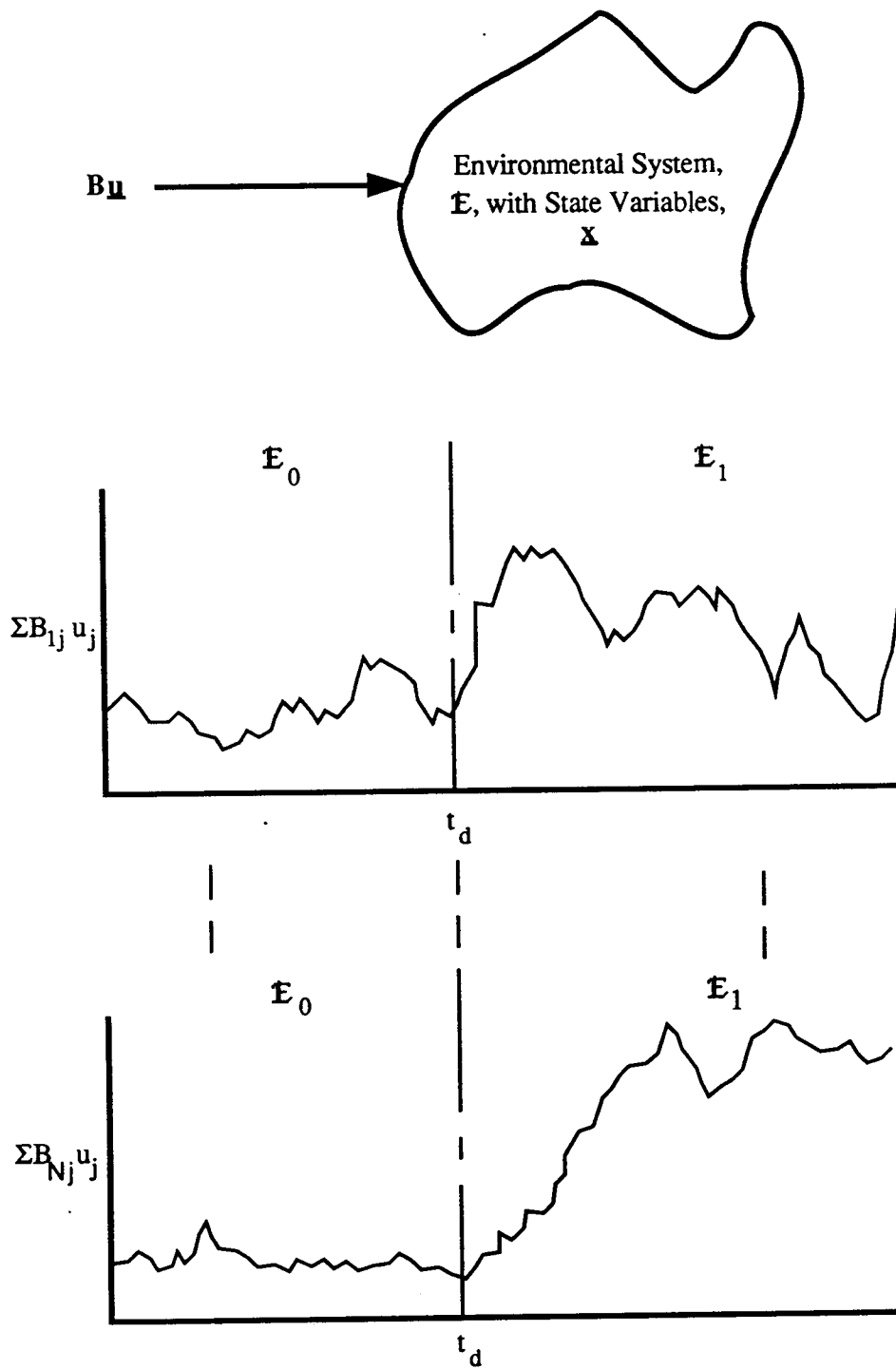


Figure 3.5. Environmental system, E , with inputs B_u before development ($t < t_d$) and after development ($t > t_d$).

\mathcal{H}_0 : The states of the environmental system, E_0 , before development are the same as the states, E_1 , after development.

\mathcal{H}_1 : The states of the environmental system, E_0 , before development are different from the states, E_1 , after development.

Estimates of the true values of the state variables, \mathbf{x} , of the environmental system can be obtained by making measurements $\mathbf{z} = \mathbf{H}\mathbf{x} + \mathbf{y}$ and by estimating the state from the systems equation, $\mathbf{x} = \mathbf{F}\mathbf{x} + \mathbf{B}\mathbf{u} + \mathbf{G}\mathbf{w}$. Combining the estimates obtained from measurements and the systems equations, the hypotheses can be stated as

$$\mathcal{H}_0: \mathbf{z}_0 = \mathbf{H}\mathbf{x}_0 + \mathbf{y}$$

$$\mathcal{H}_1: \mathbf{z}_1 = \mathbf{H}\mathbf{x}_1 + \mathbf{y}$$

where

$$\mathbf{x}_0 = \Phi\mathbf{x}_0 + \mathbf{B}\mathbf{u}_0 + \Gamma\mathbf{w}$$

$$\mathbf{x}_1 = \Phi\mathbf{x}_1 + \mathbf{B}\mathbf{u}_1 + \Gamma\mathbf{w}$$

and

\mathbf{u}_0 = The forcing functions comprised of only the natural component both before and after time, t_d , when development begins

\mathbf{u}_1 = The forcing functions comprised of the natural component before time, t_d , and including the effects of development after the time development begins

The null hypothesis, \mathcal{H}_0 , is that the observations, \mathbf{z}_0 , of the system are consistent with the statement that the state of the environmental system both before and after development is determined by natural forcing functions only. The alternative hypothesis, \mathcal{H}_1 , is that the observations, \mathbf{z}_1 , are consistent with the statement that the state of system

after development is determined by the natural forces plus the additional forcing functions result from the development.

The sampling program ($\mathbf{z} = \mathbf{H}\mathbf{x} + \mathbf{y}$) and the systems equation ($\mathbf{x} = \Phi\mathbf{x} + \mathbf{B}\mathbf{u} + \Gamma\mathbf{w}$) are the fundamental components of hypothesis testing formulated in the manner described above. Because of this, they are the keys to deciding how much in the way of resources should be devoted to either or both of these components. The kinds of questions which are appropriate in this regard are:

- Which state variables should be sampled (specification of \mathbf{H})?
- How many samples should be taken?
- How accurate should the measurements be (specification of \mathbf{R})?
- How much effort should be given to model identification, parameter estimation, and model calibration (specification of Φ and \mathbf{Q})?
- Is aggregation of state variables appropriate?

In general, these five questions represent a large number of degrees of freedom. Recognizing that answering these questions usually means a large and complex problem, solutions (or partial solutions) can be obtained only if there exist criteria for comparing various strategies for sampling and model development. One appropriate criterion for judging the effectiveness of a sample design and model development program is the time period after onset of the loading required for the model to detect the difference between the two hypotheses, \mathcal{H}_0 and \mathcal{H}_1 , given a specified tolerance for Type I error, α , and Type II error, β .

Consider the time trajectories of the state variables, $\mathbf{x}(t)$ in the ecosystem, E , of Figure 3.6, which have the true trajectory, $\mathbf{x}_0(t)$, under conditions of no man-induced environmental impacts, E_0 . They have true trajectory, $\mathbf{x}_1(t)$, for some known level of

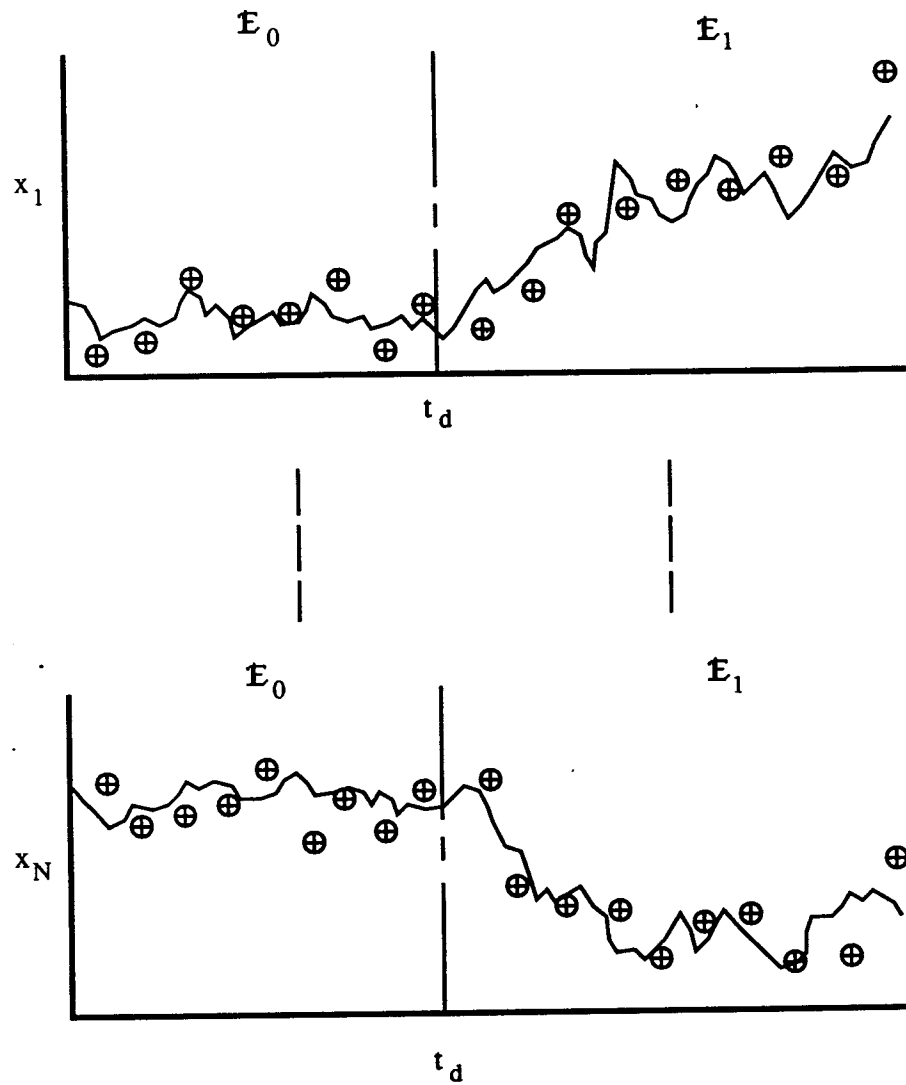


Figure 3.6. Trajectory of state variables, \mathbf{x} , in the environmental system, \mathbf{E} , before ($t < t_d$) and after ($t > t_d$) an interventions occurs. The observations, $\mathbf{z}(n)$, are also shown (\oplus).

input occurring after time, t_d , under the conditions, E_1 . Actual measurements of the constituents follow the trajectory, $\mathbf{z}(t) = [z_1(t), z_2(t), \dots, z_n(t)]$. If there are state-space systems equation of the form of equations (3.1) and (3.2) or equations (3.5) and (3.6) for the environmental system, E , then the log likelihood function, ξ_j , can be computed for the null hypothesis, \mathcal{H}_0 , and the alternate hypothesis, \mathcal{H}_1 , using equation (3.17) in conjunction with equations (3.18) through (3.20), if the model is linear, or equations (3.22) through (3.24) if the model is nonlinear. The hypothetical trajectories of the log likelihood functions, ξ_0 and ξ_1 , are shown in Figure 3.7. The log likelihood function was defined as the decision variable for the sequential test. Therefore, if at time step, $k = N$, a sample is taken and the log likelihood functions, ξ_0 and ξ_1 , are computed, the decision rule can be applied to determine whether to accept \mathcal{H}_0 , accept \mathcal{H}_1 , or continue sampling. From the previous discussion, the null hypothesis, \mathcal{H}_0 , is accepted if

$$\xi_1(N) - \xi_0(N) < \mathcal{T}_0 \quad (3.27)$$

The alternate hypothesis, \mathcal{H}_1 , is accepted if

$$\xi_1(N) - \xi_0(N) > \mathcal{T}_1 \quad (3.28)$$

If the log likelihood ratio does not satisfy the criteria given by equations (3.27) and (3.28), no decision is made and another sample is taken. Sampling continues until a decision is reached. Wald (1947) and Sage and Melsa (1971) show that the sequential test procedure will always end before an infinite number of observations have made. The log likelihood functions, ξ_j , are random variables and will vary from one realization to the next. The average number of samples required for a decision can be computed,

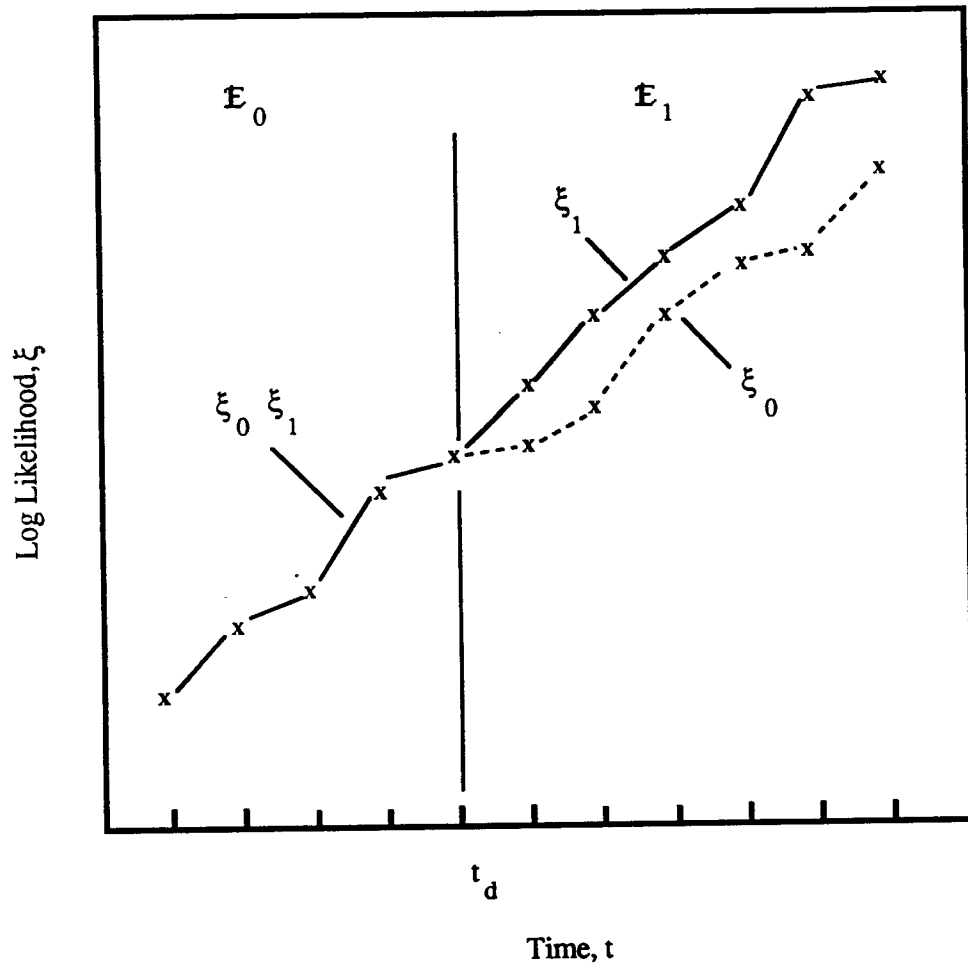


Figure 3.7. Hypothetical trajectory of decision variables ξ_0 and ξ_1 before ($t < t_d$) and after ($t > t_d$) development.

however. The more sensitive the test, the fewer number of samples will be required to reach a decision. The average number of samples required to reach a decision then provides a criterion for assessing the value of a given model/monitoring strategy. For example, given a fixed sampling frequency, $\mathbf{H}(n)$ and measurement noise variance, $\mathbf{R}(n)$, the average number of samples required to detect a change can be compared for models of various levels of complexity. In a corresponding way, the worth of data for a given level of model complexity can be determined by evaluating the way in which the time required to detect a change varies with change in the sampling frequency, $\mathbf{H}(n)$, and the measurement noise variance, $\mathbf{R}(n)$.

3.5. Application of Hypothesis Testing to Model Validity

The application of hypothesis testing to environmental assessment has been described above. Application of the method using models with state-space structure contains the implicit assumption that the models used provide valid representations of the state-space. When the validity of such models has not been established, the likelihood function generated by the Kalman filter (eq. (3.17)) can also be used as decision variable to test the following hypotheses:

\mathcal{H}_0 : The model, $\mathbf{z}(n) = \mathbf{H}(n)\mathbf{x}(n) + \mathbf{v}(n)$, gives state estimates that correctly describe the environmental system being assessed. That is, the model is correct.

\mathcal{H}_1 : The model, $\mathbf{z}(n) = \mathbf{H}(n)\mathbf{x}(n) + \mathbf{v}(n)$, gives state estimates that do not correctly describe the environmental system being assessed. That is, the model is incorrect.

In the statement of these hypotheses

$\mathbf{z}(n)$ = the observed state vector at the n^{th} time step

$\mathbf{H}(n)$ = the observation matrix at the n^{th} time step

$\mathbf{v}(n)$ = the measurement noise vector at the n^{th} time step

$\mathbf{x}(n) = \Phi[\mathbf{x}(n-1), \mathbf{w}(n-1), \mathbf{u}(n-1), (n-1)]$, the true state vector for the system at the n^{th} time step, which may be described by either linear or nonlinear model

When the observed state vector for the j^{th} hypothesis, $\mathbf{z}(n) = \mathbf{z}_j(n)$, has a normal distribution, $N(\mathbf{m}_j, \Sigma_j)$ with mean \mathbf{m}_j and variance Σ_j , then it is evident from equation (3.17), that the log likelihood function, $\xi_j(N)$, can be written as

$$2\xi_j = -[\mathbf{z}_j - \mathbf{m}_j]^T \Sigma_j^{-1} [\mathbf{z}_j - \mathbf{m}_j] \quad (3.29)$$

It is also evident then that the log likelihood function, $\xi_j(N)$, is the sum of the squares of K normally distributed random variables, where K is the product of the number of observations, N , and the number of observed state variables, L , that is, $K = NL$. Furthermore, $2\xi_j(N)$, is a χ^2 random variable with $K = NL$ degrees of freedom, a mean of K , and variance of $2K$ (Schweppe, 1973).

With this knowledge, the power of the test, $1-\beta$, the probability of rejecting the null hypothesis, \mathcal{H}_0 , when it is false, can be determined from the fraction of times that the log likelihood function $\xi(N)$, falls outside the critical region. In this first stage of testing it possible to decide, after an acceptable level of β has been specified, whether or not a given model is correct.

CHAPTER 4

LINEAR MODELS: AN ASSESSMENT OF MODEL COMPLEXITY AND DATA WORTH IN THE GLOBAL CARBON CYCLE¹

4.1. Background

The potential impact of carbon dioxide (CO₂) from anthropogenic inputs on the Earth's heat budget has been the subject of scientific interest for over a century (see, e.g., Tyndall, 1861). CO₂ is a major contributor to the greenhouse effect and therefore plays an important part in the global heat budget. Plass (1956) discussed many of the aspects of the carbon dioxide theory of climatic change, and as discussed in the Chapter 2, there have been a number of subsequent efforts to develop models of the flow of carbon on a global scale. The development of these theories also provided the impetus for testing these hypotheses with observations. In 1959, Keeling et al. (1976) began a program of measurements of atmospheric CO₂ at the observatory at Mauna Loa, Hawaii. These data have provided the documentation of the increase in atmospheric CO₂. Charney (1979) has concluded that increasing atmospheric CO₂ to twice its pre-1860 value could lead to increases in global temperatures of 3.0 ± 1.5 °C. Seidel and Keyes (1983) have attributed the increase to the combustion of fossil fuels, although this conclusion has been debated. Concern regarding the consequences of global warming has prompted the EPA to formulate strategies limiting increases of atmospheric CO₂. Relevant knowledge has been obtained both from the knowledge based on mathematical models of global carbon and from direct observations of carbon levels in the oceans, atmospheric and land. However, there is uncertainty in these estimates. A critical need identified by the EPA in

¹ This chapter is substantially the same as a refereed scientific journal publication (see Yearsley and Lettenmaier, 1987)

its analysis was the reduction of uncertainties associated with the outcomes resulting from implementation of the strategies. The objective of this chapter is to apply the methods of Chapter 3 to show how state estimation and hypothesis testing can be used to assess model complexity and data worth for linear models of the global carbon cycle.

4.2. Scope of Analysis

One of the major uncertainties in the global carbon budget is the quantification of the sources of atmospheric input. Keeling (1973) attributed the increases in atmospheric CO₂ to the combustion of fossil fuels. Stuiver (1978), however, estimated that two-thirds of the CO₂ added to the atmosphere during the period 1850-1950 resulted from the release of terrestrial biospheric carbon associated with clearing of forests, while only one-third originated from the combustion fossil fuel. Stuiver has calculated that the net global biospheric flux due to sources such as deforestation and the burning of dead organic materials was 1.2×10^9 metric tons (1.2×10^{15} grams) of carbon per year during this period. Estimates by Woodwell et al. (1978) have shown an even higher percentage of atmospheric carbon coming from biospheric sources. By contrast, Machta (1973) and Oeschger et al. (1975) treated the biota as a sink for atmospheric CO₂ rather than a source.

There has already been considerable effort devoted to the measurement of carbon fluxes and to the development of models that simulate the time-dependent fluxes between compartments (Bolin, 1981). The use of data for model identification and parameter estimation has generally been done in an ad-hoc way, however, and little effort has been devoted to quantifying the sources of uncertainty. Although recommendations for additional model development and data collection have been made (Bolin et al., 1979;

Bolin, 1981), they cannot be evaluated without determining which elements of the recommended program have highest priority.

The demonstration of the methodology in this chapter focuses on linear models for which it is assumed the model parameters are known. It is applied to testing hypotheses regarding the validity of the linear models of the global carbon cycle and then applied to testing the ability of each model to detect environmental changes as a function of measurement error and loading input.

The test of model validity can be stated in terms of the following hypotheses:

\mathcal{H}_0 : the linear model $\mathbf{z}(n) = \mathbf{H}(n)\mathbf{x}(n) + \mathbf{v}(n)$ is no different from the nonlinear reference system model describing the system behavior, i.e., the linear model is valid.

\mathcal{H}_1 : the linear model $\mathbf{z}(n) = \mathbf{H}(n)\mathbf{x}(n) + \mathbf{v}(n)$ is different from the nonlinear reference system model describing the system behavior.

As in Chapter 3, $\mathbf{z}(n)$ is the observed state vector at the n^{th} time step, $\mathbf{H}(n)$ is the observation matrix at the n^{th} time step, $\mathbf{v}(n)$ the measurement noise vector at the n^{th} time step, $\mathbf{x}(n) = \Phi(n)\mathbf{x}(n-1)$ the true state vector of the system at the n^{th} time step, and $\Phi(n)$ is the state transition matrix at the n^{th} time step.

The second type of hypothesis testing evaluates the level of model complexity and the value of data needed to assess environmental impact. For purposes of demonstrating the methodology it is worthwhile to consider the hypothesis that the terrestrial biota are a source or sink for atmospheric CO_2 . The sources of fossil fuel combustion have been well documented (Keeling, 1973), but better data and improved models are needed to adequately test the hypothesis regarding terrestrial biota (Bolin, 1981; Stuiver, 1978). Tests to examine this issue can be stated in terms of the following hypotheses:

\mathcal{H}_0 : The model $\mathbf{z}_0(n) = \mathbf{H}(n)\mathbf{x}_0(n) + \mathbf{y}(n)$ is true.

\mathcal{H}_1 : The model $\mathbf{z}_1(n) = \mathbf{H}(n)\mathbf{x}_1(n) + \mathbf{y}(n)$ is true.

where $\mathbf{x}_0(n)$ is the model with terrestrial biota making no net contribution to the global carbon cycle, and $\mathbf{x}_1(n)$ is the model with terrestrial biota making a known net contribution to the global carbon cycle.

The approach taken is to generate synthetic data with a reference system model derived from knowledge of global carbon dynamics. The reference system model is a nonlinear model, based on a construct described by Bjorkstrom (1979) and incorporating current concepts about the structure of the carbon cycle and the rates at which carbon is transferred from one compartment to another. In applying the Bjorkstrom model, it was assumed that the model was perfect (no parameter error), and the only issues are the appropriate levels of model development (complexity) and data collection. Given this assumption, the sole source of uncertainty in the generated data, is the measurement error. Only crude estimates of the measurement error associated with each of the various compartments are available. Therefore, a number of different levels of measurement error, believed to be less than actual in the case of some compartments, are used in the Monte Carlo simulations.

4.3. Model of the Global Carbon Cycle

The reference system model of the global carbon cycle (Bjorkstrom, 1979) is comprised of 15 compartments, including compartments for living terrestrial biota, soil, atmosphere, warm and cold ocean surface layers, intermediate-depth ocean layers, and deep ocean layers (see Figure 4.1). Seasonal fluctuations in atmospheric carbon, that have been observed by Keeling et al. (1976), are not included in this model. The

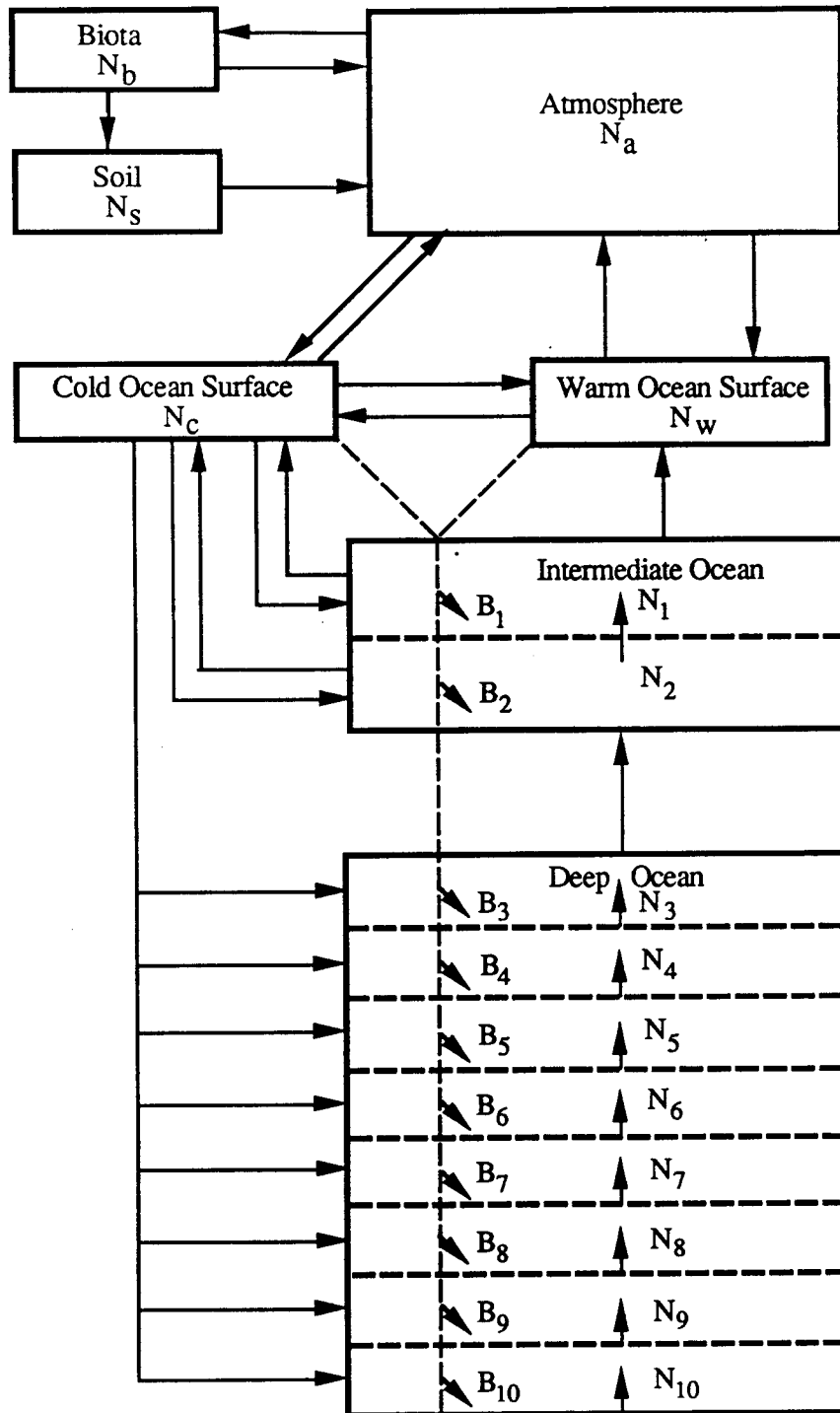


Figure 4.1. Model of global carbon cycle used for analysis (after Bjorkstrom, 1979).

dynamics of the global carbon cycle are described in detail in Appendix I and the model parameters shown in Table 4.1.

The transfer of carbon between most compartments is based on linear kinetics. The buffering action in the surface seawater associated with the chemical equilibrium of CO_2 , bicarbonate (HCO_3), and carbonate (CO_3) was modeled with the nonlinear kinetics described by Bacastow and Keeling (1973). The rate of transfer from the atmosphere to the terrestrial biota is also modeled by nonlinear kinetics similar to those used by Bacastow and Keeling (1973). Initially, the model was used to simulate the dynamics of atmospheric carbon from 1860 to 1971 using fossil fuel consumption rates estimated by Keeling (1973). The rate of transfer of carbon from the terrestrial biota to the atmosphere was assumed to be a constant over the entire period from 1860 to 1970. It was assumed that the total contribution of carbon from terrestrial biota during this period was 70×10^9 metric tons (70 gigatons) as estimated by Bolin (1977). Estimates of the pre-industrial level of average atmospheric CO_2 vary from 260 to 300 ppm (Stuiver, 1978).

For this study, pre-industrial steady-state value of atmospheric CO_2 of 285 ppm was used to determine the equilibrium conditions for all compartments are given in Table 4.1. The simulated levels of atmospheric CO_2 , using the Bjorkstrom model with this parameter set, compared well with the observations at Mauna Loa, Hawaii, reported by Keeling et al. (1976) (see Figure 4.2) Keeling et al. (1976) describe observations at the South Pole that have similar long-term trends. However, the agreement between simulated and observed atmospheric CO_2 should not be considered a verification of the Bjorkstrom model. This is because the model constructs and corresponding parameter set are not unique. Other models of the global carbon cycle have been proposed that also show good agreement between simulated and observed levels of atmospheric carbon

Table 4.1 Parameter values used in the nonlinear model of the global carbon cycle (equations I.1-15 in Appendix I)

Variable	Description	Value
k_{ac}	Transfer rate from atmosphere to cold ocean surface	$6.79 \times 10^{-2} \text{ year}^{-1}$
k_{ca}	Transfer rate from atmosphere to warm ocean surface	$1.82 \times 10^1 \text{ year}^{-1}$
k_{wc}	Transfer rate from warm ocean to cold ocean water	$8.00 \times 10^{-2} \text{ year}^{-1}$
k_{c1}	Transfer rate from cold ocean surface to ocean layer N_1	$8.33 \times 10^{-2} \text{ year}^{-1}$
k_{c2}	Transfer rate from cold ocean surface to ocean layer N_2	$2.78 \times 10^{-3} \text{ year}^{-1}$
k_{1c}	Transfer rate from ocean layer N_1 to cold ocean surface	$4.84 \times 10^{-3} \text{ year}^{-1}$
k_{2c}	Transfer rate from ocean layer N_2 to cold ocean surface	$3.38 \times 10^{-3} \text{ year}^{-1}$
k_{aw}	Transfer from atmosphere to warm ocean surface	$1.09 \times 10^{-1} \text{ year}^{-1}$
k_{wa}	Transfer from warm ocean to atmosphere	$1.77 \times 10^{-1} \text{ year}^{-1}$
k_{1w}	Transfer rate from ocean layer N_1 to warm ocean surface	$4.65 \times 10^{-3} \text{ year}^{-1}$
k_{ba}	Transfer rate from terrestrial biota to atmosphere	$3.01 \times 10^{-2} \text{ year}^{-1}$
k_{ab}	Transfer rate from atmosphere to terrestrial biota	$6.02 \times 10^{-2} \text{ year}^{-1}$
k_{sa}	Transfer rate from soil to atmosphere	$1.25 \times 10^{-2} \text{ year}^{-1}$
k_{bs}	Transfer rate from terrestrial biota to soil	$3.01 \times 10^{-2} \text{ year}^{-1}$
k_{21}	Transfer rate from ocean layer N_2 to ocean layer N_1	$4.86 \times 10^{-3} \text{ year}^{-1}$
k_{32}	Transfer rate from ocean layer N_3 to ocean layer N_2	$4.64 \times 10^{-3} \text{ year}^{-1}$
k_{43}	Transfer rate from ocean layer N_4 to ocean layer N_3	$3.74 \times 10^{-3} \text{ year}^{-1}$

Table 4.1 (continued). Parameter values used in the nonlinear model of the global carbon cycle (equations I.1-15 in Appendix I)

Variable	Description	Value
k ₅₄	Transfer rate from ocean layer N ₅ to ocean layer N ₄	3.12x10 ⁻³ year ⁻¹
k ₆₅	Transfer rate from ocean layer N ₆ to ocean layer N ₅	2.47x10 ⁻³ year ⁻¹
k ₇₆	Transfer rate from ocean layer N ₇ to ocean layer N ₆	2.02x10 ⁻³ year ⁻¹
k ₈₇	Transfer rate from ocean layer N ₈ to ocean layer N ₇	1.42x10 ⁻³ year ⁻¹
k ₉₈	Transfer rate from ocean layer N ₉ to ocean layer N ₈	1.15x10 ⁻³ year ⁻¹
k _{10,9}	Transfer rate from ocean layer N ₉ to ocean layer N ₁₀	6.41x10 ⁻⁴ year ⁻¹
	Factor determining increase in photosynthetic rate	0.25
N _b	Equilibrium value for terrestrial biota	830x10 ¹⁵ g C
N ₁₀	Equilibrium value for ocean layer 1	1600x10 ¹⁵ g C
N ₉	Equilibrium value for ocean layer 9	2100x10 ¹⁵ g C
N ₈	Equilibrium value for ocean layer 8	3200x10 ¹⁵ g C
N ₇	Equilibrium value for ocean layer 7	3300x10 ¹⁵ g C
N ₆	Equilibrium value for ocean layer 6	3700x10 ¹⁵ g C
N ₅	Equilibrium value for ocean layer 5	3900x10 ¹⁵ g C
N ₄	Equilibrium value for ocean layer 4	4000x10 ¹⁵ g C
N ₃	Equilibrium value for ocean layer 3	4200x10 ¹⁵ g C
N ₂	Equilibrium value for ocean layer 2	4000x10 ¹⁵ g C
N ₁	Equilibrium value for ocean layer 1	4200x10 ¹⁵ g C
N _s	Equilibrium value for soil	2000x10 ¹⁵ g C
N _a	Equilibrium value for atmosphere	670x10 ¹⁵ g C
N _w	Equilibrium value for warm ocean surface	462x10 ¹⁵ g C
N _c	Equilibrium value for cold ocean surface	225x10 ¹⁵ g C

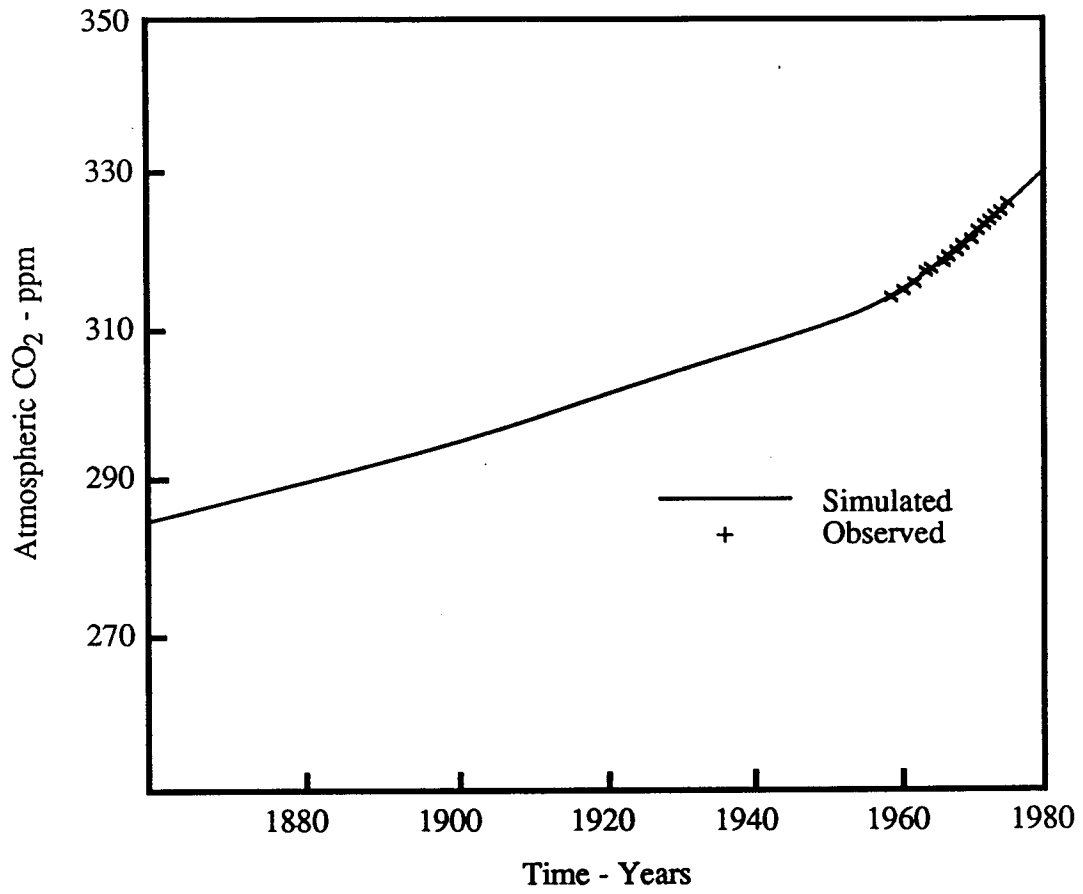


Figure 4.2. Comparison of simulated atmospheric CO₂ and observed levels at Mauna Loa, HI.

(see, e.g., Siegenthaler and Oeschger, 1978). For the purposes of this experiment, however, it was assumed that the Bjorkstrom model was perfect, and it is this model that acts as the population or universe for the Monte Carlo simulations.

A simple Euler scheme was used to solve the system of equations describing the Bjorkstrom model (Appendix I) numerically. The time step for the solution was taken as 0.5 years in order to satisfy the stability criterion for the Euler scheme imposed by the fastest rate of carbon transfer. This rate is associated with the transfer of carbon from the warm ocean surface layer to the atmosphere and has a time constant of approximately 0.55 years (Table 4.2). Because of this, the rate at which synthetic data could be sampled was limited to frequencies equal to or less than two per year.

4.4. Monte Carlo Methods

The reference system model was used to simulate a 100-year period showing the response of the global carbon cycle to two different input scenarios at two different levels of measurement noise (Table 4.2). Generation of the data sequences was accomplished by starting the model from equilibrium, with constant, but arbitrary levels of production of CO₂ from fossil fuel consumption and reduction of the terrestrial biosphere. The level of contribution from fossil fuels was comparable to estimated inputs during the last half of the 19th century. The input from terrestrial sources was chosen to be somewhat less than the estimates made by Bolin (1977) and Stuiver (1978). Each input scenario was simulated for a period of 100 years assuming that the nonlinear model was perfect. One hundred sequences, each of 100 years in length,

Table 4.2 Scenarios used to test hypotheses regarding the consumption of fossil fuels and terrestrial biota

Scenario	Fossil fuel consumption (10^{15} g C year ⁻¹)	Terrestrial biota consumption (10^{15} g C year ⁻¹)	<u>Standard deviation</u> Steady-state value
1	0.25	0.25	0.01
2	0.25	0.25	0.10
3	0.50	0.50	0.01
4	0.50	0.50	0.10

were synthesized from the simulations by superimposing normally distributed measurement noise about the simulated value. The variance associated with the measurement noise was chosen as a fixed percentage of the steady-state value for each compartment (Table 4.2). There is limited information regarding levels of uncertainty (Bolin et al., 1979) for the various compartments. Keeling et al. (1976) report a daily variability of approximately ± 1 ppm for atmospheric CO₂ levels of 320 ppm. Although observations by Keeling et al. (1976) at the South Pole are similar, there are few data available for estimating the uncertainty of the entire atmospheric CO₂ compartment. Gardner et al. (1980) estimate it to be approximately $\pm 10\%$. Estimates associated with the uncertainty in the soil compartment are as large as $\pm 50\%$ (Woodwell et al., 1978). Because of the limited information available regarding uncertainty of carbon levels in each compartment, the coefficient of variation (ratio of the standard deviation of the measurement noise to the steady-state preindustrial compartment level) in this study were varied between 1% and 10%.

4.5. Model Complexity

Linear models of the global carbon cycle with varying levels of complexity were obtained by first linearizing the 15-compartment nonlinear model about the steady-state solution. For perturbations about this steady-state, the transfer matrix, $\Phi(n)$, for the resulting linear 15-compartment model is given in Table 4.3. The complexity of the 15-compartment linear model was reduced by aggregating compartments. The aggregation process was also the parameter estimation step for the aggregated models.

The aggregate system of m' states, described by the vector $\mathbf{x}'(n)$, is related to the complete system of $m' \times m$ matrix C (Aoki, 1968) as

$$\mathbf{x}'(n) = C\mathbf{x}(n) \quad (4.1)$$

An aggregated state transition matrix, $F'(n)$, that has a minimum squared-error property (Aoki, 1968), is given by

$$F' = CFCT^T(CCT)^{-1} \quad (4.2)$$

Studies by O'Neill and Rust (1979) have shown that aggregation error is small when compartments with similar time behavior are combined. These findings can be used to reduce model order in a consistent manner. It requires, first of all, however, that the eigenvalues of the linearized 15-compartment system be determined. The eigenvalues of a linear system describe the dynamic response of each the state variables. The algorithm described by Grad and Brebner (1968) was used determine the eigenvalues. The eigenvalues for the 15-compartment system, in units of year⁻¹, are:

Table 4.3 (continued). Coefficient matrix, Φ , for 15-compartment linear model (units are year⁻¹).

	Deep/Intermediate Ocean			Soil	Atmos- phere	Warm ocean surface	Cold ocean surface
	3	2	1				
Biota					.0170		
10							.00427
9							.00595
8							.00863
7							.00919
6							.0103
5							.0119
4							.0130
3	-.00464						.0168
2	.00464	-.00824					.0278
1		.00487	-.00948				.0833
Soil				-.0125			
Atmos- phere				.0125	-.194	1.80	1.70
Warm surface			.00464		.109	-1.88	.080
Cold surface		.00339	.00484		.0679	.08	-1.97

[-2.03, -2.00, -0.0703, -0.0259, -0.00958, -0.00865, -0.00498,
 -0.00359±j 0.000728, -0.00137±j 0.000417, -0.00228±j 0.000534,
 -0.000954, 0]

where $j = \sqrt{-1}$ and signifies that the eigenvalue has an imaginary part. In linear systems the state variables with negative real eigenvalues are stable, those with positive real eigenvalues can be unstable, and those with imaginary eigenvalues have periodic (sinusoidal) behavior. Therefore, the 15-compartment linear system is stable, with six periodic modes. The eigenvalues have natural groupings. The first two (-2.03, -2.00) represent the ocean surface layers. The atmosphere, terrestrial biota, and soil are represented by the next three (-0.073, -0.0259, -0.00958), respectively. The remaining nonzero eigenvalues characterize the intermediate and deep ocean response. Closed systems, such as the global carbon cycle, have at least one eigenvalue equal to zero, reflecting the fact that the total amount of carbon in the system remains constant. The grouping of the eigenvalues, as well as physical considerations, imply three levels of aggregation. Beginning with the modes whose eigenvalues have the smallest real part, the first grouping includes the deep and intermediate ocean layers, the second includes the terrestrial biota and the soil, and the third is the two ocean surface layers.

Based on these considerations, the evaluation of model complexity was performed by postulating that the following three models would generate state estimates consistent with state estimates generated by the reference system model :

- The 15-compartment model whose state transition matrix is that given in Table 4.3
- The six-compartment model made up of the warm ocean surface layer, the cold ocean surface layer, the atmosphere, the terrestrial biota, the soil, and the aggregated intermediate and deep ocean layers.

- The four-compartment model made up of the aggregated warm and cold ocean surface layers, the aggregated terrestrial biosphere and soil, the atmosphere, and the aggregated intermediate and deep ocean layers.

The application of equation (4.2) to the 15-compartment state transition matrix of Table 4.3, for the 6-compartment model leads to the state transition matrix shown in Table 4.4.

Table 4.4 Coefficient matrix, Φ , for six-compartment linear model (units are year⁻¹)

	Biota	Deep/Intermediate ocean	Soil	Atmosphere	Warm ocean surface	Cold ocean surface
Biota	-0.602			0.0207		
Deep/Intermediate ocean		-0.00129				0.0191
Soil	0.0301		-0.0125			
Atmosphere	0.0301		0.0125	-0.198	1.80	1.70
Warm ocean surface		0.000465		0.109	-1.880	0.080
Cold ocean surface		0.000824		0.0679	0.080	-1.97

The eigenvalues for this model are:

[-2.03, 2.00, -0.0703, -0.00379, 0]

The aggregated six-compartment model preserves the important features of the fifteen-compartment model. That is, there is an eigenvalue that represents each of the principal modes of the fifteen-compartment model. The first two eigenvalues characterize the response of the surface layers, the third characterizes the response of the atmosphere, the fourth is related to the response of the terrestrial biota and the soil, and the fifth characterizes the deeper ocean. For time scales on the order of decades this model should have dynamics similar to those of the complete 15-compartment model.

The corresponding state transition matrix for the four-compartment model is shown in Table 4.5.

Table 4.5 Coefficient matrix, Φ , for four-compartment linear model (units are years⁻¹)

	Biota + soil	Deep/Inter- mediate ocean	Atmo- sphere	Ocean surface
Soil + Biota	-0.00213		0.0207	
Deep/Intermed- iate ocean		-0.00129		0.0956
Atmosphere	0.00213		-0.198	1.75
Ocean surface		0.00129	0.177	-1.85

The eigenvalues for the four-compartment model are as follows:

[-2.02, -0.0048, 0.00511, 0]

In this highly aggregated system some of the features of the more complex system have been modified. The response of the ocean surface layers is preserved, as is the response of the deeper ocean. However, aggregating the living terrestrial biota and the soil was accomplished at the expense of reducing the eigenvalues associated with the response of the atmosphere. Aggregating the terrestrial biota and the soil also has the result of coupling the soil more closely to the atmospheric compartment.

Simulations of the carbon cycle with the four different models, the true nonlinear model, the fifteen-compartment linear model, the six-compartment linear model, and the four-compartment linear model for the two different loading levels are shown in Figure 4.3. Compartments have been combined so that the results of the more complex models can be easily compared to the model with the highest level of aggregation, the four-compartment model.

4.6. Results

The test of model validity exploits the fact that the distribution for the test statistic of the null hypothesis, \mathcal{H}_0 , is known. The statistic is the log likelihood function, ξ_0 and the null hypothesis is that the j^{th} linear model is no different than the true nonlinear model used to generate the data. The probability distribution function for the log likelihood function, ξ_0 , is χ^2 with NL degrees of freedom, where N is the number of observations and L is the number of observed state variables. The log likelihood function, ξ_1 , for the alternate hypothesis, \mathcal{H}_1 , is generated by the filter for each of the postulated linear models. If ξ_1 falls within the critical region, α , for a two-tailed test on the χ^2 distribution, with NL degrees of freedom, the null hypothesis is rejected. The power of the test, $1-\beta$, is the fraction of times ξ_1 falls within the critical region.

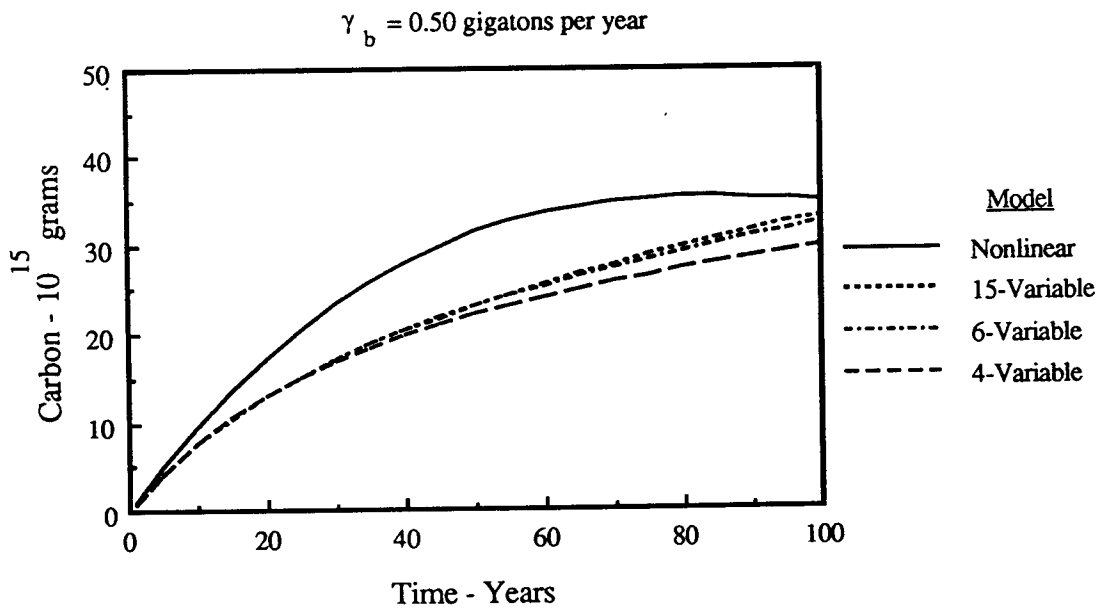
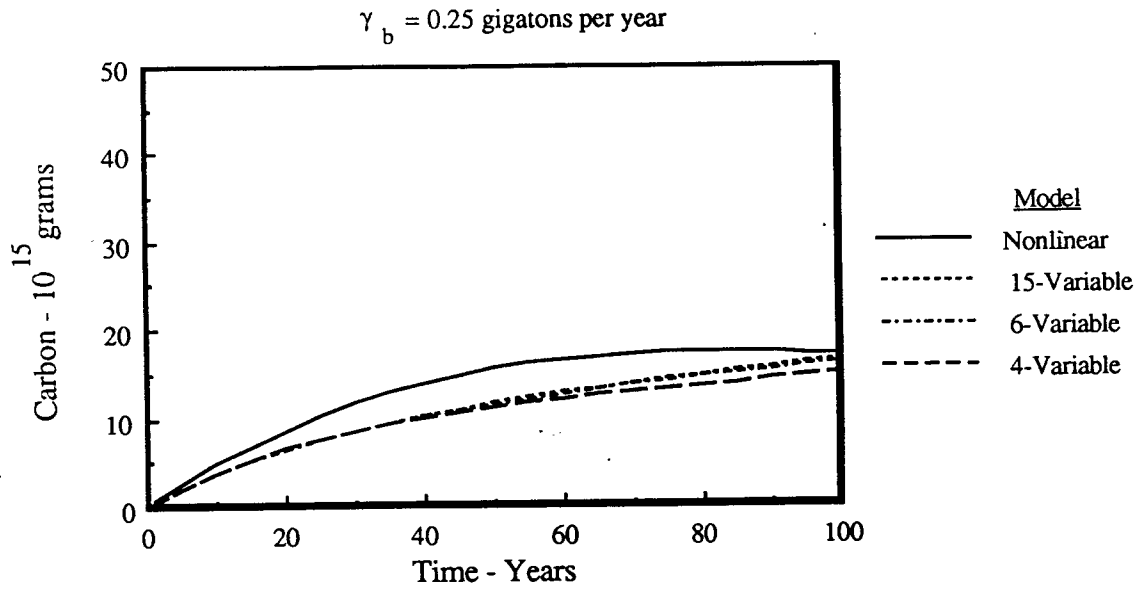


Figure 4.3 . Simulated deviations of carbon from equilibrium conditions for the atmospheric compartment. Loadings from the terrestrial biota are 0.25 and 0.5 gigatons per year.

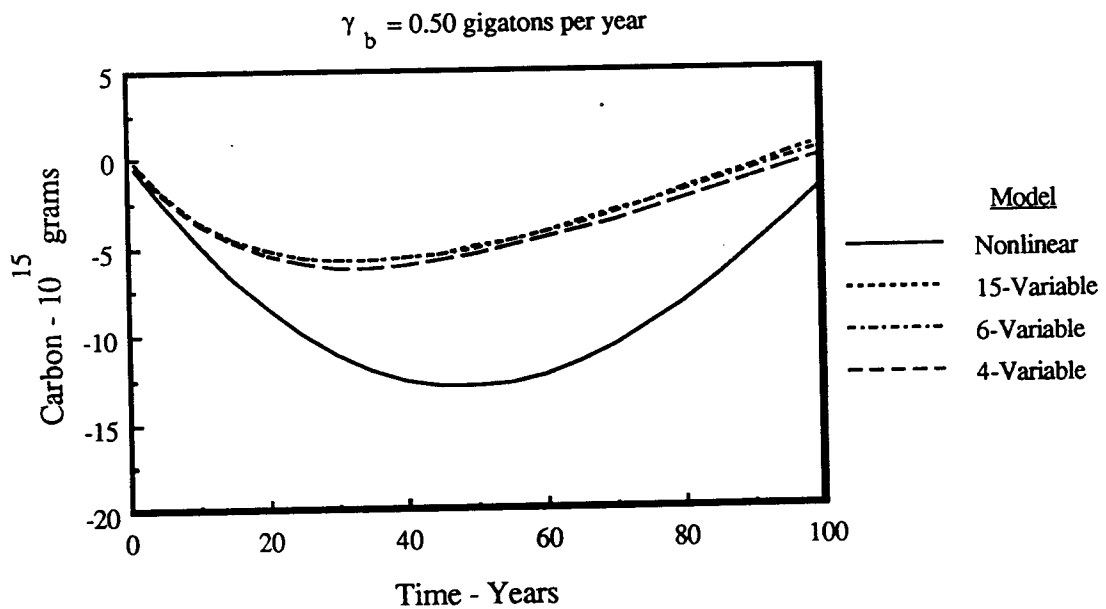
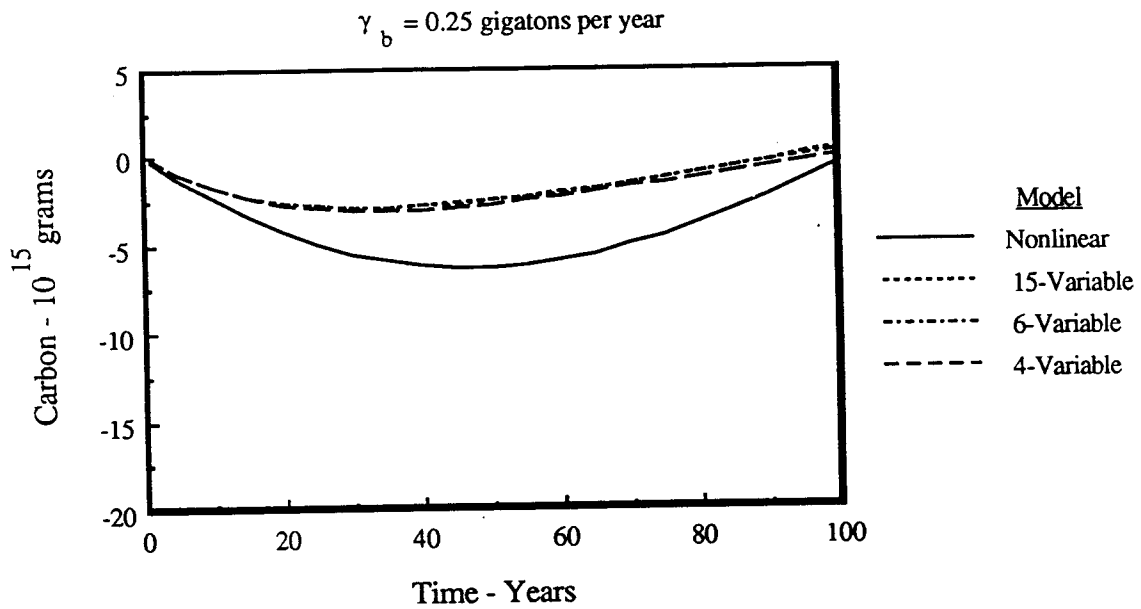


Figure 4.3 (continued) . Simulated deviations of carbon from equilibrium conditions for the terrestrial biota compartment. Loadings from the terrestrial biota are 0.25 and 0.5 gigatons per year.

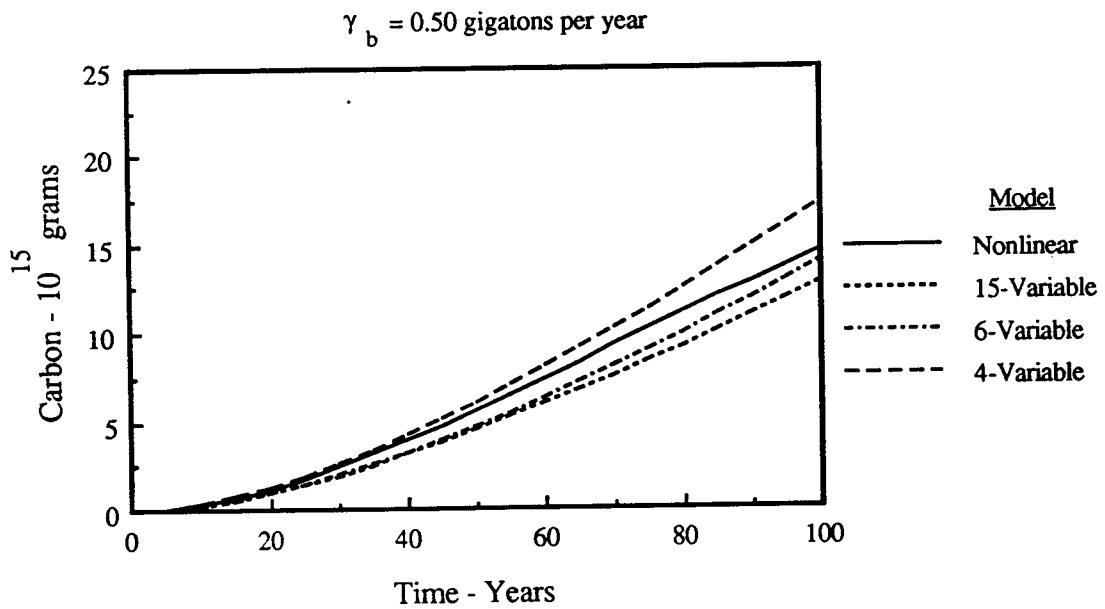
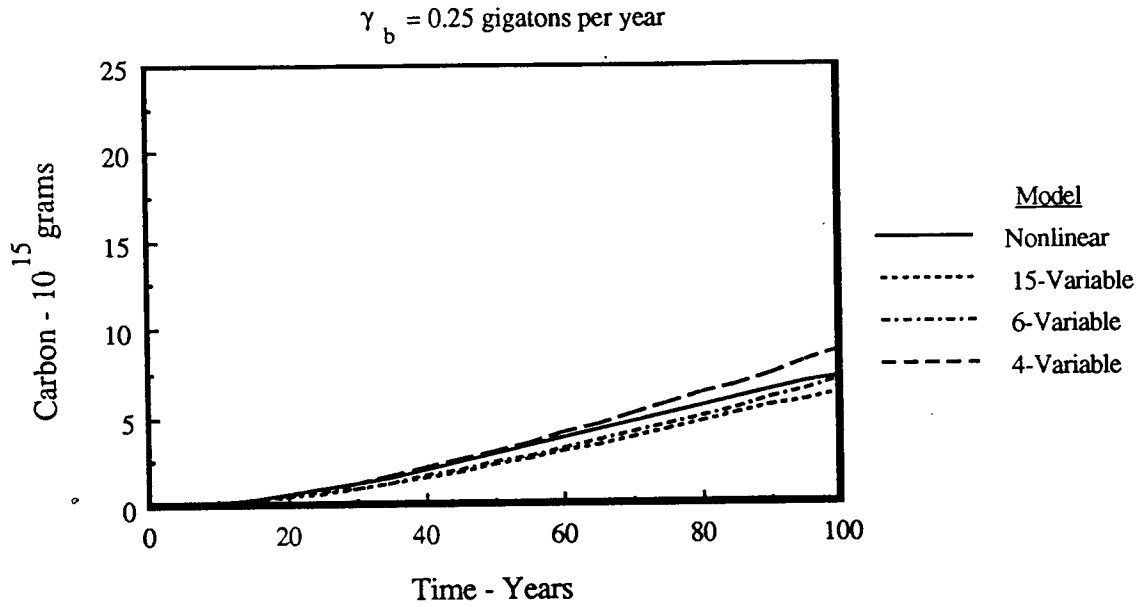


Figure 4.3 (continued). Simulated deviations of carbon from equilibrium conditions for the intermediate/deep ocean compartment. Loadings from the terrestrial biota are 0.25 and 0.5 gigatons per year.

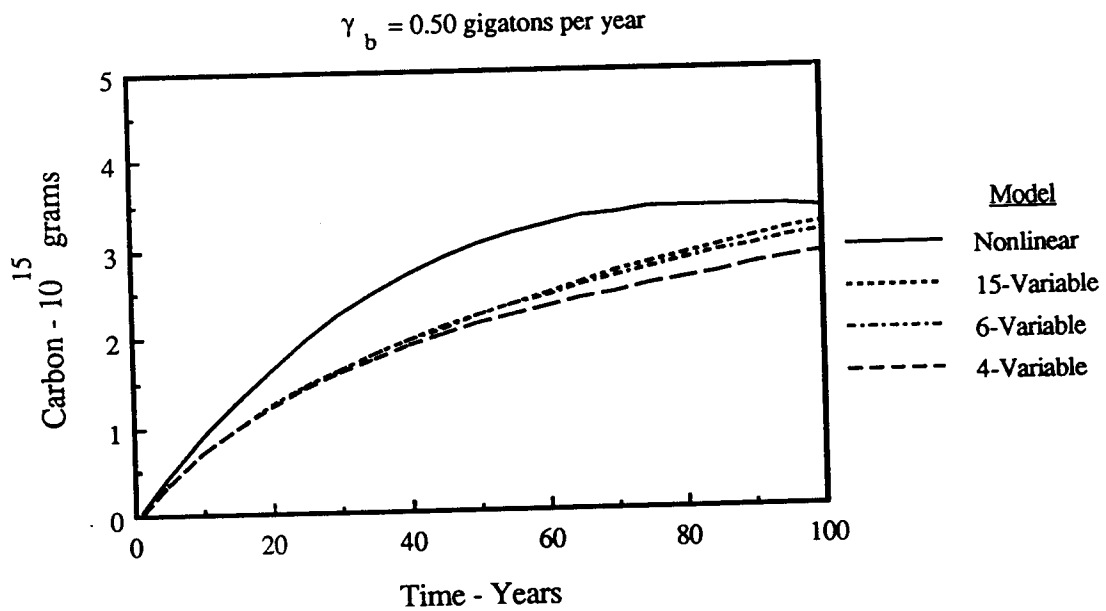
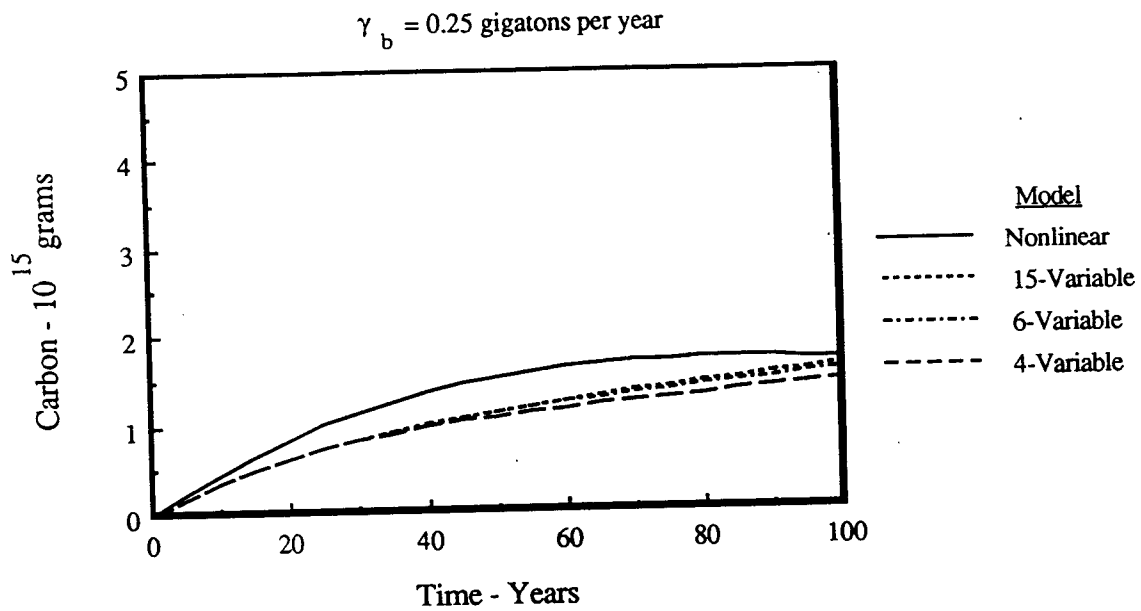


Figure 4.3 (continued). Simulated deviations of carbon from equilibrium conditions for the surface ocean compartment. Loadings from the terrestrial biota are 0.25 and 0.5 gigatons per year.

When ξ_1 has a distribution that is the same ξ_0 , the power of the test will be equal to the size of the critical region α . Congruency of the two distributions means that the postulated model is consistent, in terms of the test, with the model that generated the data. This is equivalent to stating that the postulated model is a valid one. Therefore, high levels of model validity are associated with values of $1-\beta$ that are approximately equal to α . Low levels of model validity are associated with values of $1-\beta$ close to $1-\alpha$.

The validity of each of the three linear models was tested using data generated by the reference systems model for the four scenarios described in Table 4.2. For each level of model complexity, corresponding to the fifteen-compartment, six-compartment and four-compartment models, the power of the model to discriminate against the null hypothesis was determined for a critical region $\alpha=0.05$. The trajectories of the power as a function of time, for each of the three models and for the scenarios described in Table 4.2, are shown in Figure 4.4.

In all cases in Figure 4.4, the power to reject the null hypothesis is moderately high at the beginning, indicating a moderately low level of model validity. Initially, when only limited data are available, the filter gives higher weight to the noise-corrupted measurements. As the amount of data increases, the filter begins to weight the model results more heavily, such that eventually only the differences in the mean values are important.

The power of the test to differentiate between the true nonlinear model and the linear models is influenced by both the level of the load and the measurement error. When the coefficient of variation of the error is 1% and the loading from the terrestrial biota is 0.25 gigatons per year, the hypothesis testing showed that the models were valid at all three levels of aggregation for the entire 100-year simulation period (Fig. 4.4a). Maintaining the coefficient of variation at this same level but increasing the loading rate to

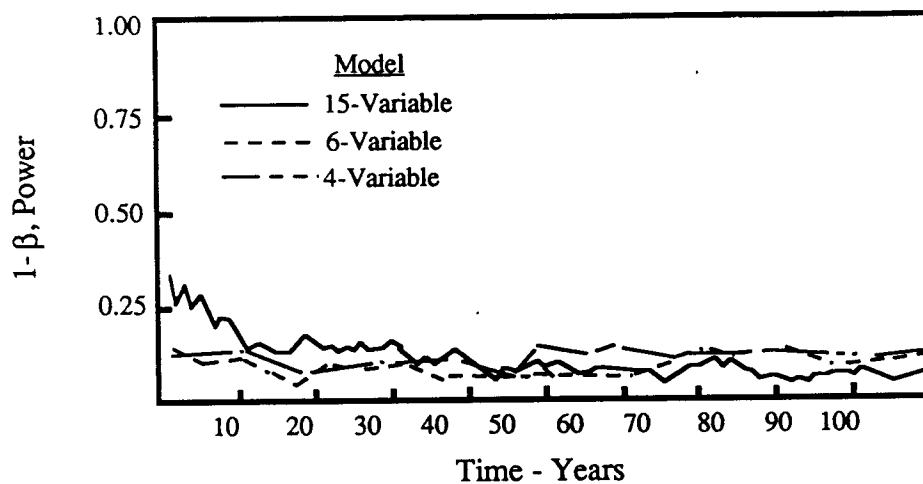
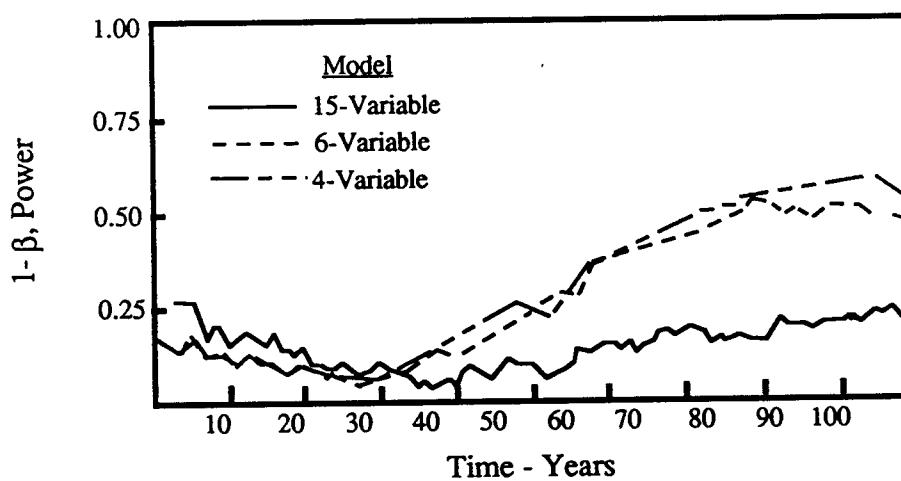
$\gamma_b = 0.25$ gigatons per year $\gamma_b = 0.50$ gigatons per year

Figure 4.4. Time history of the power to reject the null hypothesis for three models of the global carbon cycle under two different loading scenarios from the terrestrial biota and $CV = 0.01$.

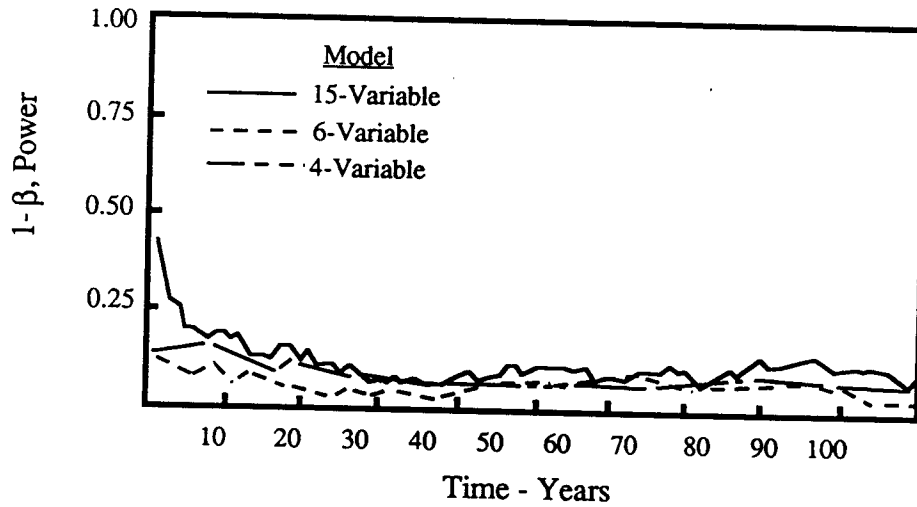
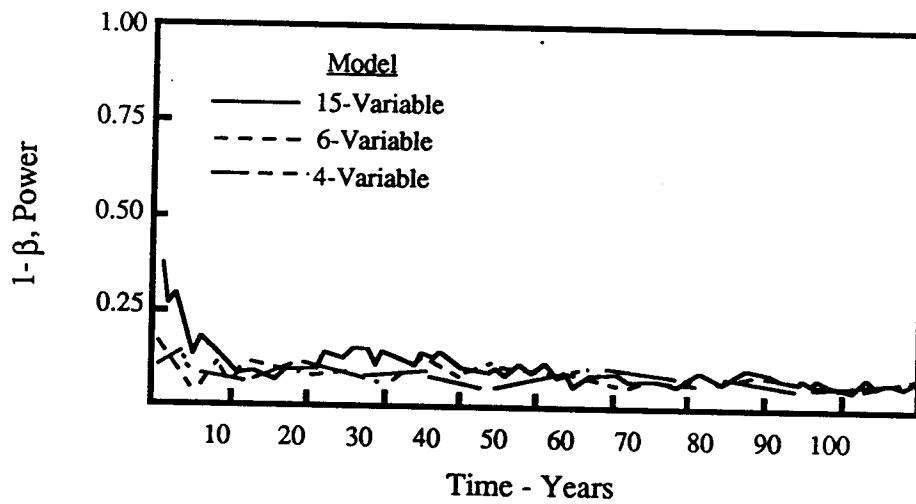
$\gamma_b = 0.25$ gigatons per year $\gamma_b = 0.50$ gigatons per year

Figure 4.4 (continued). Time history of the power to reject the null hypothesis for three models of the global carbon cycle under two different loading scenarios from the terrestrial biota and $CV = 0.10$.

0.50 gigatons per year gave rise to deterioration of the linear model simulations after approximately 40 years (Fig. 4.4b). The performance of the two models with the highest levels of aggregation, the six- and four-compartment models was the poorest. That is, they were the most likely to be discriminated from the true world. The way in which this happens can be explained by examining the contributions to the likelihood function from individual compartments. For the i^{th} compartment and given the j^{th} hypothesis, the individual contribution to the likelihood function $\xi_{i,j}$ is given by

$$\xi_{i,j,\text{obs}}(n) = \delta_{i,j}(n) \sum_{l=1}^L (\Sigma_{il,j}(n) \delta_{l,j}(n)) \quad \text{for } i = 1, \dots, L \quad (4.3)$$

with

$$\Sigma_{il,j}(n) = [\mathbf{H}_j(n) \Sigma_j(n|n-1) \mathbf{H}_j^T(n) + \mathbf{R}_j(n)]_{il}^{-1} \quad (4.4)$$

When the hypothesis, \mathcal{H}_j , is true and when the number of data, N , is large, the individual components of the likelihood function, $\xi_{i,j}$, have normal distribution with a mean of N and variance of $2N$ (Schweppe, 1973). The average value of the individual components for 100 simulations were computed for the case in which the loading from the terrestrial biota was 0.5 gigatons per year, the coefficient of variation was 1%, and the number of data, N , was 100. The results, combined so the three levels of aggregation can be easily compared, are given in Table 4.6. If the null hypothesis is true, the combined contributions should be approximately equal to NL_i , where L_i is the total number of combined states in the i^{th} aggregated compartment ($i=1,2,3,4$). The difference, Δ , between the observed value and the value that results when the null hypothesis is true is the portion of the likelihood function that contributes to rejecting the

Table 4.6. Contributions of various (combined) compartments to the likelihood function, ξ_{ij} , compared to the theoretical contribution to the likelihood function, NL_i , when the null hypothesis is true.

Compartment 1: Terrestrial biota and soil

No. of state variables in model	$\xi_{1,0}$	L_1	NL_1	$\Delta_1 = \xi_{1,0} - NL_1$
15	229	2	200	29
6	230	2	200	30
4	124	1	100	24

Compartment 2: Deep/Intermediate ocean

No. of state variables in model	$\xi_{2,0}$	L_2	NL_2	$\Delta_2 = \xi_{2,0} - NL_2$
15	1003	3	1000	3
6	101	1	100	1
4	101	1	100	1

Table 4.6 (continued). Contributions of various (combined) compartments to the likelihood function, $\xi_{i,j}$, compared to the theoretical contribution to the likelihood function, NL_i , when the null hypothesis is true.

Compartment 3: Atmosphere

No. of state variables in model	$\xi_{3,0}$	L_3	NL_3	$\Delta_3 = \xi_{3,0} - NL_3$
15	118	1	100	18
6	129	1	100	29
4	131	1	100	31

Compartment 4: Ocean surface

No. of state variables in model	$\xi_{4,0}$	L_4	NL_4	$\Delta_4 = \xi_{4,0} - NL_4$
15	200	2	200	0
6	200	2	200	0
4	100	1	100	0

Totals

No. of state variables in model	ξ_0	L	NL	$\Delta = \xi_0 - NL$
15	1560	15	1500	60
6	660	6	600	60
4	456	4	400	56

null hypothesis. These contributions are also given in Table 4.6. It is clear from Table 4.6 that the primary contribution to rejecting the null hypothesis comes from the atmospheric, terrestrial biota, and soil compartments. It is also evident from Table 4.6 that the absolute contributions from each of these compartments is nearly the same for all three levels of aggregation. However, the relative contribution is substantially less for the fifteen-compartment model because of the presence of the ten oceanic compartments. The mean of the likelihood function for the fifteen-compartment model is, therefore, influenced less by the errors in simulation of the atmosphere, terrestrial biota, and soil than the for the six- and four-compartment models. It is also apparent that the fifteen-compartment simulates the atmospheric component somewhat more accurately than do the other two more highly aggregated compartments.

When the coefficient of variation for the error was increased to 10% of the steady-state compartment values, the power to detect the null hypothesis was of the order of the level of significance of the test at both loading levels (Figs 4.4c and 4.4d). At this level of measurement error, none of the linearized, aggregated models could be discriminated from the nonlinear reference system model

Estimating the worth of measurements from a given compartment or aggregated compartment is a requirement for establishing data collection priorities. These priorities can be inferred from the way in which increases in measurement uncertainty affect the ability to detect change. For a given level of measurement error, this can be determined by the length of time (number of measurements) required for the sequential testing to reject the null hypothesis, \mathcal{H}_0 , that there is no loading against the hypothesis, \mathcal{H}_1 , that there is a given loading. This was done by defining the upper and lower threshold for equations (3.6) and (3.7) and then investigating the way in which changes in measurement error affected the time to detect a change. The upper and lower thresholds

were defined by fixing the Type I and Type II errors at $\alpha = \beta = 0.05$. The base level of measurement error was characterized by a coefficient of variation of 1% for each compartment. The coefficient of variation for a given compartment was then increased from the base level of 1% up to a maximum of 20%, while keeping other compartments at the base level.

The length of time required to detect the difference between two hypotheses, \mathcal{H}_0 and \mathcal{H}_1 , provided a measure of the importance of measurement uncertainty in the compartment for which the uncertainty was varied. Compartments in which the detection time increased rapidly with increases in measurement error could then be identified as ones with high priority for improving measurement quality, while the converse would be true for those compartments that responded slowly, or not at all, to changes in measurement error. Compartments evaluated in this way included the atmosphere, terrestrial biota, soil, ocean surface, and the intermediate/deep ocean layers. The results of this analysis for two different levels of input from the terrestrial biota are shown in Figures 4.5 through 4.9.

The compartments for which detection times change most rapidly as a function of measurement error are the living terrestrial biota and atmospheric compartments. For the six- and fifteen-compartment models, increasing the measurement error, as represented by the coefficient of variation, from 1% to 20% in the terrestrial biota or atmospheric compartments, results in an approximate two-fold increase in the time required to detect the input (Figs 4.5 and 4.6). The four-compartment model is even more sensitive to increases in the measurement error of these compartments. The effect of measurement error in the soil compartment is of less importance, but still significant (Fig 4.7). This is particularly true in the case of the four-compartment model.

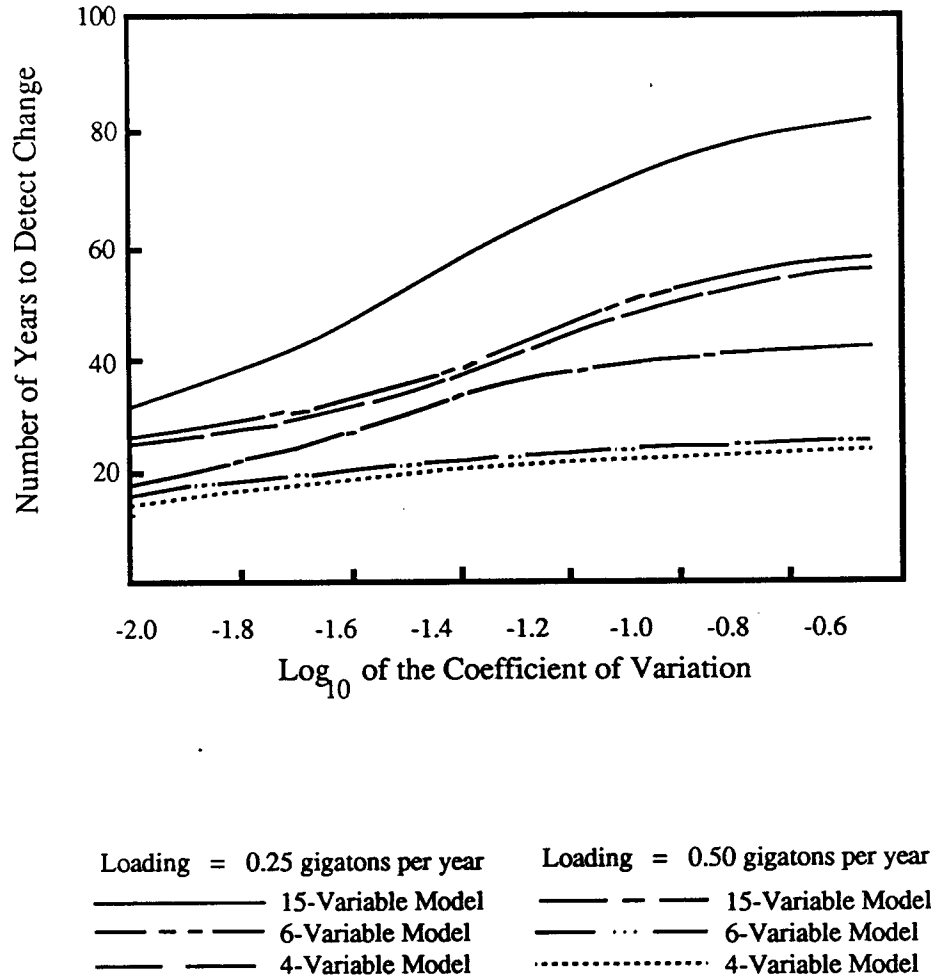


Figure 4.5. Time required to detect an input from the terrestrial biota when the measurement error of the atmospheric compartment is varied

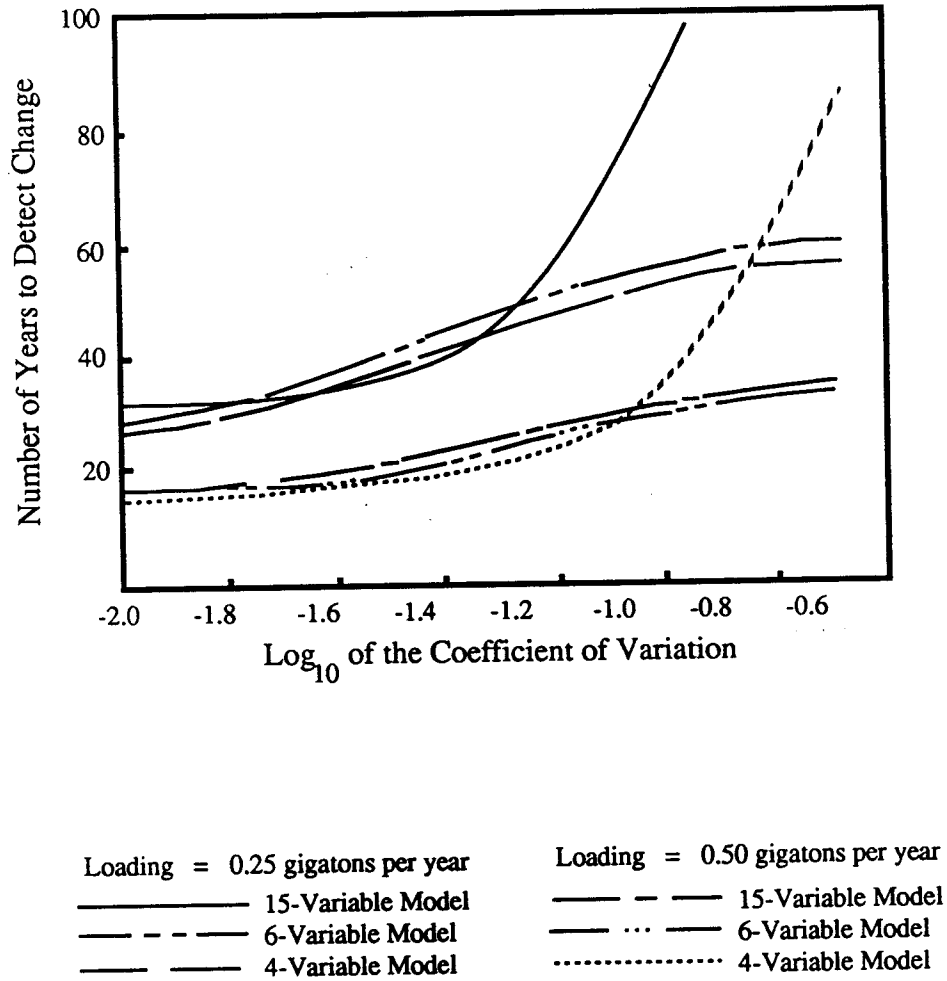


Figure 4.6. Time required to detect an input from the terrestrial biota when the measurement error of the terrestrial biota compartment is varied.

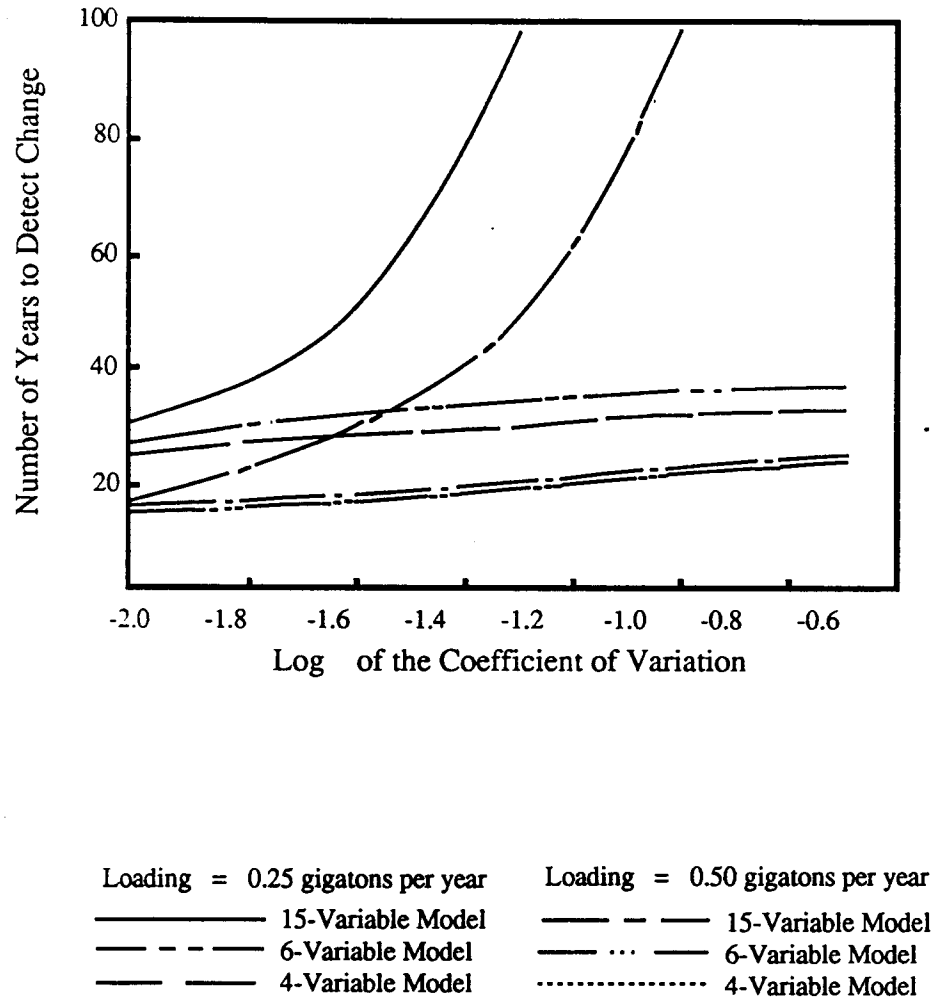
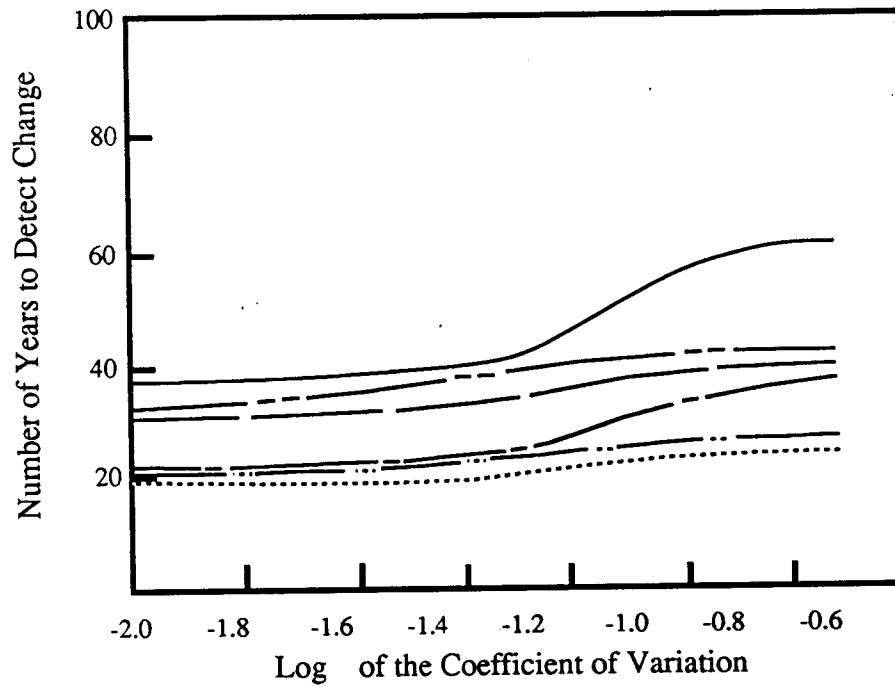


Figure 4.7. Time required to detect an input from the terrestrial biota when the measurement error of the soil compartment is varied.



Loading = 0.25 gigatons per year	Loading = 0.50 gigatons per year
————— 15-Variable Model	——— ——— 15-Variable Model
----- 6-Variable Model	——— ... —— 6-Variable Model
————— 4-Variable Model 4-Variable Model

Figure 4.8. Time required to detect an input from the terrestrial biota when the measurement error of the deep and intermediate ocean compartments are varied.

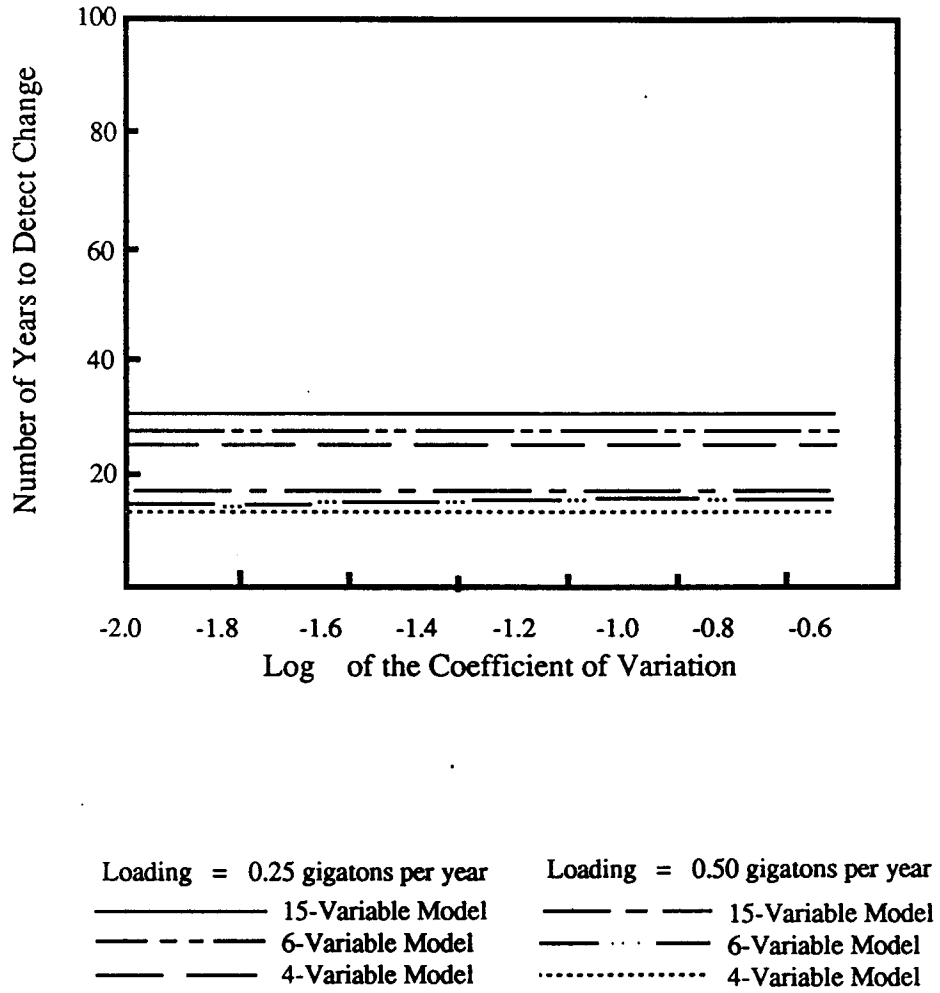


Figure 4.9. Time required to detect an input from the terrestrial biota when the measurement error of the ocean surface compartments are varied.

The role of the oceanic measurements in detecting input from terrestrial biota is very small. The deep and intermediate ocean compartment measurements have a slight effect on the detection times for the fifteen- and six-compartment models, and a somewhat larger effect on detection times for the four-compartment model (Fig. 4.8). The measurements in the two ocean surface layers have no noticeable effect on detection times for either loading level for any of the three levels of model aggregation (Fig. 4.9).

V. Summary

While the results presented in this chapter are specific to the global carbon cycle they do demonstrate the way in which linear state-space models and hypothesis testing can be used to determine the relative value of measurements compared to model complexity. These concepts were used to test model validity. They were also used to develop relationships characterizing the trade-off between model complexity and data worth when the criterion was the time to detect changes in the global carbon cycle caused by the consumption of fossil fuels and terrestrial biota. For purposes of designing sampling programs to detect such changes, the methodology illustrated the importance of the dynamic response of state variables. For detecting changes in atmospheric carbon due to fossil fuel and terrestrial biota consumption, the study showed that there was little value in measurements made in those compartments with very fast response times (the ocean surface) or very slow times (the intermediate and deep ocean).

CHAPTER 5

NONLINEAR MODELS: AN ASSESSMENT OF MODEL COMPLEXITY AND DATA WORTH IN AN HYPOTHETICAL LAKE ECOSYSTEM

5.1. Introduction

Cultural eutrophication of lakes and reservoirs, characterized by the proliferation of nuisance algal blooms, has been a major concern of state and federal environmental agencies. Excessive loadings of nutrients, particular phosphorus, and, to a lesser degree, nitrogen have been cited as the primary sources of the problem (Vollenweider, 1968). Treatment facilities for controlling these nutrients are expensive to construct and operate. Studies such as the one conducted for EPA by Horowitz and Bazel (1978) have been critical of state and federal environmental agencies for subsidizing such facilities in the absence of adequate environmental assessments. It is clear that the environmental assessments of lakes for which there is a potential for cultural eutrophication should be done with care.

The need for obtaining accurate assessments of the effects of cultural eutrophication in rivers, lakes, and reservoirs has led to the development of numerous models of lake ecosystems. These models range in complexity from the very simple models of total phosphorus (Dillon, 1975; Larsen and Mercier, 1976; Vollenweider, 1975) to very complex ecosystems models (Thomann et al., 1975; Patten et al., 1975; DiToro et al., 1975; Chen and Orlob, 1975; Scavia, 1980). While the simple models of total phosphorus are appropriate only for aquatic environments in which phosphorus is the limiting nutrient, they have proven of value for estimating the state of eutrophication in lakes as small as 3.43 hectares (Mericas and Malone, 1984) and as large as the Great Lakes system (Chapra, 1977). Development of more complex models has been in

response to the need to understand, manage, and control eutrophication problems in the broader context of growth limited by the availability of more than one nutrient and/or the availability of light. Another important factor in the development of more complex models has been the need to characterize the variability of state variables in both time and space.

Despite the attention given to the development of eutrophication models, many questions remain regarding the degree of complexity required in such models. Extensive studies both in the field and laboratory are often necessary to make such models more complex. Unfortunately, it is not always the case that these efforts lead to increases in the accuracy of the state estimates (Schindler, 1987). The development of more complex models requires additional efforts for identifying model structure and for estimating the parameters in the model once model structure has been identified. It is often difficult and expensive to design and carry out the appropriate experiments.

Another issue in the development of lake ecosystem models that has received limited attention is the characterization of the uncertainty of ecosystem models. Scavia et al. (1981) used Monte Carlo methods and first-order uncertainty to obtain variance estimates for a dynamic eutrophication model of Saginaw Bay, Lake Huron. Mericas and Malone (1984) examined the variability in total phosphorus concentrations in a small hypereutrophic lake. They conducted this examination by modifying the basic Vollenweider model so that it included stochastic processes. Ferrara and Griffin (1986) investigated the value of increase in model complexity for trophic state simulation in reservoirs by comparing the predictions from a model of total phosphorus with predictions from a multicomponent model that included three forms of phosphorus and dissolved oxygen. They used a number of test statistics for their analysis, including the root-mean-squared error, the t-statistic, and the differences in the means of the

predictions. Ferrara and Griffin (1986) concluded that for long-term, steady-state conditions there was little difference between the two models. However, for the time-dependent case the predictions from the two models were significantly different from one another.

An example in which hypothesis testing was used to assess model validity has been described by Thomann et al. (1979). They used the t-statistic to determine a verification "score" for a three-dimensional eutrophication model of Lake Ontario. Thomann et al. did not, however, extend their analysis to include making decisions about whether to accept or reject the model based upon the results of the test. Rather they used the results to make qualitative statements to describe model effectiveness.

The methodology described in Chapter 3 provides a quantitative means of both assessing model validity and detecting changes in the state of an environmental system. Once the levels of Type I and Type II error have been established the method provides a mechanism for deciding whether or not to accept the model and then to decide whether or not there has been an impact on the environment. The method for evaluating model complexity and data worth in linear state-space models was demonstrated in Chapter 4 with specific emphasis on the global carbon cycle. The spectrum of lake eutrophication models includes both linear and nonlinear models, however. Therefore, this application of hypothesis testing to the analysis of lake eutrophication models draws upon the methods for nonlinear models described in Chapter 3. Furthermore, it expands the scope of the analysis to include the role that parameter estimation plays in assessing the trade-off between model complexity and data worth.

5.2. Scope of Analysis

Models developed to assess the impacts of cultural eutrophication and to develop management strategies for controlling it, describe the flow of nutrients between and within the trophic levels of the lake ecosystem. The process of model identification and parameter estimations for these models has been based upon numerous studies both in the laboratory and in the field. The predominant approach to the development of lake ecosystems model has been to formulate them with state-space structure. There has also been a general consensus regarding the kinetics of important processes such as nutrient uptake and light limitation. Due to many of the difficulties associated with data collection and modeling, there is still debate about the validity of the structure most commonly used for ecosystem models. Nevertheless, the work described in this chapter is based upon the notion that existing lake ecosystem models, widely applied and tested under field conditions, represent the important features of these systems.

Based upon the assumption that there are ecosystems models available that describe the state space for lake ecosystems, a system of reference models was developed. The reference model system used to generate the state variables for the prototype ecosystem was comprised of two models (Fig. 5.1). One model was used to generate water temperatures and one was used to generate the ecosystem state variables. The specific lake ecosystem model used as the reference model for this analysis was based upon work done by Tetra Tech (1980). The Tetra Tech model has been used to make environmental assessments of eutrophication under a wide variety of field conditions. Examples of applications include Lake Washington (Chen and Orlob, 1975) near Seattle, Washington, San Francisco Bay (Chen and Orlob, 1975), and Lake Harding on the Chattahoochee River in Georgia (Tapp, 1978). The Electric Power Research Institute (EPRI) has supported the development of the Tetra Tech model

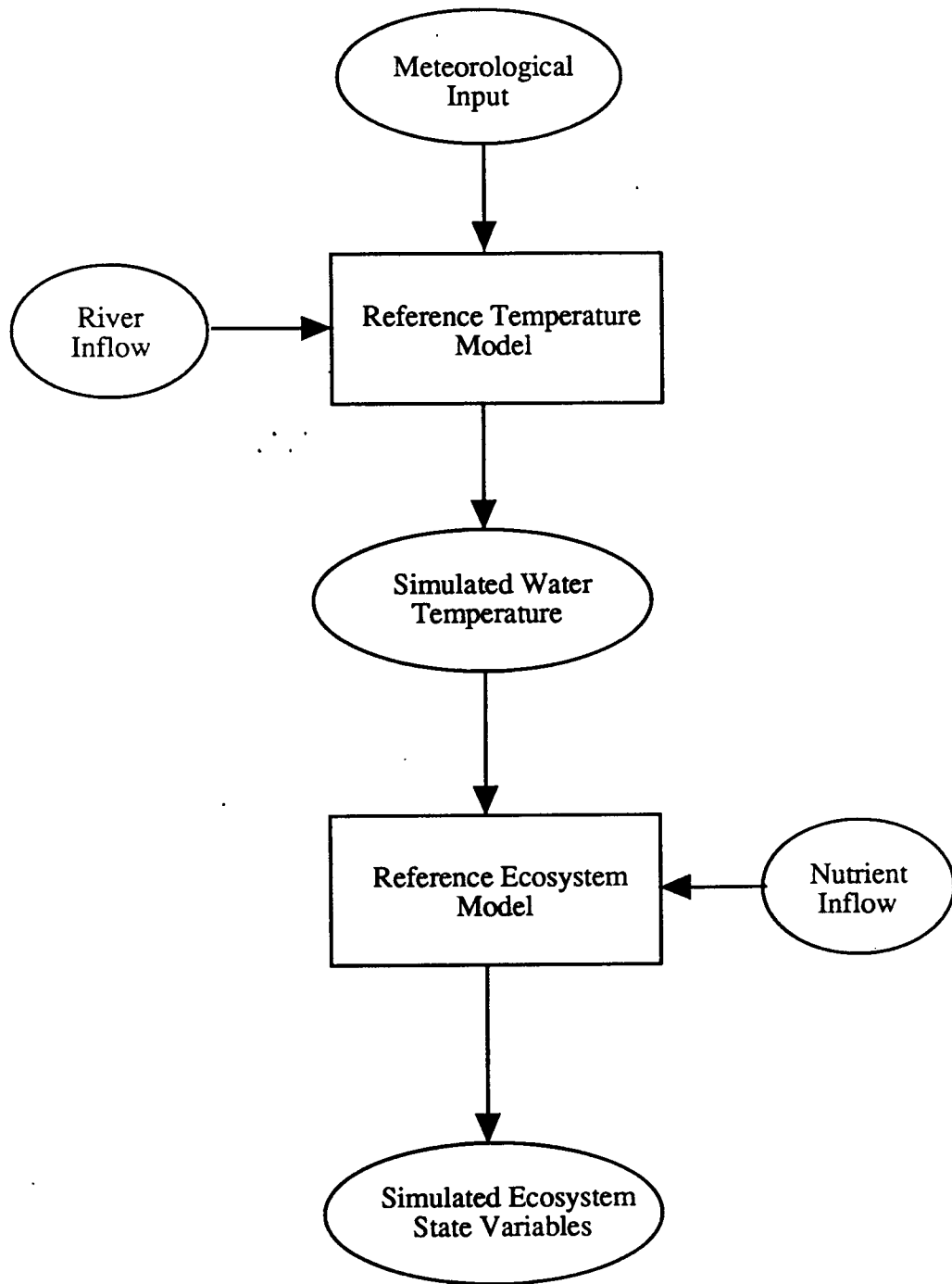


Figure 5.1 Schematic diagram of system of reference models used to generate ecosystem state variables

to evaluate the flow of energy and nutrients in power plant cooling systems. The model structure is similar to that of other well-tested models (Scavia, 1980; DiToro et al., 1975).

In the analysis of the global carbon cycle, it was assumed that the generating model was completely deterministic. This restriction was removed from the lake ecosystem model by specifying the environmental forcing functions of heat flux and nutrient loading rates as stochastic processes. The nature of the uncertainty for these forcing functions was developed from data used for the study of Lake Washington.

It was also possible to better define the nature of measurement error for lake ecosystems compared to the global carbon cycle. Estimates of the magnitudes of measurement error were obtained from the results of a number of laboratory and field studies (Bottrell et al., 1976; Marquis, 1985; EPA, 1980b and Scavia et al., 1981).

The hypothesis testing methodology of Chapter 3 was applied to the data generated with the reference system model to investigate issues of model complexity and data worth in the hypothetical lake ecosystem. Three levels of model complexity were postulated (Fig. 5.2). For each level of complexity the null hypothesis, \mathcal{H}_0 , was that the postulated model was the same as the reference system model. The alternate hypothesis, \mathcal{H}_1 , was that the postulated model was not the same as the reference model. These hypotheses formed the basis for testing the validity of each of the postulated models with respect to the data generated synthetically by the reference model.

The three levels of complexity identified in Figure 5.2 correspond roughly to the way in which ecosystems analysts increase the complexity of their analyses of lake ecosystems. The least complex model (Fig. 5.2a) corresponds to the single-compartment total phosphorus model that has been used for the analysis of steady-state

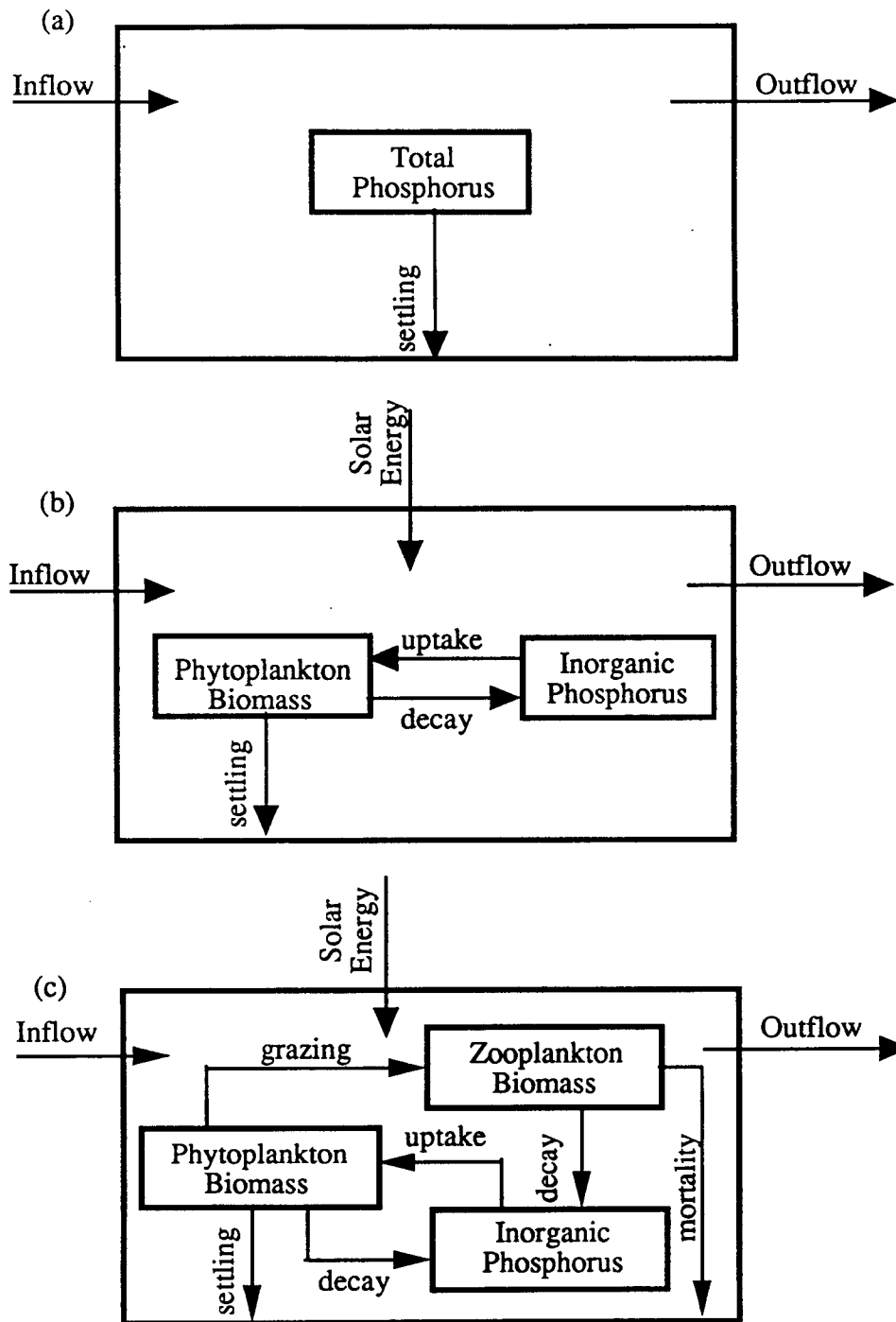


Figure 5.2. Postulated models of three different levels of complexity: (a) total phosphorus model, (b) phytoplankton and limiting nutrient model, (c) phytoplankton, limiting nutrient and zooplankton model.

(Vollenweider, 1968) and time-dependent (Chapra, 1977; Mericas and Malone, 1978; Lorenzen, 1979) conditions. The second level of complexity (Fig. 5.2b) is made up of two compartments, dissolved inorganic phosphorus and total phytoplankton population. The highest level of complexity was constructed by including zooplankton as a state variable (Fig. 5.2c).

There were two components of the analysis, model validation and environmental assessment. Hypothesis testing based upon the methodology of Chapter 3 was used as the decision-making tool. For model validation, the hypothesis testing was stated in terms of the following hypotheses:

\mathcal{H}_0 - The null hypothesis that the model generates state variables from the the same population as that from which the observations were taken.

\mathcal{H}_1 - The alternative hypothesis that model does not generate state variables from the same population as the observations.

Environmental assessment of the impact of increased phosphorus loading upon lake eutrophication was state in terms of the hypotheses:

\mathcal{H}_0 - The null hypothesis that the model and data describe a condition in which there has been no impact from increased nutrient loading.

\mathcal{H}_1 - The alternative hypothesis that model and data describe a condition in which there has been an impact from a specific level of increased nutrient loading.

The procedure used for model validation and environmental assessment was similar to that used for the model of the global carbon cycle, with two important exceptions. First of all, for the two highest levels of complexity the ecosystems models have a state-space structure based on nonlinear dynamics. It was necessary, therefore, to generate the likelihood function with the linearized Kalman filter. The other major

difference between the analysis of the lake ecosystem and the global carbon cycle was the way in which parameter estimation was treated. For the lake ecosystems model, parameter estimates were obtained from the generated data. This is in contrast with the analysis of complexity of the global carbon model for which the models of lesser complexity were obtained by aggregating the parameters of the most complex linear model. The major elements of the analysis can be summarized in the following steps:

- Step 1: Generate the time history of the state variables for the prototype lake ecosystem with the two reference systems, the thermal model and the ecosystem model. The time history of the environmental forcing functions includes a period of natural, or background conditions, followed by a period of incremental change.
- Step 2: Sample the prototype by adding measurement error to the state variables generated in Step 1, above.
- Step 3: Estimate system structure parameters and system error using the samples obtained in Step 2, above.
- Step 4: Perform hypothesis testing on background data, using the parameters obtained in Step 3, to assess model validity.
- Step 5: Perform hypothesis testing on the data collected after the incremental change in loading to assess the ability of the model/measurement system to detect environmental change.

5.3. Monte Carlo Methods

Following the generalized procedure described above, the first step was to generate the ecosystem state variables with the two reference models, the temperature model and the lake ecosystem model. The reference system model for the lake ecosystem included the following state variables:

- Zooplankton (two classes)
- Phytoplankton (three classes)
- Attached algae

- Benthic animals
- Detritus
- Organic nitrogen
- Ammonia nitrogen
- Nitrate nitrogen
- Organic phosphorus
- Orthophosphorus
- Dissolved silica
- Detritus
- Organic sediment

For purposes of investigating the nature of model complexity and data worth, the reference ecosystem was assumed to have a simple geometry (Fig. 5.3). It was assumed to be a continuously stirred tank reactor (CSTR) with no vertical or horizontal variations in the state variables.

The temperature in a lake is determined by the transfer of heat between the atmosphere and water surface, both long- and short-wave radiation, advection due to the inflow from tributaries and heat transfer across soil and water boundaries (Fig. 5.4). The state-space formulation for the temperature model is derived from the the conservation equation associated with heat transfer in well-mixed water body (Raphael, 1962; WRE, 1968; Wunderlich and Gras, 1967). The validity of this approach has been demonstrated in a number of cases, including the studies performed by WRE (1968) and Walters (1976). A more complete description of the temperature reference model is given in Appendix II. An implicit formulation of the finite difference method was used to obtain solutions to the heat budget equation.

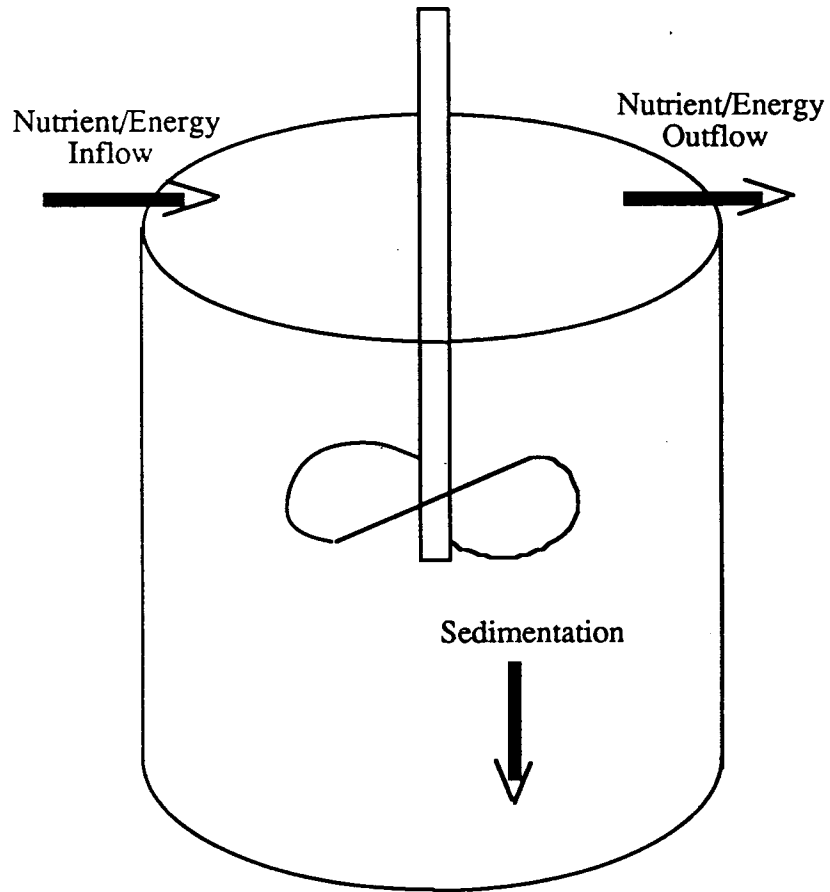


Figure 5.3 The reference ecosystem idealized as a continuously stirred tank reactor (CSTR).

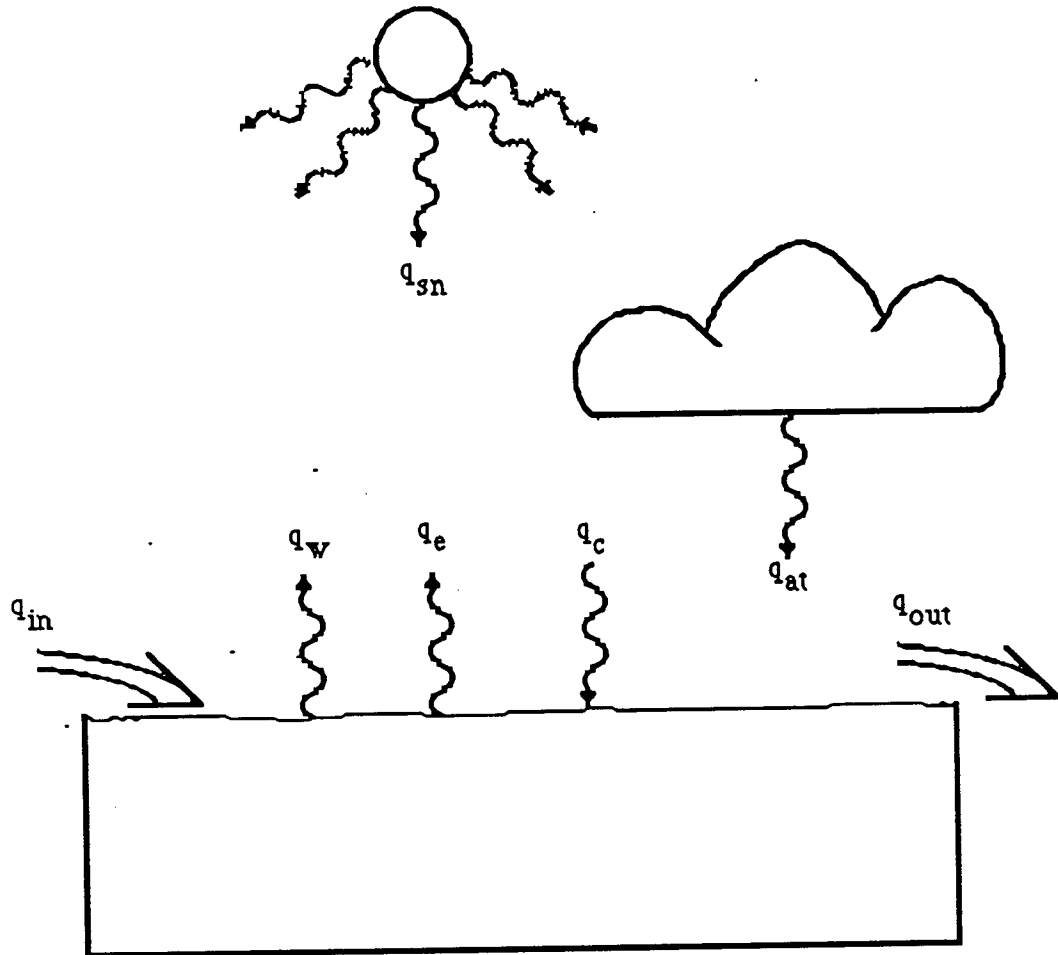


Figure 5.4 Fluxes contributing to the heat budget of the prototype lake.

The lake ecosystem model was based upon the work of Tetra Tech (1980) and was formulated in terms of the conservation equations given in Appendix III. For the hypothetical lake system of Figure 5.3, the model simulates the dynamics of the constituents enumerated above. For this model, Figure 5.5 shows the structural relationship between compartments and the nature of the energy and nutrient transfers. As in the case of the temperature model, the finite difference equations were solved by the implicit method.

The reference model pair, the temperature and ecosystem model, were used in a two-stage process to investigate model complexity and data worth. In the first stage, the primary objective was to verify that the algorithms for parameter estimation and hypothesis testing were working properly, as well as to provide conditions for which it was easier to discern how the fundamental relationships were affected by model dynamics. In this stage the two models were used to simulate daily values of the state variables with the external environmental forcing of solar radiation restricted so there was representative daily variability within a year, but no variability from year to year. Tributary inflow was assumed to be constant throughout the year. Furthermore, the parameters for the ecosystem reference model were chosen so that the reference model was of the same level of complexity as the most complex of the three models being investigated. Randomness in each of the Monte Carlo simulations, for this stage, was a result of superimposing measurement error upon reference model output.

In the second stage of analysis, the problem was made more complex by introducing year-to-year variability into the environmental forcing functions of solar radiation and tributary inflow. The complexity of the ecosystem reference model was also increased to provide a more realistic basis for analysis. Randomness was induced not only by measurement error, but by variability in the environmental forcing functions.

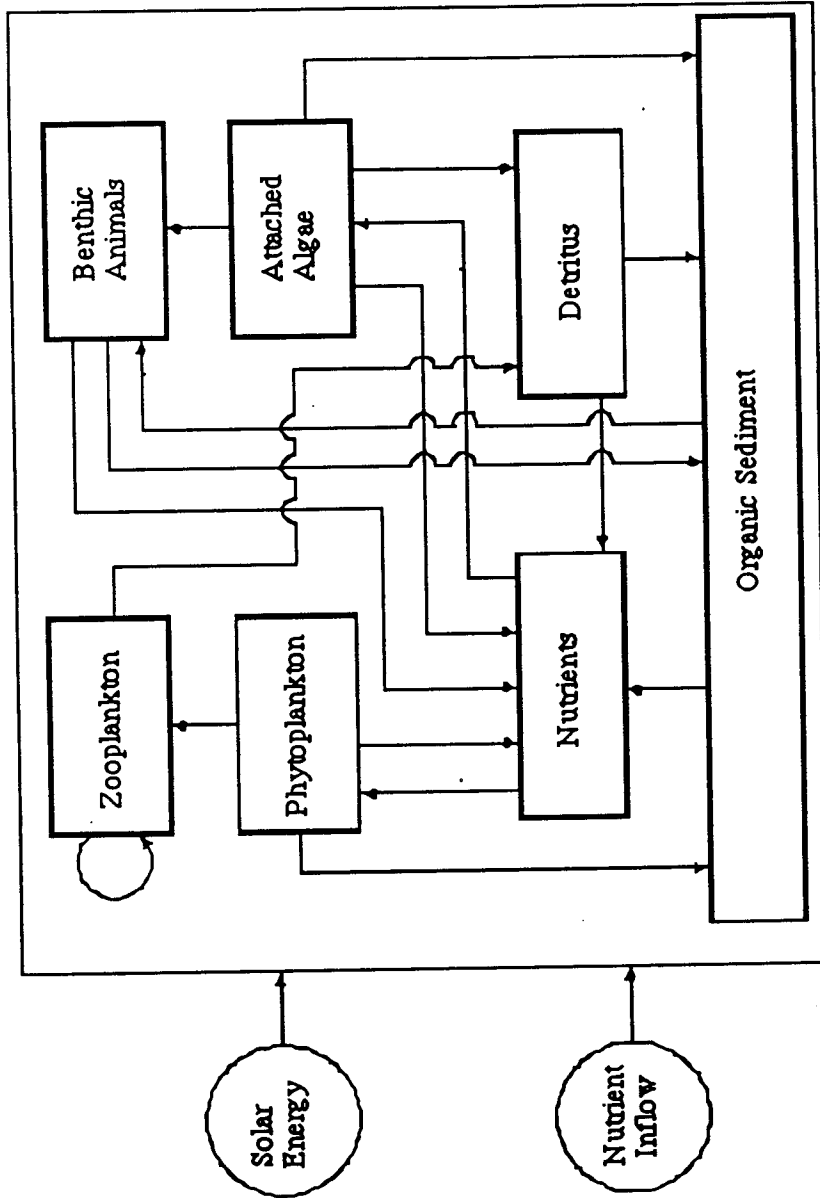


Figure 5.5 Nutrient and energy flow in prototype ecosystem

Actual environmental data was used such that the variability was representative of that which might be expected under natural conditions.

5.4. Measurement Error

In contrast to the global carbon cycle, for which estimates of typical measurement error are difficult to obtain, the extensive interest in and numerous observations of nutrient flow in lakes, rivers, estuaries, and the oceans comprise a considerable data base that can be used to characterize measurement error. The measurement error for state variables in aquatic ecosystem has several components. In a study of spatial heterogeneity in the ocean, Platt et al. (1970) separated the total variance, s_T^2 , into several components as follows:

$$s_T^2 = s_0^2 + s_1^2 + s_2^2 \quad (5.1)$$

where,

s_0^2 = the variance due to sub-sampling and analytical errors,

s_1^2 = the variance of replicates taken at the same location,

s_2^2 = the variance due to real differences between stations.

From their analysis, Platt et al. (1970) concluded that the variance of analytical/sub-sampling errors and replicates accounted for only 10% of the total variance. The real differences between stations was generally much larger, both in space and time. These results, as well as others (Harris, 1980), demonstrate the importance of "patchiness" in the variability of observations of ecosystem states in a marine environment. Similar results have been reported for lake ecosystems. Scavia et al. (1981), in their study of

variance estimates for a dynamic eutrophication model of Saginaw Bay, Lake Huron, determined the standard deviation of eight ecosystem state variables. Their results are given in Table 5.1.

Table 5.1 Range of coefficient of variation for eight ecosystem state variables in Saginaw Bay, Lake Huron (after Scavia et al., 1981).

State Variable	Coefficient of Variation (percent)
Phytoplankton	47-87
Herbivores	36-100
Carnivores	50-100
Organic-N	32-67
Ammonia	44-160
Nitrate	10-88
Organic-P	56-150
PO ₄	20-180

Marquis (1985), in a study of Moses Lake, Washington, also obtained estimates of the variability in the measurements of ecosystem state variables. Marquis (1985) estimated the coefficient of variation of NO₃-N, Total P and Chlorophyll *a* for three different sampling strategies. These strategies included: 1) identical path transects; 2) irregular path transects; and 3) composites. The results are given in Table 5.2.

In a comprehensive review of data collected during the International Biological Program (IBP), Bottrell et al. (1976) examined the methods used to estimate biomass and production of zooplankton. As part of their study they compared the efficiency of various sampling devices. The results, in terms, of the coefficients of variation are given in Table 5.3.

Table 5.2 Coefficient of variation (%) of observations of three ecosystem variables in Moses Lake, Washington using three different sampling strategies (after Marquis, 1985).

Sampling Strategy	NO ₃	Total P	Chlorophyll <u>a</u>
Identical Path Transects			
7/4/83	4	6	3
10/25/83	10	22	24
Identical and Irregular Path Transects			
7/4/83	23	9	18
10/25/83	16	14	16
Identical and Irregular Path Transects and Composites			
7/4/83	47	22	18
10/25/83	15	21	16

Table 5.3 The coefficient of variation (%) in the estimates of the numbers of several species of zooplankton using various sampling devices.

Species	Sampling Device			
	Schindler	Hand Pump	Friedinger	Ruttner
<i>Killicottia longispina</i>	30	40	31	42
<i>Polyarthra vulgaris</i>	28	40	19	23
<i>Bosmina longispina</i>	47	37	51	63
<i>Holopedium gibberum</i>	50	74	60	86
<i>Cyclops nauplii</i>	16	68	38	45
<i>Cyclops copepodites</i>	21	54	21	43

The results of these studies provide a rationale for choosing levels of measurement errors that are representative of those found in actual field studies. As described previously, both the reference model and the postulated models are based upon the assumption that the lake ecosystem behaves as a CSTR. Therefore, the measurement error includes the elements of error enumerated in equation (5.1). However, the definition of error given by Platt et al. (1970) (eq. 5.1) implies temporal as well as spatial variability. In this study of the lake ecosystem, temporal variability is excluded from the definition of measurement error. The discussion of measurement error refers only to subsampling and analytical errors, replication variance, and spatial variance. Aggregating the spatial error in this way makes it less explicit when considering the issue of space-time distribution of sampling design. Nevertheless spatial sampling strategies, such as the ones proposed by Stauffer (1988) for estimating epilimnetic chlorophyll a , can be developed to reduce the measurement error as defined for this study.

Based upon these results, three different scenarios for measurement error were considered. It was assumed that the coefficient of variation for each of the three state variables had one of three values, 10%, 30%, or 50%, and that for any given scenario this value would be the same for all state variables. This range was somewhat less than the maximum ranges shown in Tables 5.1 through 5.3, but it was necessary to limit the coefficient of variation to keep the variations small enough such that the first-order approximation was reasonable. When comparing the coefficient of variation used in this analysis it is evident that the range was large enough to represent the variability that might be experienced in a real sampling program.

The results of studies such as those done by Thomann et al. (1979) and Scavia et al. (1981) suggest that the log-normal distribution is a more reasonable characterization of the sampling error. Characterizing the sampling error with this distribution has the

additional virtue of always producing positive values for the random variables. The measurement model used for the analysis of lake ecosystems was, therefore, of the form

$$\ln \mathbf{z} = \ln \mathbf{x} + \ln \mathbf{y} \quad (5.2)$$

The measurement model was incorporated into the Monte Carlo simulations by drawing random variables from a normal distribution with mean, μ_y , and variance, σ_y , given (according to Loucks et al., 1981) by

$$\mu_y = \ln\left(\frac{\bar{x}}{\sqrt{1 + s_x^2/\bar{x}^2}}\right) \quad (5.3)$$

$$\sigma_y^2 = \ln(1 + s_x^2/\bar{x}^2) \quad (5.4)$$

where

s_x^2 = the sample variance

\bar{x} = the arithmetic mean

The normally distributed variables generated in this way were added to the natural logarithm of the value of the state variable simulated by the reference ecosystem model and then transformed into real space by taking the anti-log of the sum. The observation matrix, \mathbf{H} , that was part of the equation which generated the likelihood function (eq. (3.17)) in the filter equations also had to be treated differently. This was done by a first-order expansion (Schweppe, 1973) of the nonlinear observation matrix to give

$$\mathbf{H}^{(1)} = \mathbf{I} \mathbf{x}' \quad (5.5)$$

where

$\mathbf{H}^{(1)}$ = the first-order expansion of the observation matrix, \mathbf{H} , as defined by equation (3.24)

\mathbf{I} = the identity matrix

\mathbf{x}' = a vector whose i^{th} element is equal to $1/x_{i,\text{nom}}$

$x_{i,\text{nom}}$ = the nominal value of the i^{th} state variable along its linearized trajectory

5.5. Model of the Lake Ecosystem

5.5.1 Environmental Characteristics

Simulations of the ecosystem state variables were performed for the hypothetical lake of Figure 5.3 using the reference models described above. The primary environmental forcing functions were assumed to be similar to those that influence Lake Washington. The 20-year meteorological record (January 1952-January 1972) of observations from the U.S. Weather Service's observation station at the Seattle-Tacoma International Airport was the source for data used to describe the transfer of heat across the air-water interface of the hypothetical lake. The solar radiation portion of this record also provided the information necessary to characterize the energy available for photosynthesis. The freshwater inflow characteristics were based upon a similar period of record using data collected by the U.S. Geological Survey at the gaging station on the Cedar River at Renton, (U.S.G.S. gaging station 12-1190) Washington.

In the initial (testing) phase of this part of the study one year of weather data was picked at random from the record at Seattle-Tacoma International Airport and used to establish the heat-flux between the water surface and the atmosphere, as well as to

quantify the solar energy available for photosynthesis. Values for the inflow rate of water and dissolved inorganic phosphorus was held constant so that the behavior of the parameter estimation algorithm and the likelihood estimator could be controlled. The rate of inflow was chosen such that the lake residence time (lake volume divided by mean annual inflow) was one year.

In the second phase of the study, the meteorological data and nutrient loadings were treated as stochastic processes drawn from available data in the following way. The streamflow measurements were obtained from the record of the Cedar River gage at Renton, Washington, described above. These data were adjusted by a constant ratio such that the average annual flow, Q_{avg} , would give rise to an average lake residence time of one (1.0) year, similar to that of the first phase. The water temperature of the inflow was assumed to be equal to the monthly-averaged air temperature at the Seattle-Tacoma International Airport.

For specifying the concentrations of the primary nutrients it was assumed that total and inorganic phosphorus could be treated as flow-dependent variables in a manner similar to that done by Hirsch (1988). Hirsch (1988) treated the concentration of phosphorus as a product of a flow effect, a seasonal effect, a hysteresis effect, and noise. Hirsch's model was simplified in the simulations of the hypothetical lake ecosystem described below by modeling the total phosphorus concentration, TP, as the product of a flow effect, a deterministic component, and noise

$$TP = A * N * Q^B \quad (5.6)$$

where

TP = the total phosphorus concentration

A = the deterministic component

N = the noise component

Q = the river flow

Equation (5.9) can be written in terms of the the loading, $Q*TP$, as

$$TP_{load} = A*N*Q^{B'} \quad (5.7)$$

where $B'=B+1$.

Taking the natural logarithm of both sides gives

$$\ln TP_{load} = \ln A + \ln N + B'*Q \quad (5.8)$$

The coefficients A and B were determined from a least-squares fit of the relationship between the natural logarithm of total phosphorus loading and the natural logarithm of flow for measurements in the Cedar River at Renton, November 1970 through September 1971. The results of the least-squares analysis are given in Table 5.4. Selected results from coastal streams in the State of Washington, in an analysis of total phosphorus measurements at U.S.G.S. NASQAN stations (Faris and Lettenmaier, 1988) are also given in Table 5.4 for purposes of comparison.

The dissolved inorganic phosphorus (PO_4-P) was assumed to be a constant fraction of the total phosphorus corresponding to the mean fraction (0.75) in the record of data from the sampling station at Renton for the same period. The noise term was assumed to have a log-normal distribution with mean and variance calculated from the residuals of the least-squares fit.

Table 5.4. Slope, intercept and R^2 for least-squares analysis of equation (5.7).

Sampling Station	Intercept, ln A	Slope, B'	R^2
Cedar River at Renton, Washington	-14.425	1.577	0.67
Willapa River near Willapa, Washington	-9.864	1.081	0.74
Chehalis River near Chehalis, Washington	-9.397	0.058	0.86
Queets River near Queets, Washington	-12.756	1.358	0.66
Elwha River near Port Angeles, Wash	-12.938	1.403	0.65
Puyallup River near Puyallup, Washington	-10.865	1.299	0.38
Snohomish River near Snohomish, Washington	-11.780	1.200	0.48
Skagit River near Mount Vernon, Wash.	-18.802	1.926	0.49

5.5.2 Ecosystem Model Parameters

Once the state variables have been chosen, it is necessary to specify the parameters in the state-space model before the lake ecosystem data can be synthetically generated. The parameters required for the thermal model and the aquatic ecosystem model, as well as the specific role each of the parameters plays in the dynamics of the state-space equations, are described in Appendices II and III.

The reference models chosen to generate the ecosystem sample space are based upon constructs that derived from field experiments conducted in a number of different aquatic ecosystems. These experiments provide a basis for choosing ecosystem model parameters such that the sample space generated will be representative of of results

obtained in actual ecosystems. For example, Chen and Orlob (1975) applied a model similar to the reference model used in this thesis to simulate the ecosystems dynamics of Lake Washington reported by Chen and Orlob (1975). Scavia (1980) also has provided estimates for typical values of ecosystem parameters in the ecological modelling of Lake Ontario. Scavia et al. (1981) compiled a comprehensive survey of the statistics for ecosystems model parameter values in their study of variance estimates for a dynamic eutrophication model of Saginaw Bay. Zison et al. (1978) and Lehman et al. (1975) have also summarized estimates of parameters for ecologic models. In general, the results of these and similar studies suggest a range of parameters that lead to ecosystem dynamics typical of north temperate lakes. It is from this range that parameters were chosen for the several experiments reported below.

5.6. Model Complexity

The methods of analysis for linear state-space models have been well developed, and, as a result, the investigation of complexity for such models can be based upon a rigorous theoretical foundation. The corresponding theory for nonlinear models has not been developed nearly so well. For this reason, the analysis of model complexity for the nonlinear lake ecosystem models was organized in a way that corresponds to the approach ecologists have used in analyzing lake ecosystems. That is, it followed a trophic level approach to the examination of model complexity (Fig. 5.2). In the least complex model the only state variable was the pool of the limiting nutrient, which in this case was phosphorus. The most complex model was a three-compartment model that included the limiting nutrient, primary producers, and secondary producers.

5.6.1 Model I

The single compartment model with total phosphorus as the state variable has proved to be a useful tool for both limnological research and water quality planning. Vollenweider (1968, 1969) demonstrated the value of this approach in a comprehensive study of the nature of eutrophication of lakes and flowing waters. Vollenweider (1975) incorporated the results of additional limnological studies into a modification of his initial work. A number of others, including Dillon (1975), Dillon and Rigler (1975), Larsen and Mercier (1976) and Chapra and Tarapchak (1976), examined the response of lakes in terms of the constructs of the single compartment total phosphorus. Two typical examples of the way in which the model has been used for water quality planning were in the Great Lakes and in Long Lake, near Spokane, Washington. Chapra (1977) examined the water quality impacts of phosphorus control strategies in the Great Lakes and Patmont et al. (1987) used the model to assist the State of Washington Department of Ecology in establishing a water quality criterion for total phosphorus in Long Lake.

The total phosphorus model, assumes that the water body can be described by a continuously stirred reactor (CSTR), and the budget of total phosphorus is determined by the inflow from natural and anthropogenic sources, outflow and internal losses due to sedimentation (Fig. 5.2a). Given these assumptions and following the notation given by equation (3.1), the state-space structure of the process model for total phosphorus can be written as follows:

$$\mathbf{x}(n+1) = x_1(n+1) = \Phi_{11}(n)x_1(n) + u_1(n) + w_1(n) \quad (5.9)$$

where

$x_1(n)$ = the total phosphorus concentration in the CSTR at time, $t = n$

$$\Phi_{11}(n) = (1 - (\frac{F + w_s A_s}{V}))$$

$$u_1(n) = \frac{W(n)}{V} + F_{in} x_{1,in}$$

$w_1(n)$ = a normally distributed random variable with zero mean and variance, $Q_1(n)$

n = the time increment ($n = 1 \dots N$)

V = the volume of the water body

$W(n)$ = the total phosphorus loading from anthropogenic sources

$x_{1,in}$ = the total phosphorus concentration of the inflow

F_{in} = the inflow rate of water

F = the outflow rate of water

A_s = the lake surface area

w_s = the settling velocity

5.6.2 Model II

Model II is a two-compartment model with two state variables, the primary producers or phytoplankton and the limiting nutrient. In this case, the limiting nutrient is assumed to be phosphorus (Fig. 5.2b). This model has also been widely applied to the investigation of lake eutrophication (cf, Wang and Harleman, 1983, Imboden and Gachter, 1978; Walters, 1980; Gasperino and Soltero, 1977), although in many of these examples the spatial complexity was increased to include variability with depth.

Model II is a nonlinear model with a form similar to, but somewhat simpler than the general nonlinear form defined by equation (3.5). For the CSTR, the mass balance equations for Model II lead to the following discrete-time formulations of the process model:

$$\mathbf{x}(n+1) = \begin{bmatrix} x_1(n+1) \\ x_2(n+1) \end{bmatrix} = \begin{bmatrix} \Phi_{11}(\mathbf{x}(n),n) & \Phi_{12}(\mathbf{x}(n),n) \\ \Phi_{21}(\mathbf{x}(n),n) & \Phi_{22}(\mathbf{x}(n),n) \end{bmatrix} + \begin{bmatrix} u_1(n) \\ u_2(n) \end{bmatrix} + \begin{bmatrix} w_1(n) \\ w_2(n) \end{bmatrix} \quad (5.10)$$

where

$x_1(n)$ = the concentration of inorganic phosphorus at time $t = n$

$x_2(n)$ = the total biomass of phytoplankton at time $t = n$

$$\Phi_{11}(\mathbf{x}(n),n) = 1 - \frac{F}{V}$$

$$\Phi_{12}(\mathbf{x}(n),n) = \beta_p(R_{\Pi} - G_{\Pi})$$

$$\Phi_{21}(\mathbf{x}(n),n) = 0$$

$$\Phi_{22}(\mathbf{x}(n),n) = 1 + G_{\Pi} - R_{\Pi} - \frac{w_s}{\Delta z} - \frac{F}{V}$$

$$u_1(n) = \frac{Fx_{1,in}}{V}$$

$$u_2(n) = \frac{Fx_{2,in}}{V}$$

$\underline{w}(n)$ = a normal random vector with zero mean and covariance, $Q(n)$

$x_{1,in}$ = the concentration of inorganic phosphorus in the inflow

$x_{2,in}$ = the concentration of total biomass in the inflow

G_{Π} = the phytoplankton growth rate (see Appendix III)

R_{Π} = the phytoplankton respiration rate (see Appendix III)

Δz = the average water depth in the lake ecosystem

β_p = the ratio of phosphorus to total biomass in phytoplankton

5.6.3 Model III

Model III is a nonlinear model obtained by adding another trophic level (Wang and Harleman, 1983), secondary producers, to Model II as shown in Figure 5.2c. The state-space structure for the process model is given by

$$\mathbf{x}(n+1) = \begin{bmatrix} x_1(n+1) \\ x_2(n+1) \\ x_3(n+1) \end{bmatrix} = \begin{bmatrix} \Phi_{11}(\mathbf{x}(n),n) & \Phi_{12}(\mathbf{x}(n),n) & \Phi_{13}(\mathbf{x}(n),n) \\ \Phi_{21}(\mathbf{x}(n),n) & \Phi_{22}(\mathbf{x}(n),n) & \Phi_{23}(\mathbf{x}(n),n) \\ \Phi_{31}(\mathbf{x}(n),n) & \Phi_{32}(\mathbf{x}(n),n) & \Phi_{33}(\mathbf{x}(n),n) \end{bmatrix} \begin{bmatrix} x_1(n) \\ x_2(n) \\ x_3(n) \end{bmatrix} + \begin{bmatrix} u_1(n) \\ u_2(n) \\ u_3(n) \end{bmatrix} + \begin{bmatrix} w_1(n) \\ w_2(n) \\ w_3(n) \end{bmatrix} \quad (5.11)$$

where

$x_1(n)$ = the inorganic phosphorus at time $t=n$

$x_2(n)$ = the total biomass of phytoplankton at time $t=n$

$x_3(n)$ = the total biomass of zooplankton at time $t=n$

$$\Phi_{11}(\mathbf{x}(n),n) = 1 - \frac{F}{V}$$

$$\Phi_{12}(\mathbf{x}(n),n) = \beta_p(R_{\Pi} - G_{\Pi})$$

$$\Phi_{13}(\mathbf{x}(n),n) = \beta_{\zeta} \left(\frac{1-v}{v} \right) G_{\zeta}$$

$$\Phi_{21}(\mathbf{x}(n),n) = 0$$

$$\Phi_{22}(\mathbf{x}(n),n) = 1 + G_{\Pi} - R_{\Pi} - \frac{w_s}{\Delta z} - \frac{F}{V}$$

$$\Phi_{23}(\mathbf{x}(n),n) = \frac{G_{\zeta}}{v}$$

$$\Phi_{31}(\mathbf{x}(n),n) = 0$$

$$\Phi_{32}(\mathbf{x}(n),n) = 0$$

$$\Phi_{33}(\mathbf{x}(n),n) = 1 + G_{\zeta} - R_{\zeta} - \frac{F}{V}$$

$$u_1(n) = \frac{Fx_{1,in}}{V}$$

$$u_2(n) = \frac{Fx_{2,in}}{V}$$

$$u_{3,in}(n) = \frac{Fx_{3,in}}{V}$$

$x_{1,in}$ = the concentration of inorganic phosphorus in the inflow

$x_{2,in}$ = the concentration of total phytoplankton biomass in the inflow

$x_{3,in}$ = the concentration of total zooplankton biomass in the inflow

G_{ζ} = zooplankton growth rates (see Appendix III)

R_{ζ} = zooplankton respiration rates (see Appendix III)

β_{ζ} = ratio of organic phosphorus to total biomass in zooplankton

v = the grazing efficiency of the zooplankton

5.7. Results-Constant Environmental Conditions

The reference model and hypothesis testing software used in the analysis were extensive and complex. For purposes of testing the software, as well as to obtain insights into some of the fundamental behavior of the processes, a relatively simple problem was analyzed first. Data were generated by the ecosystems population model for an ecosystem whose level of complexity was equivalent to that of the most complex model, Model III. Values of the structural parameters used in the reference model are given in Table 5.5 and are based upon the results presented by Chen and Orlob (1975) from their work on Lake Washington.

Table 5.5. Parameter values used in the simplified ecosystem reference model.

Parameter	Value
Maximum phytoplankton growth rate	1.0 days ⁻¹
Maximum phytoplankton respiration rate	0.05 days ⁻¹
Michaelis-Menten constant for inorganic phosphorus	0.005 mg/l
Phytoplankton settling rate	0.05 m/day
Optimal solar radiation	0.025 kcal/m ² /sec
Maximum zooplankton growth rate	0.20 days ⁻¹
Maximum zooplankton respiration rate	0.02 days ⁻¹
Zooplankton mortality rate	0.03 days ⁻¹
Michaelis-Menten constant for zooplankton growth	0.50 mg/l C

The environmental forcing functions used in the part of the process also had a simple form. The lake residence time and phosphorus loading rate were specified by fixing both the tributary inflow and total phosphorus concentration at constant values. One year of daily-averaged values of solar radiation, wind speed, air temperature, cloud cover, and relative humidity, drawn at random from a 20-year data record from the Seattle-Tacoma Airport, was used to define meteorologic conditions. In the multi-year sequences of data generated for model testing, the tributary inflow, total phosphorus concentration, and daily meteorologic data remained constant throughout the simulations, based upon these values.

The meteorologic data were first used, in conjunction with the heat-balance model, to develop the thermal regime for the hypothetical reservoir (Fig. 5.3). Temperatures simulated by the heat-balance model were used to define the thermal regime for the simplified version of the ecosystem.

The simplified ecosystem reference model, with a structure identical to Model III, was used to generate sequences of the ecosystem state variables, primary nutrients, primary producers, and secondary producers. Sequences of state variables were generated for conditions representing one year of low nutrient loadings (background), followed by 25 years with a constant increment of nutrient loading added to the background. To ensure that the first year of background conditions represented a quasi-steady-state, the reference model was run an additional five years at the beginning to stabilize any errors introduced by incorrect assumptions regarding initial values of state variables. Scenarios representative of low, medium, and high phosphorus loading conditions were examined, using the background and incremental values given in Table 5.6.

Table 5.6 Scenarios for nutrient loading rate and coefficient of variation of measurement evaluated in the first stage of the ecosystem model tests.

Scenario	PO ₄ -P Conc. of Inflow	PO ₄ -P Conc. Increment	Measurement Error -CV
1	0.01 mg/l	0.001 mg/l	0.1
2	0.01 mg/l	0.001 mg/l	0.3
3	0.01 mg/l	0.001 mg/l	0.5
4	0.02 mg/l	0.002 mg/l	0.1
5	0.02 mg/l	0.002 mg/l	0.3
6	0.02 mg/l	0.002 mg/l	0.5
7	0.05 mg/l	0.005 mg/l	0.1
8	0.05 mg/l	0.005 mg/l	0.3
9	0.05 mg/l	0.005 mg/l	0.5

Each of the sequences generated in this way was basically deterministic since there was no year-to-year variability in the environmental forcing functions. However, within

the year there was natural variability in the meteorologic conditions that gave rise to seasonal (within-year) variations in water temperature and solar radiation. From each of these deterministic sequences, 26-year sequences (one year of background and 25 years of background plus increment) were generated in Monte Carlo fashion by introducing measurement error according to the model described above (eq. (5.2) and Table 5.6). The trajectories of state variables for the first five years, under the various nutrient loading conditions, are shown in Figures 5.6 through 5.8. The sequences generated from the Monte Carlo simulations were used to perform the parameter estimation, model validation, and environmental assessment.

5.7.1 Parameter Estimation

The data sequences from the Monte Carlo simulations were first used to obtain parameter estimates for Models I, II and III. It was necessary to obtain estimates of two types of parameters, those that determine the system structure, Φ (eq. (3.5)), and those that determine the system error covariance matrix, Q . Estimates of the systems structure parameters were based upon minimizing the sum of the weighted-least-squares of the difference between the observed and the simulated state variables. If $J(\theta)$ is a cost function defined by

$$J(\theta) = (\mathbf{z} - \mathbf{x})^T \mathbf{R}^{-1} (\mathbf{z} - \mathbf{x}) \quad (5.12)$$

where

\mathbf{z} = the observation vector, as before

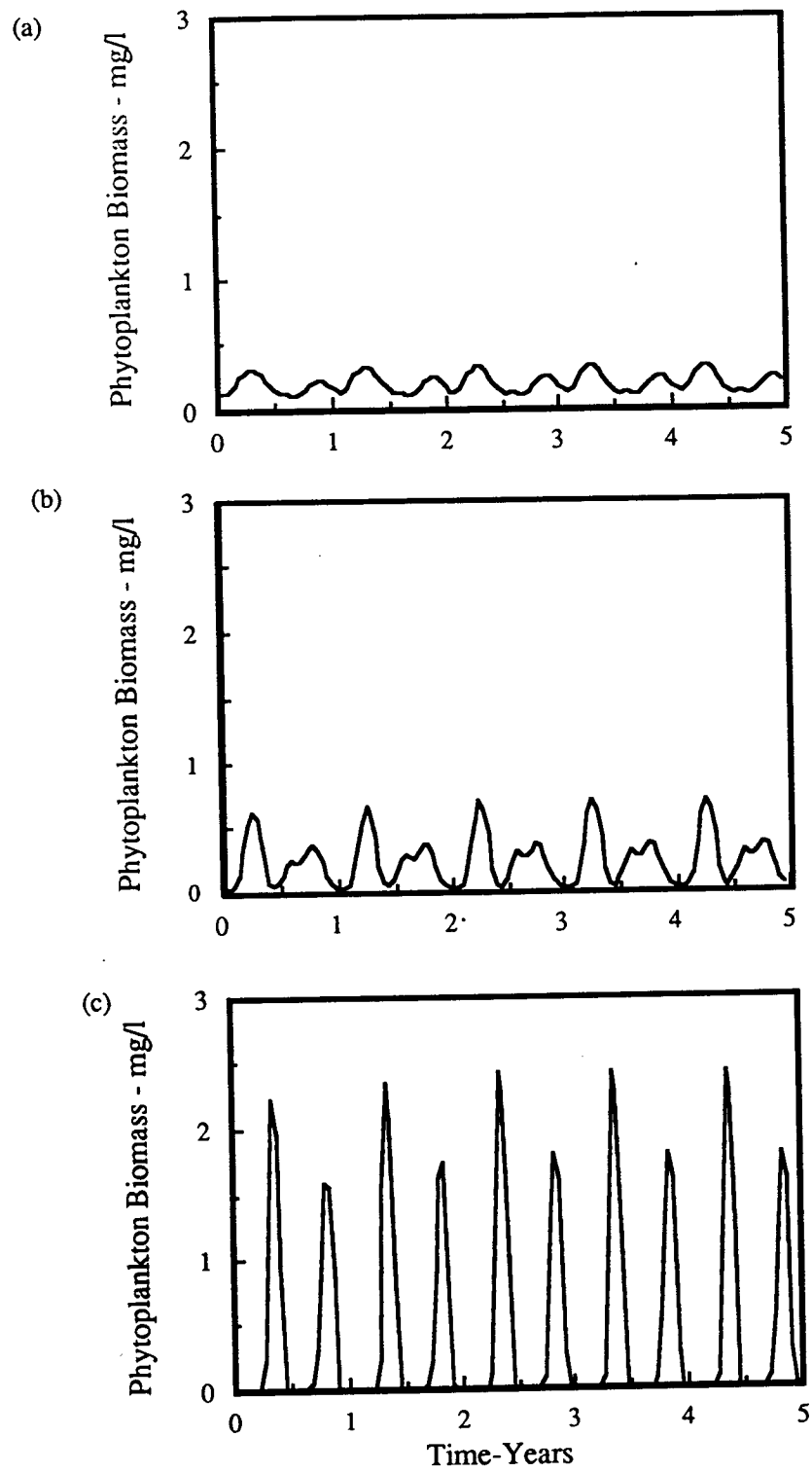


Figure 5.6. Simulated phytoplankton in reference ecosystem for three nutrient loading scenarios: (a) $P_{in} = 0.01$ mg/l; (b) $P_{in} = 0.02$ mg/l; (c) $P_{in} = 0.05$ mg/l.

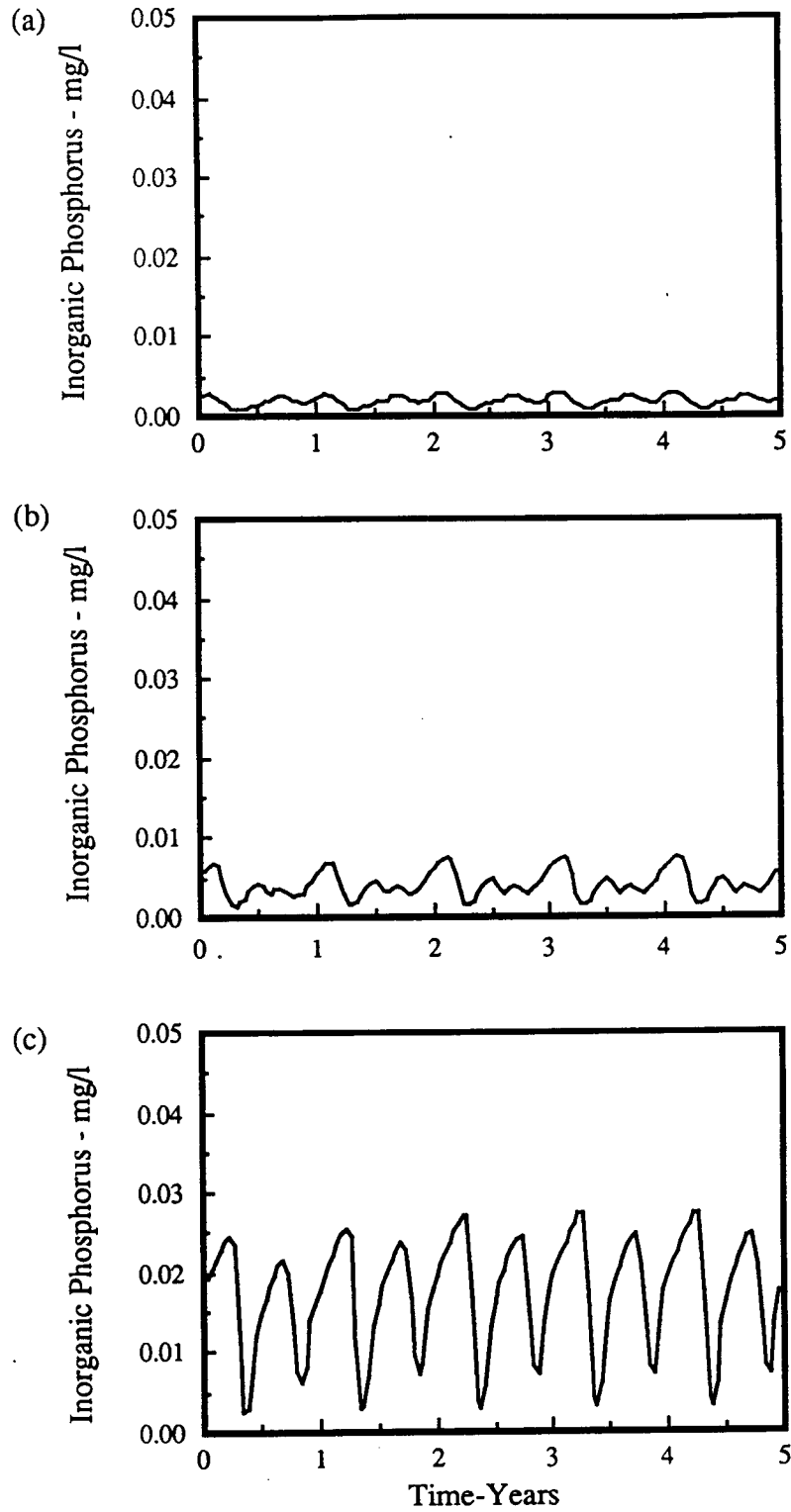


Figure 5.7. Simulated inorganic phosphorus in reference ecosystem for three nutrient loading scenarios: (a) $P_{in}=0.01$ mg/l; (b) $P_{in}=0.02$ mg/l; (c) $P_{in}=0.05$ mg/l.

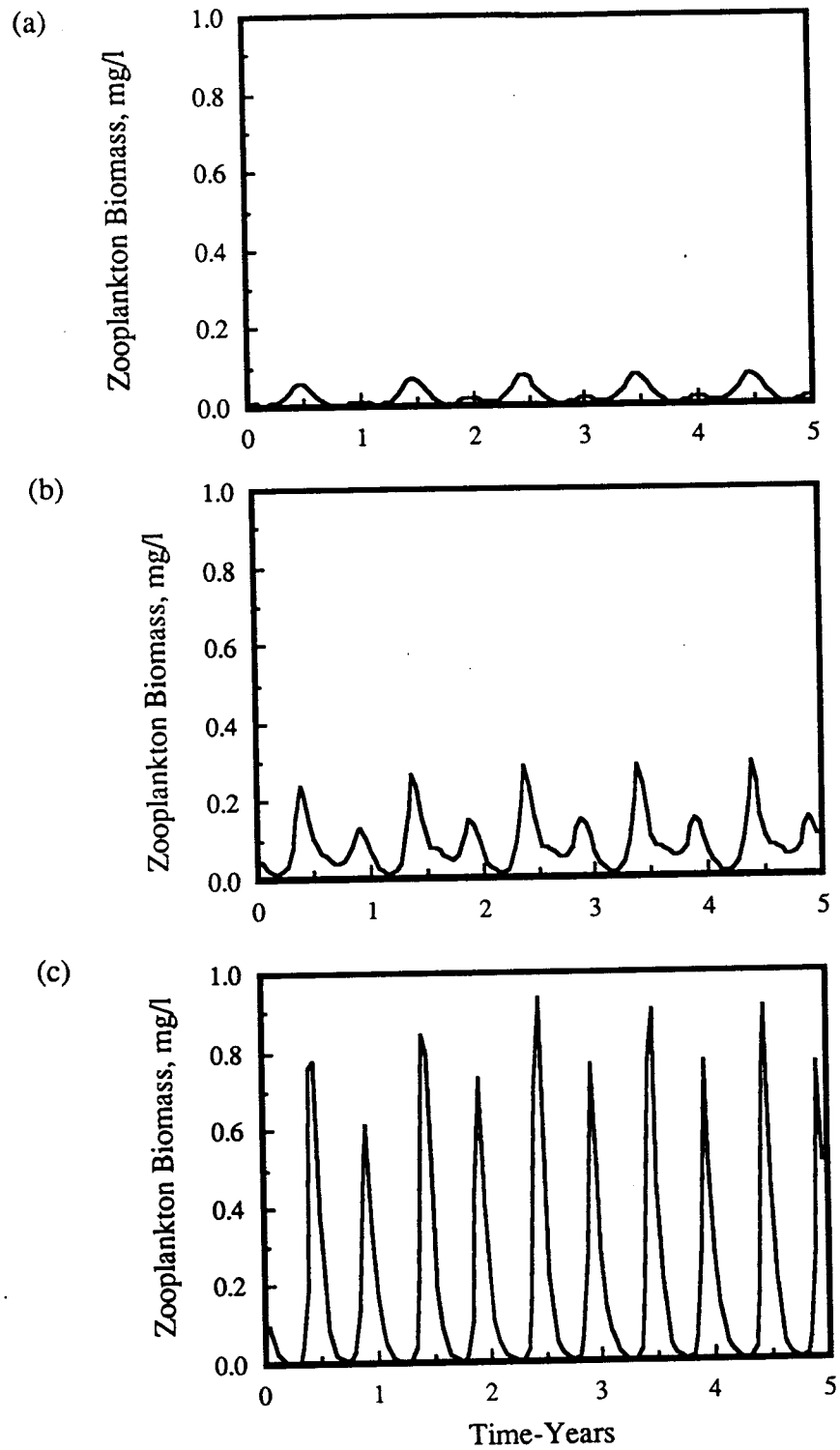


Figure 5.8. Simulated zooplankton biomass in reference ecosystem for three nutrient loading scenarios: (a) $P_{in} = 0.01$ mg/l; (b) $P_{in} = 0.02$ mg/l; (c) $P_{in} = 0.05$ mg/l.

$\underline{\theta}$ = the vector of systems parameters being estimated

\underline{x} = the vector of state variables generated by the model

\mathbf{R} = the covariance matrix for measurement error

then the parameter estimate is the set of parameters, $\underline{\theta}^*$, for which:

$$J(\underline{\theta}^*) = \min (J(\underline{\theta})) \quad (5.13)$$

The parameter set, $\underline{\theta}$, for each model was limited to include only those parameters given in Table 5.7. For Models II and III the parameters included in Table 5.7 comprise only a subset of the total number of parameters required to specify each of these models. The parameters were selected based upon their importance in the dynamics of each model. They also are representative of the range of phenomena that influence model behavior.

The simplex method for function minimization described by Nelder and Mead (1967) was used to find $J(\underline{\theta}^*)$. The efficiency and accuracy of this algorithm in obtaining parameter estimates can be improved by limiting the range of the parameter set over which the simplex must search. The numerical value of these limits was based upon the results described by Scavia et al. (1981) and Zison et al. (1978).

Parameter estimates were obtained for each of the three models with the prescribed levels of measurement accuracy (Table 5.6) using a sampling frequency of 14 days under monitoring programs with one year of background data. The background data was that portion of the sequence generated prior to the addition of the incremental increase in nutrient loading. The year of background data were first used to develop the system structure parameters (the elements of the transition matrix, Φ , in equation (3.21)).

Table 5.7. Parameter set, θ , for Models I, II, and III that were included in the estimation process.

Model I	Model II	Model III
Apparent settling velocity, w_s	Maximum phytoplankton growth rate, G_π	Maximum phytoplankton growth rate, G_π
	Maximum phytoplankton respiration rate, R_π	Maximum phytoplankton respiration rate, R_π
	Nutrient half-saturation constant, K_p	Nutrient half-saturation constant, K_p
	Light half-saturation constant, K_l	Light half-saturation constant, K_l
	Phytoplankton settling velocity, w_s	Phytoplankton settling velocity, w_s
		Maximum zooplankton growth rate, G_ζ
		Maximum zooplankton respiration rate, R_ζ
		Algal half-saturation constant, K_π

Once the parameters were estimated with equation (5.13), the residuals of the nominal trajectory (computed with estimated parameters) and the observations were used to obtain estimates of the systems error covariance matrix, Q . It was assumed that the matrix, Q , was diagonal and that contributions to the likelihood function (eq. 3.17) were distributed equally among the state variables. The diagonals of Q were estimated by finding the values for which the average value of the individual contributions to the likelihood function

$$\xi_{ij}(n) = \delta_{ij}(n) \sum_{k=1}^L (\sum_{l,j} \delta_{lj}(n)) \quad \text{for } i = 1, \dots, L \quad (5.14)$$

over all the simulations, was equal to the number of observations, N . The sum of the average individual contributions to the likelihood function, under this assumption, was equal to NL , where L was the number of state variables. This corresponded to the correct mean value for the likelihood function under the null hypothesis that the model used to generate the data and the model being validated were the same.

The mean and standard deviations of the parameters for each of the three models were estimated from the synthetically generated sequences. To perform parameter estimation, 50 such sequences were generated for each model. The estimated means and standard deviations for the parameters of each the three models, under the various scenarios of loading and measurement error are presented in Figures 5.9 through 5.11.

For Model I the mean value of the only parameter estimated, the apparent settling rate, changes as the simulated trophic state of the ecosystem changes (Fig. 5.9). For the specific environmental conditions and ecosystem parameters used in this stage, the change in the apparent settling rate does not show a consistent trend. It is interesting to note that the estimated apparent settling rate in all three cases is very close to the the value of 16 meters/year, the value obtained by Chapra (1975) in a study of data from Canadian Shield Lakes.

This result is somewhat different from that reported by Ferrara and Griffin (1986), who compared the results from a total phosphorus model similar to Model I with a multicomponent phosphorus model. Ferrara and Griffin (1986) concluded that for

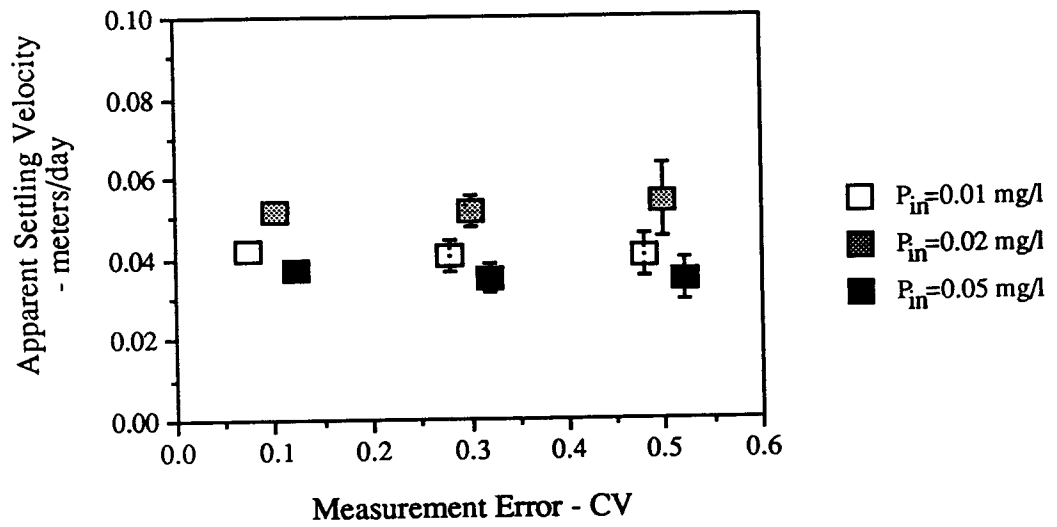


Figure 5.9. Mean and standard deviation of apparent settling velocity for Model I as a function of measurement error for three nutrient loading scenarios.

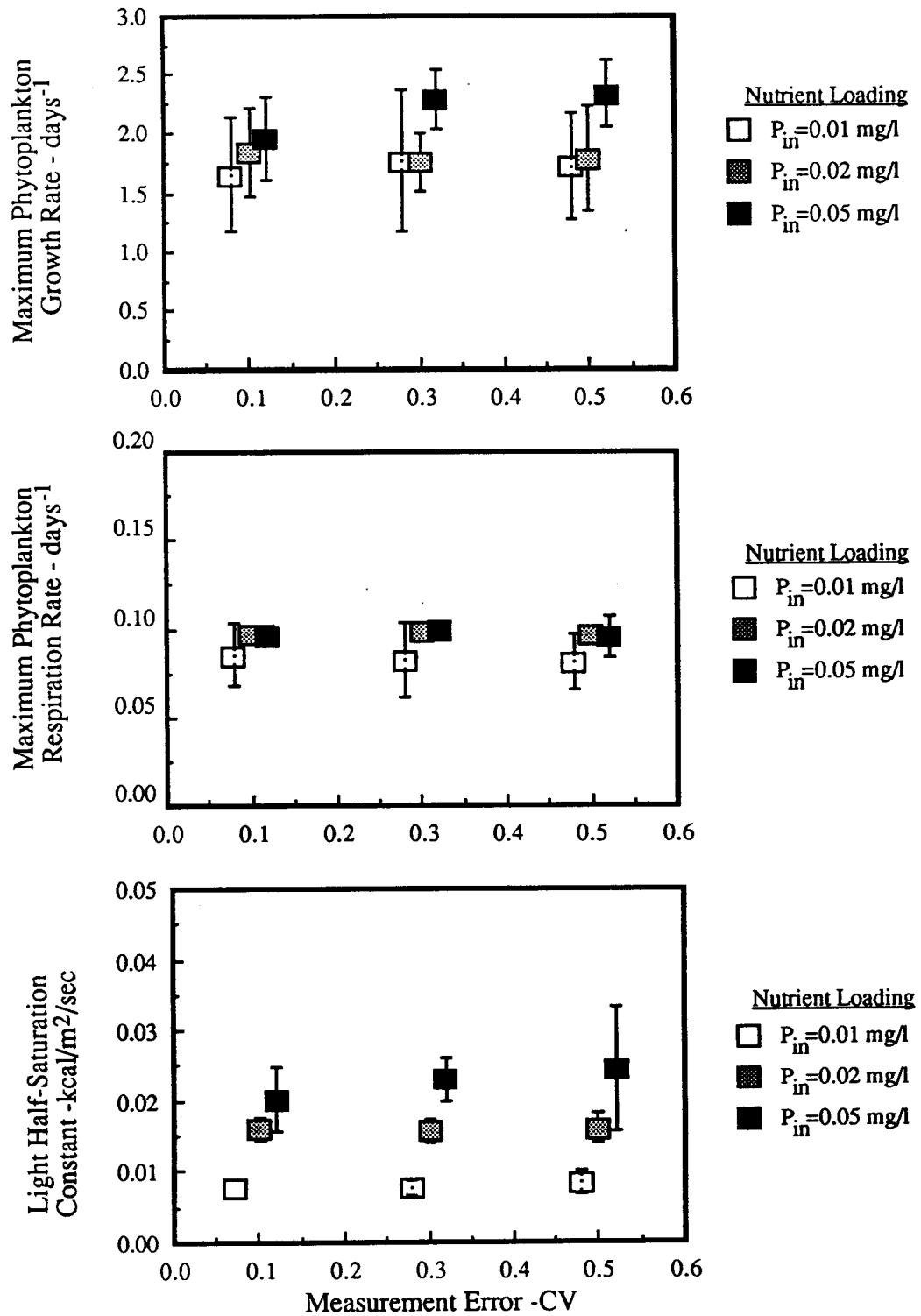


Figure 5.10. Mean and standard deviations of parameter estimates for Model II as a function of measurement error for three nutrient loading scenarios using simple ecosystem reference model.

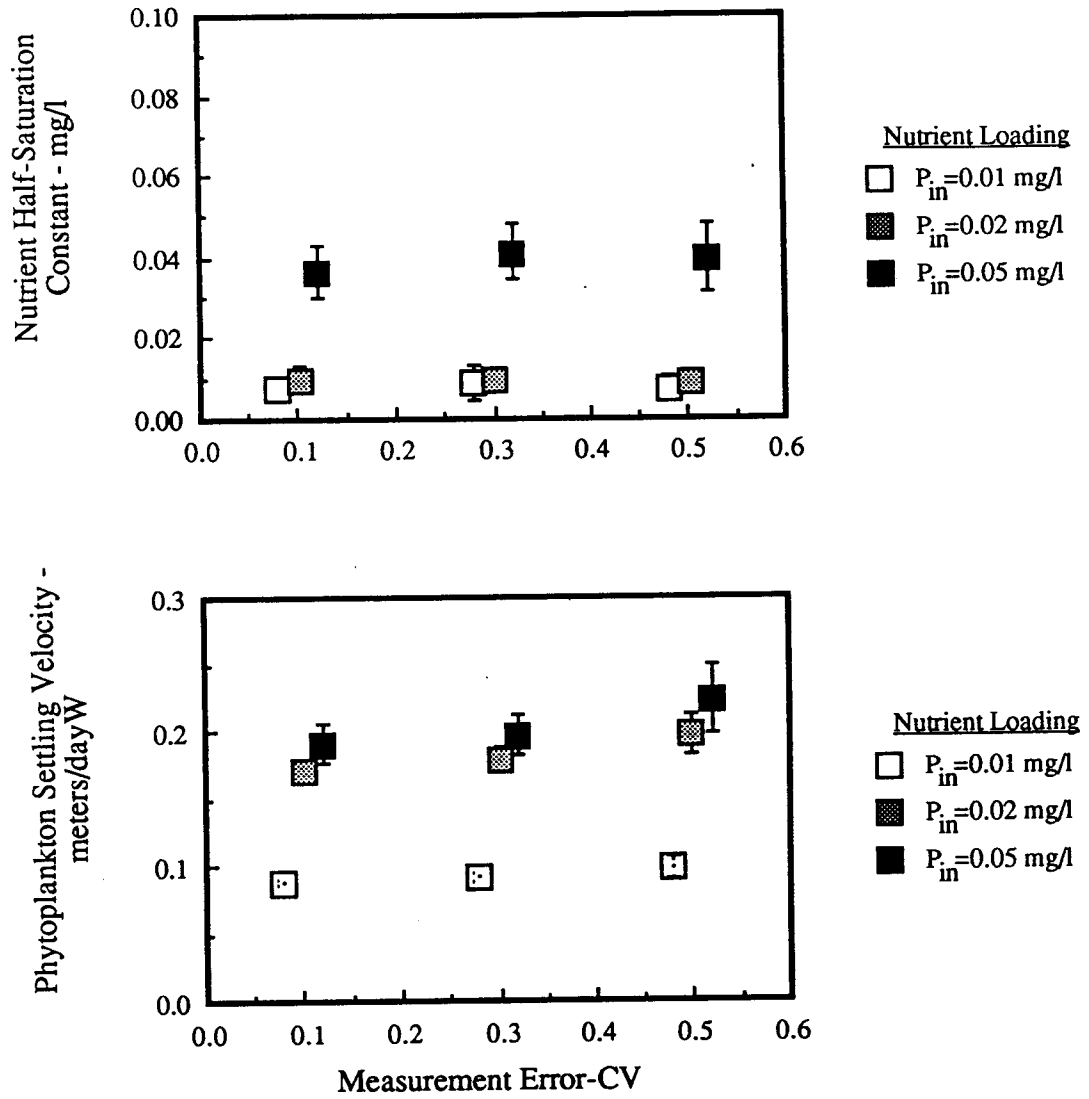


Figure 5.10 (continued). Mean and standard deviations of parameter estimates for Model II as a function of measurement error for three nutrient loading scenarios.

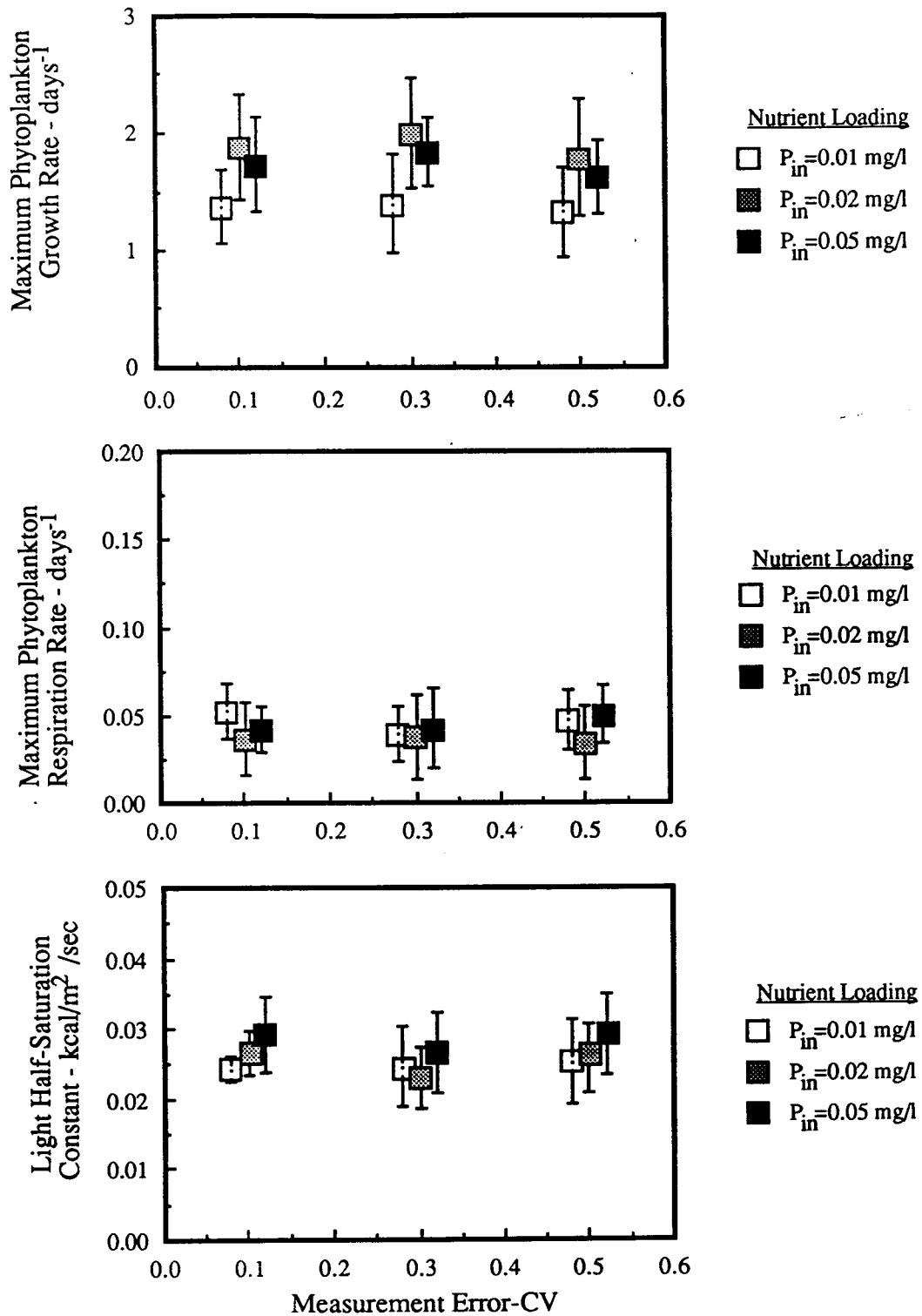


Figure 5.11. Mean and standard deviations of parameter estimates for Model III as a function of measurement error for three nutrient loading scenarios using simple ecosystem reference model .

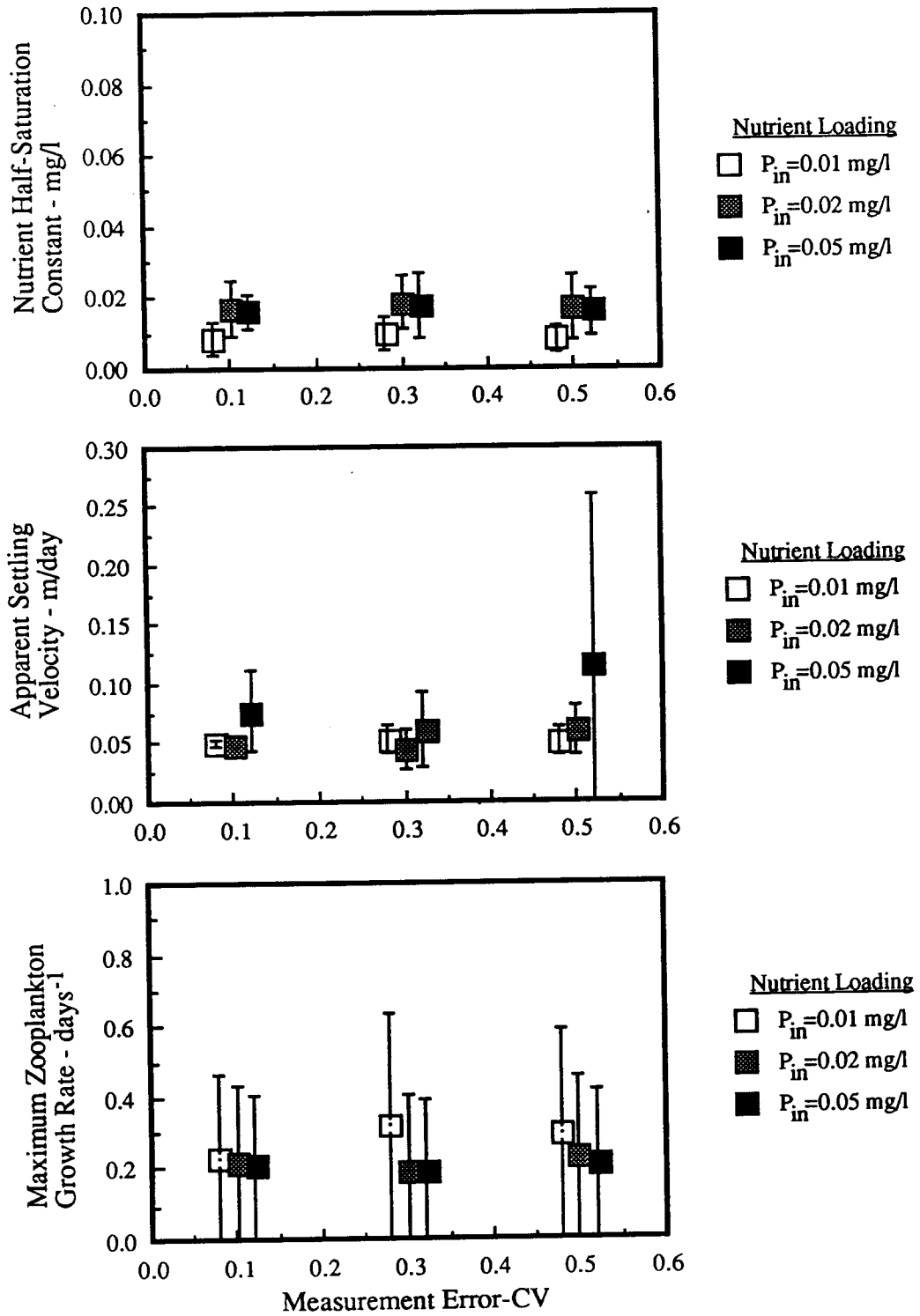


Figure 5.11(continued). Mean and standard deviations of parameter estimates for Model III as a function of measurement error for three nutrient loading scenarios using simple ecosystem reference model .

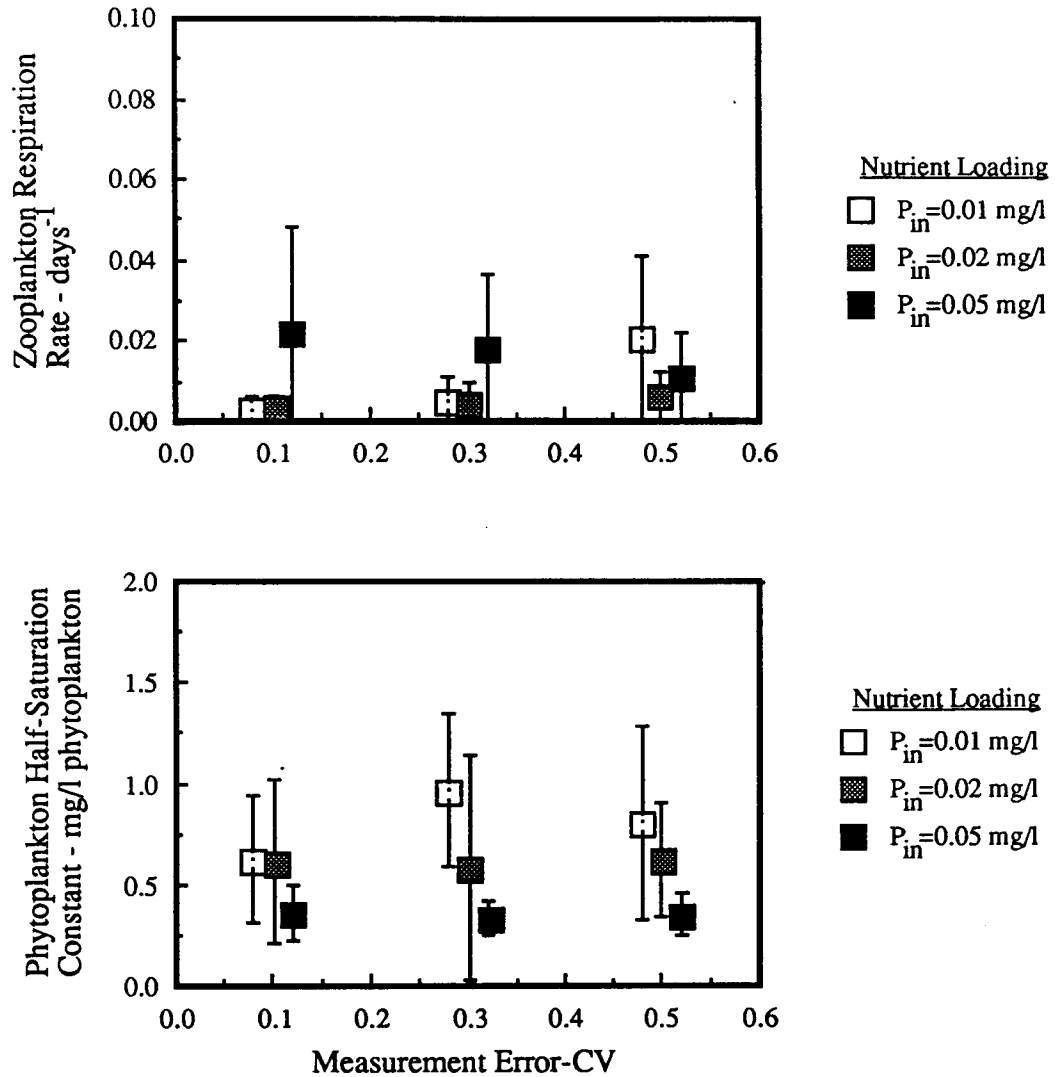


Figure 5.11(continued). Mean and standard deviations of parameter estimates for Model III as a function of measurement error for three nutrient loading scenarios using simple ecosystem reference model .

the low nutrient loading the ecosystem was biologically less active. As a result, the rates of biological uptake and deposition were diminished, resulting in a smaller net sedimentation/decay rate coefficient. However, a somewhat similar study by Scavia and Chapra (1977) found that the apparent settling velocity computed from the more complex model simulation decreased with increasing nutrient loading. The standard deviations of the parameter estimates for Model I behave consistently within each loading scenario. That is, the variability of the estimates increases as measurement error increases.

The means and standard deviations of parameter estimates for Model II are shown in Figure 5.10. The true parameter values, the ones used to generate the prototype, are given in Table 5.5. The mean of the parameter estimates is strongly influenced by the level of productivity in the prototype ecosystem. The mean values of the parameter estimates are, with the exception of the optimal solar radiation, I_s , closest to the actual parameter values used to generate the prototype when the loading rate is lowest. As the hypothetical lake becomes more eutrophic the difference between parameter estimates and the true parameter values increases, with the exception noted. The optimal solar radiation, I_s , the Michaelis-Menten constant for phosphorus uptake, K_P , and the phytoplankton settling velocity, w_s , show the most dramatic change. The changes in these parameters are evidently necessary to compensate for the increased losses due to zooplankton grazing. Zooplankton losses are not directly included in Model II and must, therefore, be affected by other processes. It is clear that an increase in the phytoplankton settling rate will lead to increased losses to compensate for zooplankton grazing. The nature of combined increases in the optimal solar radiation and Michaelis-Menten half-saturation constant is more complex, and the resulting effect upon phytoplankton losses is beyond the scope of this study. The standard deviations of the parameter estimates appear, in general, to be more influenced

by the trophic level of the hypothetical lake than by the measurement error. The phytoplankton settling velocity, w_s , is the only parameter for which the standard deviation increases consistently with increases in measurement error.

For Model III, the means and standard deviations of parameter estimates are shown in Figure 5.11, with true parameter values given in Table 5.5. Mean values of the estimated parameter are generally close to the true values. The notable exception is the maximum growth rate for phytoplankton, G_{max} . There appears to be no consistent pattern of variation of the estimated mean parameter values from the true parameter values as a function of either loading rate or measurement error. This is true of the parameter estimates for both phytoplankton and zooplankton. This implies that the variability is a result of the parameter estimation process. Because the reference system model and the most complex model (Model III) being evaluated were identical it was possible to gain some insight into the limitations of the parameter estimation process by comparing the cost functions, $J(\theta)$, for the true parameters and the estimated parameters. For a representative number of Monte Carlo simulations, the cost for the true parameters is plotted against the cost for the estimated parameters for each of the nine scenarios of Table 5.6. When the measurement error was low ($CV=0.1$) the cost function for the estimated parameters is generally greater than the cost for the true parameters. As measurement error increases, for the sampling duration and frequency used in the simulation, the parameter estimation algorithm was able to find a set of parameters for which the minimum cost was less than that for the true parameters. This implies that for these conditions, more frequent or longer duration of sampling may be required for better parameter estimates, at least for large measurement errors.

The algorithm used to estimate parameters also at the maximum loading ($P_{in}=0.05$ mg/l) and measurement error ($CV=0.5$). In a few instances, as shown in

Figure 5.12 (see arrows) the cost associated with the estimated parameters were substantially greater than the costs for the true parameters. For these cases the estimates of certain parameters were unrealistic and the corresponding simulations were poor. Figure 5.13 shows a five-year simulation of phytoplankton biomass using a parameter set whose cost function is one of those identified by the arrow in Figure 5.12. In the first year, the simulation matches, at least partially, the observed trajectory. In the ensuing years, after the intervention of the additional loading, the simulation behaves erratically. These pathologic conditions may be the result of relative minima associated with the cost function, $J(\theta)$ that are large enough to trap the simplex. It is likely that for the large measurement error either more frequent sampling or sampling over a longer duration is necessary to avoid such conditions.

5.7.2 Model Validation

After estimates of the parameters were obtained, as described above, the validity of each of the models was evaluated with the hypothesis-testing methodology. The tests were performed upon the data sequences for the period of time subsequent to the intervention associated with the incremental increase in nutrient loading. The testing done in this way is similar to the post-audit concept proposed by Thomann (1982). Conceptually, each of the models was calibrated with one year of background data. With the system parameters estimated in the calibration step, the residuals of the simulated and observed were used to determine the system error, Q , as described in Section 5.6.1. The testing of model validity was then performed on the measurements obtained after the

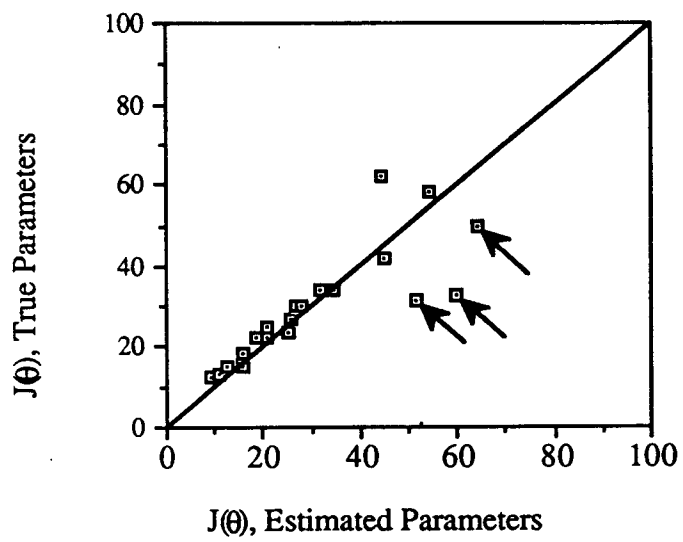


Figure 5.12 Cost function for true parameters of Model III versus cost function for estimated parameters when $P_{in}=0.05$ mg/l and $CV=0.5$.

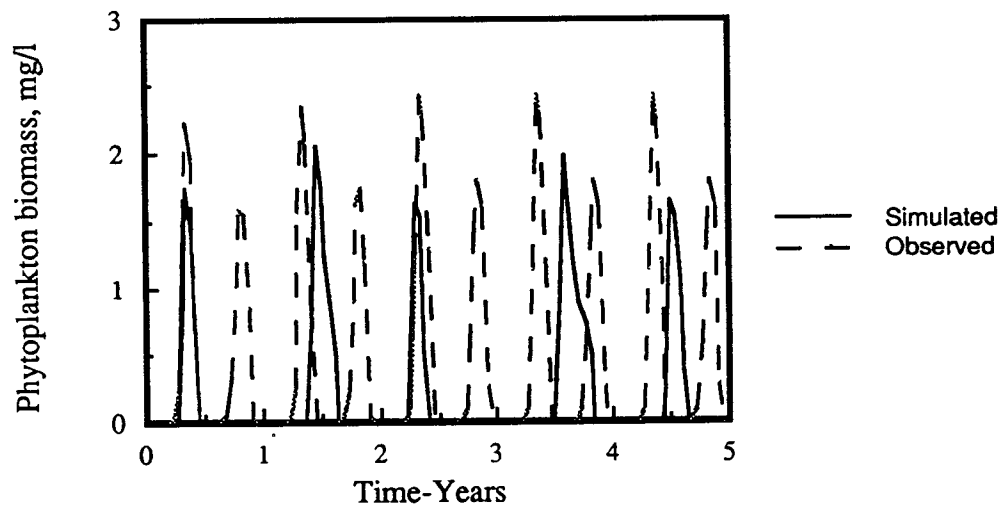


Figure 5.13 Simulated and observed trajectory of phytoplankton for parameter set with pathologic behavior (see arrows in Figure 5.12)

intervention had occurred. The threshold of the tests for model validity was based on a Type II error probability, $\beta = 0.05$. For testing model validity the results of the hypothesis testing are characterized by estimates of the power to reject the null hypothesis as a function of time for each of the scenarios. In this case the null hypothesis is that the model generates output from the same population as the reference models used to generate the synthetic population. The lower the values of power to reject the null hypothesis are, the greater is the validity of the model. The results of this part of the hypothesis testing provide an assessment of how well the model conforms to the structure described in Chapter 3.

Trajectories of the power to reject the null hypothesis, $1-\beta$, for the nine different scenarios of measurement error and nutrient loading are shown in Figures 5.14 through 5.16. These trajectories generally increase with time after the intervention. Increases in the power to reject the null hypothesis (reduced model validity) result from structural deficiencies. It may be possible to calibrate a model that is structurally incorrect, but this does not mean that such a model is necessarily a valid one. The hypothesis testing should detect deficiencies when the model is applied to conditions different from those for which it was calibrated. This was demonstrated by the results of the tests of model validity in this stage

Structural deficiencies in Model II are such that it is not possible to validate the model at any of the levels of nutrient loadings. The need to compensate for zooplankton grazing by artificially increasing other loss components such as sinking leads to incorrect model structure. The structure associated with Model II provides valid simulations during the calibration period, but is not appropriate for loading levels different than those for which it was calibrated.

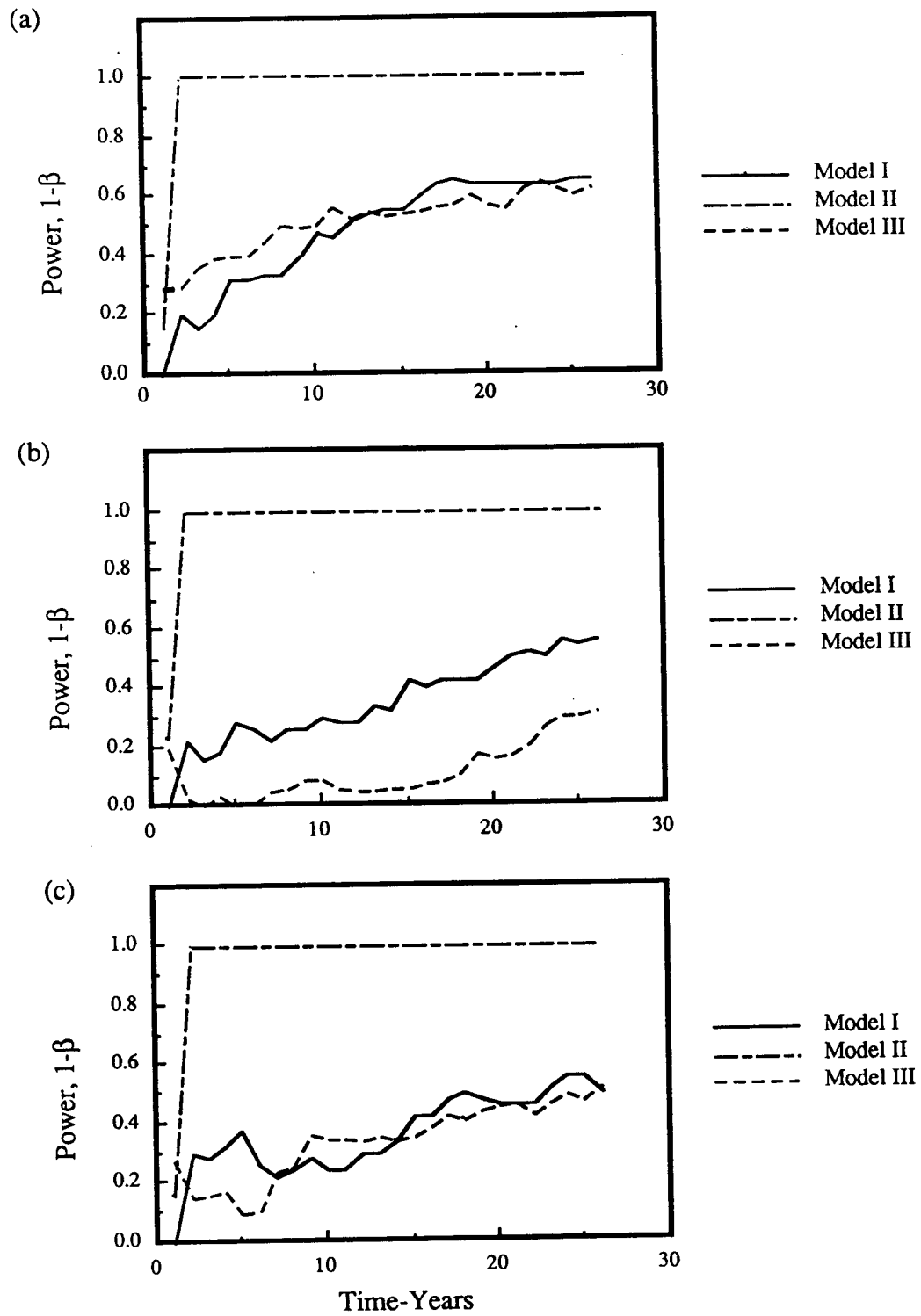


Figure 5.14. Power to reject null hypothesis for Models I, II and III when $P_{irr} = 0.01$ mg/l and measurement error is: (a) $CV=0.1$; (b) $CV=0.3$; (c) $CV=0.5$.

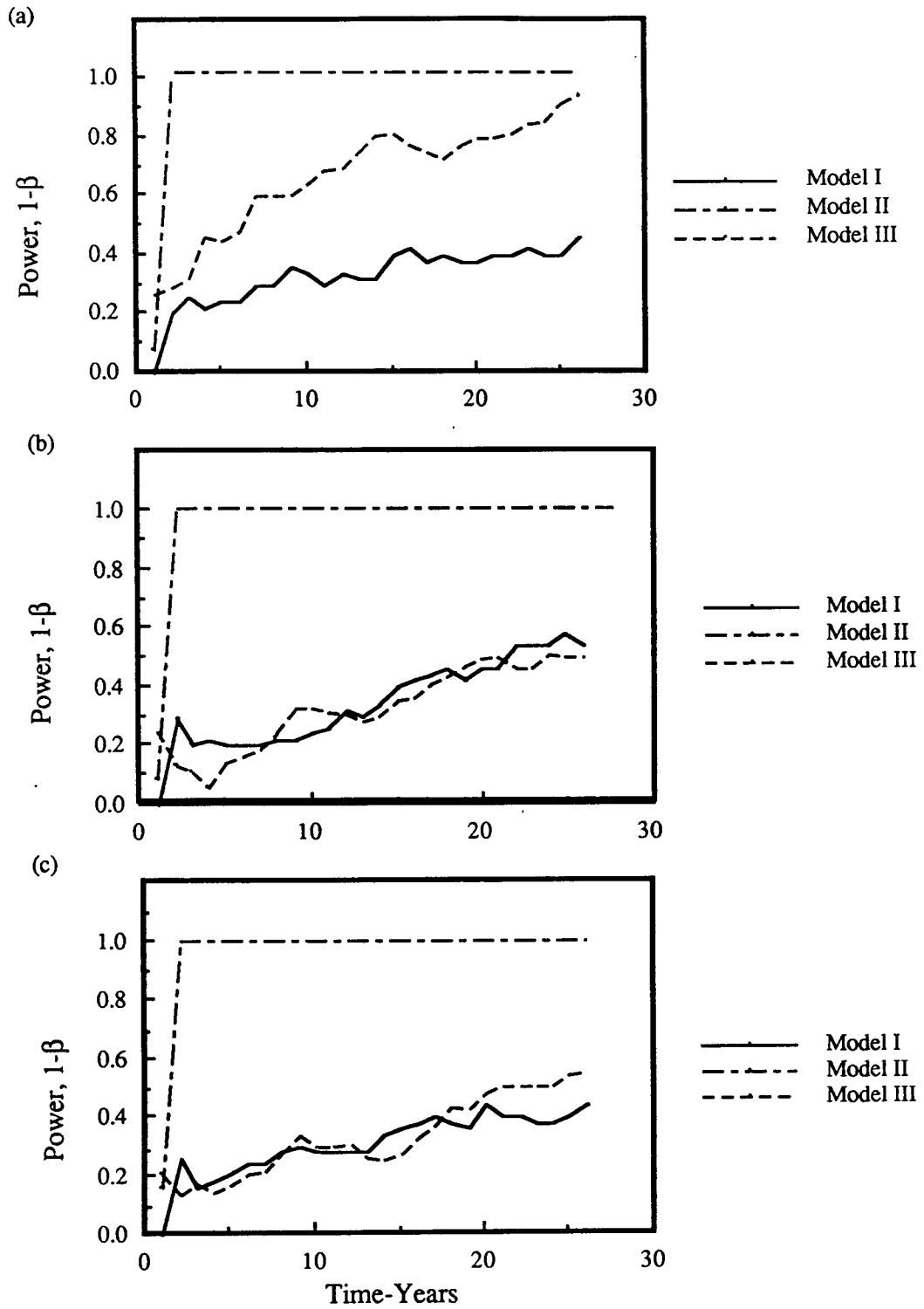


Figure 5.15. Power to reject null hypothesis for Models I, II and III when $P_{in} = 0.02 \text{ mg/l}$ and measurement error is: (a) $CV=0.1$; (b) $CV=0.3$; (c) $CV=0.5$.

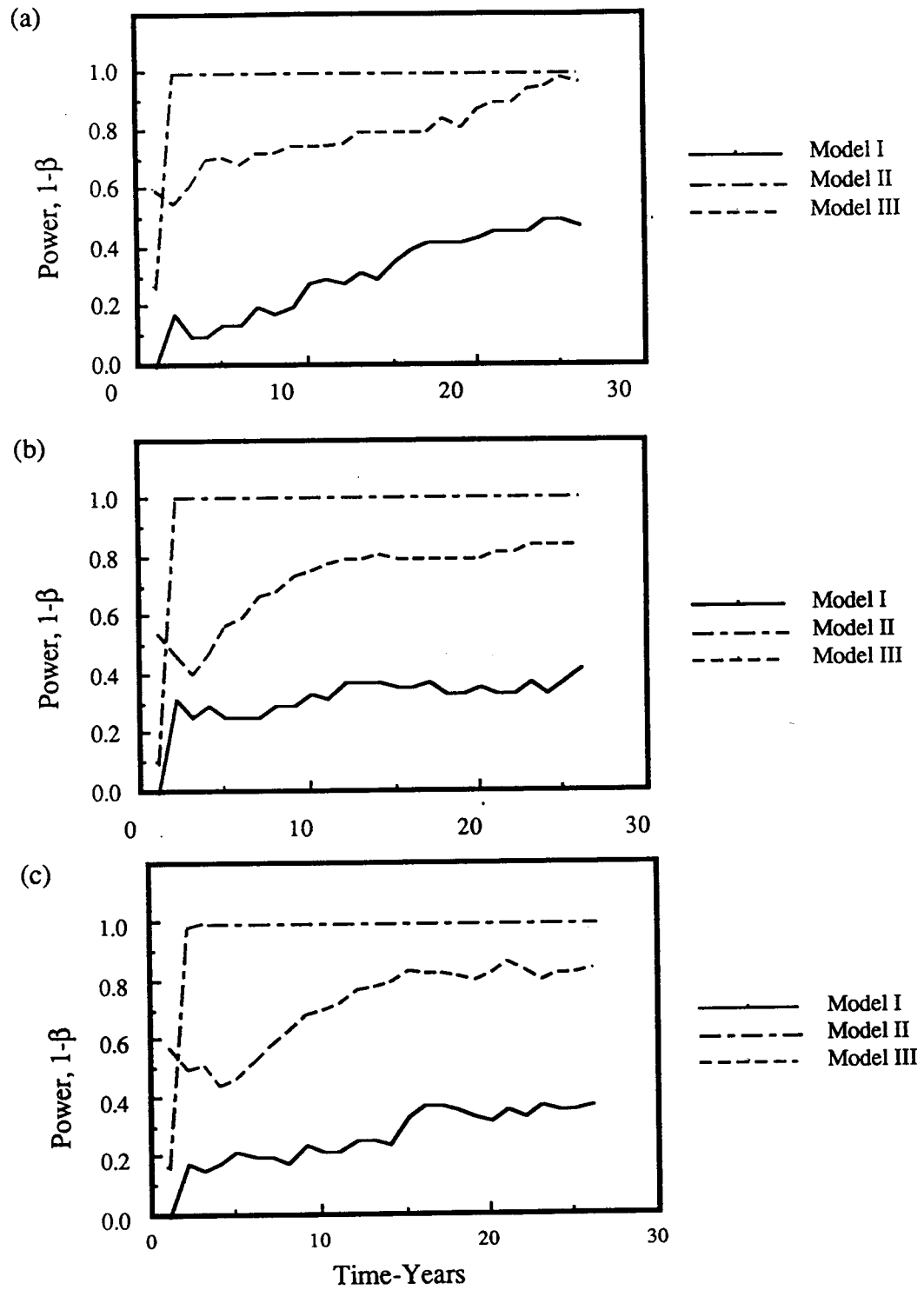


Figure 5.16. Power to reject null hypothesis for Models I, II and III when $P_{in} = 0.05$ mg/l and measurement error is: (a) $CV=0.1$; (b) $CV=0.3$; (c) $CV=0.5$.

The results for Model III are somewhat mixed. At the two lower levels of loading ($P_{in}=0.01$ mg/l, $P_{in}=0.02$ mg/l) the model behaves moderately well. The spiky nature of the plankton dynamics (Fig. 5.6) when the loading is highest ($P_{in}=0.05$ mg/l) presents difficulties for models that use unsmoothed observations. The time interval during which the maximum occurs is short compared to the sampling interval. This leads to poor parameter estimates and may contribute to the pathologic behavior described previously. The net result is poor model performance at this level of nutrient loading.

As was the case of the cost function, it was possible to compare the results of the model validity testing of Model III using estimated parameters with similar results using the true parameters. The trajectories of the power to reject the null hypothesis for Model III with the true parameters are given in Figure 5.17 for the nine scenarios of measurement error and nutrient loading. When the parameters are known the validity of the model is high, compared to the level of model validity for the estimated parameters. The results are best at the lowest level of nutrient loading (Fig. 5.17(a)) and poorest at the highest level (Fig. 5.17 (c)). At the highest level, model validity improves as the measurement error increases similar to the results obtained from the study of the linear model in Chapter 4.

5.7.3 Time to Identify Hypothesis

The final step in the analysis was to use sequential tests to estimate the average time required to identify an hypothesis, when using a given model, a given level of measurement error and a fixed sampling strategy. The threshold values, \mathcal{T}_0 and \mathcal{T}_1 (eqs. 3.13 and 3.16), were based upon Type I and Type II errors of $\alpha = \beta = 0.05$. The time to identify an hypothesis was that for which the log likelihood ratio exceeded the criteria specified by equations 3.13 and 3.16. The null hypothesis, \mathcal{H}_0 , was accepted if

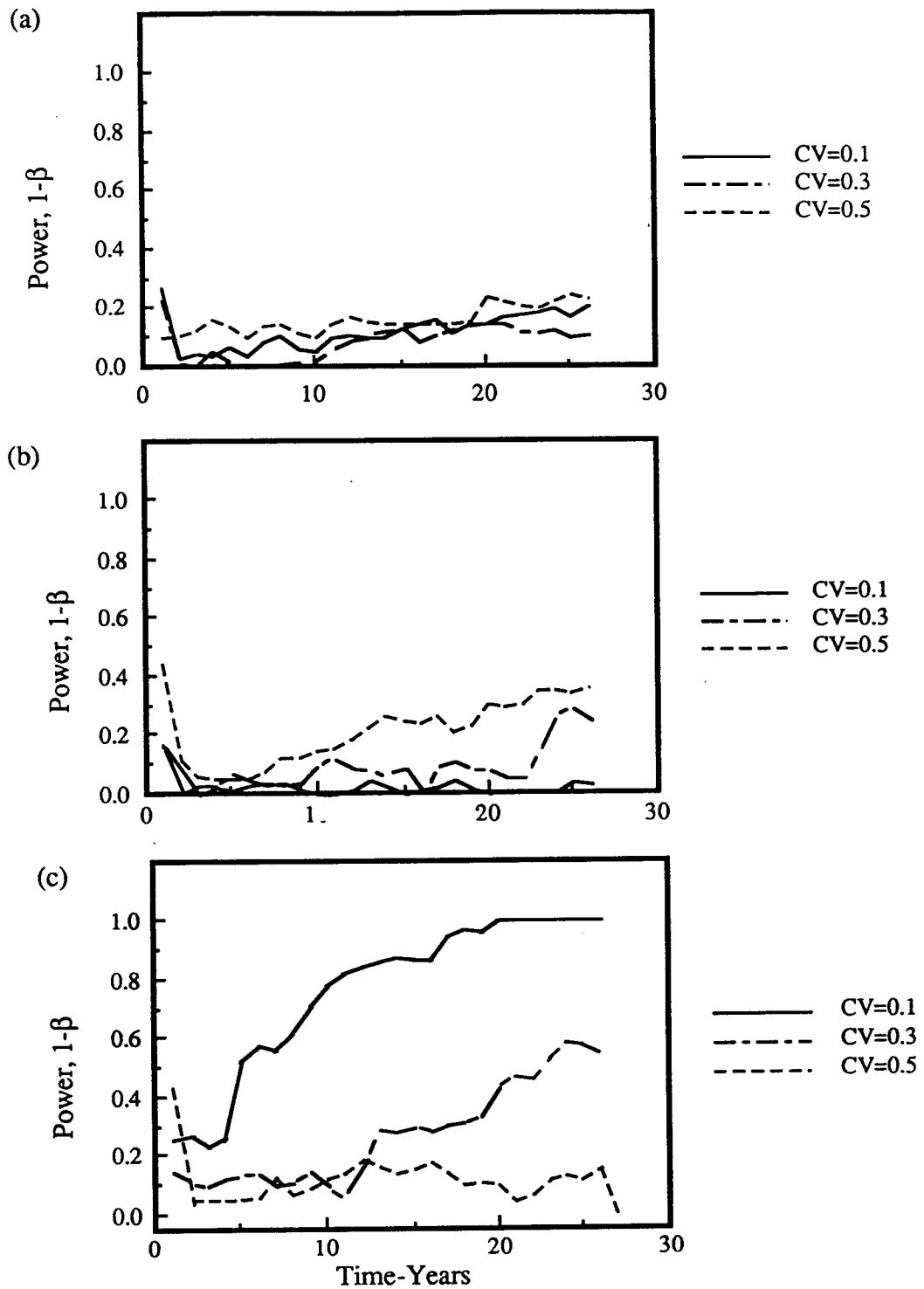


Figure 5.17. Power to reject null hypothesis for Model III with true parameters under the nutrient loading conditions; (a) $P_{in} = 0.01$ mg/l; (b) $P_{in} = 0.02$ mg/l; (c) $P_{in} = 0.05$ mg/l.

the criterion described by equation 3.13 was satisfied. The alternate hypothesis, \mathcal{H}_1 , was accepted if the criterion described by equation 3.16 was satisfied. Since the alternate hypothesis was, in fact, correct, this test also provided a measure of the effectiveness of the filter for identifying environmental impact. The results for the three models under the nine scenarios of measurement error are presented in Tables 5.8 through 5.10. Results are characterized by the time required to reach a decision regarding that hypothesis is true and by the fraction of times the correct hypothesis (\mathcal{H}_1) is chosen.

The performance of Model I with respect to detecting environmental change associated with the increase in nutrients is poorest at the lowest level of nutrient loadings. At the two higher levels of nutrient loading, Model I performs well at the lowest level of measurement error (CV=0.1), but the level of performance decreases both in terms of the time required to detect change and in fraction of time the correct choice is made as measurement error increases. The performance of Model II is unsatisfactory at all levels of nutrient loading. For the reasons discussed above, it is not adequate for detecting environmental changes at any levels of nutrient loading. Model III is most effective at the highest nutrient loading levels. This is somewhat surprising, given the parameter estimation difficulties noted in Section VII.1. The incremental change in parameters is greatest at the highest level of loading, and this is an important factor in the ability to detect change.

Table 5.8 Characteristics of Model I for identifying correct hypothesis for nine scenarios of measurement error and nutrient loading. (95% confidence limits in parentheses)

Nutrient Loading	Measurement Error-CV	Time to Determine Hypothesis	Fraction of Times \mathcal{H}_1 is Chosen
$P_{in}=0.01$ mg/l	0.1	6.8 years	0.65 (± 0.13)
$P_{in}=0.01$ mg/l	0.3	8.0 years	0.60 (± 0.14)
$P_{in}=0.01$ mg/l	0.5	10.7 years	0.48 (± 0.14)
$P_{in}=0.02$ mg/l	0.1	1.8 years	0.80 (± 0.11)
$P_{in}=0.02$ mg/l	0.3	7.5 years	0.78 (± 0.14)
$P_{in}=0.02$ mg/l	0.5	11.7 years	0.73 (± 0.13)
$P_{in}=0.05$ mg/l	0.1	1.8 years	>0.99(± 0.07)
$P_{in}=0.05$ mg/l	0.3	5.5 years	0.94 (± 0.12)
$P_{in}=0.05$ mg/l	0.5	11.0 years	0.88 (± 0.12)

Table 5.9 Characteristics of Model II for identifying correct hypothesis for nine scenarios of measurement error and nutrient loading (95% confidence limits in parentheses).

Nutrient Loading	Measurement Error-CV	Time to Determine Hypothesis	Fraction of Times \mathcal{H}_1 is Chosen
$P_{in}=0.01$ mg/l	0.1	1.0 years	0.00
$P_{in}=0.01$ mg/l	0.3	1.0 years	0.00
$P_{in}=0.01$ mg/l	0.5	1.0 years	0.00
$P_{in}=0.02$ mg/l	0.1	1.0 years	0.00
$P_{in}=0.02$ mg/l	0.3	1.0 years	0.00
$P_{in}=0.02$ mg/l	0.5	1.0 years	0.00
$P_{in}=0.05$ mg/l	0.1	1.0 years	0.00
$P_{in}=0.05$ mg/l	0.3	1.0 years	0.00
$P_{in}=0.05$ mg/l	0.5	1.0 years	0.00

Table 5.10 Characteristics of Model III for identifying correct hypothesis for nine scenarios of measurement error and nutrient loading (95% confidence limits in parentheses).

Nutrient Loading	Measurement Error-CV	Time to Determine Hypothesis	Fraction of Times H_1 is Chosen
$P_{in}=0.01$ mg/l	0.1	4.6 years	0.35 (± 0.12)
$P_{in}=0.01$ mg/l	0.3	14.2 years	0.31 (± 0.13)
$P_{in}=0.01$ mg/l	0.5	6.2 years	<0.01
$P_{in}=0.02$ mg/l	0.1	4.1 years	0.35 (± 0.14)
$P_{in}=0.02$ mg/l	0.3	5.5 years	0.05 (± 0.02)
$P_{in}=0.02$ mg/l	0.5	13.0 years	<0.01
$P_{in}=0.05$ mg/l	0.1	1.8 years	0.40 (± 0.05)
$P_{in}=0.05$ mg/l	0.3	2.4 years	0.50 (± 0.09)
$P_{in}=0.05$ mg/l	0.5	3.2 years	0.50 (± 0.08)

5.8. Results-Simulated Natural Conditions

The performance of the three ecosystem models was tested under more stringent conditions by increasing the complexity of the system of reference models and by making the environmental inputs stochastic processes. Reference model complexity was increased by adding additional compartments for phytoplankton, attached algae, zooplankton, and benthic animals as shown in Figure 5.4. The parameter values used in the more complex ecosystem reference model, using the notation described in Appendix III, are given in Table 5.11. The parameters were chosen so as to produce a range of responses from phytoplankton and zooplankton under varying conditions of available light and nutrient supply. Results reported by Lehman et al. (1975), O'Neill and Giddings (1976) and Scavia (1980) were used as guidelines for developing parameter estimates with some general characteristics of various algal and zooplankton species. The goal was not necessarily to simulate real taxa. Rather, it was an effort to generate ecosystem responses with some of the broader characteristics of various species as they have been observed in actual systems. When a variety of species is included in the model, it is reasonable to expect that the relative response of the individual species might vary as the environmental forcing functions change from year to year. In turn, this variability in response provides more stringent conditions for testing the three models.

The elements used to develop the stochastic processes for the environmental forcing functions (nutrient supply and solar energy) have been described previously in Section V of this chapter. Typical traces of river flow, solar radiation, and phosphorus concentrations are shown in Figures 5.18 through 5.20. Input levels of other major nutrients, including nitrogen and silicon, were maintained at a sufficiently high level so that the only limiting nutrient was phosphorus.

Table 5.11 Values of parameters used in the complex ecosystem reference model

<u>Benthic Animals</u>			
G_b , days ⁻¹	0.02		
R_b , days ⁻¹	0.002		
M_b , days ⁻¹	0.001		
K_b , mg/l ⁻¹	500.		
θ_b	1.047		
$\alpha_{b, sed}$	1.0		
$\alpha_{b, att}$	1.0		
B_{lim} , mg/m ²	5200.		
ϵ_b	0.50		
B_{prt}	0.75		
<u>Zooplankton</u>	<u>Type 1</u>	<u>Type 2</u>	
G_ζ , days ⁻¹	0.20	0.25	
R_ζ , days ⁻¹	0.02	0.03	
M_ζ , days ⁻¹	0.01	0.01	
K_Π , mg/l	0.50	0.30	
$\alpha_{\zeta, 1}$	1.0	0.50	
$\alpha_{\zeta, 2}$	1.0	1.0	
$\alpha_{\zeta, 3}$	0.2	0.2	
$\alpha_{\zeta, att}$	0.50	0.70	
$\alpha_{\zeta, det}$	0.1	0.1	
ZQ10	2.0	2.0	
θ_ζ	1.047	1.047	
Z_{prt}	0.75	0.75	
<u>Phytoplankton</u>	<u>Type 1</u>	<u>Type 2</u>	<u>Type 3</u>
G_Π , days ⁻¹	2.00	1.80	0.60
R_Π , days ⁻¹	0.05	0.06	0.05
K_P , mg/l	0.010	0.005	0.003
I_s , kcal/m ² /sec	0.025	0.030	0.035
PQ10	2.0	2.0	2.0
θ_Π	1.047	1.047	1.047
w , m/day	0.18	0.05	0.02

Table 5.11 (continued) Values of parameters used in the complex ecosystem reference model

<u>Detritus</u>	
K_{det} , days ⁻¹	0.10
w_{det} , days ⁻¹	0.10
θ_{det}	1.047
<u>Sediment</u>	
K_{sed} , days ⁻¹	0.0015
θ_{sed}	1.047
<u>Phosphorus</u>	
P_{alg}	0.01
P_{zoo}	0.01
P_{det}	0.01
P_{sed}	0.01
P_{ben}	0.01

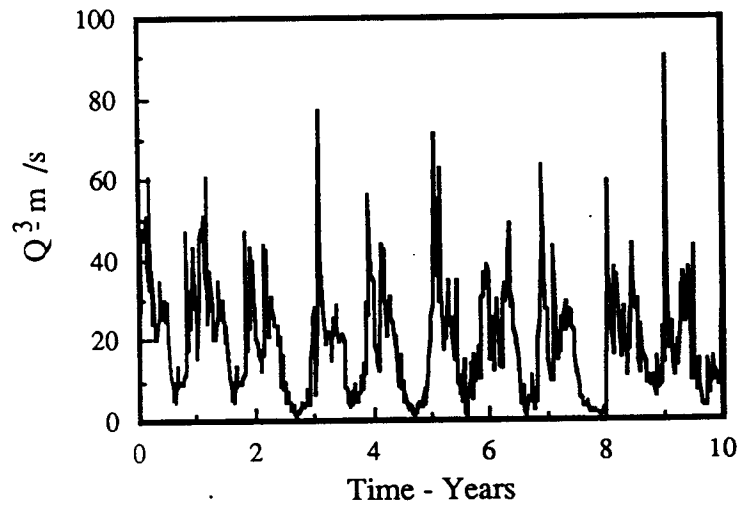


Figure 5.18. Typical ten-year trajectory of river inflow, Q , based upon data from the Cedar River at Renton, Washington.

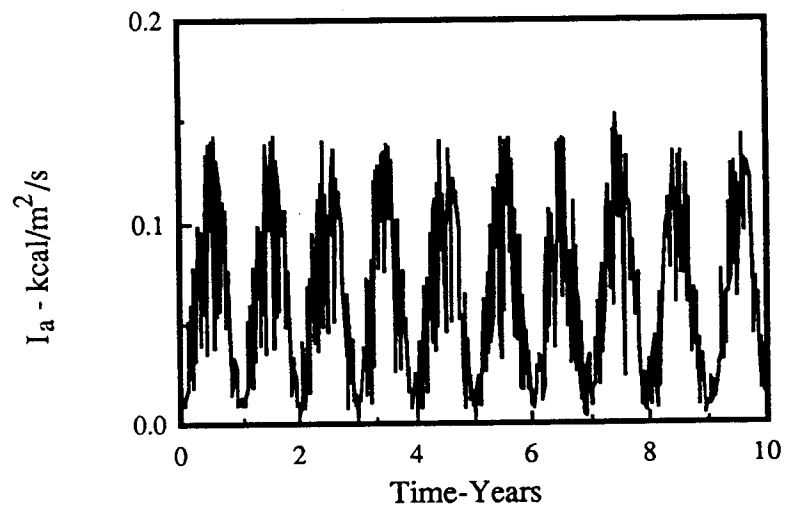


Figure 5.19. Typical ten-year trajectory of daily average solar radiation, I_a , based upon data from the Seattle-Tacoma International airport.

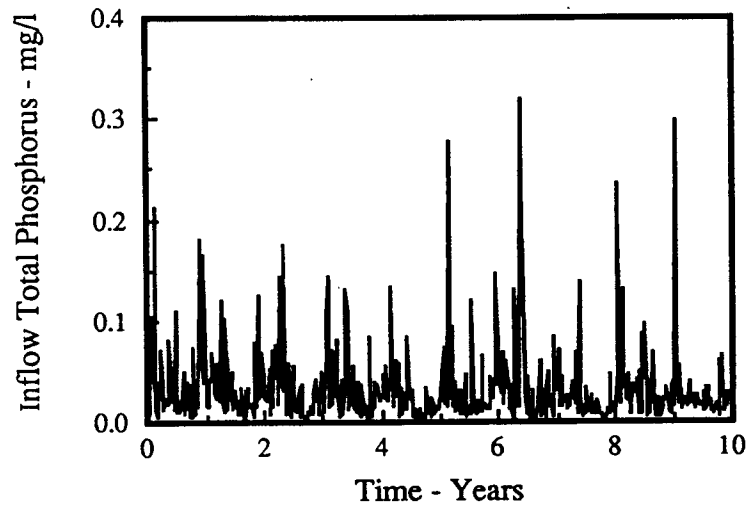


Figure 5.20 Typical ten-year trajectory of simulated total phosphorus in the river inflow based upon characteristics of the Cedar River at Renton, Washington

For the hypothesis testing 26-year sequences of state variables were generated with the ecosystem model driven by the random river flows, nutrient concentrations, and solar energy. Typical 10-year trajectories of several ecosystem state variables resulting from the coupling of these forcing functions with the ecosystem models are shown in Figures 5.21 through 5.24. The ecosystem model was run for 25 years using the environmental data for the first year. The 25-year period for startup was substantially greater than the five-year period required for the simple reference model in the testing stage. This period of time was necessary to eliminate transients associated with initial conditions, since preliminary testing showed that these transients persisted for approximately 20 years. The longer period required to eliminate transients induced by initial conditions is apparently a result of the larger and more complex model structure of the reference model used in this part of the analysis.

The environmental driving forces in the first year of the 26-year sequence were those resulting from the random processes described above. The first year was considered to be the background condition and was used for parameter estimation. Scenarios for measurement error and loading increments are given in Tables 5.12 through 5.14. Measurement error of the same levels as used in the previous Section (Table 5.7) were superimposed upon the output from the reference models. Two levels of incremental increase in the background phosphorus loading were included in the analysis. The incremental increases were assumed to be a constant fractions of the annual average background loading. These increases were introduced after the first year and applied for the remaining 25-year simulation period. The calibrated models were applied to this 25-year period to determine their effectiveness in identifying environmental impacts.

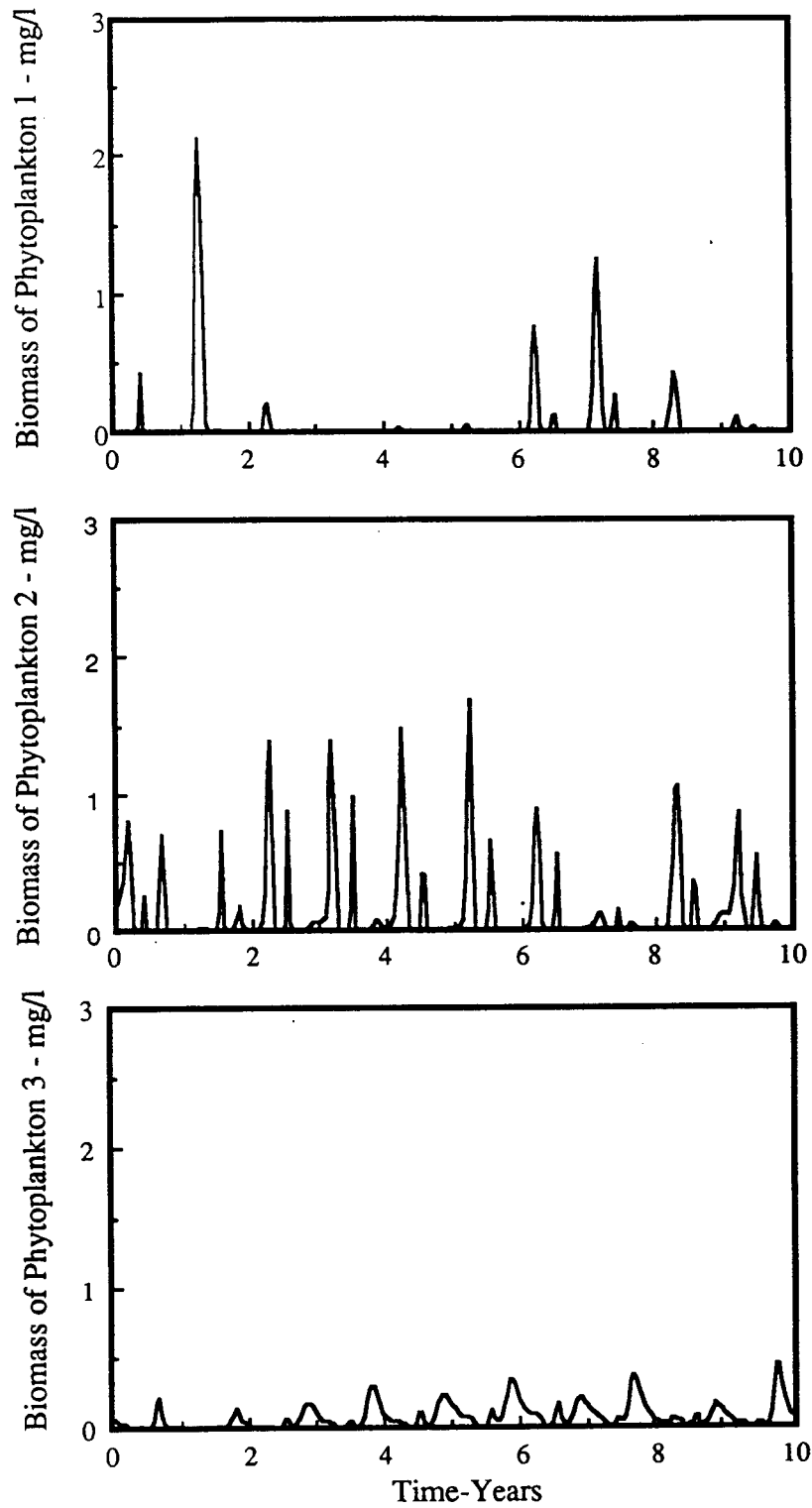


Figure 5.21. Typical ten-year trajectories for three classes of phytoplankton under simulated natural conditions.

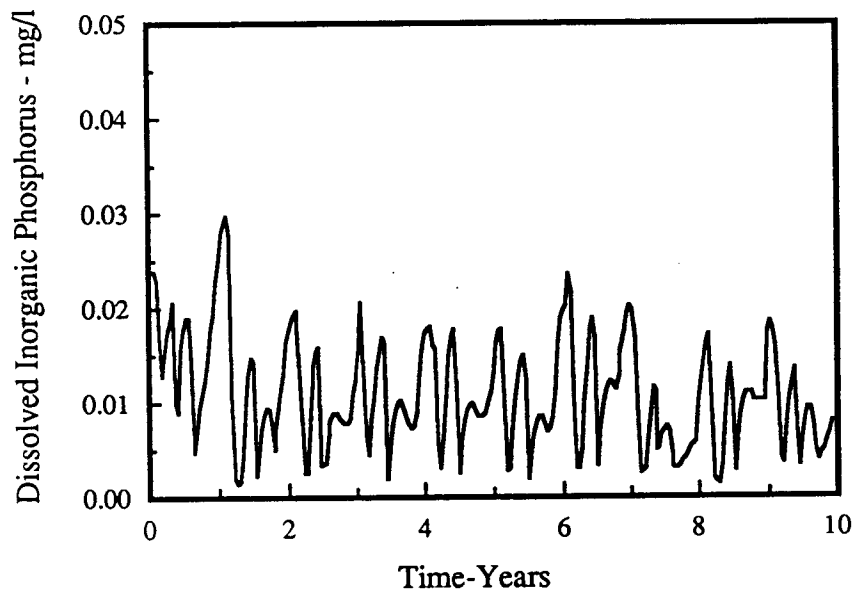


Figure 5.22. Typical ten-year trajectory of dissolved inorganic phosphorus (PO₄-P) under simulated natural conditions.

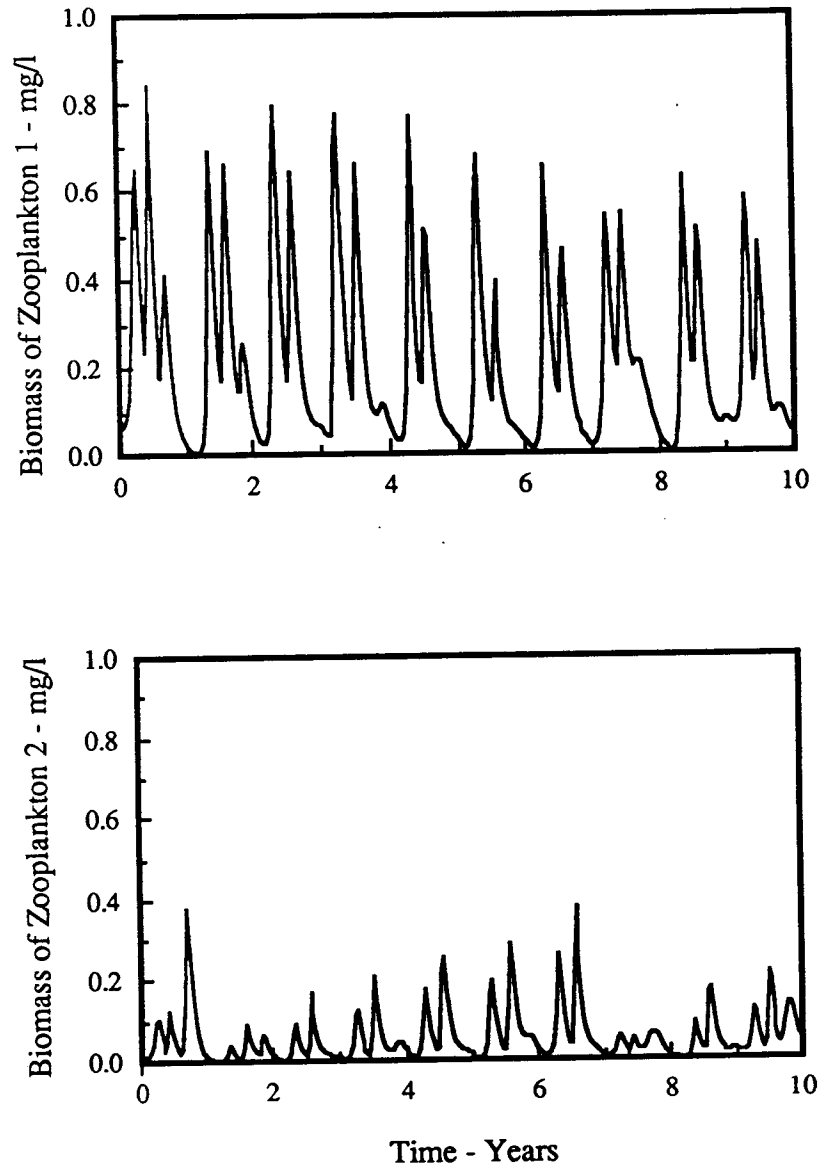


Figure 5.23. Typical ten-year trajectories for two classes of zooplankton under simulated natural conditions.

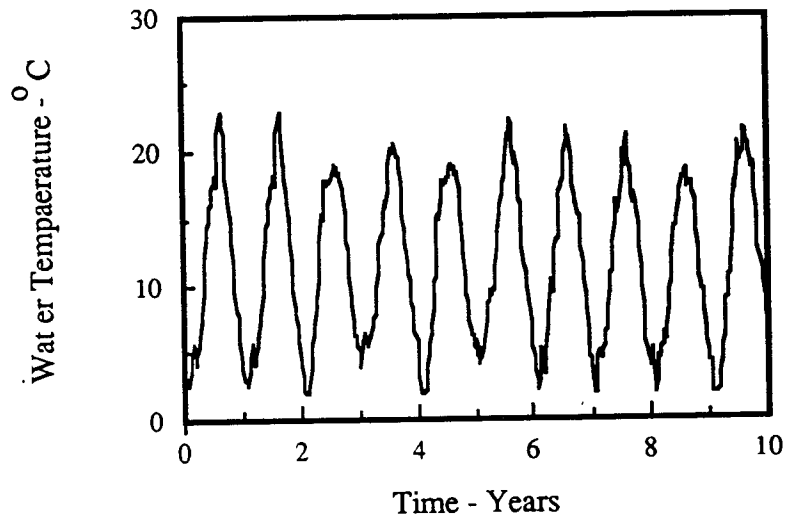


Figure 5.24 Typical ten-year trajectory of simulated water temperature in the hypothetical lake ecosystem.

5.8.1 Parameter Estimates

The parameter estimation process for this portion of the test was the same as for the first part (Section 5.7). Means and standard deviations of the system structure parameters (Φ) for Models I, II, and III are shown in Figures 5.25 through 5.27. Parameter estimates for the apparent settling velocity of Model I have means similar to those for the two highest nutrient loading rates considered in Section 5.7 (Fig. 5.9). The primary difference between the results shown in Figure 5.9 and those shown in Figure 5.25 is that measurement error plays a somewhat less important role in the variability of the estimates obtained with the natural forcing functions than for the estimates obtained under the simpler conditions considered in Section 5.7. This result does, however, support the conclusion reached previously that the value of the apparent settling velocity is a function of the environmental conditions. Under the simulated natural conditions, nutrient loading rates and lake residence times differ from one realization to the next. Despite the natural variability associated with these realizations the variability in the parameter estimates increases with measurement error, similar to results obtained in the first part of this analysis when there was no natural year-to-year variability.

Parameter estimates for Model II are shown in Figure 5.26 with the values of the same parameters used in the reference model. These estimates show some of the same characteristics of the estimates obtained in the first part of the testing. Variability of the estimates, although generally less than that found in Section 5.6 of this chapter, does not appear to be a function so much of measurement error as it is of the parameter estimation process. As in the simpler case, the parameter estimation algorithm attempts to compensate for the absence of grazing due to zooplankton by increasing the magnitude of other loss terms. As before, the settling velocity is most dramatically affected. The mean of the settling velocity estimates are more than four times that of the largest settling

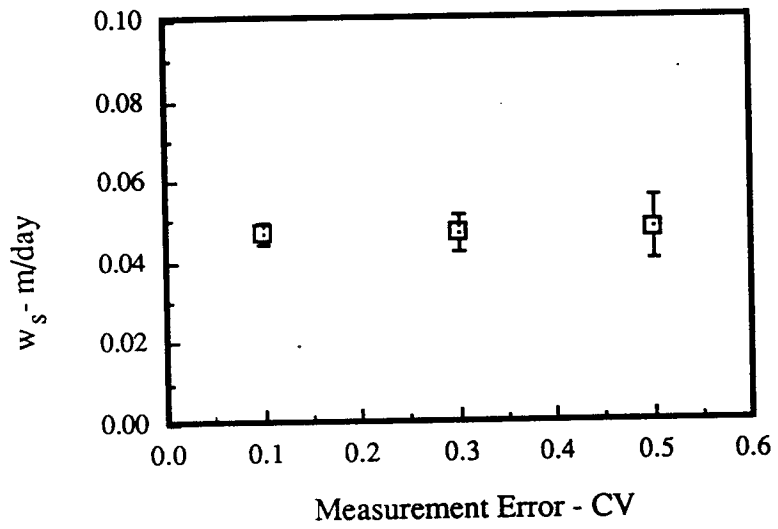


Figure 5.25. Mean and standard deviation of apparent settling velocity, w_s , for Model I using complex reference model under simulated natural conditions.

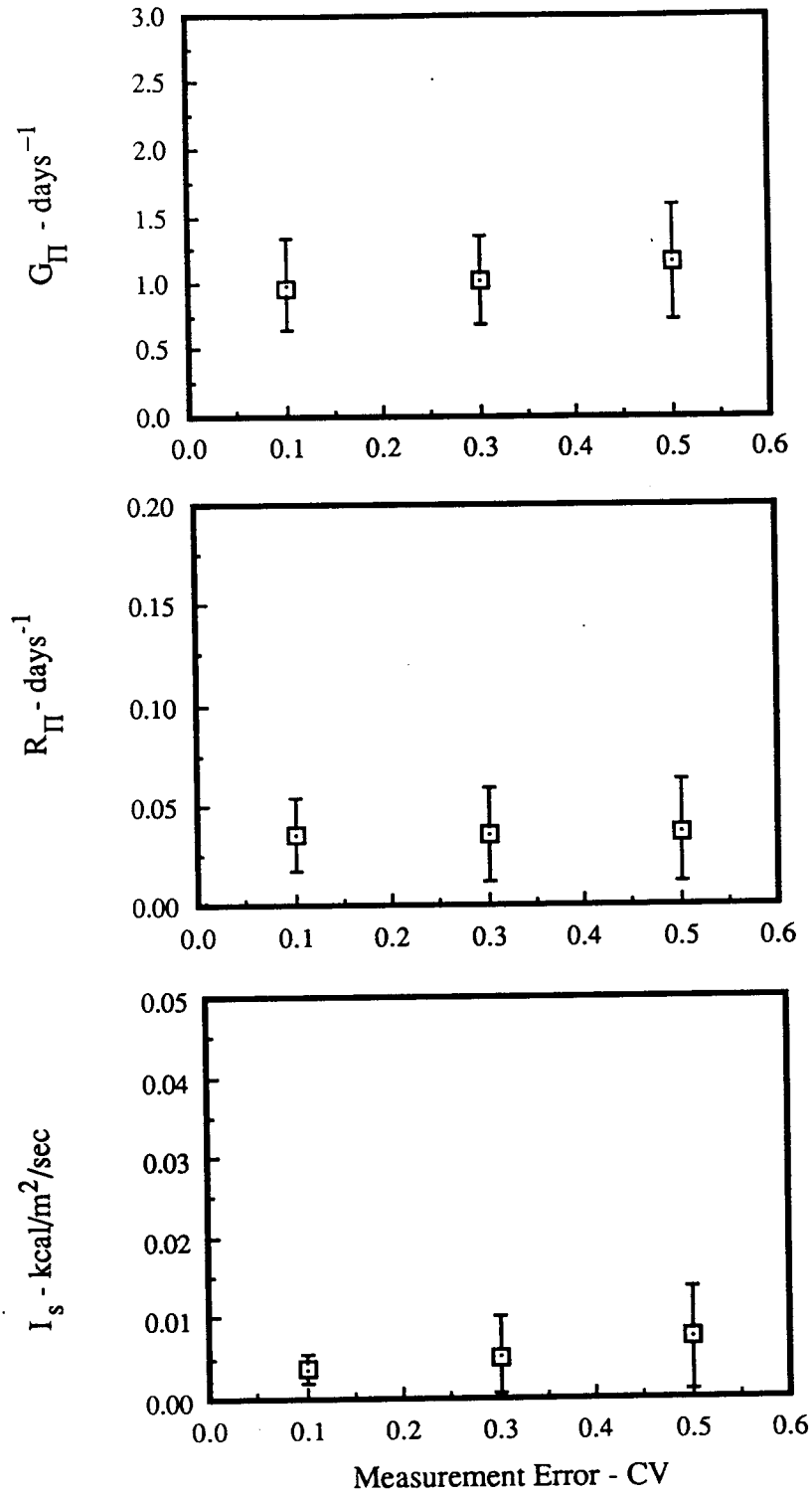


Figure 5.26. Means and standard deviations of parameter estimates for Model II using complex ecosystem reference model under simulated natural conditions.

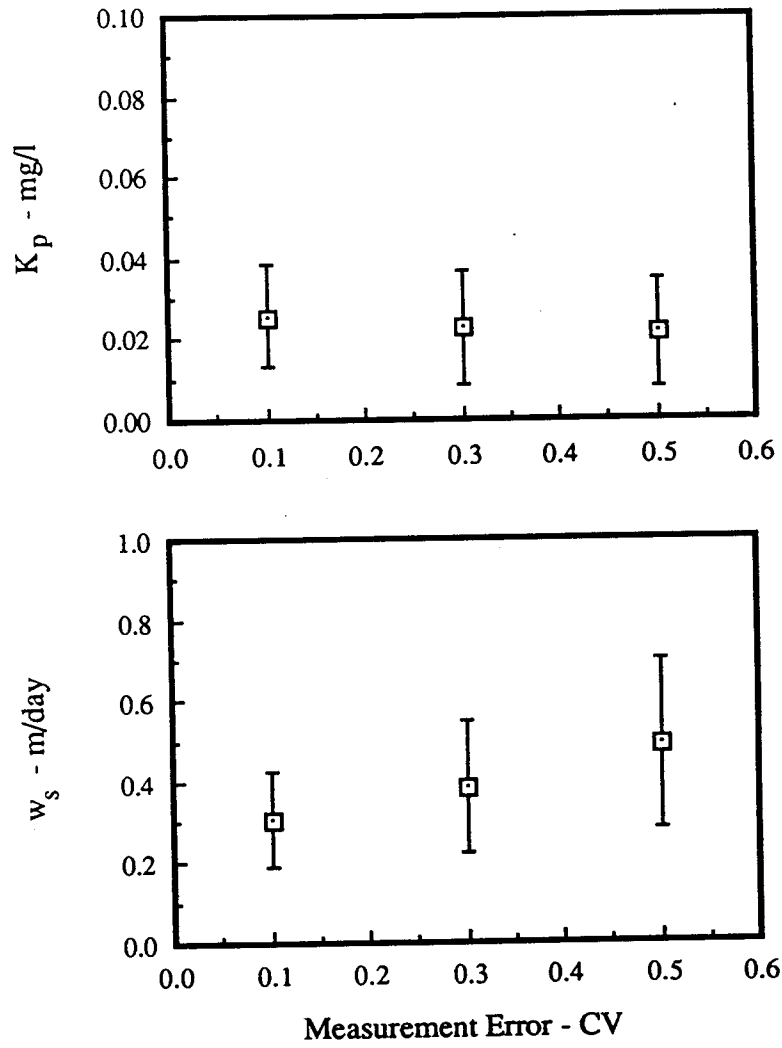


Figure 5.26 (continued). Means and standard deviations of parameter estimates for Model II derived from complex ecosystem reference under simulated natural conditions.

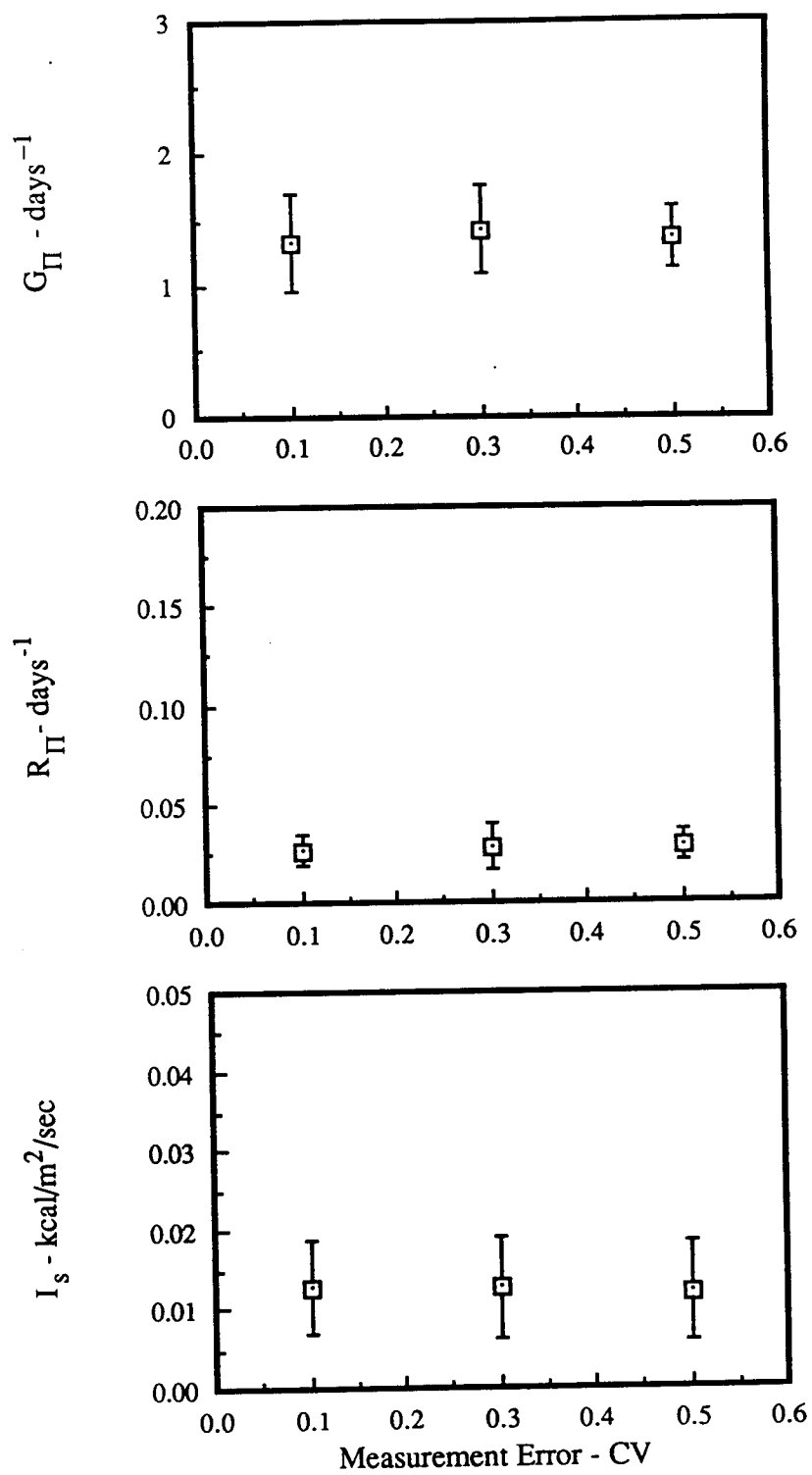


Figure 5.27. Means and standard deviations of parameter estimates for Model III using complex ecosystem reference model under natural conditions.

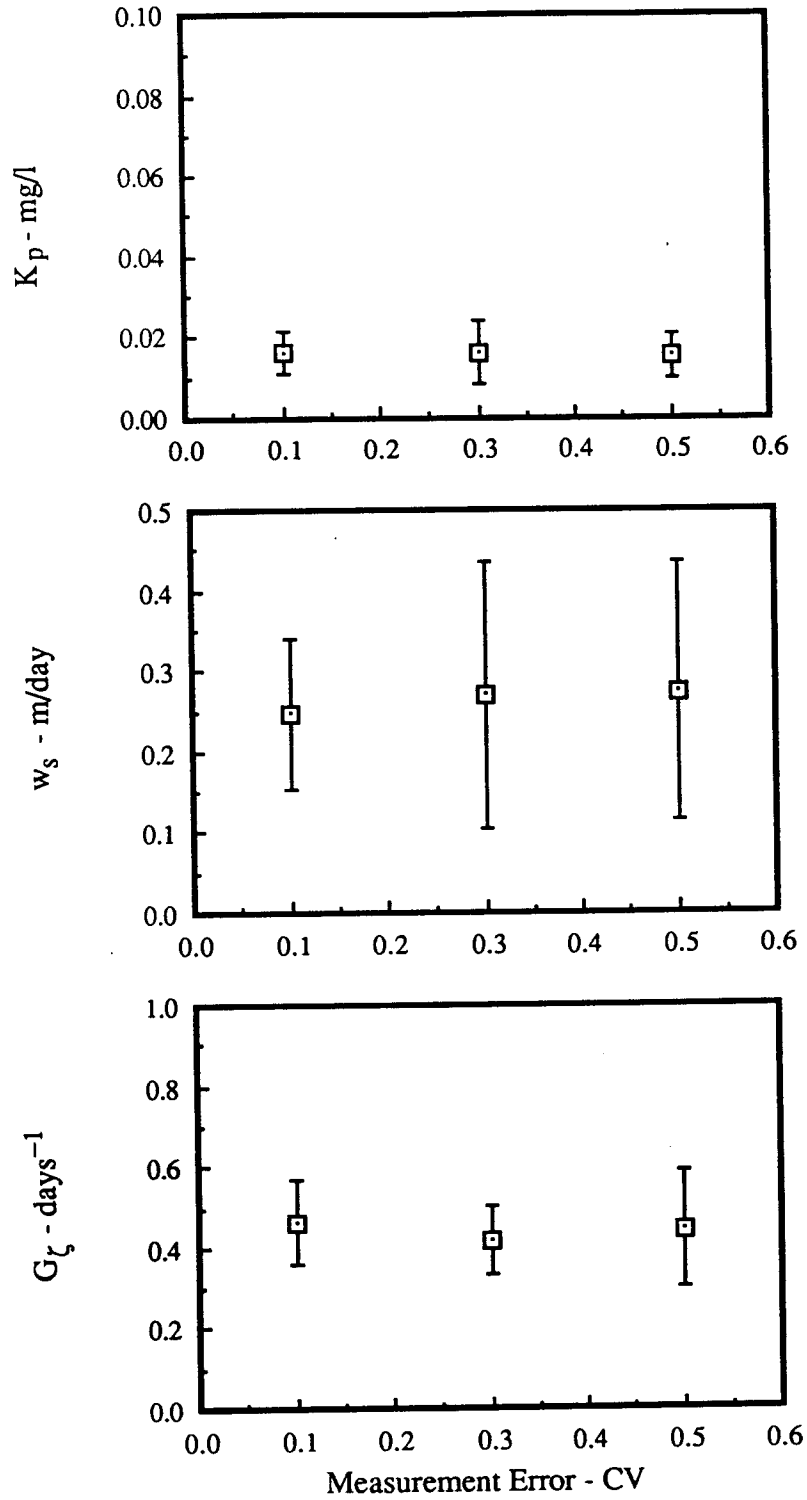


Figure 5.27 (continued). Means and standard deviations of parameter estimates for Model III using complex ecosystem reference model under simulated natural conditions.

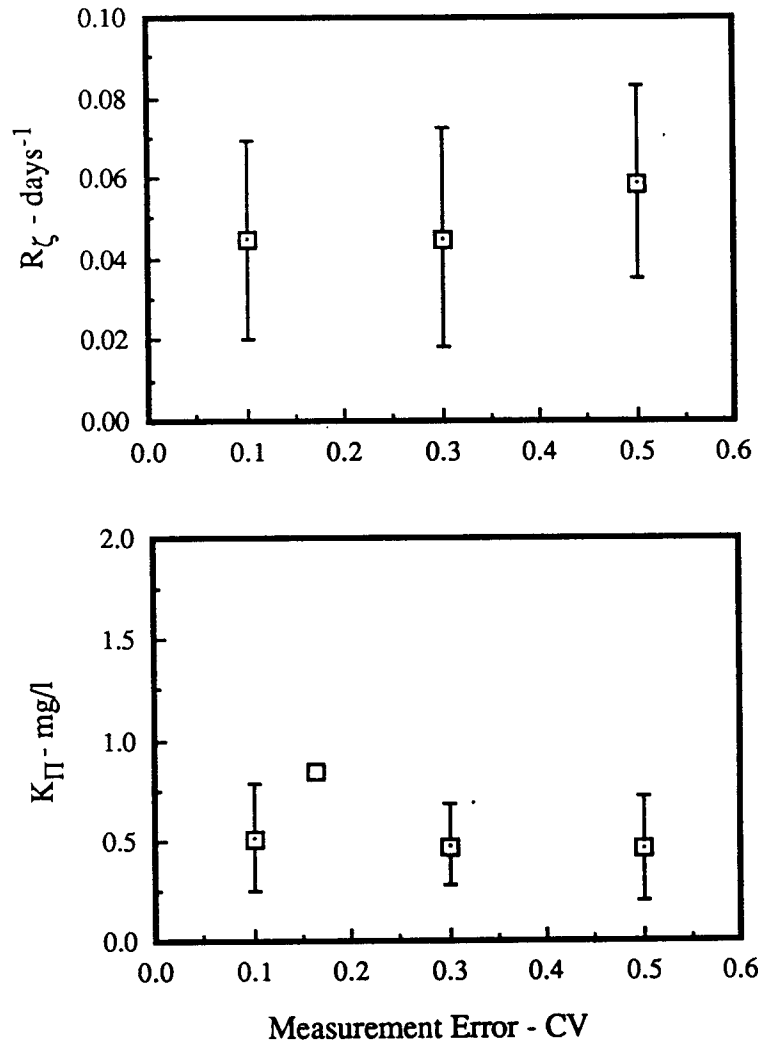


Figure 5.27 (continued). Means and standard deviations of parameter estimates for Model III using complex ecosystem reference model under simulated natural conditions.

velocity used in the reference model. The estimate of the limiting light parameter is also noticeably biased, compared to the true values. However, the direction of the bias is opposite from that found in Section 5.7.

The results for Model III, along with parameter values used in the reference model, are shown in Figure 5.27. With the possible exception of the Michaelis-Menten constant for phosphorus, parameter estimates for Model III are also not influenced greatly by variability in the measurements. The estimates are generally similar to the values used in the reference model, although this is only marginally true for the estimated respiration rate for zooplankton.

5.8.2. Model Validation

The power of the test to determine if each of the three models is the same as the reference model is shown in Figure 5.28 through 29 for each of the six scenarios examined. Estimation of the system error, Q , was a relatively simple matter for Model I and difficult for Models II and III. This is clear from the results of the model validation, which demonstrate that a value of Q can be found such that state variables generated by Model I (eq. 5.9 \geq) are statistically similar to those generated by the reference model. This is not the case for Models II and III, for which model validation results are much poorer.

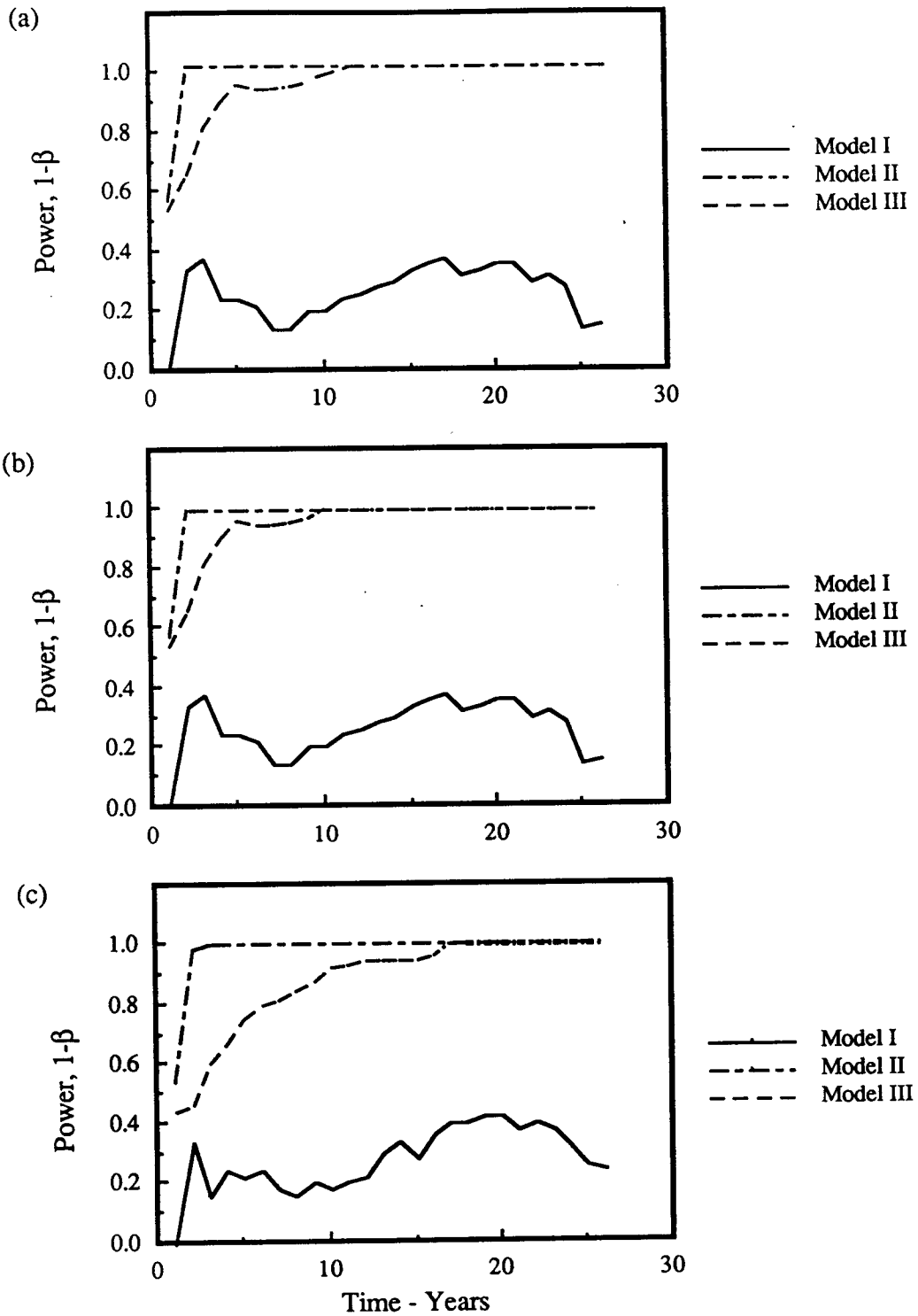


Figure 5.28. Power to reject null hypothesis for Models I, II and III under simulated natural conditions for three levels of measurement error: (a) $CV=0.1$; (b) $CV=0.3$; (c) $CV=0.5$.

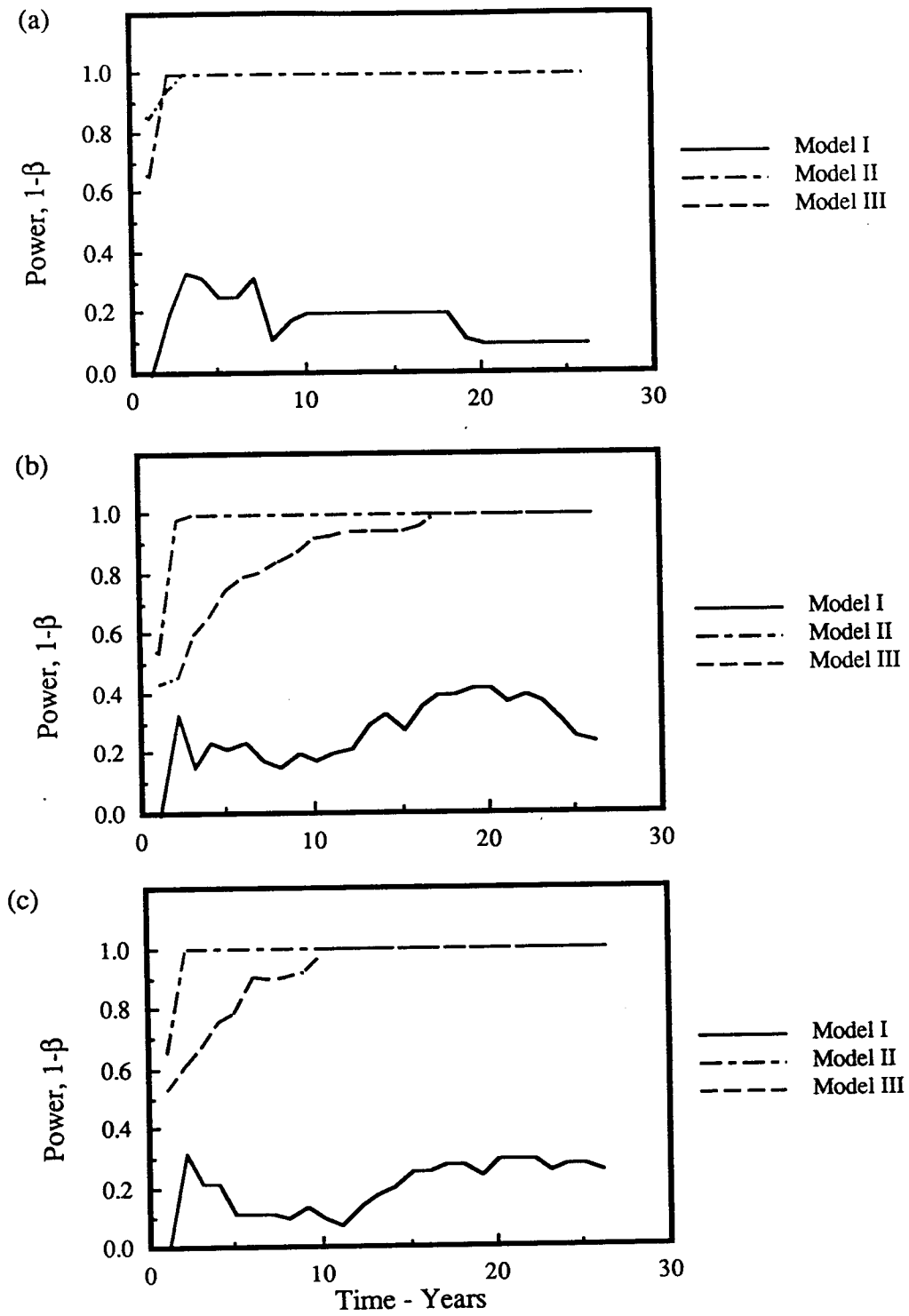


Figure 5.29. Power to reject null hypothesis for Models I, II and III under simulated natural conditions for three levels of measurement error: (a) CV=0.1; (b) CV=0.3; (c) CV=0.5.

5.8.3 Time to Determine Correct Hypothesis

The average number of years needed to decide upon an hypothesis for each of the three models, as well as the fraction of time each was able to identify the true hypothesis, \mathcal{H}_1 , are shown in Tables 5.12 through 5.14. Performance of the two most complex models was poor in this regard. Model II failed to identify the true hypothesis in any of the simulations and Model III was able to identify the true hypothesis in only a very small fraction. The failure of Model II was due to structural errors. That is, the model is not appropriate for this application. Model III performs reasonably well in terms of qualitative evaluation, but fails to pass the more rigorous demands of the hypothesis testing. Small differences between Model III and the reference model in the timing of maximum values lead to errors of sufficient magnitude that the true hypothesis cannot be easily identified.

In terms of the fraction of times the true hypothesis is identified, Model I is clearly superior to the two more complex models. However, the time required to terminate the sequential test (accept \mathcal{H}_0 or \mathcal{H}_1) is much longer for Model I than for the two more complex models. This is not surprising given that the observations used in Model I are annual averages.

Table 5.12 Characteristics of Model I for identifying correct hypothesis for six scenarios of measurement error and nutrient loading. (95% confidence limits in parentheses). Nutrient loading is given in terms of the fraction of the average annual loading from background sources.

Nutrient Loading	Measurement Error-CV	Time to Determine Hypothesis	Fraction of Times \mathcal{H}_1 is Chosen
$\Delta P=0.10$	0.1	13.5 years	0.96 (± 0.05)
$\Delta P=0.10$	0.3	15.6 years	0.88 (± 0.10)
$\Delta P=0.10$	0.5	16.1 years	0.94 (± 0.08)
$\Delta P=0.20$	0.1	6.8 years	>0.99
$\Delta P=0.20$	0.3	7.5 years	0.92 (± 0.12)
$\Delta P=0.20$	0.5	8.9 years	0.94 (± 0.11)

Table 5.13 Characteristics of Model II for identifying correct hypothesis for six scenarios of measurement error and nutrient loading. (95% confidence limits in parentheses). Nutrient loading is given in terms of the fraction of the average annual loading from background sources.

Nutrient Loading	Measurement Error-CV	Time to Determine Hypothesis	Fraction of Times \mathcal{H}_1 is Chosen
$\Delta P=0.10$	0.1	1.1 years	<0.00
$\Delta P=0.10$	0.3	1.1 years	<0.00
$\Delta P=0.10$	0.5	1.1 years	<0.00
$\Delta P=0.20$	0.1	1.1 years	<0.00
$\Delta P=0.20$	0.3	1.1 years	<0.00
$\Delta P=0.20$	0.5	1.1 years	<0.00

Table 5.14 Characteristics of Model III for identifying correct hypothesis for six scenarios of measurement error and nutrient loading. (95% confidence limits in parentheses). Nutrient loading is given in terms of the fraction of the average annual loading from background sources.

Nutrient Loading	Measurement Error-CV	Time to Determine Hypothesis	Fraction of Times \mathcal{H}_1 is Chosen
$\Delta P=0.10$	0.1	1.4 years	0.15 (± 0.16)
$\Delta P=0.10$	0.3	1.8 years	0.20 (± 0.18)
$\Delta P=0.20$	0.1	1.3 years	0.15 (± 0.16)
$\Delta P=0.20$	0.3	1.4 years	0.10 (± 0.13)
$\Delta P=0.20$	0.5	1.5 years	0.10(± 0.13)

5.9 Conclusions

The application of hypothesis testing to a nonlinear, ecosystems model has provided some insights into issues of parameter estimation, measurement error, and level of aggregation. For the ecosystems considered here, it is evident that parameter estimation is a major obstacle to the implementation of valid ecosystems models. Under conditions that can be considered quite simple, the variability in parameter estimates leads to models with a low degree of validity, even when the basic model structure is identical to the reference model. The difficulties are compounded when variability with statistical characteristics similar to natural systems is introduced.

Only a subset of the total number of ecosystems model parameters was actually included in the analysis. It can be inferred from this that parameter estimation would be extremely difficult for the complete parameter set and that, furthermore, such difficulties will increase as model complexity increases.

A somewhat surprising result of the hypothesis tests is the relatively low level of importance associated with measurement error. Except for the error of parameter estimates for Model I in the testing phase, measurement error had very little effect on the outcome of the tests. What significant differences did occur were associated with going from the middle value of measurement error ($CV=0.3$) to the highest value ($CV=0.5$). There was essentially no difference between between the middle value and the lowest value ($CV=0.1$) The one instance that did occur was one that actually favored the mid-value compared to the lowest value. This was probably an anomaly associated with the particular choice of parameters and loading levels. This seemingly anomalous result, however, does emphasize the importance of parameter estimation in affecting outcomes of the tests, compared to the effects of measurement error.

Finally, although the generality of the conclusions is limited by the way in which the problem was structured, the hypothesis testing has shown that it is difficult to obtain good results from the aggregation of nonlinear ecosystems models. In the case studied here, in terms of the ability to detect the true hypothesis, the best results occurred at the highest level of aggregation. The trade-off, however, was that the high level of aggregation induced a smoothing that made it more difficult for the model to detect change. Hence, the simplest model took a much longer time to reach the correct decision. The with the next highest level of aggregation, Model II, was clearly unsatisfactory. The mechanism for accounting for the missing state variable was not adequate for developing a valid model that could identify changes. The most complex model also failed in terms of validity and ability to detect changes. In a qualitative way the most complex model produced reasonable results, but was not able to perform well under hypothesis testing. The results do suggest that the most complex model has more power to reach a decision quickly, but that the resulting decisions are poor.

CHAPTER 6

SUMMARY AND CONCLUSIONS

6.1 Summary

The primary objective of this report was to demonstrate methods that can be used to assess model complexity and data worth in environmental systems. To achieve this objective, a paradigm was developed within the framework of hypothesis testing and state estimation.

The paradigm consisted of the following elements:

- definition of the environmental system, its spatial and temporal boundaries, and the state variables needed to characterize the system
- a process model of the environmental system with state-space structure and either linear or nonlinear dynamics
- a measurement model of the environmental system with either linear or nonlinear dynamics
- a decision variable, the log likelihood function, generated with the Kalman filter using the process and measurement models
- a null and alternate hypothesis regarding the validity of a postulated model when tested against measurements of the environmental system
- a null and alternate hypothesis for testing when an impact to the environmental system could be detected
- a decision rule for choosing the correct hypothesis

The paradigm was developed with applications to two well-known environmental systems, the global carbon cycle and a lake ecosystem. There were several reasons for choosing these two systems. First of all, they were chosen because of the interest these systems hold for environmental scientists and planners. While a great deal of effort has been devoted to analyzing these problems, much remains to be learned about them. Furthermore, there is a large body of data and research that provides the required empirical foundations for applying and testing the methodology.

Collecting environmental data is costly and time-consuming. For purposes of this report, it was assumed that the large pool of available data and knowledge was sufficient to develop a reference system model (McLaughlin and Wood, 1988) that could produce outputs characteristic of the two prototype systems. This provided a rationale for the generation of observations with Monte Carlo simulation techniques. The results of previous research were used to construct reference models of both the global carbon cycle and a lake ecosystem. Populations generated by these reference models provided the observations used in assessing both the methodology and important features of the two environmental systems.

The populations generated by the reference models were used to explore issues of model complexity and data worth for both linear and nonlinear process and measurement models. This was done, for both environmental systems, by postulating several levels of model complexity for the process models and several levels of error for the measurement models. The tests of model validity and the analysis of data worth and model complexity were performed under the controlled, idealized conditions. These conditions were established by the reference system models used to represent each of the two systems. Under these conditions, the methodology was successfully demonstrated, given certain assumptions regarding the the process and measurement models. For the global carbon cycle, the postulated process models were assumed to be perfect; i.e., no model error, and the measurement error was assumed to be normally distributed. In the case of the lake ecosystem, errors in the postulated process models were assumed to be normally distributed and the measurement error log-normally distributed.

6.2 Conclusions

6.2.1 Primary Objectives

With respect to the primary objective of demonstrating and evaluating the methodology, the results of the study led to the following conclusions:

- The methods outlined in the report, based on state estimation and hypothesis testing, provide a multivariate approach to testing validity of environmental models. The methods are sufficiently general as to be appropriate for dynamic, nonlinear models with state-space structure. In the report, the methodology for testing model validity was applied to two case studies, the global carbon cycle and the lake ecosystem. The need to perform such tests of validity for environmental models has been widely recognized (see, e.g., Friedman et al., 1984; Thomann, 1982). Applications of univariate statistics to testing the validity of air models (EPA, 1984) and lake ecosystem models (Bierman and Dolan, 1986) have been reported. However, the literature review (Chapter 2) disclosed no studies of environmental systems which used multivariate statistics in tests of model validity. Since ecosystem models have several state variables, it is important that multivariate methods be available to test model validity.

The multivariate approach was implemented in this report by using the log likelihood function as the test statistic and decision variable. It was successfully used to test the validity of three linear models of the global carbon cycle with four, six and fifteen state variables, respectively. For the lake ecosystem, it was successfully used to test the validity of a linear model with one state variable and two nonlinear models with two and three state variables, respectively.

•The method outlined in the report provides a paradigm for comparing data worth versus model complexity. This paradigm can be used for purposes of allocating resources to the task of assessing the relative value of model development compared to the collection of more and better data. In the two examples considered, the measure of utility was based upon the time required to detect an environmental change. However the methodology is not restricted in terms of the criterion used to determine the trade-offs. It can be modified or expanded to accommodate other performance criteria commonly used in environmental analysis.

6.2.2 Secondary Objective

Within the context of the experimental procedure; i.e., using data generated synthetically by a reference system model to evaluate a limited number of conditions of model complexity and measurement error, a secondary objective was to assess the role of model complexity and data worth for linear and nonlinear models based upon results from two case studies. Given these constraints, the following conclusions were reached:

• Model validity for the postulated linear models of the global carbon cycle is a function of measurement error. There may be little value in applying complex models to detect changes in environmental systems unless measurement errors are reduced to an appropriate level. For the analysis of the linear models of the global carbon cycle, it was possible to validate models at all three levels of complexity when the measurement error for state variables was large enough. Although these levels of measurement error were generally less than actual errors, they were of sufficient magnitude to obscure differences between the reference system model and the aggregated linear models at all levels of complexity. At the

lower level of model error (1% of steady-state compartment values in the scenarios considered) validity of the most highly aggregated model deteriorated substantially with time.

•For the global carbon cycle the worth of measurements associated with each state variable is a function of the dynamic response characteristics of the system. In the case of the global carbon cycle, measurements of state variables with either very small or very large response times proved to be of little value for detecting changes in compartments with response times of moderate size. Changes in the compartments of the global carbon cycle with long response times were so slow they did not contribute significantly to the test statistic at moderate time scales. Similarly, the changes in the compartments with very short response times were too small to contribute significantly. The results show that for the case of the global carbon cycle, a preference for relatively simple models results from structural considerations as well as from considerations of data needs for performing parameter estimation. Insofar as the Bjorkstrom model is an accurate representation of the true global carbon cycle, these results are applicable to that specific environmental problem. These are not all general conclusions, of course, since some systems may be more closely coupled at various time scales than is the model of the global carbon cycle used here. This specific application does demonstrate, however, the importance of systems dynamics in determining data worth and that hypothesis testing is an effective way of quantifying its value.

•When the true parameters of the postulated linear process model are perfectly known, as assumed in the case of the global carbon cycle, increases in model complexity lead to higher levels of model validity and better ability to detect change. Increases in the complexity of the postulated linear models for the global carbon cycle resulted in uniformly higher levels of model validity and generally better ability to detect change. The marginal increase in ability

to detect change, as a function of model complexity, was related to the response time of the state variables. For the inputs considered, the marginal increase was greatest in the state variables characterizing carbon levels in the atmosphere, terrestrial biota and soil. There was virtually no change in ability to detect change as function of model complexity for the state variable characterizing carbon in the ocean surface waters.

•When the parameters must be estimated, as in the case of the lake ecosystem, the models of low complexity generally perform as well as or better than the more complex models in terms of model validity and fraction of times that the correct decision is made. For the lake ecosystem examined in Chapter 5, the highly aggregated model with a single state variable, total phosphorus, generally performed better than the two more complex models. This model did require a longer time to reach a decision than the more complex models, but the more complex models had an unacceptably low rate of correct decisions, at least for the part of the experiment in which environmental forcing functions with realistic variability were used.

The principal quality of total phosphorus that makes it effective as an aggregation of the ecosystem state is that it accounts for a substantial fraction of the ecosystem response to forcing functions. The need for finding a variable that characterizes system response at a high level of aggregation is a consequence of limitations in obtaining accurate parameter estimates and the lack of an adequate rationale for successfully aggregating model compartments at intermediate levels.

•For the nonlinear lake ecosystem model, parameter estimation and hypotheses regarding model complexity and structure, play crucial roles in determining the level of model complexity at which successful environmental assessments can be performed. The limitations

associated with parameter estimation were made particularly clear in the initial phases of ecosystem model testing. In the initial phase, the most complex model analyzed was equivalent to the reference system model. The only difference was that the parameters of the most complex model were estimated from data generated by the reference system model and then corrupted by measurement error. Since the true parameters were known it was possible to specifically determine the importance of parameter estimation. For the case in which the reference model and the model used in the filter were identical, model parameters estimated from the data produced generally poor performance from the filter compared to those results obtained by using the true model parameters. This was true even though the cost function for parameter estimates of the most complex model was almost always lower than the cost function generated by the reference system model with the true parameters. Model performance, with respect to model validity, the time to detect change and the fraction of times the correct hypothesis was chosen, was significantly worse for estimated parameters compared to the true parameters.

In the report it was hypothesized that model complexity should be increased by adding higher trophic levels. The dangers of this approach were demonstrated by the difficulty of obtaining an adequate nonlinear model at an intermediate level of aggregation; i.e. the model with two trophic levels, a limiting nutrient and phytoplankton. When nonlinear losses in phytoplankton due to zooplankton grazing were aggregated into a linear phytoplankton loss term, the resulting model was inadequate when viewed in terms of the two criteria of model validity and ability to determine whether or not a change had occurred. The rationale for model aggregation at an intermediate level was based upon an *ad hoc* approach commonly used in the identification of lake ecosystems models. The *ad hoc* approach to aggregation at intermediate levels may lead to adequate models under certain conditions, particularly when the level of secondary production is low. From the results obtained in this report, this

approach can also lead to models that perform poorly. It is, therefore, important to understand the primary links between state variables before concluding that model hypotheses are appropriate and that system identification is complete.

- Measurement error is an important factor in determining the time to detect change and the fraction of time required to detect change. However, it is less important in the parameter estimation stage for complex, nonlinear models. In both case studies, the time to detect change and the fraction of time the correct hypothesis was chosen improved as measurement error decreased. As discussed previously for the global carbon cycle, the dynamics of the observed state variables are also important. For the nonlinear lake ecosystem model, measurement error was least important for the simple, linear lake model, for which the time to detect change was long at all levels.

For the range of measurement errors considered in the analysis of the nonlinear lake ecosystem model, variability in most of the parameter estimates was not a function of measurement error for the two most complex models. Intrinsic difficulties associated with nonlinear parameter estimation and variability in environmental forcing functions had a greater impact upon variability of parameters estimates than did measurement error. Since only one time/space scenario for sampling was considered, it was not possible to determine how this conclusion might be affected by increasing the frequency of sampling, sampling for a longer period or some combination of the two. For the simple, highly aggregated linear lake model, measurement error was important in parameter estimation. When environmental forcing functions with realistic variability were included, the effect of measurement error upon parameter estimates for the simple, linear lake model was greatest due to interactions (covariance) with these forcing functions.

6.3 Recommendations

It is well known that the problems of model complexity and data worth have many aspects. It was possible to explore only a few of these aspects and, not surprisingly, a number of questions were raised, either explicitly or implicitly, for which the scope of the study did not permit investigation. Some of these questions are described below.

- While the nature of the methodology can lead to dimensionality problems, an increase in the number of state variables from that used in this report is certainly practical with respect to available computing equipment. Increasing the number of state variables is more important for the lake ecosystem model than for the global carbon cycle. Only three state variables were considered in the lake ecosystem models. Filtering is practical for systems with 10 to 15 times as many variables as used in this report. Increasing the number of state variables would make it possible to more fully address two issues, increased model complexity and/or more extensive spatial monitoring.

- In this study, only a small subset of the actual number of parameters were included in the parameter estimation portion of the lake ecosystem model assessment. A complete evaluation of the limitations imposed by parameter estimation would require the inclusion of a substantial number of additional parameters. Including additional parameters in the analysis of model complexity and data worth could very well lead to less satisfactory results than were obtained in this report. However, there may be more powerful search techniques than the simplex method (Nelder and Mead, 1965) used in this study that could be applied successfully to the analysis. It also may be that certain parameters may be much more important than others. An analysis of parameter sensitivity, which was not done in this study, could lead to efficiencies in computation and perhaps in parameter estimates.

•Given the difficulties associated with parameter estimation and model validation for nonlinear models, it is worthwhile to search for state variables that describe the important features of the system in a simple way. Parameter estimation placed severe limitations on the ability to obtain valid nonlinear models of the lake ecosystem. The limitations imposed by parameter estimation compared to the relative success achieved by the simplest model provides the motivation for encapsulating the major system functions in the fewest variables and with the simplest structure. One approach to this is to find processes for which ecosystems functions can be characterized by linear models. Compartmental models (O'Neill, 1979) provide a potentially successful approach to this problem. The simple, linear total phosphorus model used in this study is a highly aggregated example of how this might work. If environmental analysts are interested in improving their capability for detecting change, however, this simple approach is not sufficient. It is for this reason that the search for a better representation of lake ecosystem dynamics than is provided by the total phosphorus model would be beneficial.

•There is a need to find better methods of estimating the process model covariance matrix, Q , and the measurement model covariance matrix, R . The analysis of system error, Q , and measurement error, R , was done in this study in a simple way. Q was estimated with the parameter estimation algorithm and R was estimated from *a priori* knowledge of the sampling error. In actual applications, this may not be possible and the use of adaptive algorithms for estimating these parameters provides a potential way for improving the model. A number of approaches have been used successfully in other areas. Todini (1976) has developed an algorithm that has been successfully applied to hydrologic modelling.

Similarly, Myers and Tapley (1979) have developed algorithms for use in aerospace applications that could as well be applied to environmental systems.

- The analysis of data worth should be extended to a more thorough evaluation of the data worth of specific compartments. In this study, only a limited evaluation of the worth of data for specific compartments was performed. It is evident, however, that measurement of certain compartments can provide more information than for others. Data worth for individual compartments is determined by both the accuracy with which they can be measured and by their importance in the dynamics of the system. For nonlinear systems, evaluating the latter characteristic is more difficult than evaluating the former. Depending upon the cost per measurement for each of the state variables, it may be useful to investigate the contribution to the total information arising from each of the state variables. The methods described in this study are appropriate for such analysis and could provide ways of quantifying optimal sampling strategies.

- The methodology should be applied to an environmental system for which there is a comprehensive set of actual measurements. The methodology described in the report has been successfully demonstrated for data generated synthetically with reference system models. The methodology should be applied to real systems for purposes of model validation. As mentioned previously, there is a need for methods to test the validity of multivariate, dynamic models of environmental systems. The hypothesis testing procedure described in the report can be applied to systems by following the paradigm developed for the two case studies.

The sequential tests for determining environmental impact can be applied to real systems in a number of ways. One is to use the tests as a way of evaluating model

complexity and data worth, as was done in the report. Real data can be used to develop reference models. The reference models, in turn, can be used to learn more about the relationships between model complexity and data worth. A more practical application of the sequential test is to use it as tool for assessing environmental quality. Once appropriate process and measurement models have been developed, the sequential test can be used to monitor the status of environmental systems and to provide a measure for determining when there has been an impact. The use of state estimation and hypothesis testing methods in these ways will result in a more systematic approach to environmental analysis.

BIBLIOGRAPHY

- Aoki, M., 1968. Control of large-scale dynamic systems by aggregation. *IEEE Transactions on Automatic Control*, AC-13: 246-253.
- Baca, R.G. and R.C. Arnett. 1976. A finite element water quality model for eutrophic lakes. BN-SA-540. Battelle Pacific Northwest Lab., Richland, Wash., 27 pp.
- Baca, R.G., W.W. Waddel, C.R. Cole, A.Brandstetter and D.B. Cearlock. 1973. EXPLORE I: A river basin water quality model. Report to the U.S. Environmental Protection Agency, Battelle-Northwest, Richland, WA.
- Bacastow, R. and C.D. Keeling. 1973. Atmospheric carbon dioxide and radiocarbon in the natural carbon cycle: II. Changes from A.D. 1700 to 2070 as deduced from a geochemical model In: G.M. Woodwell and E.V. Pecan (Editors), *Proceedings of the Conference on Carbon and the Biosphere*. CONF-720510, NTIS, Springfield, VA, pp. 87-133.
- Barnwell, T.O., Jr., and P.A. Krenkel. 1982. The use of water quality models in management decision making. *Water Science Technology*, 14: 1095-1107.
- Beck, B. and P. Young. 1976. Systematic identification of DO-BOD model structure. *Journal of Environmental Engineering, ASCE*, 102 (EE5): 909-927.
- Behrens, J.C., J.E. Beyer, O.B.G. Madsen and P.G. Thomsen. 1975. Some aspects of modelling the long-term behaviour of aquatic ecosystems. *Ecologic Modeling*, 1: 163-197.
- Bierman, V.J., Jr. and D.M. Dolan. 1986. Modeling of phytoplankton in Saginaw Bay: I. Calibration phase. *Journal of Environmental Engineering, ASCE*, 112 (EE2): 400-414.
- Bjorkstrom, A. 1979. A model of CO₂ interaction between atmosphere, oceans and land biota. In: B. Bolin, E.T. Degem, S. Kempe and P. Ketner (Editors), *The Global Carbon Cycle*. SCOPE 13, Scientific Committee on Pollution in the Environment. Wiley, New York, 491 pp.
- Bolin, B., 1977. Changes of land biota and their importance for the carbon cycle. *Science*, 196: 613-615.
- Bolin, B., E.T. Degem, S. Kempe, and P. Ketner, (Editors). 1979. *The global carbon cycle*. SCOPE 13, Scientific Committee on Pollution in the Environment. Wiley, NY, 491 pp.
- Bolin, B.(Editor). 1981. *Modeling the global carbon cycle*. SCOPE 16, Scientific Committee on Pollution in the Environment. Wiley, New York, 390 pp.
- Bottrell, H.H., A. Duncan, Z.M. Gliwicz, E. Grygierek, A. Herzig, A Hillbricht-Ilkowska, H. Kurasawa, P. Larsson and T. Weglenska. 1976. A review of

- some problems in zooplankton production studies. *Norwegian Journal of Zoology*, 24 (4): 419-456.
- Bowles, D.S. and W.J. Grenney. 1978. Steady-state river quality modeling by sequential Extended Kalman Filter. *Water Resources Research*, 14: 84-96.
- Cale, W.G., Jr., R.V. O'Neill and H.H. Shugart. 1983. Development and application of desirable ecological models. *Ecological Modelling*, 18:171-186.
- Canale, R.P., L.M. dePalma and W.F. Powers. 1980. Sampling strategies for water quality in the Great Lakes. EPA-600/3-80-055. U.S. Environmental Protection Agency, Duluth, MN. 77 pp.
- Carney, J.H., D.L. DeAngelis, R.H. Gardner, J.B. Mankin and W.M. Post. 1981. Calculation of probabilities of transfer, recurrence intervals, and positional indices for linear compartment models. Oak Ridge National Laboratories Report No. ORNL/TM-7379. 70 pp.
- Chapra, S.C. 1975. Comment on 'An empirical method of estimating the retention of phosphorus in lakes' by W.B. Kirchner and P.J. Dillon. *Water Resources Research*, 11(6): 1033-1034.
- Chapra, S.C. 1977. Total phosphorus model for the Great Lakes. *Journal of the Environmental Engineering Division, ASCE*, 103(2): 147-161.
- Chapra, S.C. and S.J. Tarapchak. 1976. A chlorophyll *a* model and its relationship to phosphorus loading plots for lakes. *Water Resources Research*, 12(6):1260-1264.
- Charney, J. 1979. Carbon dioxide and climate: A scientific assessment. National Academy of Science, National Academy Press. Washington, D.C., 22 pp.
- Chen, C.W. 1970. Concepts and utilities of ecologic model. *Journal of the Sanitary Engineering Division, ASCE*, 96 (SA5): 1085-1098.
- Chen, C.W. and G.T. Orlob. 1975. Ecologic simulation for aquatic environments. In: *Systems Analysis and Simulation in Ecology, Vol. III*. Academic Press, New York, NY. 354 pp.
- Constable, T.W. and E.A. McBean. 1979. Kalman Filtering modeling of the Speed River quality. *Journal of the Environmental Engineering Division, ASCE*, 105(5): 961-978.
- Craig, H. 1957. The natural distribution of radiocarbon and the exchange time of carbon dioxide between atmosphere and sea. *Tellus*, 9: 1-17.
- Crim, R. and N. Lovelace 1973. AUTO-QUAL modelling system. EPA-440/9-7-003. U.S. Environmental Protection Agency, Washington, D.C. 301 pp.
- Dandy, G.C. and S.F. Moore 1979. Water quality sampling programs in rivers. *Journal of the Environmental Engineering Division, ASCE*, 105: 695-712.

- Davison, E.J. 1966. A method of simplifying linear dynamic systems. *IEEE Transactions on Automatic Control*, AC-11: 93-101.
- de Caprariis, P. 1984. A note on the sufficiency of low resolution ecosystem models. *Ecological Modelling*, 21: 199-207.
- Dillon, P.J. 1975. The phosphorus budget of Cameron Lake, Ontario: The importance of flushing rate to the degree of eutrophy of lakes. *Limnology and Oceanography*, 20: 28-39.
- Dillon, P.J. and F.H. Rigler. 1975. A simple method for predicting the capacity of a lake for development based on lake trophic status. *Journal of the Fisheries Research Board of Canada*, 32:1519-1531.
- DiToro, D.M. and W.F. Matystik. 1980. Mathematical models of water quality in large lakes: 1. Lake Huron and Saginaw Bay model development, verification, and simulation. U.S. Environmental Protection Agency Report No. EPA-600/3-80-056.
- DiToro, D.M., J.J. Fitzpatrick and R.V. Thomann. 1981. Water quality analysis simulation program (WASP) and model verification program (MVP). EPA Contract No. 68-01-3872, Hydrosience, Inc., Westwood, NJ.
- DiToro, D.M., D.J. O'Connor and R.V. Thomann. 1975. Phytoplankton-zooplankton-nutrient interaction model for Western Lake Erie. In: *Systems Analysis and Simulation in Ecology*, Vol. III. Academic Press, New York, NY. 354 pp.
- Edinger, J.E. and J.C. Geyer. 1965. Heat exchange in the environment. Edison Electric Institute Report No. 65-902, New York, NY.
- Eriksson, E. and P. Welander. 1956. On a mathematical model of the carbon cycle in nature. *Tellus*, 8: 155-175.
- Faris, B. and D.P. Lettenmaier. 1988. NASQAN coastal sampling optimization. Report to the Office of Water Quality.
- Fedra, K. 1980. Estimating model prediction accuracy: A stochastic approach to ecosystem modeling. WP-80-168. IIASA, Laxenburg, Austria, 26 pp.
- Fedra, K., 1982. Environmental modeling under uncertainty: Monte Carlo simulation. WP-82-42. IIASA, Laxenburg, Austria. 68 pp.
- Fedra, K., G. van Straten and M.B. Beck. 1981. Uncertainty and arbitrariness in ecosystem modelling: A lake modelling example. *Ecological Modelling*, 13: 87-110.
- Ferrara, R.A. and T.T. Griffin. 1986. model complexity for trophic state simulations in reservoirs. In: *Proceedings EPA Stormwater and Water Quality Model Users Group Meeting*, Orlando, Florida. pp. 24-55.

- Finn, J.T. 1976. Measures of ecosystem structure and function derived from analysis of flows. *Journal of Theoretical Biology*, 56: 363-380.
- Forrester, J. 1971. *World dynamics*. Wright-Allen Press, Inc. Cambridge, MA. 142 pp.
- Friedman, R., C. Ansell, S. Diamond, and Y.Y. Haimes. 1984. The use of models for water resources management, planning, and policy. *Water Resources Research*, 20(7): 793-802.
- Gardner, R.H., J.B. Mankin and W.R. Emanuel. 1980. A comparison of three carbon models. *Ecological Modelling*, 8: 313-332.
- Gasperino, A. and R. Soltero. 1977. Phosphorus reduction and its effect on the recovery of Long Lake reservoir. Prepared for Washington State Department of Ecology by Battelle Pacific Northwest Laboratories, Richland, WA.
- Gelb, A. (Editor). 1974. *Applied optimal estimation*. MIT Press, Cambridge, MA., 374 pp.
- Ghash, B.K. 1970. *Sequential tests of statistical hypotheses*. Addison-Wesley, Reading, MA, 454 pp.
- Godfrey, K. 1983. *Compartmental models and their application*. Academic Press, New York, NY.
- Goodall, D.W. 1975. Ecosystem modeling in the desert biome. In: *Systems analysis and simulation in ecology*, Volume III, B.C. Patten (editor). Academic Press, New York, NY. pp. 73-94.
- Grad, J. and M.A. Brebner. 1968. Algorithm 343: Eigenvalues and eigenvectors of a real general matrix. *Communications of the ACM*, 11:820-826.
- Hannon, B. 1973. The structure of ecosystems. *Journal of Theoretical Biology*, 41: 535-546.
- Hansen, J., G. Russell, D. Rind, P. Stone, A. Lacis, S. Lebedeff, R. Ruedy, and L. Travis. 1981. Climate impacts of increasing atmospheric CO₂, *Science*, 213: 957-963.
- Harbeck, G.E. 1958. Water loss investigation. In: *Lake Mead Studies*, U.S. Geological Survey Paper No. 298., Washington, D.C.
- Harris, G.P. 1980. Temporal and spatial scales in phytoplankton ecology. Mechanisms, methods, models and management. *Canadian Journal of Fisheries and Aquatic Sciences*, 37: 877-900.
- Heidtke, T.M. and J.M. Armstrong. 1979. Probabilistic sampling model for water quality management. *Journal of the Water Pollution Control Federation*, 51: 2916-2927.

- Hirsch, R.M. 1988. Statistical methods and sampling design for estimating step trends in surface water quality. *Water Resources Bulletin*, 24(3): 493-503.
- Hornberger, G.M. 1980. Uncertainty in dissolved oxygen prediction due to variability in algal photosynthesis. *Water Research*, 14: 355-361.
- Hornberger, G.M. and R.C. Spear. 1980. Eutrophication in Peal Inlet-I. The problem-defining behavior and a mathematical model for the phosphorus scenario. *Water Research*, 14:29-42.
- Horowitz, J., and L. Bazel. 1977. An analysis of planning for advanced wastewater treatment (AWT). Prepared for: Headquarters, U.S. Environmental Protection Agency. 420 pp.
- Imboden, D.M. and R. Gachter. 1978. A dynamic lake model for trophic state prediction. *Ecologic Modelling*, 4:77-98.
- Innis, G.S. 1975. Role of total system models in the grassland biome study. In: *Systems analysis and simulation in ecology*, Volume III, B.C. Patten (editor). Academic Press, New York, NY. pp. 14-47.
- Isaji, T. and M. Spaulding. 1981. Numerical modeling of entrainment and far field thermal dispersion for the NEP I and II power station, Charlestown, Rhode Island. Oak Ridge National Laboratory Report No. ORNL/TM-7590, Oak Ridge, TN.
- Jamshidi, M. 1983. *Large-scale systems*. Elsevier Science Publishing Co., Inc., Amsterdam, The Netherlands, 162 pp.
- Johansen, P.A., M.W. Lorenzen, and W.W. Waddel. 1976. A multi-parameter estuary model. In: W. Ott (Editor), *Environmental Modeling and Simulation*. EPA 600/9-76-016. U.S. Environmental Protection Agency, Washington, D.C. pp. 111-114.
- Kalman, R. 1960. A new approach to linear filtering and prediction problems. *Journal of Basic Engineering, Series D, ASME*, 82: 35-45.
- Kalman, R. and R. Bucy. 1961. New results in filtering and prediction theory. *Journal of Basic Engineering, Series D, ASME*, 83: 95-108.
- Keeling, C.D. 1973. Industrial production of carbon dioxide from fossil fuels and limestone. *Tellus*, 25: 174-198.
- Keeling, C.D., Bacastow, R.B., Bainbridge, A.E., Ekdahl, C.A., Jr., Guenther, P.R., and Waterman, L.S. 1976. Atmospheric carbon dioxide variations at Mauna Loa Observatory, Hawaii. *Tellus*, 28: 538-551.
- Kitanidis, P.K., D. Veneziano and C.S. Queiroz. 1978. Sampling networks for violation of water quality standards. In: Chao-Lin Chiu (Editors), *Applications*

- of Kalman Filter to hydrology, hydraulics and water resources. University of Pittsburgh, Pittsburgh, PA., pp. 213-230.
- Koivo, A.J. and G.R. Phillips. 1971. Identification of mathematic models for DO and BOD concentrations in polluted streams from noise-corrupted measurements. *Water Resources Research*, 7: 853-862.
- Koivo, A.J. and G.R. Phillips. 1972. On determination of BOD and parameters in polluted stream models from DO measurements only. *Water Resources Research*, 8: 478-486.
- Koivo, A.J. and G.R. Phillips. 1976. Optimal estimation of DO, BOD and stream parameters using a dynamic discrete time model. *Water Resources Research*, 12: 705-711.
- Kokotovic, P.V. R.E. O'Malley, Jr. and P. Sannuti. 1976. Singular perturbations and order reduction in control theory-an overview. *Automatica*, 12: 123-132.
- Larsen, R.J. and M.L. Marx. 1981. *An Introduction to Mathematical Statistics and its Application*. Prentice-Hall, Englewood Cliffs, NJ, 536 pp.
- Larsen, D.P. and H.T. Mercier. 1976. Phosphorus retention capacity of lakes. *Journal of the Fisheries Research Board of Canada*, 33: 1742-1750.
- Lehman, J.T., D.B. Botkin, and G.E. Likens. 1975. The assumptions and rationales of a computer model of phytoplankton population dynamics. *Limnology and Oceanography*, 20(3): 343-364.
- Lettenmaier, D.P. 1975. Design of monitoring systems for detecting trends in stream quality. Tech. Report No. 39, C.W. Harris Hydraulics Lab., University of Washington, Seattle, WA. 201 pp.
- Lettenmaier, D.P. 1979. Dimensionality problems in water quality network design. *Water Resources Research*, 15: 1692-1700.
- Lettenmaier, D.P. and S.J. Burges. 1976. Use of state estimation techniques in water resource systems modeling. *Water Resources Bulletin*, 12: 83-99.
- Lewis, J.B. 1977. *Analysis of linear dynamic systems*. Matrix Publications, Inc., Champaign, Illinois. 862. pp.
- Litz, L. 1982. Order reduction of linear state-space models via optimal approximation of the nondominant modes. In: *Large Scale Systems*, A. Titli and M.G. Singh (Editors). North-Holland Publishing Co. pp. 195-202.
- Loaiciga, H.A. and M.A. Marino. 1985. An approach to parameter estimation and stochastic control in water resources with an application to reservoir operation. *Water Resources Research*, 21:1574-1584.

- Lorenzen, M.W. 1979. Effect of phosphorus control options on lake water quality. EPA-560/11-79-011, U.S. Environmental Protection Agency, Office of Toxic Substances, Washington, D.C.
- Lotka, A.J. 1956. Elements of mathematical biology. Dover, New York, NY.
- Loucks, D.P., J.R. Stedinger and D.A. Haith. 1981. Water resources systems planning and analysis Prentice-Hall Inc., Englewood Cliffs, NJ.
- Machta, L. 1973. Prediction of CO₂ in the atmosphere. In: G.M. Woodwell and E.V. Pecan (Editors), Proceedings Conference Carbon and the Biosphere. CONF-720510, NTIS, Springfield, VA, pp. 21-31.
- Mahmoud, M.S. 1982. Near-optimal control design for three-time-scale systems. In: Large Scale Systems, A. Titli and M.G. Singh (Editors). North-Holland Publishing Co. pp. 221-228.
- Marquis, S.L. 1985. A wind-driven phytoplankton model for the water quality management of Moses Lake. M.S. Thesis. University of Washington. 135 pp.
- McKenzie, D.K., L.D. Kannberg, K.L. Gore, E.M. Arnold and D.G. Watson. 1977. Design and analysis of aquatic monitoring programs at nuclear power plants. PNL-2423/NRC-10. Battelle Pacific Northwest Lab., Richland, WA. 126 pp.
- McLaughlin, D.B. and E.F. Wood. 1988. A distributed parameter approach for evaluating the accuracy of groundwater model predictions, 1: Theory. Water Resources Research, 24(7): 1037-1047.
- Meadows, D.L. and D.H. Meadows. 1972. Limits to growth; a report for the Club of Rome's project on the predicament of mankind. Universe Books, New York, NY.
- Meditch, J.S. 1973. A survey of data smoothing for linear and nonlinear dynamic systems. Automatica, 9: 151-162.
- Mericas, C.E. and R.F. Malone. 1984. Stochastic representation of a hypereutrophic lake. Journal of the Environmental Engineering Division, ASCE, 110(E2): 312-324.
- Millard, S.B., J.R. Yearsley and D.P. Lettenmaier. 1985. Space-time correlation and its effects on methods for detecting aquatic ecological changes. Canadian Journal of Fisheries and Aquatic Sciences, 42 (8): 1391-1400.
- Miller, P.C., B.D. Collier and F.L. Bunnell. 1975. Development of ecosystem modeling in the tundra biome. In: Systems analysis and simulation in ecology, Volume III, B.C. Patten (editor). Academic Press, New York, NY. pp. 95-115.
- Mitsch, W.J. 1983. Aquatic ecosystem modeling - its evolution effectiveness, and opportunities in policy issues. Prepared for AAAS/EPA Science and Engineering Fellow Program, University of Louisville, Louisville, KY Milne,

- R.D. 1965. The analysis of weakly coupled dynamical systems. *International Journal of Control*, 2: 171-199.
- Moore, S.F. 1971. The application of linear filter theory to the design and improvement of measurement systems for aquatic environments. Ph.D. Dissertation, University of California, Davis, CA. 121 pp.
- Moore, S.F., G.C. Dandy and R.J. deLucia. 1976. Describing variance with a simple water quality model and hypothetical sampling program. *Water Resources Research*, 12: 795-804.
- Myers, K.A. and B.D. Tapley. 1976. Adaptive sequential estimation with unknown noise statistics. *IEEE Transactions on Automatic Control*, AC-21: 513-520.
- Nelder, J.A. and R. Mead. 1965. A simplex method for function minimization. *Computing Journal*, 7: 308-313.
- O'Connor, D.J. and D.M. DiToro. 1970. Photosynthesis and oxygen balance in streams. *Journal of the Sanitary Engineering Division, ASCE*, 96: 641-666.
- Oeschger, H., Siegenthaler, U., Schotterer, U. and Gugelmann, A. 1975. A box diffusion model to study the carbon dioxide exchange in nature. *Tellus*, 27: 168-191.
- O'Neill, R.V. 1979. A review of linear compartmental analysis in ecosystem science. In: J.H. Matis, B.C. Patten and G.C. White (Editors), *Compartment Analysis of Ecosystem Models*. International Co-operative Publ. House. pp. 3-28.
- O'Neill, R.V. and J.M. Giddings. 1976. Population interactions and ecosystem function: Phytoplankton competition and community production. In: *Systems Analysis and Simulation in Ecology*, Vol. 4, B.C. Patten, editor, Academic Press, New York, N.Y., pp. 103-123.
- O'Neill, R.V. and B. Rust. 1979. Aggregation error in ecological models. *Ecological Modelling*, 7: 91-105.
- Ott, W.R. (editor). 1976. *Proceedings of the EPA Conference on environmental modeling and simulation*. EPA 600/9-76, Office of Research and Development, U.S. Environmental Protection Agency, Washington, D.C. 847 pp.
- Overton, W.S. 1975. The ecosystem modeling approach in the coniferous biome. In: *Systems analysis and simulation in ecology*, Volume III, B.C. Patten (editor). Academic Press, New York, NY. pp. 117-138.
- Patmont, C.R., G.J. Pelletier and M.E. Harper. 1985. Phosphorus attenuation in the Spokane River. Prepared for the State of Washington Department of Ecology by Harper-Owes, Seattle, WA, 251 pp.
- Patten, B.C., D.A. Egloff, and T.H. Richardson. 1975. Total ecosystem model for a cove in Lake Texacoma. In: B.C. Patten (Editor), *Systems Analysis and Simulation in Ecology*, Vol. 4. Academic Press, New York, NY. pp. 329-371.

- Plass, G.N. 1956. The carbon dioxide theory of climatic change. *Tellus*, 8:140-154.
- Platt, T., L.M. Dickie, and R.W. Trites. 1970. Spatial heterogeneity of phytoplankton in a near-shore environment. *Journal of the Fisheries Research Board of Canada*, 27(8):1453-1473.
- Raphael, J.M. 1962. Prediction of temperature in rivers and reservoirs. *Journal of the Power Division, ASCE*, 88(PO2): 157-181.
- Revelle, R. and H. Suess. 1957. Carbon dioxide exchange between atmosphere and ocean and the question of an increase of atmospheric carbon dioxide production. *Tellus*, 9: 18-27.
- Riley, G.A. 1965. Mathematical model of regional variations in plankton. *Limnology and Oceanograph*, 10: R202-R215.
- Riley, G.A., H. Stommel and D.F. Bumpus. 1949 Quantitative ecology of the plankton of the western north Atlantic. *Bulletin of the Bingham Oceanographic Collection*, 12:1-169.
- Roesner, L.A., P.R. Giguere and D.E. Evenson. 1981. Users' manual for the stream water quality model QUAL-II. EPA-600/9-81-015. U.S. Environmental Protection Agency, Athens, GA, 212 pp.
- Sage, A.P. and Melsa, J.L. 1973. Estimation Theory with Applications to Communications and Control. McGraw-Hill, New York, 529 pp.
- Salas, J.D., J.W. Delleur, V. Yevjevich, and W.L. Lane. 1980. Applied modeling of hydrologic time series. Water Resources Publications, Littleton, CO, 484 pp.
- Scavia, D. 1980. An ecological model of Lake Ontario. *Ecologic Modelling*, 8: 49-78.
- Scavia, D. and S.C. Chapra. 1977. Comparison of an ecological model of Lake Ontario and phosphorus loading models. *Journal of the Fisheries Research Board of Canada*, 34: 286-290.
- Scavia, D. and R.A. Park. 1976. Documentation of selected constructs and parameter values in the aquatic model CLEANER. *Ecologic Modelling*, 2:33-58.
- Scavia, D., R.P. Canale, W.F. Powers and J.L. Moody. 1981. Variance estimates for a dynamic eutrophication model of Saginaw Bay, Lake Huron. *Water Resources Research*, 17: 1115-1124.
- Schindler, D.W. 1987. Detecting ecosystem responses to anthropogenic stress. *Canadian Journal of Fisheries and Aquatic Sciences*, 44(Suppl. 1):6-25.
- Schweppe, F.C. 1973. Uncertain dynamic systems. Prentice-Hall, Englewood Cliffs, NJ, 653 pp.

- Seidel, S. and D. Keyes. 1983. Can we delay a greenhouse warming? office of Policy Analysis, U.S. Environmental Protection Agency, Washington, DC, 187 pp.
- Siegenthaler, U. and H. Oeschger. 1978. Predicting future atmosphere carbon dioxide levels. *Science*, 199: 388-395.
- Stauffer, R.E. 1988. Sampling strategies and associated errors in estimating epilimnetic chlorophyll in eutrophic lakes. *Water Resources Research*, 24 (9), 1459-1470.
- Steele, J.H. 1965. notes on some theoretical problems in production ecology. In: *Primary production in aquatic environments*, Volume 18, C.R. Goldman (editor). University of California (Berkeley) Press, Berkeley, CA, pp. 383-397.
- Streeter, H.W. and E.B. Phelps. 1925. A study of the pollution and natural purification of the Ohio River. *Public Health Bulletin No. 146*. U.S. Public Health Service, Washington, D.C. 75 pp.
- Stuiver, M. 1978. Atmospheric carbon dioxide and carbon reservoir changes. *Science*, 199: 253-258.
- Tapp, J.S. 1978. Eutrophication analysis with simple and complex models. *Journal of the Water Pollution Control Federation*, pp. 484-492.
- Tetra Tech, Inc. 1980. Methodology for evaluation of multiple power plant cooling system effects. EPRI EA-1111. Prepared for Electric Power Institute, Palo Alto, Calif.
- Thomann, R.V. 1982. Verification of water quality models. *Journal of the Environmental Engineering Division, ASCE*, 108: 923-940.
- Thomann, R.V., D.M. DiToro, R.P. Winfield and D.J. O'Connor. 1975. Mathematical modeling of phytoplankton in Lake Ontario: 1. Model development and verification. U.S. Environmental Protection Agency Report No. EPA-660/3-75-005. 177 pp.
- Thomann, R.V., R.P. Winfield and J.J. Segna. 1979. Verification analysis of Lake Ontario and Rochester Embayment three-dimensional eutrophication models. EPA-600/3-79-094. U.S. Environmental Protection Agency, Duluth, MN, 136 pp.
- Thomas, J.M., J.A. Mahaffey, K.L. Gore and D.G. Watson. 1978. Statistical methods used to assess biological impact at nuclear power plants. *Journal of Environmental Management*, 7: 269-290.
- Tiwari, J.L. and J.E. Hobbie. 1976. Random differential equations as models of ecosystems: Monte Carlo simulations. *Mathematical Bioscience*, 28: 25-44.

- Tiwari, J.L., J.E. Hobbie, J.P. Reed, D.W. Stanley and M.C. Miller. 1978. Some stochastic differential equation models of an aquatic ecosystem. *Ecological Modelling*, 4: 3-27.
- Todini, E. 1978. Mutually interactive state-parameter (MISP) estimation. In: Chao-Lin Chiu (Editors), *Applications of Kalman Filter to hydrology, hydraulics and water resources*. University of Pittsburgh, Pittsburgh, PA., pp.135-151.
- Turner, M.A. and D.L. DeAngelis. 1982. Resilience and inertia in model ecosystems: tests of some hypotheses. Oak Ridge National Laboratory Report No. ORNL/TM-7751. 61 pp.
- Tyndall, J. 1861. On the absorption and radiation of heat by gases and vapours, and on the physical connection of radiation, absorption, and conduction. *Philosophical Magazine*, 22 (Series 4): 169-194; 273-285.
- U.S. Environmental Protection Agency. 1980a. *Guideline on air quality models*. Office of Air Quality Planning and Standards, Washington, D.C.
- U.S. Environmental Protection Agency. 1980b. *Precision and accuracy data on EPA methodology for water and wastewater analyses*. Report from John A. Winter to Courtney Riordan, Office of Research and Development, Cincinnati, OH.
- Van Trees, H., 1959. *Detection, Estimation and Modulation Theory*. Wiley, New York, NY, 697 pp.
- Vollenweider, R.A. 1968. *Scientific fundamentals of the eutrophication of lakes and flowing waters, with particular reference to nitrogen and phosphorus as factors in eutrophication*. Technical Report OECD. Paris. DAS/CSI/68.27. 159 pp.
- Vollenweider, R.A. 1969. *Möglichkeiten und Grenzen elementarer Modelle der Stoffbilanz von Seen*. *Archiv für Hydrobiologie*, 66: 1-36.
- Vollenweider, R.A. 1975. *Input-output models with special reference to phosphorus loading concepts in limnology*. *Schweizerische Zeitschrift für Hydrologie*, 37(1): 53-84.
- Wald, A. 1947. *Sequential analysis*. John Wiley & Sons, Inc. New York, NY. 150 pp.
- Walters, R.A. 1976. *A numerical model of thermal stratification, primary production and nutrient cycles in deep temperate lakes*. Ph.D. Dissertation, University of Washington, 166 pp.
- Walters, R.A. 1980. *A time- and depth-dependent model for physical, chemical and biological cycles in temperate lakes*. *Ecological Modelling*, 8:79-96.
- Wang, M. and D.R.F. Harleman. 1983. *Modelling phytoplankton concentration in a stratified lake*. In *Analysis of Ecological Systems: State-of-the-Art in Ecological Modelling*, edited by W.K. Lauenroth, G.V. Skogerboe and M Flug. Elsevier Scientific Publishing Co. Amsterdam, The Netherlands, pp. 807-817.

- Ward, R.C. and D.H. Vanderholm. 1973. Cost-effectiveness methodologies for data acquisition in water quality management. *Water Resources Research*, 9: 536-545.
- Water Resources Engineers, Inc. 1975. Ecologic modelling of Puget Sound and adjacent waters. WRE11930-OWRR C2044-X U.S. Environmental Protection Agency, Washington, DC, 119 pp.
- Water Resources Engineers, Inc. 1968. Prediction of thermal energy distribution in streams and reservoirs. Prepared for the California Department of Fish and Game, Walnut, Creek, CA. 90 pp.
- Webster, J.R., J.B. Waide, and B.C. Patten. 1975. Nutrient recycling and the stability of ecosystems. In F.G. Howell, J.B. Gentry, and M.H. Smith (eds.), *Mineral recycling in southeastern ecosystems*, CONF-740513, NTIS, pp. 1-27.
- Willsky, A.S. and H.L. Jones. 1976. A generalized likelihood ratio approach to the detection and estimation of jumps in linear systems. *IEEE Transactions on Automatic Control*, 20: 108-112.
- Woodwell, G.M., R.H. Whittaker, W.A. Reiners, G.E. Likens, C.C. Delwicke, and D.B. Botkin. 1978. The biota and the world carbon budget. *Science*, 199: 141-146.
- Wunderlich, W.O. and R. Gras. 1967. Energy and mass transfer between a water surface and the atmosphere. Memorandum Report, Engineering Laboratory, TVA.
- Yearsley, J.R. and D.P. Lettenmaier. 1987. Model complexity and data worth: an assessment of changes in the global carbon budget. *Ecological Modelling*, 39: 201-226.
- Zison, S.W., W.B. Mills, D. Deimer, and C.W. Chen. 1978. Rates, constants, and kinetics formulations in surface water quality modeling. U.S. Environmental Protection Agency, Report No. EPA-600/3-78-105, 318 pp.

APPENDIX I
STATE-SPACE STRUCTURE
FOR THE
GLOBAL CARBON CYCLE

Cold Ocean Surface Layer

$$\frac{dN_c}{dt} = k_{ac}N_a - \kappa A_c P_c - k_{cw}N_c + k_{wc}N_w - \sum_{i=1}^{10} k_{ci}N_c + \sum_{i=1}^2 k_{ic}N_i - B_c \quad (I.1)$$

Warm Ocean Surface Layer

$$\frac{dN_w}{dt} = k_{aw}N_a - \kappa A_w P_w + k_w N_c - k_{wc}N_w + k_{1w}N_1 - B_w \quad (I.2)$$

Atmosphere

$$\begin{aligned} \frac{dN_a}{dt} = & \kappa A_c P_c + \kappa A_w P_w - k_{ac}N_a - k_{aw}N_a + k_{ba}N_b \\ & - k_{ab}N_b \left(1 + \beta \ln \frac{N_a}{N_{a0}}\right) + \gamma_{ff} + \gamma_b \end{aligned} \quad (I.3)$$

Terrestrial Biota

$$\frac{dN_b}{dt} = k_{ab}N_b \left(1 + \beta \ln \frac{N_a}{N_{a0}}\right) - k_{ba}N_b - k_{bs}N_b - \gamma_b \quad (I.4)$$

Soil

$$\frac{dN_s}{dt} = k_{bs} N_b - k_{sa} N_s \quad (I.5)$$

Ocean Layer 1

$$\frac{dN_1}{dt} = k_{c1} N_c - k_{1c} N_1 + k_{21} N_2 - k_{1w} N_1 + B_w + B_c - B_1 \quad (I.6)$$

Ocean Layer 2

$$\frac{dN_2}{dt} = k_{c2} N_c - k_{2c} N_2 + k_{32} N_3 - k_{21} N_2 + B_1 - B_2 \quad (I.7)$$

Ocean Layer 3

$$\frac{dN_3}{dt} = k_{c3} N_c + k_{43} N_4 - k_{32} N_3 + B_2 - B_3 \quad (I.8)$$

Ocean Layer 4

$$\frac{dN_4}{dt} = k_{c4} N_c + k_{54} N_5 - k_{43} N_4 + B_3 - B_4 \quad (I.9)$$

Ocean Layer 5

$$\frac{dN_5}{dt} = k_{c5}N_c + k_{65}N_6 - k_{54}N_5 + B_4 - B_5 \quad (\text{I.10})$$

Ocean Layer 6

$$\frac{dN_6}{dt} = k_{c6}N_c + k_{76}N_7 - k_{65}N_6 + B_5 - B_6 \quad (\text{I.11})$$

Ocean Layer 7

$$\frac{dN_7}{dt} = k_{c7}N_c + k_{87}N_8 - k_{76}N_7 + B_6 - B_7 \quad (\text{I.12})$$

Ocean Layer 8

$$\frac{dN_8}{dt} = k_{c8}N_c + k_{98}N_9 - k_{87}N_8 + B_7 - B_8 \quad (\text{I.13})$$

Ocean Layer 9

$$\frac{dN_9}{dt} = k_{c9}N_c + k_{10,9}N_{10} - k_{98}N_9 + B_8 - B_9 \quad (\text{I.14})$$

Ocean Layer 10

$$\frac{dN_{10}}{dt} = k_{c,10}N_c - k_{10,9}N_{10} + B_9 - B_{10} \quad (I.15)$$

where,

N_c = the carbon in the cold ocean surface layer reservoir, 10^{15} grams carbon,

N_w = the carbon in the warm ocean surface layer reservoir, 10^{15} grams carbon,

N_a = the carbon in the atmospheric reservoir, 10^{15} grams carbon,

N_b = the carbon in the terrestrial biota reservoir, 10^{15} grams carbon,

N_s = the carbon in the soil reservoir, 10^{15} grams carbon,

N_1 = the carbon in intermediate ocean layer 1, 10^{15} grams carbon,

N_2 = the carbon in intermediate ocean layer 2, 10^{15} grams carbon,

N_3 = the carbon in deep ocean layer 3, 10^{15} grams carbon,

· · · · ·
 · · · · ·
 · · · · ·

N_{10} = the carbon in deep ocean layer 10, 10^{15} grams carbon,

P_c = the partial pressure of CO_2 in the cold ocean surface layer, ppm,

P_w = the partial pressure of CO_2 in the warm ocean surface layer, ppm,

k_{ij} = the turnover rate for the transfer of carbon from the i^{th} compartment to the j^{th} compartment, $years^{-1}$,

β = a constant,

κ = a constant,

B_c = organic carbon in the cold ocean surface layer, 10^{15} grams carbon,

B_w = organic carbon in the warm ocean surface layer, 10^{15} grams carbon,

APPENDIX II
A DESCRIPTION
OF THE
REFERENCE MODEL FOR THERMAL ENERGY

Temperature plays an important role in the dynamics of ecosystems. Rates associated with many biological processes are a function of water temperature. In water bodies with sufficient depth such that vertical stratification occurs, the influence of water temperature upon vertical and horizontal currents can also have important effects upon population dynamics of the water body. Because temperature does influence the physics, chemistry and biology of lakes, a reference model of a lake ecosystem must include a model to generate temperature as a state variable. The most widely-used approach for simulating the temperature of a water body is the heat budget method. When the basic equations are time-averaged over a period associated with turbulent motions and the resulting Reynolds fluxes replaced by eddy coefficients of thermal diffusivity, the heat budget, in its most general form, can be written as (Walters, 1976):

$$\rho c_p \left[\frac{\partial T}{\partial t} + \frac{\partial(uT)}{\partial x} + \frac{\partial(vT)}{\partial y} + \frac{\partial(wT)}{\partial z} \right] = \rho c_p \left[\frac{\partial}{\partial x} (\kappa_x \frac{\partial T}{\partial x}) + \frac{\partial}{\partial y} (\kappa_y \frac{\partial T}{\partial y}) + \frac{\partial}{\partial z} (\kappa_z \frac{\partial T}{\partial z}) \right] + \Phi(x,y,z,t) \quad (\text{II.1})$$

where,

ρ = the density of water, kg/m³

c_p = the heat capacity of water, kcal/°C/kg

K_x, K_y, K_z = the coefficients of thermal eddy diffusivity in the x-, y-, and z-directions, respectively, m^2/sec

T = water temperature, $^{\circ}C$,

Φ = the internal source term for thermal energy, $kcal/m^3/sec$

The solution of equation (II.1) can be obtained only after the problem is completely specified. This means that the boundary conditions and initial conditions must be defined. For most lakes it is reasonable to assume that there is no heat flux through either the lake bottom and sides. The surface heat flux is given by

$$-\rho c_p K_z \left. \frac{\partial T}{\partial z} \right|_{z=0} = Q(T_{z=0}, t) \quad (II.2)$$

where,

$Q(T_{z=0}, t)$ = the net heat flux across the air-water interface.

Determination of the net heat flux, q , follows the method outlined by Tetra Tech (1980), and is computed from the following equation

$$q = q_{sn} + q_{at} - q_w - q_e + q_c \quad (II.3)$$

where,

q_{sn} = the net short-wave radiation flux through the air-water interface after losses by absorption and scattering in the atmosphere and by reflection at the interface

q_{at} = the net atmospheric (long-wave) radiation flux delivered through the interface after losses by reflection

q_w = the water surface radiation (long-wave) flux from the water surface to the atmosphere

q_e = the heat flux due to evaporation

q_c = the convective flux, or sensible heat transfer, between the water surface and the atmosphere

Atmospheric Long-Wave Radiation

The atmospheric radiation is a function of the air temperature and cloud cover and is estimated from (WRE, 1968)

$$q_{at} = 1.23 \times 10^{-16} (1.0 + 0.17 * C_1^2)(T_a + 273)^6 \quad (II.4)$$

where,

C_1 = the fraction of cloud cover,

T_a = the air temperature ($^{\circ}C$).

Long Wave Back Radiation

The long wave back radiation from the water surface is determined primarily by the absolute water temperature according in the following way

$$q_w = \epsilon \sigma T^4 \quad (II.5)$$

where,

ϵ = the emissivity of water = 0.97

σ = the Stefan-Boltzmann constant
 = 1.357×10^{-8} , kcal/m²-sec/ $^{\circ}K^4$

Tetra Tech (1980) approximated equation (II.5) by the linear relationship:

$$q_w = 6.693 \times 10^{-2} + 1.471 \times 10^{-3} T_w \quad (\text{II.6})$$

where,

T_w = the surface water temperature ($^{\circ}\text{C}$).

According to Tetra Tech (1980), equation (II.6) is accurate to within 2.1 percent over the temperature range 0°C to 30°C .

Evaporative Heat Flux

The heat flux due to evaporation can be estimated from:

$$q_e = \rho_w L_w E \quad (\text{II.7})$$

where,

ρ_w = the density of water, kg/m^3 ,

L_w = the latent heat of vaporization, Kcal/kg , = $597 - 0.57 T_w$,

E = the evaporation rate, m/sec

Studies of water loss due to evaporation (e.g., Harbeck; 1958) have shown that the evaporation rate depends upon wind speed, water temperature, air temperature and relative humidity. Harbeck (1958) developed the following empirical formula for estimating evaporation rates:

$$E = (a + bV)(e_s - e_a) \quad (\text{II.8})$$

where,

a, b = empirical constants, ($a=0.0$, $b=1.5 \times 10^{-9} \text{ mb}^{-1}$ here),

V = the wind speed at two meters above the water surface, m/sec

e_s = the saturation water vapor pressure of the air at the temperature of the water surface, mb,

e_a = the water vapor pressure of the atmosphere two meters above the water surface, mb.

The saturation water vapor pressure, a nonlinear function of the water surface temperature can be approximated by piecewise linear functions (Tetra Tech, 1980) from:

$$e_s = \alpha_j + \beta_j T_w \quad (\text{II.9})$$

where,

α_j, β_j = empirical coefficients (Tetra Tech, 1980)

Incorporating eqs. (II.8) and (II.9) into equation (II.7) gives the following:

$$q_e = \rho_w L_w (a + bV)(\alpha_j + \beta_j T_w - e_a) \quad (\text{II.10})$$

Convective Heat Flux

The convective, or sensible heat flux, can be estimated from:

$$q_c = Rq_e \quad (\text{II.11})$$

where,

$$R = \text{the Bowen ratio} = 6.1 \times 10^{-4} P \frac{T_w - T_a}{e_s - e_a} \quad (\text{II.12})$$

P = the atmospheric pressure, mb

Substituting eqs. (II.11) and (II.12) into equation (II.10) gives

$$q_c = \rho_w L_w (a + bV) (6.1 \times 10^{-4} P) (T_w - T_a) \quad (\text{II.13})$$

Data requirements for describing the flux of heat across the air-water interface include the following:

- Shortwave solar radiation
- Julian data
- Latitude
- Atmospheric turbidity
- Cloud cover
- Atmospheric pressure
- Wind speed
- Dry bulb temperature
- Relative humidity

APPENDIX III
A DESCRIPTION OF THE
REFERENCE MODEL
FOR ECOSYSTEMS DYNAMICS

The dynamics of the ecosystem are described by the general mass balance equation, which in its general form is given by

$$\begin{aligned} & \left[\frac{\partial \mathbf{c}}{\partial t} + \frac{\partial(u\mathbf{c})}{\partial x} + \frac{\partial(v\mathbf{c})}{\partial y} + \frac{\partial(w\mathbf{c})}{\partial z} \right] = \\ & \left[\frac{\partial}{\partial x} \left(\kappa_x \frac{\partial \mathbf{c}}{\partial x} \right) + \frac{\partial}{\partial y} \left(\kappa_y \frac{\partial \mathbf{c}}{\partial y} \right) + \frac{\partial}{\partial z} \left(\kappa_z \frac{\partial \mathbf{c}}{\partial z} \right) \right] + \\ & \Phi(\mathbf{x}, \mathbf{c}, t) - \Lambda(\mathbf{x}, \mathbf{c}, t) \end{aligned} \tag{III.1}$$

where,

\mathbf{c} = the vector of state variables

\mathbf{x} = the vector of spatial coordinates

κ = the coefficient of eddy diffusivity in the x-, y-, and z-direction

Φ = a source term

Λ = a sink term

When the prototype is assumed to be a continuously stirred reactor (CSTR), eq. (III.1) simplifies to

$$\frac{d\mathbf{c}}{dt} = \Phi(\mathbf{x}, \mathbf{c}, t) - \Lambda(\mathbf{x}, \mathbf{c}, t) \tag{III.2}$$

Based upon the general formulation given by eq. (III.2) and following closely the development of model structure described by Tetra Tech (1979), the specific form of equation (III.2) for the specific state variables included in this thesis is described below.

Benthic Animals

All benthic organisms are grouped into one compartment for which the conservation equation is

$$\frac{dB}{dt} = (G_b - R_b - M_b) - B_g \quad (\text{III.3})$$

where

B = the concentration of benthic animals, mg/m^2

G_b = the growth rate of benthic animals, days^{-1}

R_b = the respiration rate of benthic animals, days^{-1}

M_b = the mortality rate of benthic animals, days^{-1}

B_g = the rate at which benthic animals are grazed by predators, days^{-1}

The growth rate for benthic animals is a complex function of food density, temperature, and population density of benthic animals. Following the approach used by Tetra Tech (1979), the growth rate is characterized by

$$G_b = G_{b,\text{max}} \left(\frac{\sum_{k=1}^n \alpha_{bk} F_k}{K_b + \sum_{k=1}^n \alpha_{bk} F_k} \right) BQ_{10} \left[1 - \left(\frac{B}{B_{\text{lim}}} \right)^2 \right]$$

where

$G_{b,max}$ = the maximum growth rate of benthic animals at 20 °C, days⁻¹

K_b = Michaelis-Menten constant for benthic animal growth, mg/l

F_k = the concentration of the kth food source, mg/l

α_{bk} = the preference factor of benthic animals for the kth food source

BQ_{10} = the temperature growth function for benthic animals

B_{lim} = the limiting population level for benthic animals, mg/m²

The respiration rate is also a function of temperature, according to:

$$R_b = R_{b,20} \theta_b^{T-20}$$

where

$R_{b,20}$ = the respiration rate at 20° C, days⁻¹

θ_b = the temperature factor for benthic respiration

T = the water temperature, °C

Zooplankton

The model has the capability of simulating three groups of zooplankton with differing characteristics of feeding habits and responses to environmental factors. The mass balance equation for the dynamics of the ith zooplankton compartment is:

$$\frac{d\zeta_i}{dt} = (G_{\zeta_i} - R_{\zeta_i} - M_{\zeta_i})\zeta_i - \zeta_g - \frac{Q_{out}\zeta_i}{V} + \frac{Q_{in}\zeta_{i,in}}{V} \quad (III.4)$$

where,

G_{ζ_i} = the grazing rate for the i^{th} zooplankton compartment, days⁻¹

R_{ζ_i} = the respiration rate for the i^{th} zooplankton compartment, days⁻¹

M_{ζ_i} = the mortality rate for the i^{th} zooplankton compartment, days⁻¹

ζ_g = the rate at which zooplankton are grazed, mg /l/days⁻¹

Q_{in} = the rate of inflow to the CSTR, m³/sec

$\zeta_{i,\text{in}}$ = the concentration of the i^{th} zooplankton in the inflow, mg/l

Q_{out} = the the rate of outflow from the CSTR, m³/sec

V = the volume of the CSTR, m³

The complete description of the growth rate for zooplankton is

$$G_{\zeta_i} = G_{\zeta_i,\text{max}} \left(\frac{\sum_{k=1}^n \alpha_{\zeta_i,k} F_k}{K_{\Pi_i} + \sum_{k=1}^n \alpha_{\zeta_i,k} F_k} \right) ZQ_{10}$$

where,

$G_{\zeta_i,\text{max}}$ = the maximum growth rate of the i^{th} zooplankton compartment, days⁻¹,

K_{Π_i} = the Michaelis-Menten constant for phytoplankton consumption by the i^{th} zooplankton compartment, mg/l of phytoplankton biomass

F_k = the k^{th} food source for zooplankton, mg/l

$\alpha_{\zeta_i,k}$ = the food preference factor for the i^{th} zooplankton compartment respect to potential food item, k ,

ZQ_{10} = the temperature growth function for the i^{th} zooplankton compartment

Zooplankton respiration is assumed to have a functional relationship with the following form:

$$R_{\zeta_i} = R_{\zeta_i,20} \theta_{\zeta_i}^{T-20}$$

where,

$R_{\zeta_i,20}$ = the respiration rate of the i^{th} zooplankton compartment at 20° C, days⁻¹

θ_{ζ_i} = the temperature factor for the respiration rate of the i^{th} zooplankton compartment

Grazing rates on zooplankton are accounted for in the following manner:

$$Z_g = \sum_{j=1}^m \left[\left(\frac{\alpha_{j,i} \zeta_i}{\sum_{k=1}^n \alpha_{j,k} F_k} \right) \left(\frac{PR_j G_{pr,j}}{\epsilon_j} \right) \right]$$

where

α_{jk} = the preference factor of predator j, for food type, k

F_k = the k^{th} food type for predator j, mg/l

ϵ_j = the grazing efficiency of predator j

PR_j = the biomass associated with predator j, mg/l

$G_{pr,j}$ = the growth rate of predator j, days⁻¹

Phytoplankton

The model simulates several compartments of phytoplankton and one of attached algae. In this way, the environmental responses associated with various *taxa* can be included in the simulations. The mass balance equation for the i^{th} phytoplankton compartment is

$$\frac{d\Pi_i}{dt} = (G_{\Pi_i} - R_{\Pi_i} - \frac{w_i}{\Delta z} - \frac{Q_{\text{out}}}{V})\Pi_i + \frac{Q\Pi_{i,\text{in}}}{V} - \Pi_{i,g} \quad (\text{III.5})$$

where,

Π_i = the biomass associated with the i^{th} phytoplankton compartment, mg/l

$\Pi_{i,\text{in}}$ = the biomass of the i^{th} phytoplankton compartment in the inflow, mg/l

G_{Π_i} = the growth rate of the i^{th} phytoplankton compartment, days⁻¹

w_i = the settling rate of the i^{th} phytoplankton group, m/day

Δz = the vertical thickness of the water body, m

$\Pi_{i,g}$ = the grazing rate on the i^{th} phytoplankton compartment by all predators, mg/l/day.

The dynamics of phytoplankton growth, as described here, are based upon a growth-limiting relationship using Michaelis-Menten kinetics. Furthermore, it has been assumed that the limitation upon growth due to less-than optimal concentrations of macro-nutrients is multiplicative, according to the following:

$$G_{\Pi_i} = G_{\Pi_i, \max} \left(\frac{PO_4}{K_{P_i} + PO_4} \right) \left(\frac{NH_4 + NO_3}{K_{N_i} + NH_4 + NO_3} \right) \left(\frac{SiO_2}{K_{S_i} + SiO_2} \right) \Theta(T, I) \quad (III.7)$$

where,

$G_{\Pi_i, \max}$ = the maximum growth rate for the i^{th} phytoplankton compartment, days⁻¹,

PO_4 = the concentration of phosphorus as orthophosphate, mg/l

K_{P_i} = the Michaelis-Menten constant of the i^{th} phytoplankton compartment for inorganic phosphorus, mg/l

NH_4 = the concentration of nitrogen as ammonia, mg/l

NO_3 = the concentration of nitrogen as nitrate, mg/l

K_{N_i} = the Michaelis-Menten constant of the i^{th} phytoplankton compartment for inorganic nitrogen, mg/l

SiO_2 = the concentration of silicon as silica, mg/l

K_{S_i} = the Michaelis-Menten constant of the i^{th} phytoplankton compartment for inorganic silicon, mg/l

$\Theta(T, I)$ = the functional relationship characterizing the effects of temperature and solar energy upon growth

$$= PQ_{10} * f_L(I)$$

The relationship for the function which describes the effect of solar energy upon the growth rate is (DiToro et al., 1975):

$$f_L(I) = \frac{ef}{K_e \Delta z} (e^{-\alpha_1} - e^{-\alpha_0}) \quad (III.7)$$

where,

$$e = 2.718$$

f = the fraction of the day that solar energy is available

K_e = the light extinction coefficient, meters⁻¹

$$\alpha_1 = \frac{I_a}{I_s} e^{-K_e \Delta z},$$

$$\alpha_0 = \frac{I_a}{I_s},$$

I_a = the mean daily solar radiation, kcal/m²/sec

I_s = the optimal solar radiation, kcal/m²/sec

The light extinction coefficient, K_e , is a function of the suspended material in the water column, and is described by the following equation:

$$\lambda_e = \lambda_w + \lambda_p \sum_{i=1}^{n_p} \Pi_i + 0.3\lambda_p \sum_{i=1}^{n_z} \zeta_i + 0.7\lambda_p D \quad (\text{III.8})$$

where,

λ_w = the light extinction coefficient for distilled water, meters⁻¹

λ_p = the light extinction coefficient for suspended particulate matter, meters⁻¹

n_p = the total number of phytoplankton groups

n_z = the total number of zooplankton groups

D = the concentration of suspended detritus, mg/l

Algal respiration is defined by the relationship

$$R_{\Pi_i} = R_{\Pi_i,20} \theta_{\Pi_i}^{T-20}$$

where,

$R_{\Pi_i,20}$ = the respiration rate of the i^{th} phytoplankton compartment at 20°C, days⁻¹

θ_{Π_i} = the temperature factor for the i^{th} phytoplankton compartment

The grazing of phytoplankton by zooplankton is described by

$$\Pi_g = \sum_{j=1}^m \left[\left(\frac{\alpha_j \Pi_i}{\sum_{k=1}^n \alpha_k F_k} \right) \left(\frac{PR_j G_{prj}}{\epsilon_j} \right) \right] \quad (\text{III.9})$$

where

α_{jk} = the preference factor of predator j, for food type, k

F_k = the k^{th} food type for predator j, mg/l

ϵ_j = the grazing efficiency of predator j

PR_j = the biomass associated with predator j, mg/l

G_{prj} = the growth rate of predator j, days⁻¹

Suspended Organic Detritus

Suspended organic detritus, in this model, is derived from dead zooplankton, attached algae that have sloughed off the substrate, and excretions from zooplankton. The mass balance equation for suspended organic detritus is given by

$$\begin{aligned} \frac{dD}{dt} = & \sum_{i=1}^{n_z} (M_{\zeta_i} + Z_{i,px})\zeta_i + w_{at}\Pi_{at} + \frac{Q_n D_n}{V} - D_g \\ & - (K_{det} + \frac{w_{det}}{\Delta z} - \frac{Q_{out}}{V})D \end{aligned} \quad (III.10)$$

where

$Z_{i,px}$ = the rate at which particulate matter is excreted by the i^{th} zooplankton compartment, days⁻¹

D_g = the rate at which detritus is grazed by all consumers, mg/l/day

w_{det} = the settling velocity of detritus, m/sec

D_{in} = the concentration of detrital matter in the inflow, mg/l

$$K_{det} = K_{det,20} \theta_{det}^{T-20}$$

$K_{det,20}$ = the detrital decay constant at 20 °C, days⁻¹,

θ_{det} = the temperature factor for detrital decay

In this model, only zooplankton excrete detrital material. The rate at which the i^{th} zooplankton group does so is given by:

$$Z_{i,px} = \left(\frac{G_{\zeta_i}}{\epsilon_i} - G_{\zeta_i} \right) Z_{i,pr} \quad (III.11)$$

where,

$Z_{i,pr}$ = the particulate fraction excreted by the i^{th} zooplankton compartment.

Detrital grazing is described by the following relationship:

$$D_g = \sum_{j=1}^m \left[\left(\frac{\alpha_j D}{\sum_{k=1}^n \alpha_k F_k} \right) \left(\frac{PR_j G_{PRj}}{\epsilon_j} \right) \right] \quad (\text{III.12})$$

where,

j = the subscript of each organism feeding on detritus

Organic Sediment

Organic sediment accumulate from detritus and algae which settles to the lake bottom, mortality of benthic animals and the excretion of particulate matter by benthic animals. Sediment is grazed by benthic animals and organic nutrients decay to dissolved forms. The mass balance equation describing these processes is:

$$\frac{dS}{dt} = \sum_{i=1}^{n_p} \frac{w_i}{\Delta z} \Pi_i + \frac{w_{det}}{\Delta z} D + (M_b + B_{px}) B - S_g - K_{sed} S \quad (\text{III.13})$$

where

B_{px} = the rate at which benthic animals excrete particulate matter, days^{-1}

S_g = the rate at which sediment is grazed by all consumers, mg/l/day

K_{sed} = the rate at which organic nutrients are transformed to dissolved inorganic nutrients, days^{-1} .

The rate at which benthic animals excrete particulate matter is given by:

$$B_{pr} = \left(\frac{G_b}{\epsilon_i} - G_b \right) B_{pr} \quad (\text{III.14})$$

The temperature dependence associated with the microbiological processes affecting the decay of organic sediment is

$$K_{sed} = K_{sed20} \theta_{sed}^{T-20} \quad (\text{III.15})$$

where,

K_{sed20} = the decay rate of sediment at 20° C, days⁻¹

θ_{sed} = the temperature adjustment coefficient for sediment decay

The grazing rate of organisms upon sediment is determined from

$$S_g = \sum_{j=1}^m \left[\left(\frac{\alpha_j S}{\sum_{k=1}^n \alpha_k F_k} \right) \left(\frac{PR_j G_{prj}}{\epsilon_j} \right) \right] \quad (\text{III.16})$$

Nitrogen

Two forms of inorganic nitrogen are included in the ecosystem model: ammonia and nitrate. Ammonia is a product of the respiration and soluble excretions from aquatic organisms and of the decay of organic sediment and detritus. Both inorganic forms are utilized by phytoplankton during photosynthesis. The dynamic mass balance equations for inorganic nitrogen in the form of ammonia and nitrate are as follows:

$$\begin{aligned} \frac{d(\text{NH}_4)}{dt} = & N_{\text{det}} K_{\text{det}} D + N_{\text{sed}} K_{\text{sed}} S + N_b R_b B + \sum_{i=1}^{n_z} N_{\zeta} R_{\zeta} \zeta_i + \sum_{i=1}^{n_p} N_{\Pi} R_{\Pi} \Pi_i \\ & - \sum_{i=1}^{n_z} N_{\zeta} Z_{i,dx} \zeta_i + N_b B_{dx} B - \sum_{i=1}^{n_p} [(N_{\Pi} G_{\Pi} \Pi_i) (\frac{\text{NH}_4}{\text{NH}_4 + \text{NO}_3})] \\ & - K_{\text{NH}_4} \text{NH}_4 \end{aligned} \quad (\text{III.17})$$

$$\frac{d(\text{NO}_3)}{dt} = K_{\text{NH}_4} \text{NH}_4 - \sum_{i=1}^{n_p} [(N_{\Pi} G_{\Pi} \Pi_i) (\frac{\text{NO}_3}{\text{NH}_4 + \text{NO}_3})] \quad (\text{III.18})$$

where,

NH_4 = the concentration of ammonia nitrogen, mg/l

NO_3 = the concentration of nitrate nitrogen, mg/l

N_{det} = the nitrogen fraction of detritus

N_{sed} = the nitrogen fraction of sediment

N_b = the nitrogen fraction of benthic animal excretions

N_{ζ} = the nitrogen fraction of zooplankton excretions

N_{Π} = the nitrogen fraction of phytoplankton

$Z_{i,dx}$ = the rate at which dissolved nutrients are excreted by zooplankton, days⁻¹

B_{dx} = the rate at which dissolved nutrients are excreted by benthic animals, days⁻¹

K_{NH_4} = the rate constant for oxidation of ammonia to nitrate, days⁻¹,

The temperature dependency of the rate constant for oxidation of ammonia is

$$K_{\text{NH}_4} = K_{\text{NH}_4,20} \theta_{\text{NH}_4}^{T-20}$$

where

$K_{\text{NH}_4,20}$ = the oxidation rate at 20° C, days⁻¹

θ_{NH_4} = the temperature factor for the oxidation of ammonia

Excretion of soluble forms of nitrogen for zooplankton and benthic animals are modeled by:

$$Z_{i,\alpha} = \left(\frac{G_{\zeta}}{\epsilon_{\zeta}} - G_{\zeta} \right) (1 - Z_{i,\text{prt}}) \quad (\text{III.19})$$

$$B_{\alpha} = \left(\frac{G_B}{\epsilon_B} - G_B \right) (1 - B_{\text{prt}}) \quad (\text{III.20})$$

where

$Z_{i,\text{prt}}$ = the particulate fraction in the excreta of the i^{th} zooplankton compartment

B_{prt} = the particulate fraction in the excreta of benthic animals

Dissolved Inorganic Phosphorus (Orthophosphate)

Phosphorus is a major nutrient for aquatic organisms. Inorganic phosphorus is a product of the decay of detritus and organic sediment, the respiration of zooplankton, benthic animals and phytoplankton, and the soluble excretions of zooplankton and benthic animals. It also may be transported into a lake ecosystem by tributary river systems. The mass balance equation for orthophosphate is

$$\begin{aligned} \frac{dP}{dt} = & P_{\text{det}} K_{\text{det}} D + P_{\text{sed}} K_{\text{sed}} S + P_B R_B B + \sum_{i=1}^{n_z} P_{\zeta} R_{\zeta} \zeta_i + \sum_{i=1}^{n_p} P_{\Pi} R_{\Pi_i} \Pi_i \\ & + \sum_{i=1}^{n_z} P_{\zeta} Z_{i,\alpha} \zeta_i + P_B B_{\alpha} B - \sum_{i=1}^{n_p} P_{\Pi} G_{\Pi_i} \Pi_i \end{aligned} \quad (\text{III.21})$$

where,

P = the concentration of orthophosphate phosphorus, mg/l

P_{det} = the phosphorus fraction of detritus

P_{sed} = the phosphorus fraction of sediment

P_B = the phosphorus fraction of soluble benthic animal excretions

P_{ζ} = the phosphorus fraction of soluble zooplankton excretions

P_{Π} = the phosphorus fraction of phytoplankton cells

Silica

Silica is a major nutrient for diatoms, only, and is modeled in three different forms: dissolved silica, suspended particulate silica and sediment silica. The mass balance equations for these three forms are:

$$\frac{d(\text{Si}_d)}{dt} = K_{p\text{Si}} \text{Si}_p + K_{s\text{Si}} \text{Si}_s + \sum_{i=1}^{n_d} S_{\Pi} (R_{\Pi_i} - G_{\Pi_i}) \Pi_i \quad (\text{III.22})$$

$$\frac{d(\text{Si}_p)}{dt} = \sum_{i=1}^{n_d} S_{\Pi} \Pi_{i,g} - K_{p\text{Si}} \text{Si}_p - w_{p\text{Si}} \text{Si}_p \quad (\text{III.23})$$

$$\frac{d(\text{Si}_s)}{dt} = \sum_{i=1}^{n_d} S_{\Pi} w_{i,b} \Pi_{i,b} + w_{p\text{Si}} \text{Si}_p - K_{s\text{Si}} \text{Si}_s - w_{s\text{Si}} \text{Si}_s \quad (\text{III.24})$$

where,

S_{id} = the concentration of dissolved silica, mg/l

S_{ip} = the concentration particulate silica, mg/l

S_{is} = the concentration of sediment silica, mg/l

K_{pSi} = the rate constant for decay of particulate silica, days⁻¹

K_{sSi} = the rate constant for decay of sediment of silica, days⁻¹

n_d = the number of diatom groups in the ecosystem

S_{alg} = the silica fraction of diatom cells

w_{pSi} = the settling rate for particulate silica, days⁻¹

w_{sSi} = the rate at which sediment silica is deposited to the inorganic bottom sediments, days⁻¹

A_b = the fraction of the bottom receiving sediment deposits

APPENDIX IV
 FILTER DERIVATION
 FOR THE
 NONLINEAR ECOSYSTEMS MODELS

Models II and III for the lake ecosystem are non-linear ecosystems models. The Kalman Filter is applicable only to problems for which the systems model is linear. A number of approaches have been proposed to extend the Kalman Filter to those systems for which the model is non-linear. In general, the approaches are based upon the notion that the state variables can be expanded about some nominal trajectory to obtain a linear model of the variations. For this thesis the filters used to generate the likelihood function were derived by linearizing the equations about a nominal trajectory (Schweppe, 1973). In this case, the nominal trajectory of the state variables, $\mathbf{x}_{nom}(n)$, $n=1, \dots, N$, is given by

$$\mathbf{x}_{nom}(n+1) = \phi[\mathbf{x}_{nom}(n), n] \quad (IV.1)$$

where,

$$\mathbf{x}_{nom}(0) = \mathbf{x}_0$$

The Taylor series expansions of the the nonlinear systems and measurement models about the nominal trajectory gives:

$$\mathbf{d}_x(N+1) = \Phi^{(1)}[\mathbf{x}_{nom}(N), N] \mathbf{d}_x(N) + \Gamma[\mathbf{x}_{nom}(N), N] \mathbf{w}(N) + \dots \quad (IV.2)$$

and:

$$\mathbf{d}_z(N) = \mathbf{H}^{(1)}[\mathbf{x}_{nom}(N), N] \mathbf{d}_x(N) + \mathbf{v}(N) + \dots \quad (IV.3)$$

In Equations (IV.2) and (IV.3) the following definitions are needed:

$$\begin{aligned} \mathbf{d}_x(n) &= \mathbf{x}(n) - \mathbf{x}_{\text{nom}}(n) \\ \Phi^{(1)}[\mathbf{x}_{\text{nom}}(n), n] &= \left. \frac{\partial \phi(\mathbf{x}, n)}{\partial \mathbf{x}} \right|_{\mathbf{x}=\mathbf{x}_{\text{nom}}(n)} \\ \mathbf{H}^{(1)}[\mathbf{x}_{\text{nom}}(n), n] &= \left. \frac{\partial \mathbf{h}(\mathbf{x}, n)}{\partial \mathbf{x}} \right|_{\mathbf{x}=\mathbf{x}_{\text{nom}}(n)} \\ \mathbf{d}_z(n) &= \mathbf{z}(n) - \mathbf{h}[\mathbf{x}_{\text{nom}}(n), n] \end{aligned}$$

To first-order, with respect to the deviations, $\mathbf{d}_x(N)$, Equations (IV.2) and (IV.3) are linear and, therefore, the results of Chapter III can be applied. This leads to the filter equations:

$$\hat{\mathbf{x}}(N+1|N+1) = \hat{\mathbf{d}}_x(N+1|N+1) + \mathbf{x}_{\text{nom}}(N+1) \quad (\text{IV.4})$$

$$\begin{aligned} \hat{\mathbf{d}}_x(N+1|N+1) &= \Phi^{(1)}[\mathbf{x}_{\text{nom}}(N), N] \hat{\mathbf{d}}_x(N|N) \\ &\quad + \mathbf{K}(N+1) \{ \mathbf{z}(N+1) - \mathbf{h}[\mathbf{x}_{\text{nom}}(N+1), N+1] \\ &\quad - \mathbf{H}^{(1)}[\mathbf{x}_{\text{nom}}(N), N] \Phi^{(1)}[\mathbf{x}_{\text{nom}}(N), N] \hat{\mathbf{d}}_x(N|N) \} \end{aligned} \quad (\text{IV.5})$$

$$\mathbf{K}(N+1) = \Sigma(N+1|N+1) \mathbf{H}^{(1)}[\mathbf{x}_{\text{nom}}(N+1), N+1] \mathbf{R}^{-1}(N+1) \quad (\text{IV.6})$$

$$\begin{aligned} \Sigma(N+1|N+1) &= \{ \mathbf{H}^{(1)}[\mathbf{x}_{\text{nom}}(N+1), N+1] \mathbf{R}^{-1}(N+1) \\ &\quad \times \mathbf{H}^{(1)}[\mathbf{x}_{\text{nom}}(N+1), N+1] + \Sigma^{-1}(N+1|N) \}^{-1} \end{aligned} \quad (\text{IV.7})$$

$$\begin{aligned} \Sigma(N+1|N) &= \Phi^{(1)}[\mathbf{x}_{\text{nom}}(N), N] \Sigma(N|N) \Phi^{(1)\top}[\mathbf{x}_{\text{nom}}(N), N] \\ &\quad + \Gamma[\mathbf{x}_{\text{nom}}(N), N] \mathbf{Q}(N) \Gamma^\top[\mathbf{x}_{\text{nom}}(N), N] \end{aligned} \quad (\text{IV.8})$$

$$\Sigma(0|0) = \Psi \quad (\text{IV.9})$$

Implementing the filter equations to compute the likelihood function, ξ_i , can be done after determining the transfer matrix, $\Phi^{(1)}[\mathbf{x}_{\text{nom}}(n), n]$ for each of the models, Model II and III.

Model II

The vector of state variables for Model II is:

$$\mathbf{x}(n) = [\Pi, P]$$

where,

Π = the concentration of phytoplankton,

P = the concentration of dissolved inorganic phosphorus.

The corresponding vector of the nominal trajectory is:

$$\mathbf{x}_{\text{nom}}(n) = [\Pi_{\text{nom}}, P_{\text{nom}}]$$

The transfer matrix, $\Phi^{(1)}[\mathbf{x}_{\text{nom}}(n), n]$, for Model II is:

$$\Phi^{(1)}[\mathbf{x}_{\text{nom}}(n), n] = \begin{bmatrix} \frac{\partial \Phi_1^{(1)}}{\partial \Pi} & \frac{\partial \Phi_1^{(1)}}{\partial P} \\ \frac{\partial \Phi_2^{(1)}}{\partial \Pi} & \frac{\partial \Phi_2^{(1)}}{\partial P} \end{bmatrix} \quad (\text{IV.10})$$

where,

$$\begin{aligned} \frac{\partial \Phi_1^{(1)}}{\partial \Pi} &= [G_{\Pi} - R_{\Pi} - \frac{w}{\Delta z} - \frac{Q}{V}] \Delta t + 1. \Big|_{\mathbf{x}(n)=\mathbf{x}_{\text{nom}}(n)} \\ \frac{\partial \Phi_1^{(1)}}{\partial P} &= \frac{\mu_{\Pi} K_{\Pi} L \Theta(T) \Pi(n) \Delta t}{(K_{\Pi} + P(n))^2} \Big|_{\mathbf{x}(n)=\mathbf{x}_{\text{nom}}(n)} \\ \frac{\partial \Phi_2^{(1)}}{\partial \Pi} &= [\beta_P (R_{\Pi} - G_{\Pi})] \Delta t \Big|_{\mathbf{x}(n)=\mathbf{x}_{\text{nom}}(n)} \\ \frac{\partial \Phi_2^{(1)}}{\partial P} &= [-\beta_P \frac{\mu_{\Pi} K_{\Pi} L \Theta(T) \Pi(n)}{(K_{\Pi} + P(n))^2} - \frac{Q}{V}] \Delta t + 1. \Big|_{\mathbf{x}(n)=\mathbf{x}_{\text{nom}}(n)} \end{aligned}$$

Model III

The vector of state variables for Model III is:

$$\mathbf{x}(n) = [\Pi(n), P(n), \zeta(n)]$$

where,

Π = the concentration of phytoplankton,

P = the concentration of dissolved inorganic phosphorus

ζ = the concentration of zooplankton.

The transfer matrix, $\Phi^{(1)}[\mathbf{x}_{\text{nom}}(n), n]$, for Model III is:

$$\Phi^{(1)} [x_{\text{nom}}(n), n] = \begin{bmatrix} \frac{\partial \Phi_1^{(1)}}{\partial \Pi} & \frac{\partial \Phi_1^{(1)}}{\partial P} & \frac{\partial \Phi_1^{(1)}}{\partial \zeta} \\ \frac{\partial \Phi_2^{(1)}}{\partial \Pi} & \frac{\partial \Phi_2^{(1)}}{\partial P} & \frac{\partial \Phi_2^{(1)}}{\partial \zeta} \\ \frac{\partial \Phi_3^{(1)}}{\partial \Pi} & \frac{\partial \Phi_3^{(1)}}{\partial P} & \frac{\partial \Phi_3^{(1)}}{\partial \zeta} \end{bmatrix} \Big|_{x(n)=x_{\text{nom}}(n)} \quad (\text{IV.11})$$

where,

$$\frac{\partial \Phi_1^{(1)}}{\partial \Pi} = \left[G_{\Pi} - R_{\Pi} - \frac{w}{\Delta z} - \frac{Q}{V} - \frac{\mu_{\zeta} K_{\zeta} \Theta(T) \zeta(n)}{(K_{\zeta} + \Pi(n))^2} \right] \Delta t + 1. \Big|_{x(n)=x_{\text{nom}}(n)}$$

$$\frac{\partial \Phi_1^{(1)}}{\partial P} = \left[-\frac{\mu_{\Pi} K_P L \Theta(T) \Pi(n)}{(K_P + P(n))^2} \right] \Delta t \Big|_{x(n)=x_{\text{nom}}(n)}$$

$$\frac{\partial \Phi_1^{(1)}}{\partial \zeta} = -\frac{G_{\zeta} \Delta t}{v} \Big|_{x(n)=x_{\text{nom}}(n)}$$

$$\frac{\partial \Phi_2^{(1)}}{\partial \Pi} = \left[\beta_P (R_{\Pi} - G_{\Pi}) + \beta_P \left(\frac{1-v}{v} \right) \left(-\frac{\mu_{\zeta} K_{\Pi} \Theta(T) \zeta(n)}{(K_{\Pi} + \Pi(n))^2} \right) \right] \Delta t \Big|_{x(n)=x_{\text{nom}}(n)}$$

$$\frac{\partial \Phi_2^{(1)}}{\partial P} = \left[-\beta_P \frac{\mu_{\Pi} K_P L \Theta(T) \Pi(n)}{(K_P + P(n))^2} - \frac{Q}{V} \right] \Delta t + 1. \Big|_{x(n)=x_{\text{nom}}(n)}$$

$$\frac{\partial \Phi_2^{(1)}}{\partial \zeta} = \left[\beta_P \left(\left(\frac{1-v}{v} \right) G_{\zeta} + R_{\zeta} \right) \right] \Delta t + 1. \Big|_{x(n)=x_{\text{nom}}(n)}$$

$$\frac{\partial \Phi_3^{(1)}}{\partial \Pi} = \left[-\frac{\mu_{\zeta} K_{\Pi} \Theta(T) \zeta(n)}{(K_{\Pi} + \Pi(n))^2} \right] \Delta t \Big|_{x(n)=x_{\text{nom}}(n)}$$

$$\frac{\partial \Phi_3^{(1)}}{\partial P} = 0$$

